

PL-TR-95-2107

**METEOR-BURST MODELING AND ANALYSIS
FINAL REPORT**

**R&D EQUIPMENT INFORMATION
COMPUTER SOFTWARE PRODUCTION ITEM
SCIENTIFIC AND TECHNICAL REPORT**

**Robert I. Desourdis, Jr.
Anne K. McDonough**

**Communications Engineering Laboratory
Telecommunications and Information Systems Division
Science Applications International Corporation
261 Cedar Hill St., Bldg 'C'
Marlborough, Massachusetts 01752**

30 July 1995

Approved for public release; distribution unlimited

**Final Report
21 September 1993-21 April 1995**

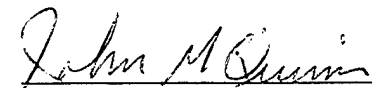
Approved for public release; distribution unlimited



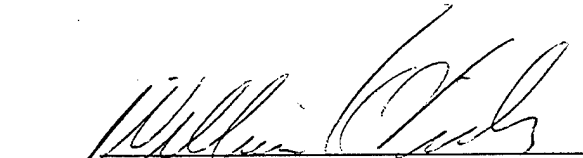
**PHILLIPS LABORATORY
Directorate of Geophysics
AIR FORCE MATERIEL COMMAND
HANSCom AFB, MA 01731-3010**

19960927 052

"This technical report has been reviewed and is approved for publication"


JOHN M. QUINN
Contract Manager


EDWARD J. BERGHORN
Branch Chief


WILLIAM K. VICKERY
Division Director

This report has been reviewed by the ESC Public Affairs Office (PA) and is releasable to the National Technical Information Service (NTIS).

Qualified requestors may obtain additional copies from the Defense Technical Information Center (DTIC). All others should apply to the National Technical Information Service (NTIS).

If your address has changed, if you wish to be removed from the mailing list, or if the addressee is no longer employed by your organization, please notify PL/IM, 29 Randolph Road, Hanscom AFB, MA 01731-3010. This will assist us in maintaining a current mailing list.

Do not return copies of this report unless contractual obligations or notices on a specific document require, that it be returned.

REPORT DOCUMENTATION PAGE			Form Approved OMB No. 0704-0188	
Public reporting burden for this collection of information is estimated to average 1 hour per response, including the time for reviewing instructions, searching existing data sources, gathering and maintaining the data needed, and completing and reviewing the collection of information. Send comments regarding this burden estimate or any other aspect of this collection of information, including suggestions for reducing this burden, to Washington Headquarters Services, Directorate for Information Operations and Reports, 1215 Jefferson Davis Highway, Suite 1204, Arlington, VA 22202-4302, and to the Office of Management and Budget, Paperwork Reduction Project (0704-0188), Washington, DC 20503.				
1. AGENCY USE ONLY (Leave blank)	2. REPORT DATE 30 July 1995	3. REPORT TYPE AND DATES COVERED Final 21 Sept 93 - 21 April 95		
4. TITLE AND SUBTITLE Meteor-Burst Modeling & Analysis: Final Report R&D Equipment Information Computer Software Production Item; Scientific & Technical Report		5. FUNDING NUMBERS C: F19628-93-C-0082 PE: 62101F PR: 4643 TA: GH WU: AA		
6. AUTHOR(S) Robert I. Desourdis, Jr. Anne K. McDonough				
7. PERFORMING ORGANIZATION NAME(S) AND ADDRESS(ES) Science Applications International Corporation Communications Engineering Laboratory 261 Cedar Hill Street, Building C Marlborough, MA 01752		8. PERFORMING ORGANIZATION REPORT NUMBER N/A		
9. SPONSORING/MONITORING AGENCY NAME(S) AND ADDRESS(ES) Phillips Laboratory 29 Randolph Road Hanscom AFB, MA 01731-3010 ATTN: John Quinn/GPIA		10. SPONSORING/MONITORING AGENCY REPORT NUMBER PL-TR-95-2107		
11. SUPPLEMENTARY NOTES NONE				
12a. DISTRIBUTION / AVAILABILITY STATEMENT Approved for public release: Distribution unlimited		12b. DISTRIBUTION CODE		
13. ABSTRACT (Maximum 200 words) This report describes a computer model for predicting the performance of meteor-burst communication links in terms of the usable meteor rate (MR) and the available channel duty cycle (DC). This model incorporates an empirical database of sporadic meteor flux, an empirical meteor velocity distribution, and detailed antenna pattern data usually provided by the National Electromagnetics Code (NEC). This program, PC METEORLINK, integrates MR and DC contributions throughout the sky region between 80 and 120 km above the earth's surface where most meteors are ionized. PC METEORLINK was derived from a VAX FORTRAN program called METEORLINK. This report describes the algorithms used in PC METEORLINK, the empirical data of meteor flux and velocity, the empirically-based formula for various meteoric physics and atmospheric parameters. It is divided into three sections. The first, R&D Equipment Information, is a User's Guide for the PC METEORLINK program. The second, Computer Software Product Item, is a Technical Manual for the program. The third, Scientific and Technical Report, presents validation results for PC METEORLINK prediction. This validation section compares PC METEORLINK predictions with data taken from the Greenland Meteor Burst Test Bed, the Jodrell Bank Experimental Station, and meteor-burst measurements performed in Kazan, Russia.				
14. SUBJECT TERMS Meteor-burst communications, modeling and simulation, Meteor-scatter modeling and analysis, Propagation modeling		15. NUMBER OF PAGES 136		
		16. PRICE CODE N/A		
17. SECURITY CLASSIFICATION OF REPORT Unclassified	18. SECURITY CLASSIFICATION OF THIS PAGE Unclassified	19. SECURITY CLASSIFICATION OF ABSTRACT Unclassified	20. LIMITATION OF ABSTRACT SAR	

CONTENTS

R&D EQUIPMENT INFORMATION (USER'S GUIDE)	1
1. INTRODUCTION	2
2. BACKGROUND	3
3. PC METEORLINK INPUTS	4
3.1 General Notes	4
3.2 Geometrical Parameters	5
3.3 Temporal Parameters	5
3.4 Integration Parameters	6
3.5 Antenna System Parameters	7
3.6 Radio-System Parameters	9
3.7 Calculation Control	10
3.8 Grids	10
4. PC METEORLINK OUTPUTS	10
5. PC METEORLINK EXECUTION	11
6. REQUIRED FILES	12
APPENDIX A: CONSTANT.DAT INPUT FILE	13
APPENDIX B: VELOCITY.DAT INPUT FILE	16
APPENDIX C: M0FLUX.DAT INPUT FILE	19
APPENDIX D: AWGAUSS.DAT INPUT FILE	36
COMPUTER SOFTWARE PRODUCT ITEM (TECHNICAL MANUAL)	44
1. INTRODUCTION	45
1.1 Summary	45
1.2 Background	47
1.3 Assumptions	48
2. OBSERVABLE METEOR TRAILS	49

3. USABLE METEOR TRAILS	51
3.1 Usability Criteria	51
3.2 Meteor Mass	52
3.3 Trail Line Density	52
4. MB LINK PERFORMANCE	58
4.1 Meteor Rate	58
4.2 Duty Cycle	64
SCIENTIFIC AND TECHNICAL REPORT (VALIDATION REPORT)	67
1. INTRODUCTION	68
1.1 Summary	68
1.2 Background	70
1.3 Assumptions	71
2. ALGORITHM DEVELOPMENT	72
2.1 Technical Background	72
2.2 Model Development	72
3. SOFTWARE DEVELOPMENT	75
4. RESULTS	75
4.1 Phillips Lab	75
4.2 Jodrell Bank	76
4.3 Calibration and Validation	78
4.4 Russian Measurements	79
4.5 Summary of Results	80
5. CONCLUSIONS AND RECOMMENDATIONS	81
APPENDIX A: GREENLAND TEST BED RESULTS	82
APPENDIX B: JODRELL BANK TEST BED RESULTS	83

R&D EQUIPMENT INFORMATION

(User's Guide)

September 5, 1995

**Prepared by
Communications Engineering Laboratory
Telecommunications and Information Systems Division
Science Applications International Corporation
261 Cedar Hill St., Bldg 'C'
Marlborough, Massachusetts 01752**

1. INTRODUCTION

SAIC's PC METEORLINK computer prediction tool was designed to model the performance of meteor-burst communication links. PC METEORLINK is a high-fidelity, first-principles model of the meteor-scatter channel that uses a detailed channel model to generate the usable meteor rate (MR) and channel duty cycle (DC) statistics. This DOS-based C++ program is an adaptation of SAIC's METEORCOM software package which predicts the performance of a much wider variety of meteor burst communication systems. METEORCOM is a family of VAX FORTRAN programs that can be used to predict the waiting time statistics associated with message delivery for arbitrary link protocols. METEORCOM also predicts the diversity improvement achieved through the use of multiple geographically-dispersed receivers. METEORCOM can be used to assess the probability of unintended intercept through its ability to predict the size and extent of the meteor burst footprint. This family of computer models has evolved over many years to become a comprehensive meteor burst communication modeling and analysis tool. This manual describes the PC version of the PC METEORLINK program. Information on the VAX-based METEORCOM software can be obtained by contacting SAIC.

PC METEORLINK has a variety of features that make it a useful modeling tool. It has been extensively validated with measured data from a variety of sources, which employed meteor-burst links with diverse link configurations. The result is a computer model which has been validated for a variety of operational environments. These link configurations include different latitudes, ranges, seasons, times of day, link geographic orientations, antenna systems, and link power budgets. Other notable features of the PC METEORLINK code include

- the use of three-dimensional, NEC-generated radiation patterns to represent antenna performance over the entire meteor-scatter region,
- sporadic meteor radiant distribution derived from extensive measurements in northern and equatorial latitudes,
- overdense and underdense meteor trail models,
- faraday rotation effects,
- solar cycle variations.

The PC METEORLINK program was designed as a first-principles model of the meteor scatter channel. It includes empirically-derived models for meteor flux, meteor mass-rate (rate of occurrence) and meteoric ionization parameters in a common volume integration to determine the total average usable meteor rate (MR) and net channel duty cycle (DC). The MR is the rate of arrival of meteors producing a received signal level (RSL) exceeding a specified minimum value. The total channel DC-value available from all properly oriented trails is measured as the percentage of time that the RSL-value is attained.

PC METEORLINK computes MR and DC, from the total incident meteor flux for a specified link-power budget, link geographic parameters, time of day, day in the year, and year in the solar cycle. The flux model used by PC METEORLINK was derived from monthly-averaged radar observations made in the Mogadishu, Somalia and the former Soviet Union. The MR and DC predictions for a given hour of a day are determined from the long-term (monthly) average flux meteor rate determined for that

hour of that day. PC METEORLINK Version 1.0 was created by converting the original VAX FORTRAN version of METEORLINK to a C++ PC computer program. PC METEORLINK Version 1.0V is an "experimental" version of PC METEORLINK that integrates each observable trail orientation over an empirically-derived meteor velocity distribution for the parent meteor.

2. BACKGROUND

Billions of meteoroids enter the earth's atmosphere each day. The vast majority of the resulting meteors are extremely small and disintegrate before reaching the ground. As these meteors burn up, they leave a trail of electrons in their wake that can reflect a radio signal. Trails can persist for up to seconds or more before being completely destroyed by diffusion, atmospheric winds, electron attachment, and recombination. The resulting meteor-burst (MB) link can provide communications for ranges up to 1200 miles. Meteoric particles of practical interest to radio communication systems range in mass from about 10^{-5} grams to about 10^2 grams, and their sizes range from about 1 cm to about below 50 microns. Many of these particles are not single solid particles but loose aggregates of smaller particles. The velocity of these meteors is bounded below by the escape velocity of a particle leaving the earth (11.3 km/sec) and is bounded above by the sum of the velocity of the earth (30 km/sec) and escape velocity from the solar system (42 km/sec) for a total velocity of 72 km/sec.

When an RF signal is incident on an electron trail, it will, in general, be scattered in all directions. The majority of the scattered energy, however, propagates along a path that satisfies the specular condition. That is, the incident and reflected angles are equal. For forward scattering of an RF signal, this condition is equivalent to the trail being contained within the tangent plane of an ellipsoid of revolution with the transmit and the receive sites at its foci. Once formed, a meteor trail immediately begins to dissipate through diffusion. After a time t , the radius of the trail is approximated by $(4Dt + r_0^2)^{1/2}$, where r_0 is the initial radius and D is the coefficient of diffusion. In addition to the diffusion effects, each trail is subject to distortion by upper atmosphere winds. Wind shear may rotate a trail by as much as 5° per second (these winds typically have velocities on the order of 25 m/sec) and can result in multipath fading of a meteor burst signal.

A meteor trail is classified as either underdense or overdense as determined by its electron volume density. Underdense trails are analyzed as if each electron in the trail were an independent scattering source. For these trails, a widely accepted model of the scattering of RF signal energy has been derived and is employed in PC METEORLINK. For overdense trails, on the other hand, the scattering effects are not nearly as straight-forward. The volume density of electrons in an overdense trail is so great that the electrons scatter from more than a single electron, that is, multiple scattering occurs. The net effect of this complex electron interaction is that radio signal does not significantly penetrate the meteor trail and most of the signal's energy is reflected in the direction that satisfies the specular condition. Several models of the scattering of radio signal energy by overdense trails have been developed. These models have been analyzed through extensive PC METEORLINK validations.

Meteor burst has been used for many years to support over-the-horizon communications at frequencies in the lower VHF band. Empirical measurements combined with theoretical predictions have demonstrated that meteor-burst systems provide near-optimum performance between about 35 and 55

MHz. Lower frequencies are not used because other propagation modes (sky wave, sporadic E, spread F, and auroral scatter) tend to dominate system performance and compromise the inherent anti-jam and low probability-of-intercept attributes of meteor-burst systems. Higher frequencies are not practical because the energy reflected by the trail decreases rapidly with increasing frequency, thus reducing the link MR and DC values. Ultimately (somewhere near 100 MHz) unrealistic requirements are imposed on the required transmitter output power and the receiver sensitivity. The highest usable frequency for a meteor-burst communication is near 100 MHz, although low duty-cycle communications have been noted at frequencies as high as 150 MHz.

3. PC METEORLINK INPUTS

The PC version of PC METEORLINK uses an input-file format similar to the "NAMELIST" format used by the VAX FORTRAN version. This format, shown below, is convenient because the input files consist of variable names (one-word convention) followed by the value(s) of that variable, such as:

variable_name = value,

Many of the input variables are represented by comma-delimited lists of values which define the transmit and receive radio system parameters for up to 12 sequential runs, that is, PC METEORLINK offers the ability to perform up to 12 sequential executions using a single input file. This feature is useful for performing parametric studies to evaluate link performance sensitivity to variations in input variables. This feature could, for example, be used to study the temporal behavior of the meteor-burst channel by executing PC METEORLINK at 12 different times of day. The total number of runs to be executed by a single PC METEORLINK input file is specified by the parameter **N_RUN**. The format required for the inputs associated with each of the **N_RUN** executions is described in the following sub-sections.

3.1 General Notes

- PC METEORLINK is not case sensitive with respect to input parameters.
- For multiple input parameters that "fill" an array, such as **MONTH** input parameter, the array can be filled by specifying each input independently, or for adjacent cells in the array with the same value, use an index parameter to tell the program, the number of values to be repeated and the parameter value to be repeated in filling the array. For example,

MONTH = 3, 3, 3, 3, 3, 3, 3, 3, 3, 3, 3, 3,

and

MONTH = 12*3,

will fill the **MONTH** input array with the same values.

- If an input parameter is missing from the input file, an error message will be issued and program execution will halt.
- For input parameters that fill an array, such as the **MONTH** input parameter, the array must be filled with at least the number of values specified by the **N_RUN** parameter. If the input parameter array does not contain enough values, an error message will be issued and program execution will halt.

- For input parameters that specify Boolean inputs, such as the **DUTY_CYCLE** input parameter, a '0' indicates FALSE and any other value will set the input parameter to TRUE.

These general notes are uniquely applicable to the PC METEORLINK program and not necessarily characteristic of "standard" C++ input formats.

3.2 Geometrical Parameters

The MB-link geometry is specified by entering the latitude and longitude of each radio station. These geographic locations are entered as integer values representing degrees, minutes, and seconds of latitude and longitude respectively. The hemisphere in which the latitude and longitude are determined is specified by the input parameters **LAT_NS** and **LNG_EW** respectively ("+" is used to represent north latitude and east longitude while "0" represents south latitude and west longitude). Since there are two MB radio stations, or antenna sites, a total of four integer values is required for each input file. The following example explains how to enter the latitude of the two radio stations.

LAT_DEG = 77, 66,

LAT_MIN = 55, 44,

LAT_SEC = 33, 22,

LAT_NS = 0, 1,

In this example, MB stations 1 and 2 are located at 77° 55' 33" S and 66° 44' 22" N latitude respectively. Notice that these variables, like all of the variables in the input file, must be terminated with a comma. The other formats required to specify the link's longitude information is similar to the latitude input format using **LNG_DEG**, **LNG_MIN**, **LNG_SEC**, and **LNG_EW** names to specify the input values.

3.3 Temporal Parameters

The date and time are required to position the earth in its orbit around the sun and thus relative to the sporadic meteor-radiant distribution. The month, day, and year are entered as integer values into comma-delimited 12-element arrays. The 12 values are used in subsequent executions of the PC METEORLINK program as specified by the input variable **N_RUN**. The "time" is represented by two 12-element

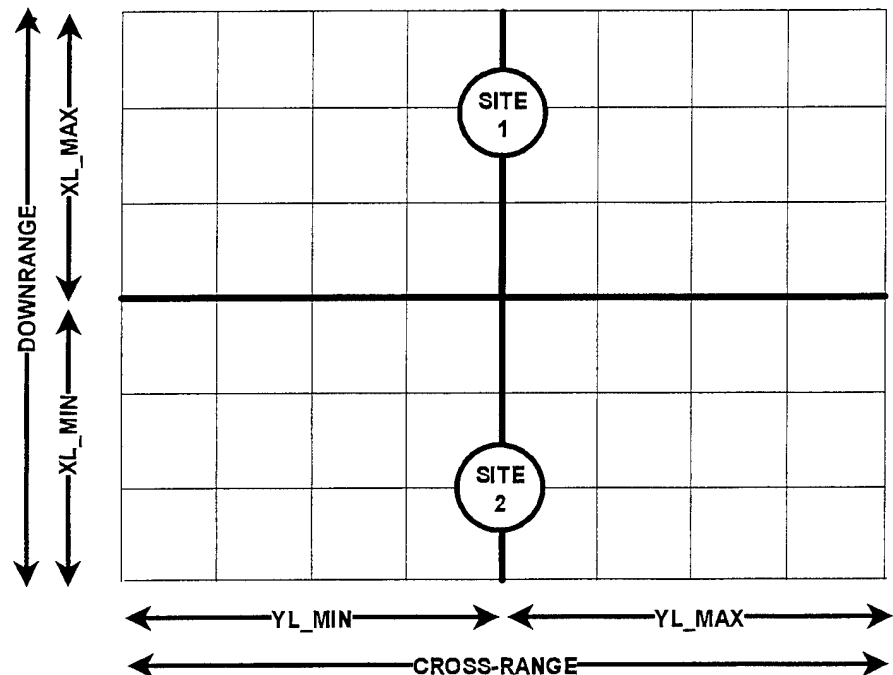


Figure 3.1 PC METEORLINK MB-link geometry

integer arrays which represent the intended hour and minute of the MB link performance to be predicted. The final parameter, **Hours_GW**, is a single integer which represents the difference between the local time and Greenwich Mean Time (GMT). This parameter is entered as the number of "hours behind GMT" and thus is a positive number for the western hemisphere. For example, the input file with the following parameters:

```

YEAR = 12*1989,
MONTH = 12*3,
DAY = 6*15, 6*1,
HOURS = 0, 4, 8, 12, 16, 20, 6*0,
MINUTES = 6*0, 6*45,
HOURS_GW = 0,

```

will be executed for the dates and times shown in Table 3.1 below.

3.4 Integration Parameters

PC METEORLINK determines the link MR and DC values by performing a spatial integration over the common sky volume illuminated by the transmit and receive antennas. In addition to these spatial integrations, PC METEORLINK version 1.0 integrates over all possible trail orientations and all possible trail electron line densities. To provide user flexibility in run time and output resolution, PC METEORLINK version 1.0 provides the capability to specify the integration parameters. These parameters are entered as integer values which are used by all 12 runs defined by a given input file. PC METEORLINK version 1.0V also integrates over meteor velocity for each trail orientation.

The Gauss quadrature integration routine implemented by PC METEORLINK requires specification of the number of integration points. The Gauss abscissas and corresponding weight values for 2, 4, 6, 8, 10, 12, 16, 20, 24, 32, 40, 48, 64, 80 and 96-point integration are stored in the file "AWGAUSS.DAT". These abscissas and weights are input by PC METEORLINK automatically upon program execution. Due to the nature of the Gauss quadrature integration, the number of integration points must be selected from the list above. The extent of the link grid is controlled by input variables **XL_MIN**, **XL_MAX**, **YL_MIN**, **YL_MAX** as shown in Figure 3.1 below. These variables are specified in kilometers.

Integrations performed by PC METEORLINK include spatial integration over the link grid (**N_XL**, **N_YL**, **N_ZL**), an angular integration to count all possible meteor-orientation (**N_AM**), a velocity

Table 3.1 Time parameters

Run	Month	Day	Year	Hour	Minute
1	March	15	1989	0	0
2	March	15	1989	4	0
3	March	15	1989	8	0
4	March	15	1989	12	0
5	March	15	1989	16	0
6	March	15	1989	20	0
7	March	1	1989	0	45
8	March	1	1989	0	45
9	March	1	1989	0	45
10	March	1	1989	0	45
11	March	1	1989	0	45
12	March	1	1989	0	45

integration to account for meteor velocity distributions (**N_VL**, version 1.0V only), and electron line density integrations for under (**N_QU**) and overdense (**N_QO**) trails. The accuracy of each integration is determined by the number of points specified. PC METEORLINK has demonstrated convergence to the second significant digit with the settings:

N_XL = 16 ,
N_YL = 16 ,
N_ZL = 8 ,
N_AM = 10 ,
N_VL = 12 ,
N_QU = 4 , and
N_QO = 8.

In practice, the user may make several executions of PC METEORLINK and examine the resulting MR and DC link grids for each link path length and antenna combination. The input parameters required to generate these grids are presented in section 3.8. (Note that only the MR grid has been implemented due to executable-image size limitations in the current PC METEORLINK program.) This procedure begins with wide integration limits resulting in excessive link grids. Examination of the distribution of MR contributions will quickly lead to a reduction in the integration limits for X and Y and a corresponding increase in accuracy. Once these limits have been found for each link scenario, input files can be created with an optimal trade-off between execution time and prediction accuracy.

3.5 Antenna System Parameters

As stated earlier, PC METEORLINK uses three-dimensional, NEC-generated radiation patterns to represent antenna performance over the entire meteor-scatter region. The "NECTOMTL" program converts NEC output files into the format used by the PC METEORLINK analysis modules. The conversion program prompts the user for the name of the file to be converted and the number of increments in azimuth and elevation angle. The antenna file created by NEC must cover the entire upper half space. Increments of 2° in ' θ ' (elevation angle) and 5° in ' ϕ ' (azimuth angle) are recommended (see Figure 3.2), but any increment which is larger than these values will work in the program although pattern granularity will suffer for intricately-lobed patterns. The 2° elevation and 5° azimuth increments require 46 values of θ and 73 values of ϕ , respectively, to cover the entire upper half space. If more than 46 θ values or 73 ϕ increments are used, the program could produce a "run time" error because the program cannot allocate enough memory for smaller increments. It

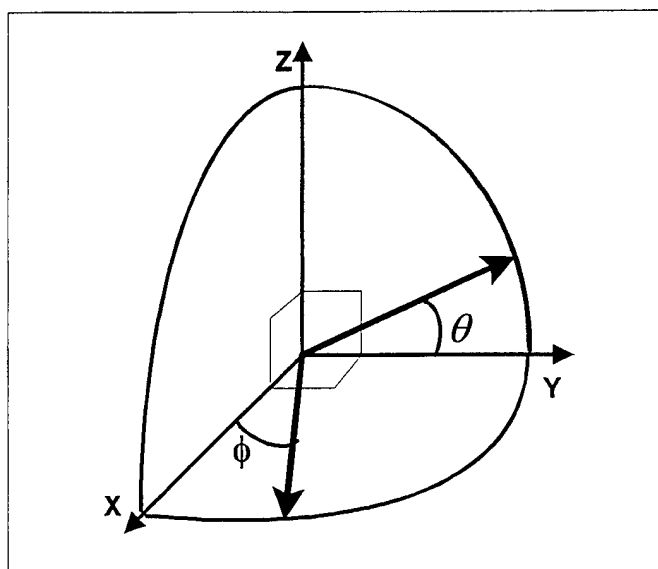


Figure 3.2 Antenna take-off angle definition

is also assumed that the ranges of θ and ϕ are $(0, \pi)$ and $(0, 2\pi)$ respectively, that is both θ and ϕ are assumed to begin at an absolute angle of 0° . It is therefore important that a range in the NEC 'RP' card (any far-field distance is acceptable) is specified. This value is needed to normalize the field strengths used in PC METEORLINK. However, a 'zero' value will for this parameter is acceptable in PC METEORLINK Version 1.0V, although it is unacceptable in Version 1.0.

The transmit and receive antenna pattern files for the two stations are specified using the input string variable **ANTENNA_FILE**. The first two files specified are the transmit and receive antennas for the site 1, while the next two files specified are the antenna patterns used for site 2. The format for specifying the antenna patterns is:

```
ANTENNA_FILE = '<path>ST1TX.MTL', '<path>ST1RX.MTL',  
'<path>ST2TX.MTL', '<path>ST2RX.MTL',
```

where:

- **<path>** is the drive and directory name where the file is located. If a path is not specified, the directory is assumed to be the same as the directory containing the PC METEORLINK executable.
- "ST1TX.MTL" is a file containing the antenna pattern for the transmit antenna at site 1,
- "ST1RX.MTL" is a file containing the antenna pattern for the receive antenna at site 1,
- "ST2TX".MTL is a file containing the antenna pattern for the transmit antenna at site 2, and
- "ST2RX.MTL" is a file containing the antenna pattern for the receive antenna at site 2.

The orientation angles of the antennas (bearing, pitch, and roll) are also specified in the input file. The bearing angle is specified in degrees with respect to true north. This parameter is a typical source of error in an input file. Improperly oriented antennas will result in long waiting times and negligible duty cycle. Antenna pattern pitch and roll are useful in the analysis of the performance of airborne antenna systems. Antenna systems near to the earth's surface should have pitch and roll angles of 0° . Therefore, NEC must be used to accurately account for pitch and roll angles in antenna systems near the ground. The bearing, pitch, and roll are specified using the input variable names, **BEARING**, **PITCH**, and **ROLL** using the following format:

```
BEARING_DEG = WW.W, XX.X, YY.Y, ZZ.Z,
```

```
PITCH_DEG = WW.W, XX.X, YY.Y, ZZ.Z,
```

```
ROLL_DEG = WW.W, XX.X, YY.Y, ZZ.Z,
```

where WW.W, XX.X, YY.Y, and ZZ.Z, are specified in the number of degrees. W and X specify the values for the transmit and receive antennas at site 1, respectively. Y and Z specify the values for the transmit and receive antennas at site 2, respectively.

In PC METEORLINK Version 1.0, the bearing angles **BEARING_DEG** correspond to the antenna pointing angle measured east of true north, that is, clockwise from north. In Version 1.0V, the meaning of **BEARING_DEG** depends upon the "sign" of the value used in the input file. If a bearing angle is entered as 0° ($< 0.01^\circ$) or negative, then this value is *added* to the actual bearing angle pointing from one site to the second site. In other words, the bearing angle becomes a pointing "offset" from the Great

Circle path between sites. Otherwise, the bearing angle serves as the absolute pointing angle measured east of north as in Version 1.0.

The antenna heights are specified in kilometers using the input variable name **HANT_KM**. The format for indicating the antenna height is:

HANT_KM = XX.XX, YY.YY

where **XX.XX** is the height of the antennas at site 1 in kilometers and **YY.YY** is the height of the antennas at site 2. These heights are used to model ground-air and air-air MB links in which the radio LOS range is extended.

3.6 Radio-System Parameters

The radio-system parameters include transmit frequency, transmit power, transmitter system losses, antenna patterns, required received power, minimum burst duration, and index of the transmit site. The transmit system losses generally consist of cable, connector, and mismatch losses. The required received power at the antenna terminals must be calculated considering the external noise temperature, the receiver's noise figure, the insertion loss of the cable and the cable's physical temperature, and the minimum required signal-to-noise ratio (SNR) per bit.

The required SNR is computed from the required E_b/N_o , the bit transmission rate, system losses and coding gain. The required E_b/N_o can be found by referring to the appropriate BER curve for the desired modulation scheme. These curves can be found in a number of well-known sources. The sum of the required SNR (dB) and the noise power (dBm) yields the required signal level at the receiver input. The required power at the antenna terminals is the sum of this value and the insertion loss of the cable. The minimum burst duration is the length of time that a scattered signal must exceed the receiver's threshold for it be considered a usable trail. Trails with a duration less than the specified trail duration are not considered usable on the MB link. The transmitter index identifies the transmit site, using the index, i_{Tx} , and the receive site using the parameter, which is set to one for the transmit site.

The transmit frequency in MegaHertz for the two stations is indicated by the format:

FREQUENCY_MHZ = XX.XX, YY.YY,

where **XX.XX** and **YY.YY** are the transmit frequencies for site 1 and 2, respectively.

The values following **PT_DBW** define the transmit power in dBW for each of the 12 PC METEORLINK runs. The values following **PRREQ_DBM** indicate the required receive power in dB below one milliWatt for each of the 12 PC METEORLINK runs. The transmit line losses in dB for the two stations is specified using the **LTX_DB** variable name. The values following **TAU_SEC** define the required minimum burst duration in seconds for each of the 12 PC METEORLINK runs. The integer values following **INDEX_TX** indicate which station (1 or 2) is the transmit site for each of the 12 PC METEORLINK runs.

3.7 Calculation Control

DUTY_CYCLE is another flag which controls the execution of PC METEORLINK. A value of "TRUE" for this variable tells PC METEORLINK to compute link DC as well as the MR value, while a value of "FALSE" forces PC METEORLINK to compute the MR only. Setting this value to "FALSE" will save computer time. The flag **FARADAY** is a logical flag that controls the execution of PC METEORLINK. Setting FARADAY to 'TRUE,' that is, any non-zero integer value, forces the program to compute the Faraday rotation angles of transmit and receive electric vectors. If **FARADAY** is set to 'FALSE,' that is, a '0,' Faraday effects are not included in the MR and DC calculations.

3.8 Grids

As stated previously, the usable meteor rate output grid can be generated by PC METEORLINK to determine which part of the meteoric sky volume produces the greatest usable rate contribution. The MR output grid will be generated if the input variable name controlling these grids is set to TRUE. The various grids employed in the VAX METEORLINK program are listed in the table below with their input variable names and the extension of file that contains the output grids. At present, PC METEORLINK Version 1.0 provides no grid output, while Version 1.0V provides only the MR-contribution grid output as highlighted in Table 3.3.

4. PC METEORLINK OUTPUTS

PC METEORLINK always computes the average MR value and may also compute the channel DC value for the link specified in the input file. The input variables described in Section 3.6 determine whether or not the DC value is computed in addition to the MR value. PC METEORLINK will output the MR value, corresponding waiting time, DC value (%), percentage of MR from underdense trails, percentage of DC from underdense trails, and total flux of suitable oriented meteor trails. The format of the output is shown in Figure 3.3

METEORLINK RESULTS															
						REQUIRE D				PERFORMANCE			Underdense Portion of		Total
DATE TIME Tx						Rx	Burst	Meteor	Waiting	Duty	Meteor	Duty	Observable	Flux	
Run	Mo	Day	Year	Hr	Min	Site	Power (dBW)	Duration (sec)	Rate (Mpm)	Time (min)	Cycle (%)	Cycle (%)	Cycle (%)	Flux (Mpm)	
1	3	15	1989	00:00		1	29.5	-120.0	0.040	1.85E-01	5.41E+00	0.00E+00	9.40E+01	0.00E+00	2.85E+02
2	3	15	1989	04:00		1	29.5	-120.0	0.040	1.33E-01	5.67E+00	0.00E+00	9.60E+01	0.00E+00	2.95E+02
Mean Values:										1.85E-01	5.41E+00	0.00E+00	9.50E+01	0.00E+00	2.90E+02

Figure 3.3 Sample PC METEORLINK output

Figure 3.3 Sample PC METEORLINK output

PC METEORLINK will output these values to the screen and two output files. The output files will have the same prefix as the input file. The output file with the suffix ".OUT" will have the same format as shown above. The output file with the suffix ".TXT" will use spaces to delimit values so that output can be easily "read" by a spreadsheet program such as Microsoft Excel. If output grids have been computed, files will be created for each type of grid with the same prefix as the input file. The file suffixes are listed in Table 3.2. Spaces are used to delimit values so that output can be easily read by a spreadsheet program such as Microsoft Excel.

Table 3.2 Grid file suffix definitions (only **MR_GRID** is currently implemented)

GRID DESCRIPTION	INPUT VARIABLE	FILE EXTENSION
MR contributions above each point in the LINK grid	MR_GRID	.MR
DC contributions above each point in the LINK grid	DC_GRID	.DC
Percentage of MR contributions from underdense meteor trails above each point in the LINK grid	UPMR_GRID	.UMR
Percentage of DC contributions from underdense meteor trails above each point in the LINK grid	UPDC_GRID	.UDC
Antenna azimuth and elevation angles for which the MR (or DC) contribution exceeds a percentage FRCT_MR (or FRCT_DC) of the net MR (or DC) above each point in the LINK grid	ANTAZ_GRID ANTEL_GRID	.AZ .EL
Average gain product of transmit and receive field vectors in dB above each point in the LINK grid	GTGR_GRID	.GTR
Faraday rotation angles for transmit and receive electric vectors if and only if FARADAY = .TRUE.	FARADAY_GRID	.FAR

5. PC METEORLINK EXECUTION

The user can execute PC METEORLINK in an interactive or non-interactive mode. In interactive mode, the user simply types "MLINK" at the MS-DOS prompt. A list of input files in the directory that PC METEORLINK resides will be listed. The user can abort execution by hitting the "ESCAPE" key. Or by using the "←", "→", "↑", and "↓" to move around and hitting the "ENTER" key, a user can choose the desired input file. In non-interactive mode, the user simply types MLINK <path>inputfile.INP at the MS-DOS prompt, and PC METEORLINK will be executed using the desired input file.

At the beginning of PC METEORLINK execution, the program dynamically allocates memory for the several arrays, including those containing integration values and antenna gain patterns. If PC METEORLINK cannot allocate enough memory, an error message will be issued and the program execution will halt. PC METEORLINK can use only base DOS memory, not extended memory. Therefore, it is recommended that PC METEORLINK is executed with as much base memory as possible. If the program will not execute, then use the following suggestions to reduce the amount of dynamically allocated memory required:

- start PC METEORLINK with as much base memory as possible,
- limit the number of output grids (one or zero in the present configuration),
- reduce the number of ϕ and θ values in the antenna pattern file (if possible for accuracy), and
- reduce the number of integration points (**N_XL**, **N_YL**, **N_ZL**, **N_AM**, **N_VL**) until the computed MR and DC values begins to change significantly.

As previously stated, the maximum available memory should be "free" for use by PC METEORLINK. 'Resetting' a PC before executing the program or initiating a large number of executions would arguably provide the 'best' solution.

6. REQUIRED FILES

The following files must be located in the same directory as the PC METEORLINK executable:

CONSTANT.DAT (Appendix A)

VELOCITY.DAT (Appendix B)

M0FLUX.DAT (Appendix C)

AWGAUSS.DAT (Appendix D)

These files are provided in the indicated appendices. Of these files, only **CONSTANT.DAT** should be altered by the user interested in further calibration of the PC METEORLINK program (either version) and then only after careful consultation with the available MB references. Note that the constants in **CONSTANT.DAT** have different meaning depending on which PC METEORLINK version is being employed. These differences are critical to the operation of the respective programs and are described in Appendix A.

7. APPENDIX A: CONSTANT.DAT INPUT FILE

This appendix contains the CONSTANT.DAT input file. Although the number and names of arguments defined by CONSTANT.DAT are the same for both PC METEORLINK Version 1.0 and Version 1.0V, some of the arguments differ in their meaning and use in the respective algorithms. These differences are annotated below. Note that only Version 1.0V values are shown in the file below.

```

//*****
//*****
//1030 IMPORTANT CONSTANTS
//*****
//*****
// constants.140
const float hMImin_km = 80.0; ..... Both versions: maximum height of meteoric ionization
const float hMImax_km = 120.0; ..... Both versions: minimum height of meteoric ionization
const float Rc      = 9.0; ..... Version 1.0: Flux cell correlation coefficient
                                   Version 1.0V: Index used to select desired expression for
                                   the ionization coefficient (see Final Report)

const float VeOh_kmps = 29.77; ..... Both versions: Earth's heliocentric speed (unused)
const float m_VmOh    = 0.0; ..... Both versions: Slope of heliocentric meteor speed (unused)
const float b_VmOh    = 1.0; ..... Version 1.0: Intercept of heliocentric speed (unused)
                                   Version 1.0V: Scale factor to divide sporadic flux values

const float Re_m      = 2.8178e-15; ..... Both versions: Classical electron radius (m)
const float m_theta   = 0.0189; ..... Both versions: Constant for absent algorithm (unused)
const float m_Hmax    = 49.0; ..... Version 1.0: Slope of height curve of maximum ionization
                                   as a function of meteor speed
                                   Version 1.0V: (1) "zero," if the height of maximum
                                   ionization is equal to b_Hmax
                                   (2) Slope of height curve of maximum
                                   ionization as a function of meteor
                                   speed, if m_Hmax > 0 and b_Hmax > 0
                                   (3) Coefficient on the log10 of meteor
                                   speed for the height curve of maximum
                                   ionization, if m_Hmax > 0 and
                                   b_Hmax < 0

const float b_Hmax    = -3.3; ..... Version 1.0: Intercept of height curve of maximum
                                   ionization
                                   Version 1.0V: (1) height of maximum ionization if
                                   m_Hmax = 0
                                   (2) Intercept of height curve of maximum
                                   ionization as a function of meteor
                                   speed, if m_Hmax > 0 and b_Hmax > 0
                                   (3) Coefficient on the log10 of maximum
                                   electron line density for the height

```

curve of maximum ionization, if
 $m_Hmax > 0$ and $b_Hmax < 0$

const float qO_MAX = 1.0e18; Both versions: maximum electron line density considered
 const float EXP_thr = 1.0; Both versions: absent algorithm (unused)
 const float m_eRo = 7.35e6; Version 1.0: slope of meteor height dependence as
 exponent on 10 used to compute the initial
 trail radius (height in kilometers)
 Version 1.0V: Constant multiplier for initial radius
 expression
 const float b_eRo = 1.0; Version 1.0: Intercept of meteor height dependence
 as
 exponent on 10 used to compute the initial
 trail radius (height in kilometers)
 Version 1.0V: Exponent on meteor speed (cm/s) used in
 the expression for initial radius
 const float m_eD = 0.0225; Both versions: slope of meteor height dependence as
 exponent on 10 used to compute the
 ambipolar diffusion rate (height in
 kilometers)
 const float b_eD = -1.40; Both versions: intercept of meteor height dependence as
 exponent on 10 used to compute the
 ambipolar diffusion rate (height in
 kilometers)
 const int NLTA_smp = 25; Both versions: number of attachment spline samples
 const float Be_Nm = 0.25; Both versions: $\beta_e N_m$, attachment factor on q
 const int SLRmin_yr = 1974; Both versions: base year for solar cycle scaling
 const float SLRavg = 1.5; Both versions: average factor for solar cycle scaling
 const float SLRmax = 0.5; Both versions: maximum amplitude of assumed
 sinusoidal solar cycle behavior
 const float zeta_D = 1.0; Both versions: underdense diffusion rate scale factor
 const float PLASMA_factor = 1.0; Both versions: plasma resonance amplification factor
 const float CsL_EXP = 2.40; Both versions: mass-rate exponent for MB link
 const float CsR_EXP = 1.0; Version 1.0: mass-rate exponent for sporadic flux radar
 Version 1.0V: (1) mass-rate exponent is CsL_EXP for
 sporadic flux on MB link if
 $CsR_EXP > 0.0$
 (2) mass-rate exponent varies with
 elongation angle with CsL_EXP as a
 constant on the MB link if
 $CsR_EXP \leq 0.0$
 const float qMI_radar_Epm = 1.2e13; Version 1.0: minimum radar-detectable line density
 Version 1.0V: minimum radar-detectable line density
 (unused)
 const float lmda_radar_m = 8.0; Version 1.0: radar signal wavelength

Version 1.0V: radar signal wavelength (unused)
 const float RoMI_radar_m = 1.2; Version 1.0: initial trail radius for radar-detectable trails at
 height of maximum ionization
 Version 1.0V: initial trail radius for radar-detectable trails
 at height of maximum ionization (unused)
 const float hMI_radar_km = 96.0; Version 1.0: height of maximum ionization for radar-
 detectable meteor trails
 Version 1.0V: height of maximum ionization for radar-
 detectable meteor trails (unused)
 const float PHASE_shift_dg = 95.0; Version 1.0: phase shift for underdense/overdense
 threshold
 Version 1.0V: (1) 2.4×10^{14} if PHASE_shift_dg = 0.0
 (2) phase shift for underdense/overdense
 threshold if PHASE_shift_dg > 0.0
 const float Q_ERR = 0.0001; Both versions: error in overdense line density
 approximation search routine
 const float t_ERR = 0.0001; Both versions: error in overdense line density
 peak-power time-search routine
 const float mo = 6.5e-4; Both versions: minimum detectable meteor mass in
 sporadic flux density distribution

8. APPENDIX B: VELOCITY.DAT INPUT FILE

This appendix contains the **VELOCITY.DAT** data file providing values for the meteor velocity number-density function. These values should not be changed by the user.

```
//      SPORADIC METEOR VELOCITY DENSITY VS. ELONGATION ANGLE
```

```
//
```

```
// Elongation Angle Bins
```

```
//E_A_Bins 5.0, 15.0, 25.0, 35.0, 45.0,
```

```
//E_A_Bins 55.0, 65.0, 75.0, 85.0, 95.0,
```

```
//E_A_Bins 105.0, 115.0, 125.0, 135.0, 145.0,
```

```
//E_A_Bins 155.0, 165.0, 175.0,
```

```
// Meteor-Speed Bins
```

```
//M_S_Bins 11.0, 13.0, 15.0, 17.0, 19.0, 21.0, 23.0, 25.0, 27.0, 29.0, 31.0, 33.0,
```

```
//M_S_Bins 35.0, 37.0, 39.0, 41.0, 43.0, 45.0, 47.0, 49.0, 51.0, 53.0, 55.0, 57.0,
```

```
//M_S_Bins 59.0, 61.0, 63.0, 65.0, 67.0, 69.0, 71.0, 73.0,
```

```
// Meteor Speed Density Values
```

```
// Each column represents a single density function
```

```
// Each row corresponds to the various elongation-angle values
```

```
// 11-13 km/sec
```

```
0.0, 0.0, 0.0, 0.0, 0.0, 0.0, 0.0, 0.0, 0.1,
```

```
0.1, 0.1, 0.1, 0.1, 0.1, 0.1, 0.1, 0.1, 0.0,
```

```
// 13-15 km/sec
```

```
0.0, 0.0, 0.0, 0.0, 0.8, 2.7, 4.2, 5.0, 5.4,
```

```
6.0, 6.3, 6.4, 6.9, 6.9, 7.0, 7.9, 10.5, 8.5,
```

```
// 15-17 km/sec
```

```
0.0, 0.0, 0.1, 2.4, 8.6, 10.8, 11.1, 11.8, 13.2,
```

```
16.6, 19.9, 22.7, 26.6, 32.0, 40.4, 56.2, 89.4, 91.4,
```

```
// 17-19 km/sec
```

```
0.0, 0.0, 0.8, 3.0, 9.4, 12.6, 13.2, 14.0, 15.4,
```

```
19.0, 23.8, 29.8, 37.3, 48.3, 52.5, 35.9, 0.0, 0.0,
```

```
// 19-21 km/sec
```

```
0.0, 0.2, 0.7, 3.0, 6.7, 8.9, 10.6, 12.7, 15.2,
```

```
19.1, 22.9, 27.3, 29.2, 12.7, 0.0, 0.0, 0.0, 0.0,
```

```
// 21-23 km/sec
```

```
0.0, 0.2, 0.5, 1.2, 3.8, 6.3, 8.5, 11.2, 13.7,
```

```
16.5, 17.1, 13.7, 0.0, 0.0, 0.0, 0.0, 0.0, 0.0,
```

```
// 23-25 km/sec
```

```
0.0, 0.1, 0.1, 0.8, 2.8, 4.5, 6.2, 8.9, 11.4,
```

```
12.1, 8.5, 0.0, 0.0, 0.0, 0.0, 0.0, 0.0, 0.0,
```

```
// 25-27 km/sec
```

```
0.0, 0.0, 0.2, 0.7, 2.3, 3.6, 4.8, 6.8, 8.6,
```

6.8, 1.4, 0.0, 0.0, 0.0, 0.0, 0.0, 0.0, 0.0,
 // 27-29 km/sec
 0.0, 0.0, 0.1, 0.6, 1.9, 3.0, 4.1, 5.5, 6.5,
 2.9, 0.0, 0.0, 0.0, 0.0, 0.0, 0.0, 0.0, 0.0,
 // 29-31 km/sec
 0.0, 0.0, 0.2, 0.7, 1.9, 2.8, 3.7, 4.9, 4.9,
 1.0, 0.0, 0.0, 0.0, 0.0, 0.0, 0.0, 0.0, 0.0,
 // 31-33 km/sec
 0.0, 0.0, 0.1, 0.6, 2.1, 3.0, 3.6, 4.5, 3.5,
 0.0, 0.0, 0.0, 0.0, 0.0, 0.0, 0.0, 0.0, 0.0,
 // 33-35 km/sec
 0.0, 0.0, 0.1, 0.4, 2.1, 3.3, 3.7, 4.3, 2.1,
 0.0, 0.0, 0.0, 0.0, 0.0, 0.0, 0.0, 0.0, 0.0,
 // 35-37 km/sec
 0.0, 0.0, 0.0, 0.4, 2.1, 3.7, 4.0, 4.1, 0.0,
 0.0, 0.0, 0.0, 0.0, 0.0, 0.0, 0.0, 0.0, 0.0,
 // 37-39 km/sec
 0.0, 0.0, 0.0, 0.4, 2.1, 4.2, 4.3, 3.8, 0.0,
 0.0, 0.0, 0.0, 0.0, 0.0, 0.0, 0.0, 0.0, 0.0,
 // 39-41 km/sec
 0.0, 0.0, 0.0, 0.3, 2.0, 4.6, 4.7, 2.5, 0.0,
 0.0, 0.0, 0.0, 0.0, 0.0, 0.0, 0.0, 0.0, 0.0,
 // 41-43 km/sec
 0.0, 0.0, 0.1, 0.3, 1.9, 4.8, 5.0, 0.0, 0.0,
 0.0, 0.0, 0.0, 0.0, 0.0, 0.0, 0.0, 0.0, 0.0,
 // 43-45 km/sec
 0.0, 0.1, 0.2, 0.5, 2.0, 4.7, 4.8, 0.0, 0.0,
 0.0, 0.0, 0.0, 0.0, 0.0, 0.0, 0.0, 0.0, 0.0,
 // 45-47 km/sec
 0.0, 0.2, 0.3, 0.9, 2.4, 4.5, 3.2, 0.0, 0.0,
 0.0, 0.0, 0.0, 0.0, 0.0, 0.0, 0.0, 0.0, 0.0,
 // 47-49 km/sec
 0.1, 0.3, 0.6, 1.5, 3.1, 4.3, 0.0, 0.0, 0.0,
 0.0, 0.0, 0.0, 0.0, 0.0, 0.0, 0.0, 0.0, 0.0,
 // 49-51 km/sec
 0.2, 0.6, 1.1, 2.5, 4.3, 4.3, 0.0, 0.0, 0.0,
 0.0, 0.0, 0.0, 0.0, 0.0, 0.0, 0.0, 0.0, 0.0,
 // 51-53 km/sec
 0.4, 1.2, 1.9, 4.0, 6.1, 3.6, 0.0, 0.0, 0.0,
 0.0, 0.0, 0.0, 0.0, 0.0, 0.0, 0.0, 0.0, 0.0,
 // 53-55 km/sec
 0.7, 2.0, 3.1, 6.1, 8.5, 0.0, 0.0, 0.0, 0.0,
 0.0, 0.0, 0.0, 0.0, 0.0, 0.0, 0.0, 0.0, 0.0,
 // 55-57 km/sec

1.3, 3.2, 4.9, 9.0, 11.1, 0.0, 0.0, 0.0, 0.0,
 0.0, 0.0, 0.0, 0.0, 0.0, 0.0, 0.0, 0.0, 0.0,
 // 57-59 km/sec
 2.4, 4.9, 7.3, 12.7, 12.0, 0.0, 0.0, 0.0, 0.0,
 0.0, 0.0, 0.0, 0.0, 0.0, 0.0, 0.0, 0.0, 0.0,
 // 59-61 km/sec
 4.2, 7.3, 10.2, 16.7, 0.0, 0.0, 0.0, 0.0, 0.0,
 0.0, 0.0, 0.0, 0.0, 0.0, 0.0, 0.0, 0.0, 0.0,
 // 61-63 km/sec
 6.8, 10.2, 13.7, 19.1, 0.0, 0.0, 0.0, 0.0, 0.0,
 0.0, 0.0, 0.0, 0.0, 0.0, 0.0, 0.0, 0.0, 0.0,
 // 63-65 km/sec
 10.4, 13.6, 17.2, 12.1, 0.0, 0.0, 0.0, 0.0, 0.0,
 0.0, 0.0, 0.0, 0.0, 0.0, 0.0, 0.0, 0.0, 0.0,
 // 65-67 km/sec
 14.8, 16.7, 19.4, 0.0, 0.0, 0.0, 0.0, 0.0, 0.0,
 0.0, 0.0, 0.0, 0.0, 0.0, 0.0, 0.0, 0.0, 0.0,
 // 67-69 km/sec
 19.0, 18.2, 17.2, 0.0, 0.0, 0.0, 0.0, 0.0, 0.0,
 0.0, 0.0, 0.0, 0.0, 0.0, 0.0, 0.0, 0.0, 0.0,
 // 69-71 km/sec
 20.9, 15.4, 0.0, 0.0, 0.0, 0.0, 0.0, 0.0, 0.0,
 0.0, 0.0, 0.0, 0.0, 0.0, 0.0, 0.0, 0.0, 0.0,
 // 71-73 km/sec
 16.4, 5.5, 0.0, 0.0, 0.0, 0.0, 0.0, 0.0, 0.0,
 0.0, 0.0, 0.0, 0.0, 0.0, 0.0, 0.0, 0.0, 0.0,
 // 73-75 km/sec
 2.3, 0.0, 0.0, 0.0, 0.0, 0.0, 0.0, 0.0, 0.0,
 0.0, 0.0, 0.0, 0.0, 0.0, 0.0, 0.0, 0.0, 0.0

9. APPENDIX C: M0FLUX.DAT INPUT FILE

This appendix contains the M0FLUX.DAT data file providing values for the sporadic meteor flux density distribution for meteors exceeding mass m_0 . These values should not be changed by the user.

// Monthly Sporadic Meteor Flux Density in Meteors / km² * hr * sr

//

// JANUARY

// 80-90 North Ecliptic Latitude

4.4, 4.4, 4.4, 4.4, 4.4, 4.4, 4.4, 4.4, 4.4, 4.4, 4.4, 4.4, 4.4,
4.4, 4.4, 4.4, 4.4, 4.4, 4.4, 4.4, 4.4, 4.4, 4.4, 4.4, 4.4, 4.4,
4.4, 4.4, 4.4, 4.4, 4.4, 4.4, 4.4, 4.4, 4.4, 4.4, 4.4, 4.4, 4.4,
4.4, 4.4, 4.4, 4.4, 4.4, 4.4, 4.4, 4.4, 4.4, 4.4, 4.4, 4.4, 4.4,

// 65-80 North Ecliptic Latitude

4.0, 1.8, 1.8, 1.8, 1.8, 1.8, 1.8, 1.8, 1.8, 3.0, 3.0, 3.0,
3.0, 3.0, 3.0, 3.0, 3.0, 2.9, 2.9, 2.9, 2.9, 2.9, 2.9, 2.9,
2.9, 2.7, 2.7, 2.7, 2.7, 2.7, 2.7, 2.7, 2.7, 1.3, 1.3, 1.3,
1.3, 1.3, 1.3, 1.3, 1.3, 4.0, 4.0, 4.0, 4.0, 4.0, 4.0, 4.0, 4.0,

// 50-65 North Ecliptic Latitude

2.4, 5.8, 5.8, 5.8, 5.8, 2.3, 2.3, 2.3, 2.3, 1.3, 1.3, 1.3,
1.3, 4.3, 4.3, 4.3, 4.3, 11.3, 11.3, 11.3, 11.3, 6.2, 6.2, 6.2,
6.2, 6.2, 6.2, 6.2, 6.2, 1.6, 1.6, 1.6, 1.6, 1.1, 1.1, 1.1,
1.1, 1.2, 1.2, 1.2, 1.2, 2.1, 2.1, 2.1, 2.1, 2.4, 2.4, 2.4,

// 35-50 North Ecliptic Latitude

2.1, 2.1, 2.1, 2.4, 2.4, 2.4, 1.9, 1.9, 1.9, 0.9, 0.9, 0.9,
0.7, 0.7, 0.7, 2.8, 2.8, 2.8, 13.3, 13.3, 13.3, 24.3, 24.3, 24.3,
18.6, 18.6, 18.6, 10.4, 10.4, 10.4, 3.3, 3.3, 3.3, 1.7, 1.7, 1.7,
0.4, 0.4, 0.4, 0.3, 0.3, 0.3, 0.2, 0.2, 0.2, 0.6, 0.6, 0.6,

// 20-35 North Ecliptic Latitude

0.3, 0.3, 0.3, 0.6, 0.6, 0.6, 1.2, 1.2, 1.2, 1.5, 1.5, 1.5,
2.0, 2.0, 2.0, 4.0, 4.0, 4.0, 19.9, 19.9, 19.9, 15.3, 15.3, 15.3,
31.7, 31.7, 31.7, 26.7, 26.7, 26.7, 6.5, 6.5, 6.5, 4.1, 4.1, 4.1,
0.9, 0.9, 0.9, 0.0, 0.0, 0.0, 0.1, 0.1, 0.1, 0.1, 0.1, 0.1,

// 0-20 North Ecliptic Latitude

0.0, 0.0, 0.0, 0.4, 0.4, 1.0, 1.0, 3.9, 3.9, 2.6, 2.6, 4.3,
4.3, 7.3, 7.3, 10.2, 10.2, 14.4, 14.4, 48.9, 48.9, 31.2, 31.2, 26.7,
26.7, 71.5, 71.5, 20.2, 20.2, 8.7, 8.7, 10.7, 10.7, 5.9, 5.9, 5.5,
5.5, 2.6, 2.6, 2.1, 2.1, 0.0, 0.0, 0.0, 0.0, 0.0, 0.0, 0.0,

// 0-20 South Ecliptic Latitude

0.0, 0.2, 0.2, 0.6, 0.6, 0.5, 0.5, 1.6, 1.6, 4.1, 4.1, 8.6,
8.6, 20.2, 20.2, 47.8, 47.8, 25.7, 25.7, 54.6, 54.6, 21.8, 21.8, 21.8,
21.8, 59.7, 59.7, 29.5, 29.5, 12.0, 12.0, 4.6, 4.6, 13.5, 13.5, 11.5,
11.5, 5.5, 5.5, 0.2, 0.2, 0.3, 0.3, 0.0, 0.0, 0.0, 0.0, 0.0,

// 20-35 South Ecliptic Latitude

0.0, 0.0, 0.0, 0.4, 0.4, 0.4, 0.3, 0.3, 0.3, 11.0, 11.0, 11.0,
 16.3, 16.3, 16.3, 31.0, 31.0, 31.0, 21.0, 21.0, 21.0, 20.9, 20.9, 20.9,
 17.9, 17.9, 17.9, 14.4, 14.4, 14.4, 59.9, 59.9, 59.9, 6.0, 6.0, 6.0,
 2.4, 2.4, 2.4, 1.6, 1.6, 1.6, 0.4, 0.4, 0.4, 0.2, 0.2, 0.2,
 // 35-50 South Ecliptic Latitude
 0.1, 0.1, 0.1, 0.0, 0.0, 0.0, 0.9, 0.9, 0.9, 2.7, 2.7, 2.7,
 1.8, 1.8, 1.8, 3.9, 3.9, 3.9, 16.2, 16.2, 16.2, 54.4, 54.4, 54.4,
 86.3, 86.3, 86.3, 51.0, 51.0, 51.0, 8.8, 8.8, 8.8, 5.1, 5.1, 5.1,
 0.2, 0.2, 0.2, 0.9, 0.9, 0.9, 0.2, 0.2, 0.2, 0.9, 0.9, 0.9,
 // 50-65 South Ecliptic Latitude
 0.3, 0.5, 0.5, 0.5, 0.5, 0.3, 0.3, 0.3, 0.3, 0.6, 0.6, 0.6,
 0.6, 3.1, 3.1, 3.1, 3.1, 9.9, 9.9, 9.9, 9.9, 24.4, 24.4, 24.4,
 24.4, 32.0, 32.0, 32.0, 32.0, 66.4, 66.4, 66.4, 66.4, 2.2, 2.2, 2.2,
 2.2, 0.4, 0.4, 0.4, 0.4, 4.2, 4.2, 4.2, 4.2, 0.3, 0.3, 0.3,
 // 65-80 South Ecliptic Latitude
 2.0, 1.6, 1.6, 1.6, 1.6, 1.6, 1.6, 1.6, 1.6, 0.7, 0.7, 0.7,
 0.7, 0.7, 0.7, 0.7, 0.7, 3.4, 3.4, 3.4, 3.4, 3.4, 3.4, 3.4,
 3.4, 7.0, 7.0, 7.0, 7.0, 7.0, 7.0, 7.0, 7.0, 2.9, 2.9, 2.9,
 2.9, 2.9, 2.9, 2.9, 2.9, 2.0, 2.0, 2.0, 2.0, 2.0, 2.0,
 // 80-90 South Ecliptic Latitude
 3.5, 3.5, 3.5, 3.5, 3.5, 3.5, 3.5, 3.5, 3.5, 3.5, 3.5, 3.5,
 3.5, 3.5, 3.5, 3.5, 3.5, 3.5, 3.5, 3.5, 3.5, 3.5, 3.5, 3.5,
 3.5, 3.5, 3.5, 3.5, 3.5, 3.5, 3.5, 3.5, 3.5, 3.5, 3.5, 3.5,
 3.5, 3.5, 3.5, 3.5, 3.5, 3.5, 3.5, 3.5, 3.5, 3.5, 3.5, 3.5,
 // FEBRUARY
 // 80-90 North Ecliptic Latitude
 2.2, 2.2, 2.2, 2.2, 2.2, 2.2, 2.2, 2.2, 2.2, 2.2, 2.2, 2.2,
 2.2, 2.2, 2.2, 2.2, 2.2, 2.2, 2.2, 2.2, 2.2, 2.2, 2.2, 2.2,
 2.2, 2.2, 2.2, 2.2, 2.2, 2.2, 2.2, 2.2, 2.2, 2.2, 2.2, 2.2,
 2.2, 2.2, 2.2, 2.2, 2.2, 2.2, 2.2, 2.2, 2.2, 2.2, 2.2, 2.2,
 // 65-80 North Ecliptic Latitude
 1.6, 1.6, 1.6, 2.2, 2.2, 2.2, 2.2, 2.2, 2.2, 2.2, 2.2, 3.8,
 3.8, 3.8, 3.8, 3.8, 3.8, 3.8, 2.9, 2.9, 2.9, 2.9, 2.9,
 2.9, 2.9, 2.9, 2.0, 2.0, 2.0, 2.0, 2.0, 2.0, 2.0, 2.0, 2.6,
 2.6, 2.6, 2.6, 2.6, 2.6, 2.6, 1.6, 1.6, 1.6, 1.6, 1.6,
 // 50-65 North Ecliptic Latitude
 1.3, 1.3, 1.3, 1.4, 1.4, 1.4, 1.4, 1.1, 1.1, 1.1, 1.1, 2.9,
 2.9, 2.9, 2.9, 6.0, 6.0, 6.0, 6.0, 6.0, 6.0, 6.0, 6.0, 5.8,
 5.8, 5.8, 5.8, 2.4, 2.4, 2.4, 2.4, 0.9, 0.9, 0.9, 0.9, 0.8,
 0.8, 0.8, 0.8, 1.2, 1.2, 1.2, 1.2, 1.2, 1.2, 1.2, 1.2, 1.3,
 // 35-50 North Ecliptic Latitude
 1.2, 1.2, 1.2, 0.5, 0.5, 0.5, 1.0, 1.0, 1.0, 1.0, 1.0, 1.0,
 2.5, 2.5, 2.5, 10.2, 10.2, 10.2, 17.1, 17.1, 17.1, 20.9, 20.9, 20.9,
 9.3, 9.3, 9.3, 4.8, 4.8, 4.8, 0.4, 0.4, 0.4, 0.4, 0.4, 0.4,

0.2, 0.2, 0.2, 1.3, 1.3, 1.3, 1.2, 1.2, 1.2, 1.2, 1.2, 1.2,
 // 20-35 North Ecliptic Latitude
 1.0, 1.0, 1.0, 1.1, 1.1, 1.1, 1.2, 1.2, 1.2, 2.1, 2.1, 2.1,
 3.7, 3.7, 3.7, 12.7, 12.7, 12.7, 10.9, 10.9, 10.9, 33.9, 33.9, 33.9,
 14.4, 14.4, 14.4, 9.9, 9.9, 9.9, 5.5, 5.5, 5.5, 3.1, 3.1, 3.1,
 0.5, 0.5, 0.5, 0.2, 0.2, 0.2, 0.2, 0.2, 0.2, 0.3, 0.3, 0.3,
 // 0-20 North Ecliptic Latitude
 0.7, 0.3, 0.3, 0.5, 0.5, 1.4, 1.4, 1.4, 1.4, 3.2, 3.2, 5.9,
 5.9, 7.8, 7.8, 25.3, 25.3, 19.7, 19.7, 15.5, 15.5, 25.6, 25.6, 32.5,
 32.5, 7.1, 7.1, 6.7, 6.7, 13.6, 13.6, 6.8, 6.8, 3.7, 3.7, 0.9,
 0.9, 0.2, 0.2, 0.2, 0.2, 0.1, 0.1, 0.1, 0.1, 0.7, 0.7, 0.7,
 // 0-20 South Ecliptic Latitude
 0.3, 0.3, 0.3, 0.6, 0.6, 0.1, 0.1, 6.9, 6.9, 14.6, 14.6, 8.0,
 8.0, 22.6, 22.6, 14.0, 14.0, 8.5, 8.5, 18.7, 18.7, 33.8, 33.8, 7.3,
 7.3, 1.9, 1.9, 2.7, 2.7, 10.4, 10.4, 2.2, 2.2, 3.3, 3.3, 0.9,
 0.9, 0.0, 0.0, 0.1, 0.1, 0.1, 0.1, 0.2, 0.2, 0.3, 0.3, 0.3,
 // 20-35 South Ecliptic Latitude
 0.1, 0.1, 0.1, 0.3, 0.3, 0.3, 3.9, 3.9, 3.9, 8.8, 8.8, 8.8,
 5.2, 5.2, 5.2, 5.1, 5.1, 5.1, 10.9, 10.9, 10.9, 16.6, 16.6, 16.6,
 91.5, 91.5, 91.5, 0.9, 0.9, 0.9, 3.3, 3.3, 3.3, 0.4, 0.4, 0.4,
 0.1, 0.1, 0.1, 0.0, 0.0, 0.0, 0.0, 0.0, 0.0, 0.1, 0.1, 0.1,
 // 35-50 South Ecliptic Latitude
 0.0, 0.0, 0.0, 0.0, 0.0, 0.0, 0.0, 0.0, 0.0, 0.0, 0.0, 0.0,
 0.2, 0.2, 0.2, 3.3, 3.3, 3.3, 27.7, 27.7, 27.7, 53.8, 53.8, 53.8,
 22.2, 22.2, 22.2, 3.2, 3.2, 3.2, 0.0, 0.0, 0.0, 0.1, 0.1, 0.1,
 0.0, 0.0, 0.0, 0.0, 0.0, 0.0, 0.0, 0.0, 0.0, 0.0, 0.0, 0.0,
 // 50-65 South Ecliptic Latitude
 0.0, 0.0, 0.0, 0.0, 0.0, 0.0, 0.0, 0.0, 0.0, 0.0, 0.0, 0.8,
 0.8, 0.8, 0.7, 0.7, 0.7, 0.7, 2.3, 2.3, 2.3, 2.3, 35.4,
 35.4, 35.4, 50.0, 50.0, 50.0, 50.0, 0.0, 0.0, 0.0, 0.0, 0.0,
 0.0, 0.0, 0.0, 0.1, 0.1, 0.1, 0.1, 0.0, 0.0, 0.0, 0.0, 0.0,
 // 65-80 South Ecliptic Latitude
 0.0, 0.0, 0.0, 0.0, 0.0, 0.0, 0.0, 0.0, 0.0, 0.0, 0.0, 0.0,
 0.0, 0.0, 0.0, 0.0, 0.0, 0.0, 0.0, 0.3, 0.3, 0.3, 0.3, 0.3,
 0.3, 0.3, 0.3, 0.0, 0.0, 0.0, 0.0, 0.0, 0.0, 0.0, 0.0, 0.0,
 0.0, 0.0, 0.0, 0.0, 0.0, 0.0, 0.0, 0.0, 0.0, 0.0, 0.0, 0.0,
 // 80-90 South Ecliptic Latitude
 0.0, 0.0, 0.0, 0.0, 0.0, 0.0, 0.0, 0.0, 0.0, 0.0, 0.0, 0.0,
 0.0, 0.0, 0.0, 0.0, 0.0, 0.0, 0.0, 0.0, 0.0, 0.0, 0.0, 0.0,
 0.0, 0.0, 0.0, 0.0, 0.0, 0.0, 0.0, 0.0, 0.0, 0.0, 0.0, 0.0,
 0.0, 0.0, 0.0, 0.0, 0.0, 0.0, 0.0, 0.0, 0.0, 0.0, 0.0, 0.0,
 // MARCH
 // 80-90 North Ecliptic Latitude
 1.6, 1.6, 1.6, 1.6, 1.6, 1.6, 1.6, 1.6, 1.6, 1.6, 1.6, 1.6,

1.6, 1.6, 1.6, 1.6, 1.6, 1.6, 1.6, 1.6, 1.6, 1.6, 1.6, 1.6,
 1.6, 1.6, 1.6, 1.6, 1.6, 1.6, 1.6, 1.6, 1.6, 1.6, 1.6, 1.6,
 1.6, 1.6, 1.6, 1.6, 1.6, 1.6, 1.6, 1.6, 1.6, 1.6, 1.6, 1.6,
 // 65-80 North Ecliptic Latitude
 1.6, 1.6, 1.6, 1.6, 1.6, 1.6, 1.6, 2.2, 2.2, 2.2, 2.2, 2.2,
 2.2, 2.2, 2.2, 7.8, 7.8, 7.8, 7.8, 7.8, 7.8, 7.8, 7.8, 4.7,
 4.7, 4.7, 4.7, 4.7, 4.7, 4.7, 4.7, 0.3, 0.3, 0.3, 0.3, 0.3,
 0.3, 0.3, 0.3, 1.0, 1.0, 1.0, 1.0, 1.0, 1.0, 1.0, 1.0, 1.6,
 // 50-65 North Ecliptic Latitude
 0.5, 0.5, 0.5, 2.8, 2.8, 2.8, 2.8, 2.2, 2.2, 2.2, 2.2, 4.5,
 4.5, 4.5, 4.5, 7.8, 7.8, 7.8, 7.8, 12.4, 12.4, 12.4, 12.4, 18.4,
 18.4, 18.4, 18.4, 3.9, 3.9, 3.9, 3.9, 1.4, 1.4, 1.4, 1.4, 0.3,
 0.3, 0.3, 0.3, 0.5, 0.5, 0.5, 0.5, 1.3, 1.3, 1.3, 1.3, 0.5,
 // 35-50 North Ecliptic Latitude
 2.4, 2.4, 1.9, 1.9, 1.9, 1.4, 1.4, 1.4, 1.0, 1.0, 1.0, 3.0,
 3.0, 3.0, 5.1, 5.1, 5.1, 21.2, 21.2, 21.2, 24.3, 24.3, 24.3, 23.6,
 23.6, 23.6, 13.3, 13.3, 13.3, 6.7, 6.7, 6.7, 1.6, 1.6, 1.6, 2.4,
 2.4, 2.4, 1.4, 1.4, 1.4, 0.8, 0.8, 0.8, 5.6, 5.6, 5.6, 2.4,
 // 20-35 North Ecliptic Latitude
 2.0, 2.0, 1.0, 1.0, 1.0, 0.5, 0.5, 0.5, 1.6, 1.6, 1.6, 2.5,
 2.5, 2.5, 3.5, 3.5, 3.5, 5.1, 5.1, 5.1, 7.6, 7.6, 7.6, 23.5,
 23.5, 23.5, 10.3, 10.3, 10.3, 15.1, 15.1, 15.1, 5.1, 5.1, 5.1, 1.7,
 1.7, 1.7, 1.8, 1.8, 1.8, 0.6, 0.6, 0.6, 2.2, 2.2, 2.2, 2.2,
 // 0-20 North Ecliptic Latitude
 0.3, 0.3, 0.3, 0.1, 0.1, 0.1, 0.1, 0.5, 0.5, 1.6, 1.6, 5.0,
 5.0, 6.1, 6.1, 9.0, 9.0, 18.8, 18.8, 11.7, 11.7, 5.1, 5.1, 10.5,
 10.5, 38.1, 38.1, 24.3, 24.3, 21.5, 21.5, 20.9, 20.9, 10.2, 10.2, 6.6,
 6.6, 13.6, 13.6, 0.2, 0.2, 0.1, 0.1, 0.1, 0.1, 0.3, 0.3, 0.3,
 // 0-20 South Ecliptic Latitude
 0.1, 0.2, 0.2, 0.0, 0.0, 0.0, 0.0, 0.5, 0.5, 5.5, 5.5, 8.4,
 8.4, 22.2, 22.2, 21.0, 21.0, 42.1, 42.1, 53.0, 53.0, 27.3, 27.3, 70.0,
 70.0, 13.5, 13.5, 3.6, 3.6, 4.9, 4.9, 9.6, 9.6, 2.7, 2.7, 2.6,
 2.6, 0.2, 0.2, 0.0, 0.0, 0.0, 0.0, 0.0, 0.0, 0.3, 0.3, 0.1,
 // 20-35 South Ecliptic Latitude
 0.0, 0.0, 0.0, 0.0, 0.0, 0.0, 0.0, 0.0, 1.4, 1.4, 1.4, 14.1,
 14.1, 14.1, 15.9, 15.9, 15.9, 61.3, 61.3, 61.3, 72.1, 72.1, 72.1, 5.5,
 5.5, 5.5, 4.4, 4.4, 4.4, 8.1, 8.1, 8.1, 8.0, 8.0, 8.0, 0.4,
 0.4, 0.4, 0.0, 0.0, 0.0, 0.0, 0.0, 0.0, 0.0, 0.0, 0.0, 0.0,
 // 35-50 South Ecliptic Latitude
 0.0, 0.0, 0.0, 0.0, 0.0, 0.0, 0.0, 0.0, 0.0, 0.0, 0.0, 0.0,
 0.0, 0.0, 6.1, 6.1, 6.1, 64.5, 64.5, 64.5, 10.8, 10.8, 10.8, 11.6,
 11.6, 11.6, 6.2, 6.2, 6.2, 1.2, 1.2, 1.2, 0.8, 0.8, 0.8, 1.6,
 1.6, 1.6, 0.1, 0.1, 0.1, 0.7, 0.7, 0.7, 0.1, 0.1, 0.1, 0.0,
 // 50-65 South Ecliptic Latitude

1.8, 1.8, 1.8, 0.1, 0.1, 0.1, 0.2, 0.2, 0.2, 0.2, 4.0,
 4.0, 4.0, 4.0, 6.3, 6.3, 6.3, 6.3, 21.4, 21.4, 21.4, 21.4, 0.0,
 0.0, 0.0, 0.0, 1.6, 1.6, 1.6, 1.6, 0.2, 0.2, 0.2, 0.2, 0.9,
 0.9, 0.9, 0.9, 0.6, 0.6, 0.6, 0.6, 1.3, 1.3, 1.3, 1.3, 1.8,
 // 65-80 South Ecliptic Latitude
 1.0, 1.0, 1.0, 1.0, 1.0, 1.0, 1.0, 1.0, 12.1, 12.1, 12.1, 12.1,
 12.1, 12.1, 12.1, 12.1, 5.0, 5.0, 5.0, 5.0, 5.0, 5.0, 5.0, 22.6,
 22.6, 22.6, 22.6, 22.6, 22.6, 22.6, 22.6, 3.8, 3.8, 3.8, 3.8, 3.8,
 3.8, 3.8, 3.8, 3.8, 8.3, 8.3, 8.3, 8.3, 8.3, 8.3, 8.3, 8.3,
 // 80-90 South Ecliptic Latitude
 1.1, 1.1, 1.1, 1.1, 1.1, 1.1, 1.1, 1.1, 1.1, 1.1, 1.1, 1.1,
 1.1, 1.1, 1.1, 1.1, 1.1, 1.1, 1.1, 1.1, 1.1, 1.1, 1.1, 1.1,
 1.1, 1.1, 1.1, 1.1, 1.1, 1.1, 1.1, 1.1, 1.1, 1.1, 1.1, 1.1,
 1.1, 1.1, 1.1, 1.1, 1.1, 1.1, 1.1, 1.1, 1.1, 1.1, 1.1, 1.1,
 // APRIL
 // 80-90 North Ecliptic Latitude
 0.6, 0.6, 0.6, 0.6, 0.6, 0.6, 0.6, 0.6, 0.6, 0.6, 0.6, 0.6,
 0.6, 0.6, 0.6, 0.6, 0.6, 0.6, 0.6, 0.6, 0.6, 0.6, 0.6, 0.6,
 0.6, 0.6, 0.6, 0.6, 0.6, 0.6, 0.6, 0.6, 0.6, 0.6, 0.6, 0.6,
 0.6, 0.6, 0.6, 0.6, 0.6, 0.6, 0.6, 0.6, 0.6, 0.6, 0.6, 0.6,
 // 65-80 North Ecliptic Latitude
 1.2, 1.2, 1.2, 1.2, 1.2, 1.7, 1.7, 1.7, 1.7, 1.7, 1.7, 1.7,
 1.7, 2.2, 2.2, 2.2, 2.2, 2.2, 2.2, 2.2, 2.2, 2.1, 2.1, 2.1,
 2.1, 2.1, 2.1, 2.1, 2.1, 0.4, 0.4, 0.4, 0.4, 0.4, 0.4, 0.4,
 0.4, 1.6, 1.6, 1.6, 1.6, 1.6, 1.6, 1.6, 1.6, 1.2, 1.2, 1.2,
 // 50-65 North Ecliptic Latitude
 1.1, 0.6, 0.6, 0.6, 0.6, 0.8, 0.8, 0.8, 0.8, 1.3, 1.3, 1.3,
 1.3, 3.5, 3.5, 3.5, 3.5, 8.3, 8.3, 8.3, 8.3, 18.3, 18.3, 18.3,
 18.3, 6.5, 6.5, 6.5, 6.5, 2.9, 2.9, 2.9, 2.9, 1.3, 1.3, 1.3,
 1.3, 0.8, 0.8, 0.8, 0.8, 1.6, 1.6, 1.6, 1.6, 1.1, 1.1, 1.1,
 // 35-50 North Ecliptic Latitude
 1.5, 1.5, 1.5, 1.9, 1.9, 1.9, 1.0, 1.0, 1.0, 20.1, 20.1, 20.1,
 7.5, 7.5, 7.5, 9.6, 9.6, 9.6, 32.9, 32.9, 32.9, 29.1, 29.1, 29.1,
 21.6, 21.6, 21.6, 8.4, 8.4, 8.4, 3.2, 3.2, 3.2, 3.2, 3.2, 3.2,
 2.2, 2.2, 2.2, 2.8, 2.8, 2.8, 3.2, 3.2, 3.2, 0.8, 0.8, 0.8,
 // 20-35 North Ecliptic Latitude
 1.5, 1.5, 1.5, 0.8, 0.8, 0.8, 1.4, 1.4, 1.4, 20.1, 20.1, 20.1,
 3.5, 3.5, 3.5, 5.5, 5.5, 5.5, 9.0, 9.0, 9.0, 34.3, 34.3, 34.3,
 21.3, 21.3, 21.3, 24.7, 24.7, 24.7, 16.8, 16.8, 16.8, 4.1, 4.1, 4.1,
 1.4, 1.4, 1.4, 0.6, 0.6, 0.6, 0.6, 0.6, 0.6, 0.5, 0.5, 0.5,
 // 0-20 North Ecliptic Latitude
 0.1, 0.1, 0.1, 0.3, 0.3, 0.5, 0.5, 1.4, 1.4, 3.5, 3.5, 6.3,
 6.3, 13.7, 13.7, 14.8, 14.8, 28.8, 28.8, 11.7, 11.7, 15.6, 15.6, 31.0,
 31.0, 16.8, 16.8, 20.2, 20.2, 23.8, 23.8, 14.0, 14.0, 8.8, 8.8, 2.4,

2.4, 0.0, 0.0, 0.0, 0.0, 0.1, 0.1, 0.0, 0.0, 0.0, 0.0, 0.1,
 // 0-20 South Ecliptic Latitude
 0.0, 0.0, 0.0, 0.2, 0.2, 1.2, 1.2, 4.0, 4.0, 8.1, 8.1, 12.9,
 12.9, 15.7, 15.7, 38.9, 38.9, 42.8, 42.8, 25.1, 25.1, 42.4, 42.4, 13.6,
 13.6, 13.8, 13.8, 1.9, 1.9, 11.9, 11.9, 19.6, 19.6, 8.2, 8.2, 4.4,
 4.4, 0.3, 0.3, 0.0, 0.0, 0.0, 0.0, 0.0, 0.0, 0.0, 0.0, 0.0,
 // 20-35 South Ecliptic Latitude
 0.0, 0.0, 0.0, 0.3, 0.3, 0.3, 3.8, 3.8, 3.8, 1.8, 1.8, 1.8,
 4.7, 4.7, 4.7, 36.2, 36.2, 36.2, 38.6, 38.6, 38.6, 77.0, 77.0, 77.0,
 22.3, 22.3, 22.3, 2.2, 2.2, 2.2, 3.7, 3.7, 3.7, 10.1, 10.1, 10.1,
 0.6, 0.6, 0.6, 0.0, 0.0, 0.0, 0.0, 0.0, 0.0, 0.0, 0.0, 0.0,
 // 35-50 South Ecliptic Latitude
 0.0, 0.0, 0.0, 0.0, 0.0, 0.0, 0.1, 0.1, 0.1, 0.0, 0.0, 0.0,
 1.4, 1.4, 1.4, 31.3, 31.3, 31.3, 38.3, 38.3, 38.3, 11.8, 11.8, 11.8,
 5.8, 5.8, 5.8, 0.3, 0.3, 0.3, 1.4, 1.4, 1.4, 5.3, 5.3, 5.3,
 0.2, 0.2, 0.2, 0.0, 0.0, 0.0, 0.0, 0.0, 0.0, 0.0, 0.0, 0.0,
 // 50-65 South Ecliptic Latitude
 0.0, 0.7, 0.7, 0.7, 0.7, 0.1, 0.1, 0.1, 0.1, 0.0, 0.0, 0.0,
 0.0, 1.4, 1.4, 1.4, 1.4, 122.7, 122.7, 122.7, 122.7, 123.8, 123.8, 123.8,
 123.8, 1.4, 1.4, 1.4, 1.4, 0.4, 0.4, 0.4, 0.4, 0.9, 0.9, 0.9,
 0.9, 0.2, 0.2, 0.2, 0.2, 1.4, 1.4, 1.4, 1.4, 0.0, 0.0, 0.0,
 // 65-80 South Ecliptic Latitude
 0.6, 0.6, 0.6, 0.6, 0.6, 0.8, 0.8, 0.8, 0.8, 0.8, 0.8, 0.8,
 0.8, 0.0, 0.0, 0.0, 0.0, 0.0, 0.0, 0.0, 0.0, 6.3, 6.3, 6.3,
 6.3, 6.3, 6.3, 6.3, 6.3, 3.0, 3.0, 3.0, 3.0, 3.0, 3.0, 3.0,
 3.0, 3.1, 3.1, 3.1, 3.1, 3.1, 3.1, 3.1, 3.1, 0.6, 0.6, 0.6,
 // 80-90 South Ecliptic Latitude
 0.0, 0.0, 0.0, 0.0, 0.0, 0.0, 0.0, 0.0, 0.0, 0.0, 0.0, 0.0,
 0.0, 0.0, 0.0, 0.0, 0.0, 0.0, 0.0, 0.0, 0.0, 0.0, 0.0, 0.0,
 0.0, 0.0, 0.0, 0.0, 0.0, 0.0, 0.0, 0.0, 0.0, 0.0, 0.0, 0.0,
 0.0, 0.0, 0.0, 0.0, 0.0, 0.0, 0.0, 0.0, 0.0, 0.0, 0.0, 0.0,
 // MAY
 // 80-90 North Ecliptic Latitude
 1.07, 1.07, 1.07, 1.07, 1.07, 1.07, 1.07, 1.07, 1.07, 1.07, 1.07, 1.07,
 1.07, 1.07, 1.07, 1.07, 1.07, 1.07, 1.07, 1.07, 1.07, 1.07, 1.07, 1.07,
 1.07, 1.07, 1.07, 1.07, 1.07, 1.07, 1.07, 1.07, 1.07, 1.07, 1.07, 1.07,
 1.07, 1.07, 1.07, 1.07, 1.07, 1.07, 1.07, 1.07, 1.07, 1.07, 1.07, 1.07,
 // 65-80 North Ecliptic Latitude
 2.2, 2.2, 2.2, 2.2, 2.2, 2.0, 2.0, 2.0, 2.0, 2.0, 2.0, 2.0,
 2.0, 4.1, 4.1, 4.1, 4.1, 4.1, 4.1, 4.1, 4.1, 2.4, 2.4, 2.4,
 2.4, 2.4, 2.4, 2.4, 2.4, 1.5, 1.5, 1.5, 1.5, 1.5, 1.5, 1.5,
 1.5, 1.6, 1.6, 1.6, 1.6, 1.6, 1.6, 1.6, 1.6, 2.2, 2.2, 2.2,
 // 50-65 North Ecliptic Latitude
 2.6, 2.8, 2.8, 2.8, 2.8, 1.0, 1.0, 1.0, 1.0, 4.3, 4.3, 4.3,

4.3, 6.9, 6.9, 6.9, 6.9, 10.1, 10.1, 10.1, 10.1, 6.7, 6.7, 6.7,
 6.7, 4.8, 4.8, 4.8, 4.8, 3.9, 3.9, 3.9, 3.9, 0.9, 0.9, 0.9,
 0.9, 2.6, 2.6, 2.6, 2.6, 0.9, 0.9, 0.9, 0.9, 2.6, 2.6, 2.6,
 // 35-50 North Ecliptic Latitude
 2.1, 2.1, 1.1, 1.1, 1.1, 0.7, 0.7, 0.7, 1.7, 1.7, 1.7, 9.0,
 9.0, 9.0, 11.1, 11.1, 11.1, 18.8, 18.8, 18.8, 24.0, 24.0, 24.0, 30.1,
 30.1, 30.1, 16.1, 16.1, 16.1, 8.1, 8.1, 8.1, 3.3, 3.3, 3.3, 2.2,
 2.2, 2.2, 3.7, 3.7, 3.7, 6.6, 6.6, 6.6, 5.6, 5.6, 5.6, 2.1,
 // 20-35 North Ecliptic Latitude
 0.3, 0.3, 0.1, 0.1, 0.1, 0.5, 0.5, 0.5, 2.6, 2.6, 2.6, 6.3,
 6.3, 6.3, 28.1, 28.1, 28.1, 52.1, 52.1, 52.1, 36.6, 36.6, 36.6, 35.4,
 35.4, 35.4, 27.0, 27.0, 27.0, 18.3, 18.3, 18.3, 3.5, 3.5, 3.5, 3.1,
 3.1, 3.1, 3.3, 3.3, 3.3, 1.8, 1.8, 1.8, 1.5, 1.5, 1.5, 0.3,
 // 0-20 North Ecliptic Latitude
 0.0, 0.0, 0.0, 0.1, 0.1, 0.2, 0.2, 0.9, 0.9, 10.8, 10.8, 19.8,
 19.8, 39.8, 39.8, 23.8, 23.8, 27.8, 27.8, 48.5, 48.5, 51.4, 51.4, 47.1,
 47.1, 57.9, 57.9, 35.5, 35.5, 59.4, 59.4, 23.5, 23.5, 7.1, 7.1, 7.3,
 7.3, 1.4, 1.4, 0.8, 0.8, 0.3, 0.3, 0.2, 0.2, 0.1, 0.1, 0.0,
 // 0-20 South Ecliptic Latitude
 0.0, 0.0, 0.0, 0.0, 0.0, 0.0, 0.0, 2.6, 2.6, 7.3, 7.3, 6.2,
 6.2, 17.3, 17.3, 23.2, 23.2, 22.6, 22.6, 29.9, 29.9, 21.7, 21.7, 18.9,
 18.9, 14.2, 14.2, 45.3, 45.3, 45.0, 45.0, 34.6, 34.6, 15.0, 15.0, 6.4,
 6.4, 1.4, 1.4, 0.8, 0.8, 0.1, 0.1, 0.3, 0.3, 0.0, 0.0, 0.0,
 // 20-35 South Ecliptic Latitude
 0.0, 0.0, 0.0, 0.0, 0.0, 0.2, 0.2, 0.2, 2.0, 2.0, 2.0, 13.9,
 13.9, 13.9, 27.2, 27.2, 27.2, 23.2, 23.2, 23.2, 55.5, 55.5, 55.5, 39.5,
 39.5, 39.5, 11.7, 11.7, 11.7, 11.9, 11.9, 11.9, 11.2, 11.2, 11.2, 2.7,
 2.7, 2.7, 0.2, 0.2, 0.2, 0.0, 0.0, 0.0, 0.0, 0.0, 0.0, 0.0,
 // 35-50 South Ecliptic Latitude
 0.1, 0.1, 0.0, 0.0, 0.0, 0.1, 0.1, 0.1, 0.1, 0.1, 0.1, 1.5,
 1.5, 1.5, 13.1, 13.1, 13.1, 40.9, 40.9, 40.9, 25.7, 25.7, 25.7, 9.3,
 9.3, 9.3, 4.9, 4.9, 4.9, 1.4, 1.4, 1.4, 0.7, 0.7, 0.7, 2.2,
 2.2, 2.2, 0.5, 0.5, 0.5, 0.1, 0.1, 0.1, 0.0, 0.0, 0.0, 0.1,
 // 50-65 South Ecliptic Latitude
 0.5, 1.3, 1.3, 1.3, 1.3, 0.7, 0.7, 0.7, 0.7, 2.8, 2.8, 2.8,
 2.8, 0.9, 0.9, 0.9, 0.9, 23.8, 23.8, 23.8, 23.8, 0.7, 0.7, 0.7,
 0.7, 1.6, 1.6, 1.6, 1.6, 0.8, 0.8, 0.8, 0.8, 0.7, 0.7, 0.7,
 0.7, 0.6, 0.6, 0.6, 0.6, 0.6, 0.6, 0.6, 0.6, 0.5, 0.5, 0.5,
 // 65-80 South Ecliptic Latitude
 1.8, 1.8, 1.8, 1.8, 1.8, 0.0, 0.0, 0.0, 0.0, 0.0, 0.0, 0.0,
 0.0, 0.2, 0.2, 0.2, 0.2, 0.2, 0.2, 0.2, 0.2, 0.8, 0.8, 0.8,
 0.8, 0.8, 0.8, 0.8, 0.8, 0.0, 0.0, 0.0, 0.0, 0.0, 0.0, 0.0,
 0.0, 1.4, 1.4, 1.4, 1.4, 1.4, 1.4, 1.4, 1.4, 1.8, 1.8, 1.8,
 // 80-90 South Ecliptic Latitude

5.5, 5.5, 5.5, 5.5, 5.5, 5.5, 5.5, 5.5, 5.5, 5.5, 5.5, 5.5,
5.5, 5.5, 5.5, 5.5, 5.5, 5.5, 5.5, 5.5, 5.5, 5.5, 5.5, 5.5,
5.5, 5.5, 5.5, 5.5, 5.5, 5.5, 5.5, 5.5, 5.5, 5.5, 5.5, 5.5,
5.5, 5.5, 5.5, 5.5, 5.5, 5.5, 5.5, 5.5, 5.5, 5.5, 5.5, 5.5,

// JUNE

// 80-90 North Ecliptic Latitude

0.3, 0.3, 0.3, 0.3, 0.3, 0.3, 0.3, 0.3, 0.3, 0.3, 0.3, 0.3,
0.3, 0.3, 0.3, 0.3, 0.3, 0.3, 0.3, 0.3, 0.3, 0.3, 0.3, 0.3,
0.3, 0.3, 0.3, 0.3, 0.3, 0.3, 0.3, 0.3, 0.3, 0.3, 0.3, 0.3,
0.3, 0.3, 0.3, 0.3, 0.3, 0.3, 0.3, 0.3, 0.3, 0.3, 0.3, 0.3,

// 65-80 North Ecliptic Latitude

3.3, 3.3, 3.3, 3.3, 3.3, 4.8, 4.8, 4.8, 4.8, 4.8, 4.8, 4.8,
4.8, 4.3, 4.3, 4.3, 4.3, 4.3, 4.3, 4.3, 4.3, 3.1, 3.1, 3.1,
3.1, 3.1, 3.1, 3.1, 3.1, 2.2, 2.2, 2.2, 2.2, 2.2, 2.2, 2.2,
2.2, 2.4, 2.4, 2.4, 2.4, 2.4, 2.4, 2.4, 2.4, 3.3, 3.3, 3.3,

// 50-65 North Ecliptic Latitude

1.9, 1.9, 1.9, 1.9, 1.9, 2.9, 2.9, 2.9, 2.9, 5.0, 5.0, 5.0,
5.0, 4.9, 4.9, 4.9, 4.9, 5.3, 5.3, 5.3, 5.3, 10.2, 10.2, 10.2,
10.2, 9.6, 9.6, 9.6, 9.6, 1.2, 1.2, 1.2, 1.2, 2.7, 2.7, 2.7,
2.7, 2.0, 2.0, 2.0, 2.0, 4.9, 4.9, 4.9, 4.9, 1.9, 1.9, 1.9,

// 35-50 North Ecliptic Latitude

0.6, 0.5, 0.5, 0.5, 0.7, 0.7, 0.7, 1.0, 1.0, 1.0, 2.7, 2.7,
2.7, 6.9, 6.9, 6.9, 23.2, 23.2, 23.2, 13.7, 13.7, 13.7, 16.4, 16.4,
16.4, 19.5, 19.5, 19.5, 4.4, 4.4, 4.4, 2.2, 2.2, 2.2, 2.2, 2.2,
2.2, 6.5, 6.5, 6.5, 3.5, 3.5, 3.5, 0.8, 0.8, 0.8, 0.6, 0.6,

// 20-35 North Ecliptic Latitude

0.2, 0.2, 0.2, 0.2, 0.4, 0.4, 0.4, 0.6, 0.6, 0.6, 7.5, 7.5,
7.5, 17.5, 17.5, 17.5, 24.0, 24.0, 24.0, 11.3, 11.3, 11.3, 26.7, 26.7,
26.7, 30.8, 30.8, 30.8, 16.0, 16.0, 16.0, 11.2, 11.2, 11.2, 4.8, 4.8,
4.8, 4.1, 4.1, 4.1, 0.8, 0.8, 0.8, 0.3, 0.3, 0.3, 0.2, 0.2,

// 0-20 North Ecliptic Latitude

0.0, 0.1, 0.1, 0.0, 0.0, 0.3, 0.3, 5.4, 5.4, 4.6, 4.6, 13.6,
13.6, 27.2, 27.2, 33.6, 33.6, 36.6, 36.6, 31.5, 31.5, 12.0, 12.0, 16.1,
16.1, 28.7, 28.7, 36.0, 36.0, 45.0, 45.0, 31.1, 31.1, 7.2, 7.2, 4.2,
4.2, 2.6, 2.6, 0.8, 0.8, 0.4, 0.4, 0.1, 0.1, 0.1, 0.1, 0.0,

// 0-20 South Ecliptic Latitude

0.0, 0.0, 0.0, 0.1, 0.1, 0.6, 0.6, 2.2, 2.2, 4.1, 4.1, 17.5,
17.5, 12.6, 12.6, 38.3, 38.3, 28.4, 28.4, 12.8, 12.8, 19.2, 19.2, 21.5,
21.5, 20.7, 20.7, 64.1, 64.1, 60.8, 60.8, 33.4, 33.4, 14.7, 14.7, 6.4,
6.4, 3.3, 3.3, 0.5, 0.5, 0.1, 0.1, 0.0, 0.0, 0.0, 0.0, 0.0,

// 20-35 South Ecliptic Latitude

0.2, 0.3, 0.3, 0.3, 0.6, 0.6, 0.6, 3.7, 3.7, 3.7, 10.4, 10.4,
10.4, 19.8, 19.8, 19.8, 21.5, 21.5, 21.5, 31.9, 31.9, 31.9, 12.0, 12.0,
12.0, 15.3, 15.3, 15.3, 12.5, 12.5, 12.5, 8.4, 8.4, 8.4, 5.5, 5.5,

5.5, 1.2, 1.2, 1.2, 0.4, 0.4, 0.4, 0.2, 0.2, 0.2, 0.2, 0.2,
 // 35-50 South Ecliptic Latitude
 0.3, 0.0, 0.0, 0.0, 0.6, 0.6, 0.6, 1.6, 1.6, 1.6, 4.4, 4.4,
 4.4, 26.5, 26.5, 26.5, 17.9, 17.9, 17.9, 44.5, 44.5, 44.5, 21.5, 21.5,
 21.5, 3.1, 3.1, 3.1, 1.6, 1.6, 1.6, 0.7, 0.7, 0.7, 1.0, 1.0,
 1.0, 1.6, 1.6, 1.6, 1.3, 1.3, 1.3, 0.8, 0.8, 0.8, 0.3, 0.3,
 // 50-65 South Ecliptic Latitude
 0.3, 1.3, 1.3, 1.3, 1.3, 2.8, 2.8, 2.8, 2.8, 2.4, 2.4, 2.4,
 2.4, 65.1, 65.1, 65.1, 65.1, 4.6, 4.6, 4.6, 4.6, 4.9, 4.9, 4.9,
 4.9, 0.9, 0.9, 0.9, 0.9, 0.3, 0.3, 0.3, 0.3, 0.3, 0.3, 0.3,
 0.3, 1.0, 1.0, 1.0, 1.0, 0.7, 0.7, 0.7, 0.7, 0.3, 0.3, 0.3,
 // 65-80 South Ecliptic Latitude
 2.6, 2.6, 2.6, 2.6, 2.6, 1.6, 1.6, 1.6, 1.6, 1.6, 1.6, 1.6,
 1.6, 0.7, 0.7, 0.7, 0.7, 0.7, 0.7, 0.7, 0.7, 0.5, 0.5, 0.5,
 0.5, 0.5, 0.5, 0.5, 0.5, 0.5, 0.5, 0.5, 0.5, 0.5, 0.5, 0.5,
 0.5, 1.3, 1.3, 1.3, 1.3, 1.3, 1.3, 1.3, 1.3, 2.6, 2.6, 2.6,
 // 80-90 South Ecliptic Latitude
 4.9, 4.9, 4.9, 4.9, 4.9, 4.9, 4.9, 4.9, 4.9, 4.9, 4.9, 4.9,
 4.9, 4.9, 4.9, 4.9, 4.9, 4.9, 4.9, 4.9, 4.9, 4.9, 4.9, 4.9,
 4.9, 4.9, 4.9, 4.9, 4.9, 4.9, 4.9, 4.9, 4.9, 4.9, 4.9, 4.9,
 4.9, 4.9, 4.9, 4.9, 4.9, 4.9, 4.9, 4.9, 4.9, 4.9, 4.9, 4.9,
 // JULY
 // 80-90 North Ecliptic Latitude
 6.4, 6.4, 6.4, 6.4, 6.4, 6.4, 6.4, 6.4, 6.4, 6.4, 6.4, 6.4,
 6.4, 6.4, 6.4, 6.4, 6.4, 6.4, 6.4, 6.4, 6.4, 6.4, 6.4, 6.4,
 6.4, 6.4, 6.4, 6.4, 6.4, 6.4, 6.4, 6.4, 6.4, 6.4, 6.4, 6.4,
 6.4, 6.4, 6.4, 6.4, 6.4, 6.4, 6.4, 6.4, 6.4, 6.4, 6.4, 6.4,
 // 65-80 North Ecliptic Latitude
 13.4, 1.8, 1.8, 1.8, 1.8, 1.8, 1.8, 1.8, 1.8, 1.4, 1.4, 1.4,
 1.4, 1.4, 1.4, 1.4, 1.4, 3.9, 3.9, 3.9, 3.9, 3.9, 3.9, 3.9,
 3.9, 7.1, 7.1, 7.1, 7.1, 7.1, 7.1, 7.1, 7.1, 4.0, 4.0, 4.0,
 4.0, 4.0, 4.0, 4.0, 4.0, 13.4, 13.4, 13.4, 13.4, 13.4, 13.4,
 // 50-65 North Ecliptic Latitude
 3.5, 0.9, 0.9, 0.9, 0.9, 1.1, 1.1, 1.1, 1.1, 2.2, 2.2, 2.2,
 2.2, 2.8, 2.8, 2.8, 2.8, 4.6, 4.6, 4.6, 4.6, 10.2, 10.2, 10.2,
 10.2, 3.9, 3.9, 3.9, 3.9, 14.5, 14.5, 14.5, 14.5, 7.5, 7.5, 7.5,
 7.5, 11.4, 11.4, 11.4, 11.4, 4.7, 4.7, 4.7, 4.7, 3.5, 3.5, 3.5,
 // 35-50 North Ecliptic Latitude
 0.2, 0.2, 0.2, 0.2, 0.2, 0.2, 3.1, 3.1, 3.1, 5.0, 5.0, 5.0,
 6.9, 6.9, 6.9, 27.8, 27.8, 27.8, 31.5, 31.5, 31.5, 13.7, 13.7, 13.7,
 20.9, 20.9, 20.9, 20.0, 20.0, 20.0, 5.5, 5.5, 5.5, 10.6, 10.6, 10.6,
 5.5, 5.5, 5.5, 2.3, 2.3, 2.3, 0.5, 0.5, 0.5, 0.1, 0.1, 0.1,
 // 20-35 North Ecliptic Latitude
 0.1, 0.1, 0.1, 0.6, 0.6, 0.6, 3.9, 3.9, 3.9, 13.3, 13.3, 13.3,

44.7, 44.7, 44.7, 55.7, 55.7, 55.7, 73.4, 73.4, 73.4, 45.1, 45.1, 45.1,
 40.1, 40.1, 40.1, 28.8, 28.8, 28.8, 19.6, 19.6, 19.6, 8.3, 8.3, 8.3,
 2.1, 2.1, 2.1, 0.2, 0.2, 0.2, 0.1, 0.1, 0.1, 0.1, 0.1, 0.1,
 // 0-20 North Ecliptic Latitude
 0.0, 0.3, 0.3, 0.6, 0.6, 2.4, 2.4, 0.3, 0.3, 1.6, 1.6, 12.1,
 12.1, 25.3, 25.3, 78.6, 78.6, 130.0, 130.0, 69.2, 69.2, 39.1, 39.1, 22.7,
 22.7, 20.9, 20.9, 60.3, 60.3, 15.1, 15.1, 15.0, 15.0, 5.5, 5.5, 8.9,
 8.9, 6.3, 6.3, 0.3, 0.3, 0.1, 0.1, 0.0, 0.0, 0.1, 0.1, 0.0,
 // 0-20 South Ecliptic Latitude
 0.0, 0.0, 0.0, 0.0, 0.0, 0.0, 0.0, 0.0, 1.8, 1.8, 2.0,
 2.0, 7.5, 7.5, 13.9, 13.9, 17.5, 17.5, 38.6, 38.6, 45.6, 45.6, 40.9,
 40.9, 33.8, 33.8, 14.5, 14.5, 15.1, 15.1, 3.2, 3.2, 13.4, 13.4, 3.1,
 3.1, 6.8, 6.8, 0.8, 0.8, 0.0, 0.0, 0.0, 0.0, 0.0, 0.0, 0.0,
 // 20-35 South Ecliptic Latitude
 0.0, 0.0, 0.0, 0.0, 0.0, 0.0, 0.0, 0.0, 1.0, 1.0, 1.0,
 14.7, 14.7, 14.7, 26.7, 26.7, 26.7, 22.9, 22.9, 22.9, 26.2, 26.2, 26.2,
 60.9, 60.9, 60.9, 32.9, 32.9, 32.9, 11.0, 11.0, 11.0, 4.1, 4.1, 4.1,
 2.4, 2.4, 2.4, 0.2, 0.2, 0.2, 0.0, 0.0, 0.0, 0.0, 0.0, 0.0,
 // 35-50 South Ecliptic Latitude
 0.0, 0.0, 0.0, 0.0, 0.0, 0.0, 0.0, 0.0, 0.1, 0.1, 0.1,
 6.8, 6.8, 6.8, 8.0, 8.0, 8.0, 35.4, 35.4, 35.4, 13.4, 13.4, 13.4,
 3.7, 3.7, 3.7, 3.2, 3.2, 3.2, 3.3, 3.3, 3.3, 1.4, 1.4, 1.4,
 4.3, 4.3, 4.3, 1.4, 1.4, 1.4, 0.1, 0.1, 0.1, 0.0, 0.0, 0.0,
 // 50-65 South Ecliptic Latitude
 0.0, 0.0, 0.0, 0.0, 0.0, 0.0, 0.0, 0.0, 3.4, 3.4, 3.4,
 3.4, 24.1, 24.1, 24.1, 24.1, 32.4, 32.4, 32.4, 32.4, 16.1, 16.1, 16.1,
 16.1, 8.1, 8.1, 8.1, 8.1, 0.8, 0.8, 0.8, 0.8, 0.5, 0.5, 0.5,
 0.5, 1.6, 1.6, 1.6, 1.6, 0.5, 0.5, 0.5, 0.5, 0.0, 0.0, 0.0,
 // 65-80 South Ecliptic Latitude
 2.6, 0.0, 0.0, 0.0, 0.0, 0.0, 0.0, 0.0, 15.3, 15.3, 15.3,
 15.3, 15.3, 15.3, 15.3, 15.3, 19.8, 19.8, 19.8, 19.8, 19.8, 19.8, 19.8,
 19.8, 1.6, 1.6, 1.6, 1.6, 1.6, 1.6, 1.6, 0.4, 0.4, 0.4,
 0.4, 0.4, 0.4, 0.4, 0.4, 2.6, 2.6, 2.6, 2.6, 2.6, 2.6, 2.6,
 // 80-90 South Ecliptic Latitude
 6.3, 6.3, 6.3, 6.3, 6.3, 6.3, 6.3, 6.3, 6.3, 6.3, 6.3, 6.3,
 6.3, 6.3, 6.3, 6.3, 6.3, 6.3, 6.3, 6.3, 6.3, 6.3, 6.3, 6.3,
 6.3, 6.3, 6.3, 6.3, 6.3, 6.3, 6.3, 6.3, 6.3, 6.3, 6.3, 6.3,
 6.3, 6.3, 6.3, 6.3, 6.3, 6.3, 6.3, 6.3, 6.3, 6.3, 6.3, 6.3,
 // AUGUST
 // 80-90 North Ecliptic Latitude
 8.2, 8.2, 8.2, 8.2, 8.2, 8.2, 8.2, 8.2, 8.2, 8.2, 8.2, 8.2,
 8.2, 8.2, 8.2, 8.2, 8.2, 8.2, 8.2, 8.2, 8.2, 8.2, 8.2, 8.2,
 8.2, 8.2, 8.2, 8.2, 8.2, 8.2, 8.2, 8.2, 8.2, 8.2, 8.2, 8.2,
 8.2, 8.2, 8.2, 8.2, 8.2, 8.2, 8.2, 8.2, 8.2, 8.2, 8.2, 8.2,

// 65-80 North Ecliptic Latitude

2.9, 2.9, 2.9, 2.9, 2.9, 2.9, 2.9, 2.4, 2.4, 2.4, 2.4, 2.4,
2.4, 2.4, 2.4, 7.7, 7.7, 7.7, 7.7, 7.7, 7.7, 7.7, 7.7, 7.7,
7.7, 7.7, 7.7, 7.7, 7.7, 7.7, 7.7, 8.4, 8.4, 8.4, 8.4, 8.4,
8.4, 8.4, 8.4, 4.5, 4.5, 4.5, 4.5, 4.5, 4.5, 4.5, 4.5, 2.9,

// 50-65 North Ecliptic Latitude

1.6, 1.6, 1.6, 1.0, 1.0, 1.0, 1.0, 2.4, 2.4, 2.4, 2.4, 3.6,
3.6, 3.6, 3.6, 12.8, 12.8, 12.8, 12.8, 14.2, 14.2, 14.2, 14.2, 20.6,
20.6, 20.6, 20.6, 12.7, 12.7, 12.7, 12.7, 7.2, 7.2, 7.2, 7.2, 4.0,
4.0, 4.0, 4.0, 2.6, 2.6, 2.6, 2.6, 2.1, 2.1, 2.1, 2.1, 1.6,

// 35-50 North Ecliptic Latitude

0.3, 0.3, 0.3, 1.3, 1.3, 1.3, 1.2, 1.2, 1.2, 1.8, 1.8, 1.8,
6.1, 6.1, 6.1, 7.1, 7.1, 7.1, 9.6, 9.6, 9.6, 15.4, 15.4, 15.4,
9.9, 9.9, 9.9, 10.5, 10.5, 10.5, 3.7, 3.7, 3.7, 4.3, 4.3, 4.3,
1.8, 1.8, 1.8, 0.7, 0.7, 0.7, 0.6, 0.6, 0.6, 0.6, 0.6, 0.6,

// 20-35 North Ecliptic Latitude

0.4, 0.4, 0.4, 1.2, 1.2, 1.2, 3.5, 3.5, 3.5, 7.9, 7.9, 7.9,
12.2, 12.2, 12.2, 13.3, 13.3, 13.3, 15.0, 15.0, 15.0, 27.8, 27.8, 27.8,
28.4, 28.4, 28.4, 10.6, 10.6, 10.6, 6.9, 6.9, 6.9, 4.8, 4.8, 4.8,
1.2, 1.2, 1.2, 0.5, 0.5, 0.5, 0.2, 0.2, 0.2, 0.3, 0.3, 0.3,

// 0-20 North Ecliptic Latitude

0.0, 0.2, 0.2, 0.5, 0.5, 1.6, 1.6, 3.5, 3.5, 15.2, 15.2, 26.5,
26.5, 38.2, 38.2, 20.6, 20.6, 21.8, 21.8, 34.0, 34.0, 40.3, 40.3, 51.1,
51.1, 27.6, 27.6, 15.8, 15.8, 11.6, 11.6, 10.1, 10.1, 5.0, 5.0, 3.7,
3.7, 1.2, 1.2, 0.5, 0.5, 0.2, 0.2, 0.0, 0.0, 0.0, 0.0, 0.0,

// 0-20 South Ecliptic Latitude

0.7, 0.3, 0.3, 0.5, 0.5, 0.7, 0.7, 1.6, 1.6, 9.3, 9.3, 12.9,
12.9, 26.7, 26.7, 26.4, 26.4, 13.7, 13.7, 17.9, 17.9, 55.5, 55.5, 41.8,
41.8, 38.1, 38.1, 24.6, 24.6, 30.0, 30.0, 20.0, 20.0, 16.1, 16.1, 4.4,
4.4, 2.4, 2.4, 1.1, 1.1, 0.6, 0.6, 0.2, 0.2, 0.3, 0.3, 0.7,

// 20-35 South Ecliptic Latitude

3.0, 3.0, 3.0, 0.9, 0.9, 0.9, 1.4, 1.4, 1.4, 1.7, 1.7, 1.7,
3.1, 3.1, 3.1, 3.8, 3.8, 3.8, 21.3, 21.3, 21.3, 18.2, 18.2, 18.2,
41.2, 41.2, 41.2, 26.0, 26.0, 26.0, 13.6, 13.96, 13.6, 12.2, 12.2, 12.2,
2.6, 2.6, 2.6, 2.1, 2.1, 2.1, 1.0, 1.0, 1.0, 1.7, 1.7, 1.7,

// 35-50 South Ecliptic Latitude

5.0, 5.0, 5.0, 8.3, 8.3, 8.3, 2.1, 2.1, 2.1, 1.3, 1.3, 1.3,
2.8, 2.8, 2.8, 3.0, 3.0, 3.0, 3.5, 3.5, 3.5, 19.2, 19.2, 19.2,
12.0, 12.0, 12.0, 2.3, 2.3, 2.3, 0.4, 0.4, 0.4, 0.7, 0.7, 0.7,
1.5, 1.5, 1.5, 1.6, 1.6, 1.6, 1.6, 1.6, 1.6, 3.2, 3.2, 3.2,

// 50-65 South Ecliptic Latitude

0.8, 0.8, 0.8, 50.2, 50.2, 50.2, 50.2, 4.2, 4.2, 4.2, 4.2, 3.8,
3.8, 3.8, 3.8, 11.0, 11.0, 11.0, 11.0, 11.1, 11.1, 11.1, 11.1, 5.8,
5.8, 5.8, 5.8, 1.4, 1.4, 1.4, 1.4, 0.6, 0.6, 0.6, 0.6, 1.7,

1.7, 1.7, 1.7, 0.4, 0.4, 0.4, 0.4, 0.5, 0.5, 0.5, 0.5, 0.8,
 // 65-80 South Ecliptic Latitude
 0.0, 0.0, 0.0, 0.0, 0.0, 0.0, 0.0, 5.5, 5.5, 5.5, 5.5, 5.5,
 5.5, 5.5, 5.5, 11.0, 11.0, 11.0, 11.0, 11.0, 11.0, 11.0, 11.0, 5.9,
 5.9, 5.9, 5.9, 5.9, 5.9, 5.9, 5.9, 0.4, 0.4, 0.4, 0.4, 0.4,
 0.4, 0.4, 0.4, 0.5, 0.5, 0.5, 0.5, 0.5, 0.5, 0.5, 0.5, 0.0,
 // 80-90 South Ecliptic Latitude
 4.1, 4.1, 4.1, 4.1, 4.1, 4.1, 4.1, 4.1, 4.1, 4.1, 4.1, 4.1,
 4.1, 4.1, 4.1, 4.1, 4.1, 4.1, 4.1, 4.1, 4.1, 4.1, 4.1, 4.1,
 4.1, 4.1, 4.1, 4.1, 4.1, 4.1, 4.1, 4.1, 4.1, 4.1, 4.1, 4.1,
 4.1, 4.1, 4.1, 4.1, 4.1, 4.1, 4.1, 4.1, 4.1, 4.1, 4.1, 4.1,
 // SEPTEMBER
 // 80-90 North Ecliptic Latitude
 7.9, 7.9, 7.9, 7.9, 7.9, 7.9, 7.9, 7.9, 7.9, 7.9, 7.9, 7.9,
 7.9, 7.9, 7.9, 7.9, 7.9, 7.9, 7.9, 7.9, 7.9, 7.9, 7.9, 7.9,
 7.9, 7.9, 7.9, 7.9, 7.9, 7.9, 7.9, 7.9, 7.9, 7.9, 7.9, 7.9,
 7.9, 7.9, 7.9, 7.9, 7.9, 7.9, 7.9, 7.9, 7.9, 7.9, 7.9, 7.9,
 // 65-80 North Ecliptic Latitude
 5.1, 5.1, 5.1, 5.9, 5.9, 5.9, 5.9, 5.9, 5.9, 5.9, 5.9, 7.1,
 7.1, 7.1, 7.1, 7.1, 7.1, 7.1, 7.1, 8.2, 8.2, 8.2, 8.2, 8.2,
 8.2, 8.2, 8.2, 9.0, 9.0, 9.0, 9.0, 9.0, 9.0, 9.0, 9.0, 8.2,
 8.2, 8.2, 8.2, 8.2, 8.2, 8.2, 5.1, 5.1, 5.1, 5.1, 5.1,
 // 50-65 North Ecliptic Latitude
 3.8, 3.8, 4.3, 4.3, 4.3, 11.3, 11.3, 11.3, 15.9, 15.9, 15.9, 18.6,
 18.6, 18.6, 12.4, 12.4, 12.4, 6.6, 6.6, 6.6, 7.0, 7.0, 7.0, 18.6,
 18.6, 18.6, 12.4, 12.4, 12.4, 6.6, 6.6, 6.6, 7.0, 7.0, 7.0, 0.6,
 0.6, 0.6, 2.3, 2.3, 2.3, 1.8, 1.8, 1.8, 1.6, 1.6, 1.6, 3.8,
 // 35-50 North Ecliptic Latitude
 0.5, 0.5, 0.8, 0.8, 0.8, 2.1, 2.1, 2.1, 4.2, 4.2, 4.2, 3.2,
 3.2, 3.2, 4.6, 4.6, 4.6, 9.6, 9.6, 9.6, 10.3, 10.3, 10.3, 10.3,
 10.3, 10.3, 9.3, 9.3, 9.3, 11.1, 11.1, 11.1, 4.7, 4.7, 4.7, 0.7,
 0.7, 0.7, 0.4, 0.4, 0.4, 0.2, 0.2, 0.2, 0.2, 0.2, 0.2, 0.5,
 // 20-35 North Ecliptic Latitude
 26.7, 26.7, 58.9, 58.9, 58.9, 1.4, 1.4, 1.4, 2.2, 2.2, 2.2, 5.0,
 5.0, 5.0, 8.5, 8.5, 8.5, 21.9, 21.9, 21.9, 15.0, 15.0, 15.0, 14.8,
 14.8, 14.8, 14.0, 14.0, 14.0, 6.5, 6.5, 6.5, 3.4, 3.4, 3.4, 1.4,
 1.4, 1.4, 0.2, 0.2, 0.2, 0.1, 0.1, 0.1, 0.1, 0.1, 0.1, 26.7,
 // 0-20 North Ecliptic Latitude
 0.0, 0.4, 0.4, 1.3, 1.3, 1.9, 1.9, 3.9, 3.9, 19.6, 19.6, 14.3,
 14.3, 14.3, 14.3, 20.0, 20.0, 23.6, 23.6, 25.3, 25.3, 21.8, 21.8, 34.2,
 34.2, 30.5, 30.5, 22.7, 22.7, 15.3, 15.3, 11.8, 11.8, 9.1, 9.1, 2.3,
 2.3, 0.7, 0.7, 0.4, 0.4, 0.2, 0.2, 0.0, 0.0, 0.0, 0.0, 0.0,
 // 0-20 South Ecliptic Latitude
 0.7, 1.9, 1.9, 2.2, 2.2, 0.9, 0.9, 9.2, 9.2, 16.8, 16.8, 30.2,

30.2, 40.6, 40.6, 36.0, 36.0, 34.0, 34.0, 50.8, 50.8, 44.3, 44.3, 48.4,
48.4, 54.1, 54.1, 30.0, 30.0, 27.6, 27.6, 18.2, 18.2, 17.2, 17.2, 10.2,
10.2, 7.3, 7.3, 1.3, 1.3, 5.0, 5.0, 0.8, 0.8, 0.5, 0.5, 0.7,

// 20-35 South Ecliptic Latitude

2.7, 2.7, 2.1, 2.1, 2.1, 1.7, 1.7, 1.7, 1.0, 1.0, 1.0, 5.9,
5.9, 5.9, 29.0, 29.0, 29.0, 21.1, 21.1, 21.1, 48.6, 48.6, 48.6, 41.6,
41.6, 41.6, 26.4, 26.4, 26.4, 15.1, 15.1, 15.1, 5.9, 5.9, 5.9, 3.3,
3.3, 3.3, 5.6, 5.6, 5.6, 1.9, 1.9, 1.9, 5.7, 5.7, 5.7, 2.7,

// 35-50 South Ecliptic Latitude

4.8, 4.8, 9.2, 9.2, 9.2, 0.6, 0.6, 0.6, 3.5, 3.5, 3.5, 2.5,
2.5, 2.5, 7.6, 7.6, 7.6, 9.5, 9.5, 9.5, 21.6, 21.6, 21.6, 10.4,
10.4, 10.4, 5.6, 5.6, 5.6, 0.9, 0.9, 0.9, 1.8, 1.8, 1.8, 1.2,
1.2, 1.2, 3.1, 3.1, 3.1, 1.6, 1.6, 1.6, 10.0, 10.0, 10.0, 4.8,

// 50-65 South Ecliptic Latitude

35.6, 35.6, 35.6, 5.8, 5.8, 5.8, 5.8, 7.7, 7.7, 7.7, 7.7, 3.4,
3.4, 3.4, 3.4, 10.0, 10.0, 10.0, 10.0, 17.5, 17.5, 17.5, 17.5, 5.2,
5.2, 5.2, 5.2, 7.1, 7.1, 7.1, 7.1, 5.1, 5.1, 5.1, 5.1, 1.9,
1.9, 1.9, 1.9, 1.2, 1.2, 1.2, 1.2, 8.6, 8.6, 8.6, 8.6, 35.6,

// 65-80 South Ecliptic Latitude

3.7, 3.7, 3.7, 2.2, 2.2, 2.2, 2.2, 2.2, 2.2, 2.2, 2.2, 10.6,
10.6, 10.6, 10.6, 10.6, 10.6, 10.6, 10.6, 15.7, 15.7, 15.7, 15.7, 15.7,
15.7, 15.7, 15.7, 3.3, 3.3, 3.3, 3.3, 3.3, 3.3, 3.3, 3.3, 3.0,
3.0, 3.0, 3.0, 3.0, 3.0, 3.0, 3.0, 3.7, 3.7, 3.7, 3.7, 3.7,

// 80-90 South Ecliptic Latitude

8.8, 8.8, 8.8, 8.8, 8.8, 8.8, 8.8, 8.8, 8.8, 8.8, 8.8, 8.8,
8.8, 8.8, 8.8, 8.8, 8.8, 8.8, 8.8, 8.8, 8.8, 8.8, 8.8, 8.8,
8.8, 8.8, 8.8, 8.8, 8.8, 8.8, 8.8, 8.8, 8.8, 8.8, 8.8, 8.8,
8.8, 8.8, 8.8, 8.8, 8.8, 8.8, 8.8, 8.8, 8.8, 8.8, 8.8, 8.8,

// OCTOBER

// 80-90 North Ecliptic Latitude

13.7, 13.7, 13.7, 13.7, 13.7, 13.7, 13.7, 13.7, 13.7, 13.7, 13.7, 13.7,
13.7, 13.7, 13.7, 13.7, 13.7, 13.7, 13.7, 13.7, 13.7, 13.7, 13.7, 13.7,
13.7, 13.7, 13.7, 13.7, 13.7, 13.7, 13.7, 13.7, 13.7, 13.7, 13.7, 13.7,
13.7, 13.7, 13.7, 13.7, 13.7, 13.7, 13.7, 13.7, 13.7, 13.7, 13.7, 13.7,

// 65-80 North Ecliptic Latitude

7.3, 7.3, 7.3, 7.3, 7.3, 5.9, 5.9, 5.9, 5.9, 5.9, 5.9, 5.9,
5.9, 4.3, 4.3, 4.3, 4.3, 4.3, 4.3, 4.3, 4.3, 11.4, 11.4, 11.4,
11.4, 11.4, 11.4, 11.4, 11.4, 8.0, 8.0, 8.0, 8.0, 8.0, 8.0, 8.0,
8.0, 6.1, 6.1, 6.1, 6.1, 6.1, 6.1, 6.1, 7.3, 7.3, 7.3,

// 50-65 North Ecliptic Latitude

0.9, 2.1, 2.1, 2.1, 2.1, 3.9, 3.9, 3.9, 3.9, 2.6, 2.6, 2.6,
2.6, 10.4, 10.4, 10.4, 10.4, 10.1, 10.1, 10.1, 10.1, 22.0, 22.0, 22.0,
22.0, 17.3, 17.3, 17.3, 17.3, 11.8, 11.8, 11.8, 11.8, 6.8, 6.8, 6.8,
6.8, 1.4, 1.4, 1.4, 1.4, 1.4, 1.4, 1.4, 1.4, 0.9, 0.9, 0.9,

// 35-50 North Ecliptic Latitude

0.6, 0.6, 0.6, 1.3, 1.3, 1.3, 2.4, 2.4, 2.4, 2.4, 2.4, 2.4,
2.9, 2.9, 2.9, 4.2, 4.2, 4.2, 7.2, 7.2, 7.2, 16.1, 16.1, 16.1,
12.7, 12.7, 12.7, 20.3, 20.3, 20.3, 7.7, 7.7, 7.7, 2.9, 2.9, 2.9,
0.8, 0.8, 0.8, 0.5, 0.5, 0.5, 0.2, 0.2, 0.2, 0.3, 0.3, 0.3,

// 20-35 North Ecliptic Latitude

0.3, 0.3, 0.3, 0.6, 0.6, 0.6, 4.0, 4.0, 4.0, 4.2, 4.2, 4.2,
7.3, 7.3, 7.3, 13.3, 13.3, 13.3, 9.8, 9.8, 9.8, 27.8, 27.8, 27.8,
14.5, 14.5, 14.5, 13.7, 13.7, 13.7, 8.0, 8.0, 8.0, 3.7, 3.7, 3.7,
1.0, 1.0, 1.0, 0.2, 0.2, 0.2, 0.2, 0.2, 0.2, 0.2, 0.2, 0.2,

// 0-20 North Ecliptic Latitude

0.4, 0.3, 0.3, 1.2, 1.2, 2.4, 2.4, 7.3, 7.3, 8.2, 8.2, 16.6,
16.6, 20.0, 20.0, 15.0, 15.0, 23.6, 23.6, 24.4, 24.4, 46.8, 46.8, 41.5,
41.5, 43.2, 43.2, 16.8, 16.8, 17.1, 17.1, 7.7, 7.7, 4.9, 4.9, 3.9,
3.9, 0.5, 0.5, 0.4, 0.4, 0.1, 0.1, 0.1, 0.1, 0.4, 0.4, 0.4,

// 0-20 South Ecliptic Latitude

1.0, 0.3, 0.3, 0.9, 0.9, 3.7, 3.7, 4.4, 4.4, 23.4, 23.4, 30.2,
30.2, 50.0, 50.0, 40.6, 40.6, 42.3, 42.3, 48.0, 48.0, 63.7, 63.7, 79.0,
79.0, 48.9, 48.9, 20.7, 20.7, 24.7, 24.7, 39.6, 39.6, 18.2, 18.2, 7.0,
7.0, 6.0, 6.0, 4.8, 4.8, 0.2, 0.2, 0.1, 0.1, 1.0, 1.0, 1.0,

// 20-35 South Ecliptic Latitude

0.3, 0.3, 0.3, 5.0, 5.0, 5.0, 1.4, 1.4, 1.4, 1.8, 1.8, 1.8,
22.4, 22.4, 22.4, 50.5, 50.5, 50.5, 43.9, 43.9, 43.9, 74.9, 74.9, 74.9,
39.3, 39.3, 39.3, 30.8, 30.8, 30.8, 12.0, 12.0, 12.0, 9.8, 9.8, 9.8,
3.0, 3.0, 3.0, 0.3, 0.3, 0.3, 0.2, 0.2, 0.2, 0.2, 0.2, 0.2,

// 35-50 South Ecliptic Latitude

0.2, 0.2, 0.2, 0.5, 0.5, 0.5, 1.1, 1.1, 1.1, 1.3, 1.3, 1.3,
1.2, 1.2, 1.2, 2.3, 2.3, 2.3, 2.0, 2.0, 2.0, 13.7, 13.7, 13.7,
20.6, 20.6, 20.6, 3.8, 3.8, 3.8, 3.0, 3.0, 3.0, 2.1, 2.1, 2.1,
0.7, 0.7, 0.7, 0.2, 0.2, 0.2, 0.0, 0.0, 0.0, 0.2, 0.2, 0.2,

// 50-65 South Ecliptic Latitude

0.0, 0.1, 0.1, 0.1, 0.1, 0.8, 0.8, 0.8, 0.8, 0.5, 0.5, 0.5,
0.5, 4.1, 4.1, 4.1, 4.1, 2.5, 2.5, 2.5, 2.5, 10.2, 10.2, 10.2,
10.2, 5.9, 5.9, 5.9, 5.9, 0.9, 0.9, 0.9, 0.9, 0.5, 0.5, 0.5,
0.5, 2.0, 2.0, 2.0, 2.0, 0.0, 0.0, 0.0, 0.0, 0.0, 0.0, 0.0,

// 65-80 South Ecliptic Latitude

0.2, 0.2, 0.2, 0.2, 0.2, 0.2, 0.2, 0.2, 0.2, 0.2, 0.2, 0.2,
0.2, 9.4, 9.4, 9.4, 9.4, 9.4, 9.4, 9.4, 9.4, 8.0, 8.0, 8.0,
8.0, 8.0, 8.0, 8.0, 8.0, 4.5, 4.5, 4.5, 4.5, 4.5, 4.5, 4.5,
4.5, 4.9, 4.9, 4.9, 4.9, 4.9, 4.9, 4.9, 4.9, 0.2, 0.2, 0.2,

// 80-90 South Ecliptic Latitude

2.0, 2.0, 2.0, 2.0, 2.0, 2.0, 2.0, 2.0, 2.0, 2.0, 2.0, 2.0,
2.0, 2.0, 2.0, 2.0, 2.0, 2.0, 2.0, 2.0, 2.0, 2.0, 2.0, 2.0,
2.0, 2.0, 2.0, 2.0, 2.0, 2.0, 2.0, 2.0, 2.0, 2.0, 2.0, 2.0,

2.0, 2.0, 2.0, 2.0, 2.0, 2.0, 2.0, 2.0, 2.0, 2.0, 2.0, 2.0,
// NOVEMBER
// 80-90 North Ecliptic Latitude
15.2, 15.2, 15.2, 15.2, 15.2, 15.2, 15.2, 15.2, 15.2, 15.2, 15.2, 15.2,
15.2, 15.2, 15.2, 15.2, 15.2, 15.2, 15.2, 15.2, 15.2, 15.2, 15.2, 15.2,
15.2, 15.2, 15.2, 15.2, 15.2, 15.2, 15.2, 15.2, 15.2, 15.2, 15.2, 15.2,
15.2, 15.2, 15.2, 15.2, 15.2, 15.2, 15.2, 15.2, 15.2, 15.2, 15.2, 15.2,
// 65-80 North Ecliptic Latitude
15.5, 15.5, 15.5, 15.5, 15.5, 15.5, 15.5, 5.3, 5.3, 5.3, 5.3, 5.3,
5.3, 5.3, 5.3, 7.1, 7.1, 7.1, 7.1, 7.1, 7.1, 7.1, 7.1, 4.8,
4.8, 4.8, 4.8, 4.8, 4.8, 4.8, 4.8, 2.7, 2.7, 2.7, 2.7, 2.7,
2.7, 2.7, 2.7, 7.1, 7.1, 7.1, 7.1, 7.1, 7.1, 7.1, 7.1, 15.5,
// 50-65 North Ecliptic Latitude
2.9, 2.9, 2.9, 6.8, 6.8, 6.8, 6.8, 13.6, 13.6, 13.6, 13.6, 4.8,
4.8, 4.8, 4.8, 3.3, 3.3, 3.3, 3.3, 1.2, 1.2, 1.2, 1.2, 3.5,
3.5, 3.5, 3.5, 11.4, 11.4, 11.4, 11.4, 1.8, 1.8, 1.8, 1.8, 2.8,
2.8, 2.8, 2.8, 1.4, 1.4, 1.4, 1.4, 2.1, 2.1, 2.1, 2.1, 2.9,
// 35-50 North Ecliptic Latitude
1.2, 1.2, 1.2, 4.8, 4.8, 4.8, 3.5, 3.5, 3.5, 5.1, 5.1, 5.1,
3.7, 3.7, 3.7, 1.4, 1.4, 1.4, 1.4, 1.4, 1.4, 6.2, 6.2, 6.2,
4.9, 4.9, 4.9, 3.5, 3.5, 3.5, 3.3, 3.3, 3.3, 1.7, 1.7, 1.7,
0.8, 0.8, 0.8, 0.9, 0.9, 0.9, 0.0, 0.0, 0.0, 0.6, 0.6, 0.6,
// 20-35 North Ecliptic Latitude
0.7, 0.7, 0.7, 3.2, 3.2, 3.2, 3.7, 3.7, 3.7, 2.6, 2.6, 2.6,
4.5, 4.5, 4.5, 3.2, 3.2, 3.2, 9.9, 9.9, 9.9, 19.9, 19.9, 19.9,
21.3, 21.3, 21.3, 11.6, 11.6, 11.6, 9.7, 9.7, 9.7, 4.8, 4.8, 4.8,
0.8, 0.8, 0.8, 0.2, 0.2, 0.2, 0.2, 0.2, 0.2, 0.1, 0.1, 0.1,
// 0-20 North Ecliptic Latitude
0.3, 1.0, 1.0, 1.6, 1.6, 2.4, 2.4, 1.2, 1.2, 4.3, 4.3, 9.7,
9.7, 13.1, 13.1, 13.9, 13.9, 27.4, 27.4, 29.2, 29.2, 27.4, 27.4, 29.9,
29.9, 23.0, 23.0, 16.4, 16.4, 24.0, 24.0, 13.6, 13.6, 4.1, 4.1, 14.8,
14.8, 1.6, 1.6, 0.5, 0.5, 0.5, 0.5, 0.0, 0.0, 0.0, 0.0, 0.3,
// 0-20 South Ecliptic Latitude
0.0, 0.6, 0.6, 0.6, 0.6, 3.4, 3.4, 4.4, 4.4, 9.0, 9.0, 19.3,
19.3, 19.8, 19.8, 18.6, 18.6, 36.0, 36.0, 32.0, 32.0, 46.8, 46.8, 53.0,
53.0, 51.0, 51.0, 42.0, 42.0, 14.0, 14.0, 10.1, 10.1, 9.7, 9.7, 4.9,
4.9, 1.8, 1.8, 10.1, 10.1, 0.7, 0.7, 0.6, 0.6, 0.1, 0.1, 0.0,
// 20-35 South Ecliptic Latitude
0.0, 0.0, 0.0, 0.6, 0.6, 0.6, 5.1, 5.1, 5.1, 7.7, 7.7, 7.7,
14.5, 14.5, 14.5, 37.7, 37.7, 37.7, 42.0, 42.0, 42.0, 55.6, 55.6, 55.6,
26.7, 26.7, 26.7, 10.3, 10.3, 10.3, 7.4, 7.4, 7.4, 9.8, 9.8, 9.8,
5.7, 5.7, 5.7, 0.0, 0.0, 0.0, 0.2, 0.2, 0.2, 0.1, 0.1, 0.1,
// 35-50 South Ecliptic Latitude
0.0, 0.0, 0.0, 0.8, 0.8, 0.8, 0.2, 0.2, 0.2, 0.9, 0.9, 0.9,

5.3, 5.3, 5.3, 9.5, 9.5, 9.5, 15.1, 15.1, 15.1, 28.1, 28.1, 28.1,
 8.9, 8.9, 8.9, 16.8, 16.8, 16.8, 31.5, 31.5, 31.5, 4.5, 4.5, 4.5,
 2.2, 2.2, 2.2, 1.9, 1.9, 1.9, 0.0, 0.0, 0.0, 0.0, 0.0, 0.0,
 // 50-65 South Ecliptic Latitude
 0.2, 0.2, 0.2, 0.7, 0.7, 0.7, 0.7, 0.4, 0.4, 0.4, 0.4, 0.8,
 0.8, 0.8, 0.8, 14.3, 14.3, 14.3, 14.3, 18.6, 18.6, 18.6, 18.6, 28.4,
 28.4, 28.4, 28.4, 57.8, 57.8, 57.8, 57.8, 16.3, 16.3, 16.3, 16.3, 12.7,
 12.7, 12.7, 12.7, 0.0, 0.0, 0.0, 0.0, 0.0, 0.0, 0.0, 0.0, 0.2,
 // 65-80 South Ecliptic Latitude
 0.8, 0.8, 0.8, 0.8, 0.8, 0.8, 0.8, 6.8, 6.8, 6.8, 6.8, 6.8,
 6.8, 6.8, 6.8, 4.3, 4.3, 4.3, 4.3, 4.3, 4.3, 4.3, 4.3, 13.9,
 13.9, 13.9, 13.9, 13.9, 13.9, 13.9, 13.9, 2.6, 2.6, 2.6, 2.6, 2.6,
 2.6, 2.6, 2.6, 0.4, 0.4, 0.4, 0.4, 0.4, 0.4, 0.4, 0.4, 0.8,
 // 80-90 South Ecliptic Latitude
 1.8, 1.8, 1.8, 1.8, 1.8, 1.8, 1.8, 1.8, 1.8, 1.8, 1.8, 1.8,
 1.8, 1.8, 1.8, 1.8, 1.8, 1.8, 1.8, 1.8, 1.8, 1.8, 1.8, 1.8,
 1.8, 1.8, 1.8, 1.8, 1.8, 1.8, 1.8, 1.8, 1.8, 1.8, 1.8, 1.8,
 1.8, 1.8, 1.8, 1.8, 1.8, 1.8, 1.8, 1.8, 1.8, 1.8, 1.8, 1.8,
 // DECEMBER
 // 80-90 North Ecliptic Latitude
 2.4, 2.4, 2.4, 2.4, 2.4, 2.4, 2.4, 2.4, 2.4, 2.4, 2.4, 2.4,
 2.4, 2.4, 2.4, 2.4, 2.4, 2.4, 2.4, 2.4, 2.4, 2.4, 2.4, 2.4,
 2.4, 2.4, 2.4, 2.4, 2.4, 2.4, 2.4, 2.4, 2.4, 2.4, 2.4, 2.4,
 2.4, 2.4, 2.4, 2.4, 2.4, 2.4, 2.4, 2.4, 2.4, 2.4, 2.4, 2.4,
 // 65-80 North Ecliptic Latitude
 2.6, 1.8, 1.8, 1.8, 1.8, 1.8, 1.8, 1.8, 1.8, 0.9, 0.9, 0.9,
 0.9, 0.9, 0.9, 0.9, 0.9, 1.6, 1.6, 1.6, 1.6, 1.6, 1.6, 1.6,
 1.6, 1.1, 1.1, 1.1, 1.1, 1.1, 1.1, 1.1, 1.1, 1.8, 1.8, 1.8,
 1.8, 1.8, 1.8, 1.8, 1.8, 2.6, 2.6, 2.6, 2.6, 2.6, 2.6, 2.6,
 // 50-65 North Ecliptic Latitude
 0.8, 1.9, 1.9, 1.9, 1.9, 0.8, 0.8, 0.8, 0.8, 1.3, 1.3, 1.3,
 1.3, 0.6, 0.6, 0.6, 0.6, 4.2, 4.2, 4.2, 4.2, 5.1, 5.1, 5.1,
 5.1, 2.1, 2.1, 2.1, 2.1, 3.2, 3.2, 3.2, 3.2, 1.6, 1.6, 1.6,
 1.6, 0.5, 0.5, 0.5, 0.5, 0.3, 0.3, 0.3, 0.3, 0.8, 0.8, 0.8,
 // 35-50 North Ecliptic Latitude
 0.1, 0.1, 0.1, 1.5, 1.5, 1.5, 1.4, 1.4, 1.4, 3.2, 3.2, 3.2,
 3.9, 3.9, 3.9, 2.0, 2.0, 2.0, 7.3, 7.3, 7.3, 9.3, 9.3, 9.3,
 6.9, 6.9, 6.9, 10.7, 10.7, 10.7, 14.3, 14.3, 14.3, 0.9, 0.9, 0.9,
 1.2, 1.2, 1.2, 0.1, 0.1, 0.1, 0.1, 0.1, 0.1, 0.1, 0.1, 0.1,
 // 20-35 North Ecliptic Latitude
 0.1, 0.1, 0.1, 0.3, 0.3, 0.3, 1.3, 1.3, 1.3, 2.6, 2.6, 2.6,
 4.1, 4.1, 4.1, 5.8, 5.8, 5.8, 6.5, 6.5, 6.5, 18.6, 18.6, 18.6,
 24.6, 24.6, 24.6, 28.8, 28.8, 28.8, 11.5, 11.5, 11.5, 2.2, 2.2, 2.2,
 0.6, 0.6, 0.6, 0.1, 0.1, 0.1, 0.1, 0.1, 0.1, 0.0, 0.0, 0.0,

// 0-20 North Ecliptic Latitude

0.0, 0.3, 0.3, 0.6, 0.6, 1.2, 1.2, 1.4, 1.4, 3.3, 3.3, 4.1,
4.1, 5.3, 5.3, 13.3, 13.3, 10.6, 10.6, 11.5, 11.5, 4.8, 4.8, 19.0,
19.0, 22.5, 22.5, 19.6, 19.6, 8.1, 8.1, 6.5, 6.5, 9.7, 9.7, 6.0,
6.0, 0.7, 0.7, 0.2, 0.2, 0.0, 0.0, 0.0, 0.0, 0.0, 0.0, 0.0,

// 0-20 South Ecliptic Latitude

0.0, 0.0, 0.0, 0.0, 0.0, 0.1, 0.1, 1.2, 1.2, 4.5, 4.5, 6.1,
6.1, 5.5, 5.5, 4.9, 4.9, 6.5, 6.5, 9.6, 9.6, 22.9, 22.9, 27.9,
27.9, 35.9, 35.9, 12.6, 12.6, 7.9, 7.9, 14.0, 14.0, 15.5, 15.5, 8.6,
8.6, 2.4, 2.4, 0.8, 0.8, 0.3, 0.3, 0.1, 0.1, 0.0, 0.0, 0.0,

// 20-35 South Ecliptic Latitude

0.0, 0.0, 0.0, 0.0, 0.0, 0.0, 0.5, 0.5, 0.5, 1.0, 1.0, 1.0,
7.2, 7.2, 7.2, 8.3, 8.3, 8.3, 15.8, 15.8, 15.8, 15.0, 15.0, 15.0,
16.5, 16.5, 16.5, 16.4, 16.4, 16.4, 12.2, 12.2, 12.2, 5.3, 5.3, 5.3,
13.5, 13.5, 13.5, 2.3, 2.3, 2.3, 0.1, 0.1, 0.1, 0.3, 0.3, 0.3,

// 35-50 South Ecliptic Latitude

0.0, 0.0, 0.0, 0.3, 0.3, 0.3, 0.2, 0.2, 0.2, 3.3, 3.3, 3.3,
8.9, 8.9, 8.9, 6.4, 6.4, 6.4, 16.8, 16.8, 16.8, 28.8, 28.8, 28.8,
32.9, 32.9, 32.9, 33.2, 33.2, 33.2, 15.1, 15.1, 15.1, 3.7, 3.7, 3.7,
7.1, 7.1, 7.1, 0.4, 0.4, 0.4, 0.8, 0.8, 0.8, 0.6, 0.6, 0.6,

// 50-65 South Ecliptic Latitude

0.2, 1.2, 1.2, 1.2, 1.2, 7.3, 7.3, 7.3, 7.3, 18.2, 18.2, 18.2,
18.2, 13.1, 13.1, 13.1, 13.1, 6.7, 6.7, 6.7, 6.7, 53.9, 53.9, 53.9,
53.9, 82.5, 82.5, 82.5, 82.5, 0.2, 0.2, 0.2, 0.2, 0.0, 0.0, 0.0,
0.0, 0.9, 0.9, 0.9, 0.9, 11.4, 11.4, 11.4, 11.4, 0.2, 0.2, 0.2,

// 65-80 South Ecliptic Latitude

10.0, 2.9, 2.9, 2.9, 2.9, 2.9, 2.9, 2.9, 2.9, 3.8, 3.8, 3.8,
3.8, 3.8, 3.8, 3.8, 3.8, 38.8, 38.8, 38.8, 38.8, 38.8, 38.8, 38.8,
38.8, 89.4, 89.4, 89.4, 89.4, 89.4, 89.4, 89.4, 89.4, 0.4, 0.4, 0.4,
0.4, 0.4, 0.4, 0.4, 0.4, 10.0, 10.0, 10.0, 10.0, 10.0, 10.0, 10.0,

// 80-90 South Ecliptic Latitude

21.8, 21.8, 21.8, 21.8, 21.8, 21.8, 21.8, 21.8, 21.8, 21.8, 21.8,
21.8, 21.8, 21.8, 21.8, 21.8, 21.8, 21.8, 21.8, 21.8, 21.8, 21.8,
21.8, 21.8, 21.8, 21.8, 21.8, 21.8, 21.8, 21.8, 21.8, 21.8, 21.8,
21.8, 21.8, 21.8, 21.8, 21.8, 21.8, 21.8, 21.8, 21.8, 21.8, 21.8,

10. APPENDIX D: AWGAUSS.DAT INPUT FILE

This appendix contains the AWGAUSS.DAT data file providing values for the Gauss quadrature employed in both PC METEORLINK Versions 1.0 and 1.0V. These values should *not* be changed by the user.

15

```
const int PGauss[3][15]= {2  4  6  8 10 12 16 20 24 32 40 48 64 80 96
```

```
1  2  4  7 11 16 22 30 40 52 68 88 112 144 184
```

```
1  3  6 10 15 21 29 39 51 67 87 111 143 183 231}
```

2

```
0.577350269189626    1.0000000000000000
```

4

```
0.339981043584856    0.652145154862546
```

```
0.861136311594053    0.347854845137454
```

6

```
0.238619186083197    0.467913934572691
```

```
0.661209386466265    0.360761573048139
```

```
0.932469514203152    0.171324492379170
```

8

```
0.183434642495650    0.362683783378362
```

```
0.525532409916329    0.313706645877887
```

```
0.796666477413627    0.222381034453374
```

```
0.960289856497536    0.101228536290376
```

10

```
0.148874338981631    0.295524224714753
```

```
0.433395394129247    0.269266719309996
```

```
0.679409568299024    0.219086362515982
```

```
0.865063366688985    0.149451349150581
```

```
0.973906528517172    0.066671344308688
```

12

```
0.125233408511469    0.249147045813403
```

```
0.367831498998180    0.233492536538355
```

```
0.587317954286617    0.203167426723066
```

```
0.769902674194305    0.160078328543346
```

```
0.904117256370475    0.106939325995318
```

```
0.981560634246719    0.047175336386512
```

16

```
0.095012509837637440185    0.189450610455068496285
```

```
0.281603550779258913230    0.182603415044923588867
```

```
0.458016777657227386342    0.169156519395002538189
```

```
0.617876244402643748447    0.149595988816576732081
```

```
0.755404408355003033895    0.124628971255533872052
```

```
0.865631202387831743880    0.095158511682492784810
```

0.944575023073232576078	0.062253523938647892863
0.989400934991649932596	0.027152459411754094852

20

0.076526521133497333755	0.152753387130725850698
0.227785851141645078080	0.149172986472603746788
0.373706088715419560673	0.142096109318382051329
0.510867001950827098004	0.131688638449176626898
0.636053680726515025453	0.118194531961518417312
0.746331906460150792614	0.101930119817240435037
0.839116971822218823395	0.083276741576704748725
0.912234428251325905868	0.062672048334109063570
0.963971927277913791268	0.040601429800386941331
0.993128599185094924786	0.017614007139152118312

24

0.064056892862605626085	0.127938195346752156974
0.191118867473616309159	0.125837456346828296121
0.315042679696163374387	0.121670472927803391204
0.433793507626045138487	0.115505668053725601353
0.545421471388839535658	0.107444270115965634783
0.648093651936975569252	0.097618652104113888270
0.740124191578554364244	0.086190161531953275917
0.820001985973902921954	0.073346481411080305734
0.886415527004401034213	0.059298584915436780746
0.938274552002732758524	0.044277438817419806169
0.974728555971309498198	0.028531388628933663181
0.995187219997021360180	0.012341229799987199547

32

0.048307665687738316235	0.096540088514727800567
0.144471961582796493485	0.095638720079274859419
0.239287362252137074545	0.093844399080804565639
0.331868602282127649780	0.091173878695763884713
0.421351276130635345364	0.087652093004403811143
0.506899908932229390024	0.083311924226946755222
0.587715757240762329041	0.078193895787070306472
0.663044266930215200975	0.072345794108848506225
0.732182118740289680387	0.065822222776361846838
0.794483795967942406963	0.058684093478535547145
0.849367613732569970134	0.050998059262376176196
0.896321155766052123965	0.042835898022226680657
0.934906075937739689171	0.034273862913021433103
0.964762255587506430774	0.025392065309262059456
0.985611511545268335400	0.016274394730905670605
0.997263861849481563545	0.007018610009470096600

40

0.038772417506050821933	0.077505947978424811264
0.116084070675255208483	0.077039818164247965588
0.192697580701371099716	0.076110361900626242372
0.268152185007253681141	0.074723169057968264200
0.341994090825758473007	0.072886582395804059061
0.413779204371605001525	0.070611647391286779695
0.483075801686178712909	0.067912045815233903826
0.549467125095128202076	0.064804013456601038075
0.612553889667980237953	0.061306242492928939167
0.671956684614179548379	0.057439769099391551367
0.727318255189927103281	0.053227846983936824355
0.778305651426519387695	0.048695807635072232061
0.824612230833311663196	0.043870908185673271992
0.865959503212259503821	0.038782167974472017640
0.902098806968874296728	0.033460195282547847393
0.932812808278676533361	0.027937006980023401098
0.957916819213791655805	0.022245849194166957262
0.977259949983774262663	0.016421058381907888713
0.990726238699457006453	0.010498284531152813615
0.998237709710559200350	0.004521277098533191258

48

0.032380170962869362033	0.064737696812683922503
0.097004699209462698930	0.064466164435950082207
0.161222356068891718056	0.063924238584648186624
0.224763790394689061225	0.063114192286254025657
0.287362487355455576736	0.062039423159892663904
0.348755886292160738160	0.060704439165893880053
0.408686481990716729916	0.059114839698395635746
0.466902904750958404545	0.057277292100403215705
0.523160974722233033678	0.055199503699984162868
0.577224726083972703818	0.052890189485193667096
0.628867396776513623995	0.050359035553854474958
0.677872379632663905212	0.047616658492490474826
0.724034130923814654674	0.044674560856694280419
0.767159032515740339254	0.041545082943464749214
0.807066204029442627083	0.038241351065830706317
0.843588261624393530711	0.034777222564770438893
0.876572020274247885906	0.031167227832798088902
0.905879136715569672822	0.027426509708356948200
0.931386690706554333114	0.023570760839324379141
0.952987703160430860723	0.019616160457355527814
0.970591592546247250461	0.015579315722943848728
0.984124583722826857745	0.011477234579234539490
0.993530172266350757548	0.007327553901276262102
0.998771007252426118601	0.003153346052305838633

64

0.024350292663424432509	0.048690957009139720383
0.072993121787799039450	0.048575467441503426935
0.121462819296120554470	0.048344762234802957170
0.169644420423992818037	0.047999388596458307728
0.217423643740007084150	0.047540165714830308662
0.264687162208767416374	0.046968182816210017325
0.311322871990210956158	0.046284796581314417296
0.357220158337668115950	0.045491627927418144480
0.402270157963991603696	0.044590558163756563060
0.446366017253464087985	0.043583724529323453377
0.489403145707052957479	0.042473515123653589007
0.531279464019894545658	0.041262563242623528610
0.571895646202634034284	0.039953741132720341387
0.611155355172393250249	0.038550153178615629129
0.648965471254657339858	0.037055128540240046040
0.685236313054233242564	0.035472213256882383811
0.719881850171610826849	0.033805161837141609392
0.752819907260531896612	0.032057928354851553585

0.783972358943341407610	0.030234657072402478868
0.813265315122797559742	0.028339672614259483228
0.840629296252580362752	0.026377469715054658672
0.865999398154092819761	0.024352702568710873338
0.889315445995114105853	0.022270173808383254159
0.910522137078502805756	0.020134823153530209372
0.929569172131939575821	0.017951715775697343085
0.946411374858402816062	0.015726030476024719322
0.961008799652053718919	0.013463047896718642598
0.973326827789910963742	0.011168139460131128819
0.983336253884625956931	0.008846759826363947723
0.991013371476744320739	0.006504457968978362856
0.996340116771955279347	0.004147033260562467635
0.999305041735772139457	0.001783280721696432947

0.019511383256793997654	0.039017813656306654811
0.058504437152420668629	0.038958395962769531199
0.097408398441584599063	0.038839651059051968932
0.136164022809143886559	0.038661759774076463327
0.174712291832646812559	0.038424993006959423185
0.212994502857666132572	0.038129711314477638344
0.250952358392272120493	0.037776364362001397490
0.288528054884511853109	0.037365490238730490027
0.325664370747701914619	0.036897714638276008839
0.362304753499487315619	0.036373749905835978044
0.398393405881969227024	0.035794393953416054603
0.433875370831756093062	0.035160529044747593496
0.468696615170544477036	0.034473120451753928794
0.502804111888784987594	0.033733214984611522817
0.536145920897131932020	0.032941939397645401383
0.568671268122709784725	0.032100498673487773148
0.600330622829751743155	0.031210174188114701642
0.631075773046871966248	0.030272321759557980661
0.660859898986119801736	0.029288369583267847693
0.689637644342027600771	0.028259816057276862397
0.717365185362099880254	0.027188227500486380674
0.744000297583597272317	0.026075235767565117903
0.769502420135041373866	0.024922535764115491105
0.793832717504605449949	0.023731882865930101293
0.816954138681463470371	0.022505090246332461926
0.838831473580255275617	0.021244026115782006389
0.859431406663111096977	0.019950610878141998929
0.878722567678213828704	0.018626814208299031429
0.896675579438770683194	0.017274652056269306359
0.913263102571757654165	0.015896183583725688045
0.928459877172445795953	0.014493508040509076117
0.942242761309872674752	0.013068761592401339294
0.954590766343634905493	0.011624114120797826916
0.965485089043799251452	0.010161766041103064521
0.974909140585727793386	0.008683945269260858426
0.982848572738629070418	0.007192904768117312753
0.989291302499755531027	0.005690922451403198649
0.994227540965688277892	0.004180313124694895237
0.997649864398237688900	0.002663533589512681669
0.999553822651630629880	0.001144950003186941534

0.016276744849602969579	0.032550614492363166242
0.048812985136049731112	0.032516118713868835987
0.081297495464425558994	0.032447163714064269364
0.113695850110665920911	0.032343822568575928429
0.145973714654896941989	0.032206204794030250669
0.178096882367618602759	0.032034456231992663218
0.210031310460567203603	0.031828758894411006535
0.241743156163840012328	0.031589330770727168558
0.273198812591049141487	0.031316425596861355813
0.304364944354496353024	0.031010332586313837423
0.335208522892625422616	0.030671376123669149014
0.365696861472313635031	0.030299915420827593794
0.395797649828908603285	0.029896344136328385984
0.425478988407300545365	0.029461089958167905970
0.454709422167743008636	0.028994614150555236543
0.483457973920596359768	0.028497411065085385646
0.511694177154667673586	0.027970007616848334440
0.539388108324357436227	0.027412962726029242823
0.566510418561397168404	0.026826866725591762198
0.593032364777572080694	0.026212340735672413913
0.618925840125468570386	0.025570036005349361499
0.644163403784967106798	0.024900633222483610288
0.668718310043916153953	0.024204841792364691282
0.692564536642171561344	0.023483399085926219842
0.715676812348967626225	0.022737069658329374001
0.738030643744400132851	0.021966644438744349195
0.759602341176647498703	0.021172939892191298988
0.780369043867433217604	0.020356797154333324595
0.800308744139140817229	0.019519081140145022410
0.819400310737931675539	0.018660679627411467385
0.837623511228187121494	0.017782502316045260838
0.854959033434601455463	0.016885479864245172450
0.871388505909296502874	0.015970562902562291381
0.886894517402420416057	0.015038721026994938006
0.901460635315852341319	0.014090941772314860916
0.915071423120898074206	0.013128229566961572637
0.927712456722308690965	0.012151604671088319635
0.939370339752755216932	0.011162102099838498591
0.950032717784437635756	0.010160770535008415758
0.959688291448742539300	0.009148671230783386633
0.968326828463264212174	0.008126876925698759217
0.975939174585136466453	0.007096470791153865269
0.982517263563014677447	0.006058545504235961683

0.988054126329623799481	0.005014202742927517693
0.992543900323762624572	0.003964554338444686674
0.995981842987209290650	0.002910731817934946408
0.998364375863181677724	0.001853960788946921732
0.999689503883230766828	0.000796792065552012429

COMPUTER SOFTWARE PRODUCT ITEM

(Technical Manual)

September 5, 1995

Prepared by
Communications Engineering Laboratory
Telecommunications and Information Systems Division
Science Applications International Corporation
261 Cedar Hill St., Bldg 'C'
Marlborough, Massachusetts 01752

1. INTRODUCTION

1.1 Summary

This report presents work performed for the Phillips Laboratory by Science Applications International Corporation (SAIC) to convert its proprietary VAX-based METEORLINK meteor-burst computer model to software capable of operation on an IBM-compatible personal computer (PC). The VAX version of METEORLINK was written in FORTRAN 77 using several VAX VMS-unique features for I/O and pseudo-structured programming. The PC METEORLINK program was written in the Borland Turbo C++ language by directly translating the original FORTRAN source code. This translation was completed successfully and several test cases were performed using the VAX and PC versions driven by the same input parameters. These test cases demonstrated essentially identical results with the exception of insignificant numerical differences due to the different computing platforms. The initial PC translation of the VAX METEORLINK program was designated "Version 1.0" of the "PC METEORLINK" computer program.

SAIC sought to improve the MB modeling algorithms employed in the PC METEORLINK program, Version 1.0, by adding an empirical meteor velocity distribution, a meteor mass-based distribution of sporadic meteor flux, and several other improved algorithms. The addition of the meteor velocity distribution required the addition of additional integration loops for meteor speed for each modeled meteor radiant. This enhanced version of the PC METEORLINK program has been designated "Version 1.0V". A measurement-prediction comparison has been performed using Version 1.0V of the PC METEORLINK program with comparisons drawn to results obtained with the VAX METEORLINK program in several earlier publications [1, 2, 3]. The results of this comparison exhibit improvement of model behavior in several respects, but the amount of speed dependence produces distortion in the normal diurnal variation in excess of anticipated values. Although this distortion is apparent, and indicates that better empirical models should be considered, the overall model predictions represent an improvement over the Version 1.0 capability to accurately model the performance of an MB communications link.

METEORLINK Version 1.0V calibration and validation were performed with data taken from three MB-link measurement campaigns, including the Greenland Meteor Burst Test Bed [4], the Jodrell Bank Engineering Station [5] in the United Kingdom, and Kazan State University [6] in

-
1. R. I. Desourdis, Jr., S. C. Merrill, J. H. Wojtaszek and K. Hernandez, Meteor burst link performance sensitivity to antenna pattern, power margin and range, *IEEE MILCOM'88 Conf. Proc.*, Vol. 1, October 1988, pp. 14.5.1-14.5.7.
 2. R. I. Desourdis, Jr., J. C. Ostergaard, and A. D. Bailey, "Meteor burst computer model validation using high-latitude measurements," *IEEE MILCOM'91 Conf. Proc.*, Vol. 2, McLean, Virginia, November 1991, pp. 22.1.1-22.1.5.
 3. R. I. Desourdis, et. al., "Advanced Meteor-Burst Radio for Multi-Media Communications," *IEEE MILCOM'94 Conf. Proc.*, Vol. 2, Ft. Monmouth, New Jersey, October 1994, pp. 685-689.
 4. R. I. Desourdis, Jr., V. V. Sidorov, A. V. Karpov, R. G. Huziashev, L. A. Epictetov, and D. W. Brown, "A Russian meteor burst communications experiment and measurement-prediction comparison," *IEEE MILCOM'92 Conf. Proc.*, Vol. 1, San Diego, October 1992, pp. 1.6.1-1.6.5.
 5. A. C. B. Lovell, *Meteor Astronomy*, University Press, Oxford, New York, 1954, pp. 112-115.

Russia. The results show that both Versions 1.0 and 1.0V of the PC METEORLINK program yield similar accuracy although the two models differ significantly in their calculation of the usable meteor rate (MR) and duty cycle (DC). The complete results of the Greenland Test Bed measurement-prediction comparison with Version 1.0 and Version 1.0V predictions appear in Appendix A of a companion report [7]. A comparison of model prediction accuracy for the Greenland measurements alone is shown in Figure 1.1 and described in Section 4 of this report. Figures 1.2a and 1.2b are plots of the daily-average MR value measured at Jodrell Bank in 1950-51 with the corresponding Version 1.0 and 1.0V predictions. The complete set of month by month Jodrell Bank predictions are provided in of a companion report [7]. Although development of Version 1.0V was motivated in part due reduce the excessive METEORLINK prediction for the Autumn MR values, the effect was not altered by incorporating a more accurate meteor velocity distribution. Other physical parameters, such as the sporadic meteor flux density or meteor velocity distributions, may have produced or maintained this phenomena. Finally, MB measurements performed in Russia during April (radar) and May (forward scatter) were compared with Version 1.0V predictions as shown in the scatter plots of Figures 1.3a and 1.3b.

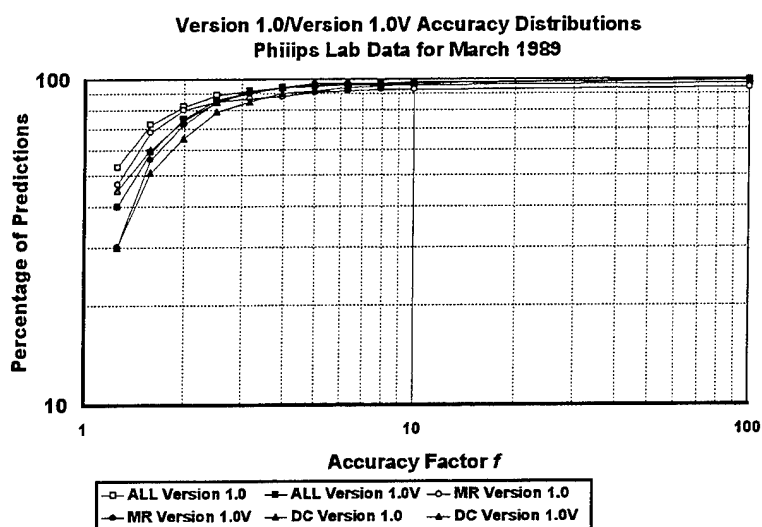


Figure 1.1 Greenland prediction accuracy comparison

There reports were written as part of this effort in addition to translation and modification of the original VAX FORTRAN version of METEORLINK. into a Turbo C++ program for the PC. The software is accompanied by a "User's Guide" addressing both Versions 1.0 and 1.0V of the PC METEORLINK program. It must be noted that the Version 1.0V files can be "read" by the Version 1.0 program, but use of Version 1.0 input files with Version 1.0V will lead to an I/O error. For example, the number of meteor speed integration points is a required input parameter, although the Version 1.0 program does not use this parameter. The second report describes many of the PC METEORLINK algorithms, particularly those which were altered in developing Version 1.0V from Version 1.0. Algorithms shared by both programs, particularly the development of the geometric model of meteor trail scatter, were referenced from a recent publication [8]. Finally, this report and the associated Appendices A and B of the companion

6. R. I. Desourdis, Jr., V. V. Sidorov, A. V. Karpov, R. G. Huziashev, L. A. Epictetov, and D. W. Brown, *Ibid.*

7. Science Applications International Corporation, *R&D Equipment Information (User's Guide)*, Contract # F19628-93-C-0082, CDRL A005, Marlborough, Mass., September 1995.

8. R. I. Desourdis, "Modeling and Analysis of Meteor Burst Communications," Chapter 3, *Meteor Burst Communications: Theory and Practice*, John Wiley & Sons, New York, March, 1993, pp. 59-342.

report [7] present preliminary results from the measurement-prediction comparison performed using Phillips Lab data collected in Greenland and radar data collected in England at Jodrell Bank, respectively, as well as the Kazan measurements.

This report describes the algorithms employed in the PC METEORLINK Version 1.0 and 1.0V C++ computer programs used to produce the measurement-prediction comparison results described in this report and other publications [1, 2, 3]. The reader will note that many of the basic derivations assumed in this report were published elsewhere [7].

1.2 Background

This technical manual describes the algorithms employed in the PC METEORLINK computer program, Versions 1.0 and 1.0V. The "1.0V" Version employs "velocity-based" prediction algorithms intended to increase model fidelity and, ultimately, improve MB-link performance predictions. These algorithms include the integration of usable meteor rate with respect to meteor speed using an empirical distribution for meteor velocity. In addition, Version 1.0V replaces the Version 1.0 sporadic meteor distribution based on minimum electron line density with the corresponding distribution of sporadic meteors whose mass exceeds a minimum specified value. Finally, the height of maximum ionization is determined numerically as a function of meteor speed and maximum trail electron line density.

The PC METEORLINK program is authored in the C++ language and was originally translated directly from the FORTRAN 77 version developed for the VAX 3600. In other words, PC METEORLINK Version 1.0 is intended to reproduce the current VAX METEORLINK Version 1.40 results as closely as possible given the difference in platforms. An earlier version of

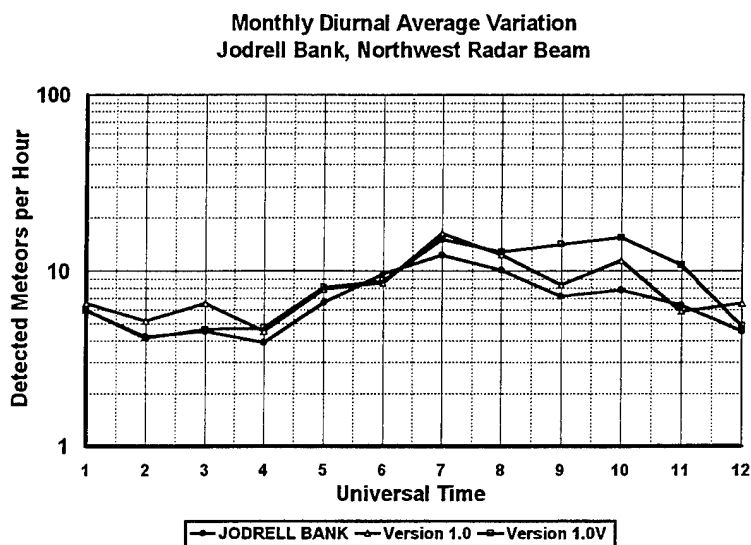


Figure 1.2a Monthly MR Comparison for the Northwest Beam

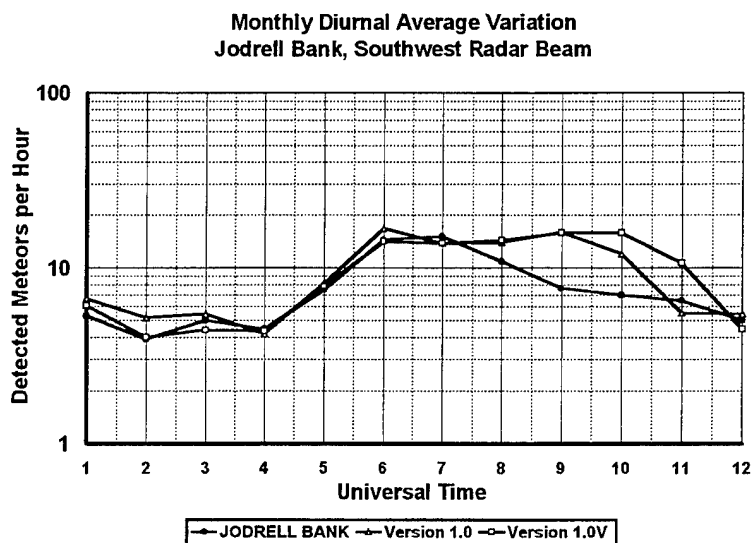


Figure 1.2b Monthly MR Comparison for the Southwest Beam

the VAX METEORLINK program was provided to the Phillips Laboratory as part of a contract executed to calibrate and, subsequently, validate the VAX METEORLINK program. The measurements of meteor arrival rate (MR), duty cycle (DC), and other link-performance parameters used in this validation were extracted from the extensive meteor-burst data base collected in Greenland by the Phillips Laboratory [9]. In fact, a limited validation of the PC METEORLINK Version 1.0V program was performed using a subset of the data employed in the original VAX METEORLINK validation. This Version 1.0V validation is described in a companion report [10].

1.3 Assumptions

This report uses symbols and definitions adopted by Chapter 3 of *Meteor Burst Communications: Theory and Practice* [11]. This book chapter provides a detailed derivation of the algorithms employed in the original VAX METEORLINK program as well as complete validation results not previously published. This report will not attempt to reproduce material presented in this book except to the extent that it is necessary to explain the differences between the PC METEORLINK Version 1.0V

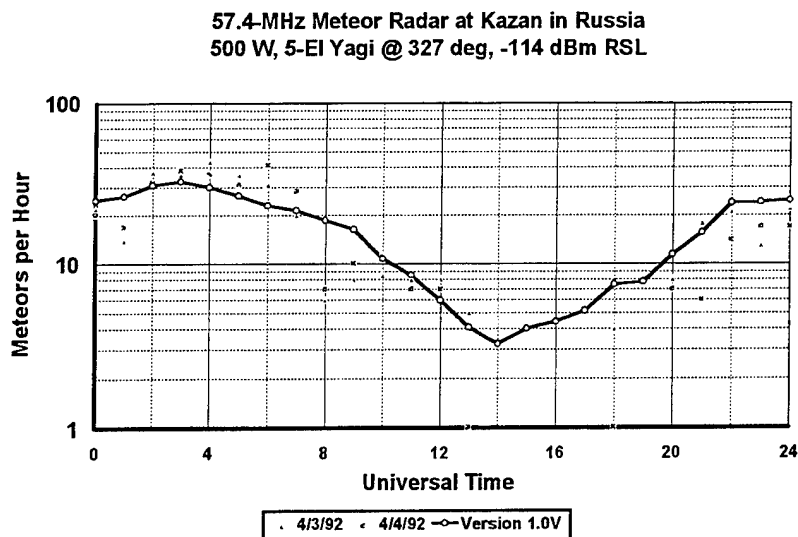


Figure 1.3a Kazan radar (backscatter) measurements

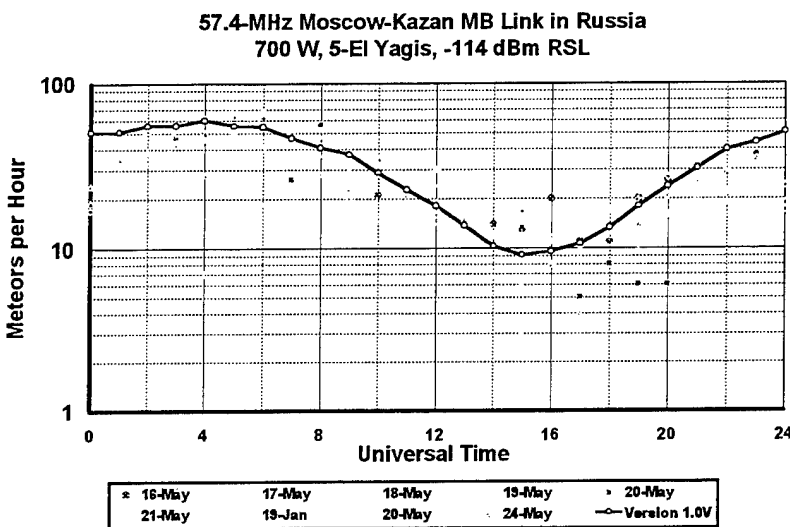


Figure 1.3b Moscow-Kazan forward-scatter MB link

9. *The RADC High Latitude Meteor Scatter Test Bed*, by J. C. Ostergaard, J. E. Rasmussen, M. J. Sowa, J. M. Quinn, and P. A. Kossey, RADC-TR-86-74 ADA180550, Hanscom Air Force Base, Massachusetts, July 1986, Unlimited Distribution.

10. Science Applications International Corporation, *Scientific and Technical Report*, Contract # F19628-93-C-0082, CDRL A003, Marlborough, Mass., September 1995.

11. R. I. Desourdis, "Modeling and Analysis of Meteor Burst Communications," Chapter 3, *Meteor Burst Communications: Theory and Practice*, John Wiley & Sons, New York, March, 1993, pp. 59-342.

and Version 1.0. It will also be assumed that the reader is familiar with the terminology of meteor-burst communications, such as meteor rate, duty cycle, underdense meteor rate, etc. and the fundamentals of meteor astronomy and physics.

Appendix A in Chapter 3 of *Meteor Burst Communications: Theory and Practice* contains a complete development of useful coordinate systems for modeling MB links. In this report, only the LINK (L), METEOR (M), and ORBITAL coordinate systems defined in this reference will be employed. Many other coordinate systems are defined in this reference, but these three systems can be used to meet the objectives of this technical report. The L and M systems are used to determine the spatial orientations of meteor trails essential to effective radiowave scattering, i.e., *link-observable* meteor trails. The O system is used to represent these link-observable trails using the coordinate conventions used to define the incident flux of sporadic meteors and the meteor velocity distribution.

2. OBSERVABLE METEOR TRAILS

The L system is defined such that the x_L axis passes through the geographic coordinates of the transmit and receive antennas. The y_L axis crosses the x_L axis halfway between these coordinates, and the z_L axis is defined in the normal right-handed sense pointing along the zenith (see Figure 2.1). At a given scatter point, $\rho_s^L = (x_s^L, y_s^L, z_s^L)$, in the L system, the $x_M - y_M$ plane in the M system defines observable (i.e. potentially usable) orientation of meteor trails. This plane is tangent to the confocal surface of revolution (ellipsoid) defined by the antenna coordinates as foci. It can be defined by its normal vector $\mathbf{n}_s^L = \mathbf{r}_{s1}^L + \mathbf{r}_{s2}^L$, where the two r-vectors point from the transmit and receive antennas to the scatter point ρ_s^L . The M system is used to define observable trail orientations with unit vectors $\hat{\mathbf{v}}_m^M$ [12] and then transformed into the L system as $\hat{\mathbf{v}}_m^L$. Through a series of transformations [13], $\hat{\mathbf{v}}_m^L$ is subsequently transformed into the corresponding unit vector for meteor velocity in the O system,

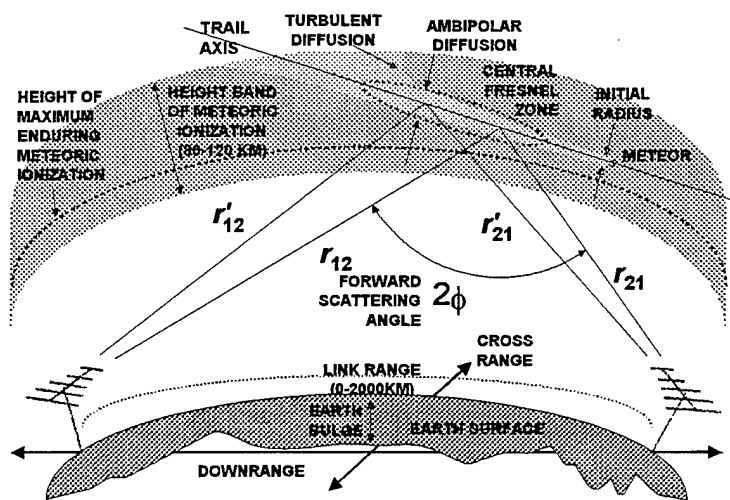


Figure 2.1 Link coordinate system

12. M. L. Meeks and J. C. James, "On the influence of meteor-radiant distributions in meteor-scatter communication," *Proc. IRE*, Vol. 45, December 1957, p. 1725.

13. R. I. Desourdis, "Modeling and Analysis of Meteor Burst Communications," *Ibid.*, pp. 292-295.

given by \hat{v}_m^0 .

The *apparent* meteor speed is assumed to be $v_a = |\mathbf{v}_m^M| = |\mathbf{v}_m^L| = |\mathbf{v}_m^0|$, where the effects negligible (for present purposes) of atmospheric deceleration, diurnal aberration, and zenith attraction [14] are ignored. These latter transformations account for the transmit and receive antenna coordinates and heights above ground, time of day, and day in the year. In the parent reference [15], the O system is defined such that the x_0 axis points in the direction of the sun, that is, the helion. As a result, the elongation angle is given by $\varepsilon = \cos^{-1}(-\hat{v}_{m2}^0)$, where $\hat{v}_m^0 = \langle \hat{v}_{m1}^0, \hat{v}_{m2}^0, \hat{v}_{m3}^0 \rangle$ defines the vector components. All METEORLINK versions employ an O system rotated 90° from this orientation, such that the x_0 axis always points in the earth's antapex direction and $\varepsilon = \cos^{-1}(-\hat{v}_{m1}^0)$.

The probability that a meteor will arrive with speed v_a at elongation angle ε is determined from the empirical velocity distribution $p(|\hat{v}_m^0|, \hat{v}_m^0) = p(v_a, \hat{v}_m^0)$ depicted in Figure 2.2. This two-dimensional density function gives the discrete probability for velocity values defined within intervals of 2 km/sec from 11 to 73 km/sec (32 values) and elongation angle values lying with intervals defined in 10° increments from 0° (apex) to 180° (antapex). In general, the density function $p(v_a, \hat{v}_m^0) = p(v_a, \varepsilon)$ must satisfy

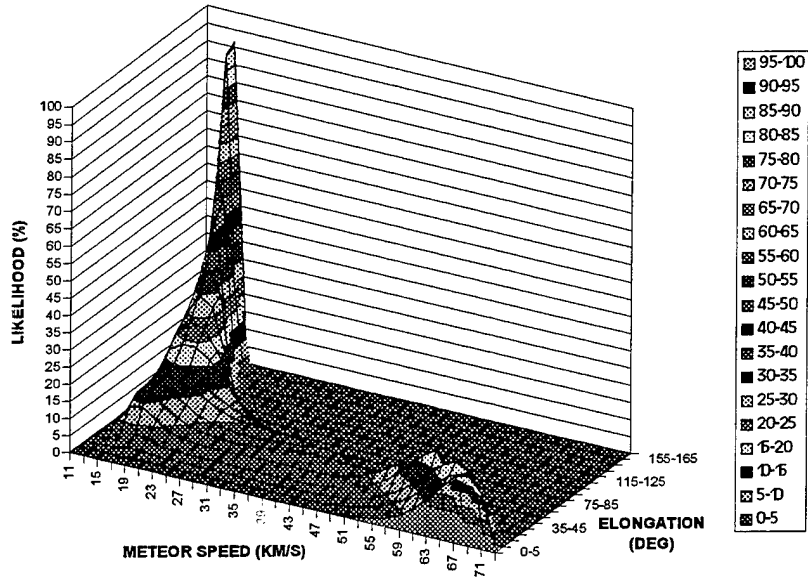


Figure 2.2 Empirically-Derived Sporadic Meteor Velocity Distribution

$$2\pi \kappa_n \int_0^\pi \int_{11}^{73} p(v_a, \varepsilon) \sin \varepsilon dv_a d\varepsilon = 1.0 \quad (2.1)$$

to avoid distorting the empirical distribution of sporadic meteor radiant. The available empirical discrete meteor velocity density function [16] satisfies

$$\sum_{j=1}^{32} p_{ij} = 1.0 \quad (2.2)$$

14. D. W. R. McKinley, *Meteor Science and Engineering*, McGraw-Hill, New York, 1961, p. 34.

15. R. I. Desourdis, *Ibid.*, pp. 286-289.

16. V. V. Sidorov, *personal communication*.

for each ε interval $i = 1, 2, \dots, 18$. Eq. 2.1 can then be expressed as

$$2\pi \kappa_n \sum_{i=1}^{18} \left[\sum_{j=1}^{32} p_{ij} \int_{(i-1)\frac{\pi}{10}}^{i\frac{\pi}{10}} \sin \varepsilon d\varepsilon \right] = 2\pi \kappa_n \sum_{i=1}^{18} \left[\int_{(i-1)\frac{\pi}{10}}^{i\frac{\pi}{10}} \sin \varepsilon d\varepsilon \right] = 1.0$$

so the normalization constant is given by

$$\begin{aligned} \kappa_n &= \left\{ 2\pi \sum_{i=1}^{18} \left[\int_{(i-1)\frac{\pi}{10}}^{i\frac{\pi}{10}} \sin \varepsilon d\varepsilon \right] \right\}^{-1} \\ &= \left\{ 2\pi \int_0^{\pi} \sin \varepsilon d\varepsilon \right\}^{-1} \\ &= \frac{1}{4\pi} \end{aligned}$$

In practice, the density function $p(v_a, \varepsilon)$ appears in a ratio such that the normalization factor κ_n does not impact the computed MR or DC values as will be shown in a subsequent section.

The trail-scatter point ρ_s^L and the unit meteor direction vector \hat{v}_m^L define the geometric criteria for a meteor trail to produce a usable signal at the receiver. In fact, meteor trails meeting the geometric criteria (ρ_s^L, \hat{v}_m^L) are defined to be *observable* meteor trails. In other words, all meteors passing through ρ_s^L forming a trail with direction \hat{v}_m^L will be suitably positioned relative to the transmit and receive antenna locations to produce a usable received signal. These observability criteria are a necessary condition for trail scatter as modeled by both Versions 1.0 and 1.0V of PC METEORLINK. To produce a usable received signal, however, the trail-forming meteor must exceed a certain minimum mass which is dependent on both meteor speed and link power-budget parameters.

3. USABLE METEOR TRAILS

3.1 Usability Criteria

The minimum performance requirements for an MB-link necessarily include the required received power P_r^* from the "meteor burst" and the minimum burst duration τ^* . Thus, given the observability criteria (ρ_s^L, \hat{v}_m^L) , a meteor trail is deemed *usable* if it meets the equipment-dependent criteria (P_r^*, τ^*) . The objectives of the PC METEORLINK computer programs are to determine the MB link MR and DC values resulting from meteor trails that meet both the observability criteria (ρ_s^L, \hat{v}_m^L) and the usability criteria (P_r^*, τ^*) .

3.2 Meteor Mass

The METEORLINK programs compute the minimum electron line density q_{sm}^* for each observable trail with velocity vector $\mathbf{v}_m^L = v_a \hat{\mathbf{v}}_m^L$. This minimum density q_{sm}^* is determined such that a minimum power of P_r^* Watts is delivered to the receiver for a minimum time τ^* seconds. In other words, the meteor trail provides a scatter path with total maximum path loss (MAPL) not exceeding L^* dB. The minimum meteor mass m_{sm}^* required to this line density is given by

$$m_{sm}^*(\rho_s^L, \mathbf{v}_m^L, L^*, \tau^*) = \frac{\mu H_P}{\beta_I(v_a) \cos(\chi_{sm})} \hat{q}_{sm}^*(\rho_s^L, \mathbf{v}_m^L, L^*, \tau^*) \quad (3.1a)$$

where

$$\hat{q}_{sm}^*(\rho_s^L, \mathbf{v}_m^L, L^*, \tau^*) = \frac{4 q_{sm}^*(\rho_s^L, \mathbf{v}_m^L, L^*, \tau^*)}{9 \exp(H_e) [1 - \exp(H_e)/3]^2} \quad (3.1b)$$

with

$$H_e = \frac{\hat{H}_I - h_s}{H_P} \quad (3.1c)$$

and

μ = average mass of a meteoric atom

$\beta_I(v_a)$ = number of free electrons ionized by a single meteoric atom

H_P = atmospheric scale height at the true height

χ_{sm} = included angle between the trail vector $\hat{\mathbf{v}}_m^L$ and the zenith (vertical) at ρ_s^L

\hat{H}_I = height of maximum ionization

h_s = height of the trail-scatter point ρ_s^L above sea level in the L system.

In Eqs. 3.1, the dependence of line density q and therefore mass m on received power threshold P_r^* and minimum duration τ^* is determined from modifications to the classical trail-scatter models [17].

3.3 Trail Line Density

Underdense Trail-Scatter Model

For each observable trail, both METEORLINK Versions 1.0 and 1.0V compute the minimum required underdense (long wavelength) line density $q_{sm}^*(\rho_s^L, \mathbf{v}_m^L, L^*, \tau^*) = q_{sm}^{LU}(\rho_s^L, \mathbf{v}_m^L, L^*, \tau^*)$. This computation begins with the calculation of the classic underdense trail model coefficients

17. G. R. Suger, "Radio propagation by reflections from meteor trails," *Proc. IEEE*, Vol. 52, February 1964, pp. 116-136.

$$a_1^{LU} = \frac{16\pi^2}{r_e^2 \lambda^3} r_1 r_2 (r_1 + r_2) \sin^2(\gamma_{sm}) \quad (3.2a)$$

$$a_2^{LU} = 32 \frac{\pi^2}{\lambda^2} \cos^2(\phi_s) D_U \quad (3.2b)$$

$$a_3^{LU} = 8 \frac{\pi^2}{\lambda^2} \cos^2(\phi_s) r_0^2 \quad (3.2c)$$

so that

$$q_{sm}^{LU}(\rho_s^L, \mathbf{v}_m^L, L^*, \tau^*) = \sqrt{a_1^{LU} \exp(a_2^{LU} \tau^* + a_3^{LU}) / l^*} \quad (3.3)$$

where the MB system loss

$$l^* = 10^{(L^*/10)} \quad (3.4)$$

with

$$L^* = P_t + G_{sm}^{12} - L_t - L_r - P_r^* \quad (3.5)$$

r_0 = initial radius of the meteor trail

λ = signal wavelength

ϕ_s = included angle between \mathbf{r}_{s1}^L and \mathbf{r}_{s1}^L at the trail scatter point (see Figure 2.1)

γ_{sm} = angle between the trail vector $\hat{\mathbf{v}}_m^L$ and \mathbf{r}_{s1}^L , where \mathbf{r}_{s1}^L vector pointing from the transmit antenna to scatter point)

D_U = underdense trail diffusion rate

and $r_i = |\mathbf{r}_{si}^L|$ for $i = 1, 2$. The factor $\sin^2(\gamma_{sm}) = 1 - \sin^2(\phi_s) \cos^2(\beta_{sm})$ from the classical formulation where $\beta_{sm} = \cos^{-1}[\cos(\gamma_{sm})/\sin(\phi_s)]$ is the angle between the propagation plane and the plane containing observable meteor trails through the point ρ_s^L .

Empirically-derived approximations are used for diffusion rate and initial radius. The diffusion rate is dependent only on trail height and is given by

$$D = D_U = 10^{0.0225h_s - 1.58} \text{ m}^2 / \text{ s} \quad [18] \quad (3.6a)$$

while the initial radius is dependent on both height and meteor speed from

18. E. L. Murray, Ambipolar diffusion of a meteor trail and its relation with height, *Planet. Space Sci.*, Vol. 1, 1959, pp. 125-129.

$$r_0(v_a, h_s) = \frac{2.58 \times 10^{12} v_a^{0.8}}{n_a(h_s)} \text{ m [19]} \quad (3.6b)$$

where $n_a(h_s)$ is the atmospheric particle density at height h_s .

The term G_{sm}^{12} in Eq. 3.5 is the dot product of the normalized transmit and receive electric field vectors (in dB) at each trail scatter point. In symbols, G_{sm}^{12} is defined as

$$G_{sm}^{12} = 10 \log_{10} \left\| \tilde{e}_{s11}^V (\tilde{e}_{s21}^V)^c + \rho \left[\tilde{e}_{s12}^V (\tilde{e}_{s22}^V)^c + \tilde{e}_{s31}^V (\tilde{e}_{s31}^V)^c \right] \right\| \quad (3.7)$$

In this expression, the factor ρ is defined as the plasma resonance amplification factor which affects only the transverse electric-field vector scattered from the trail. Measurements and theory have established that $\rho \cong 2$ for a brief period after trail formation when the dielectric constant passes through the value

$$\kappa = 1 - N_e \lambda^2 r_e / e \cong -1.4 \quad (3.8a)$$

where the electron volume density at time $t = \tau^*$ is given by

$$N_e = \frac{q}{e \pi r_i^2} = \frac{q}{e \pi (4D\tau^* + r_0^2)} \quad (3.8b)$$

If the minimum required line density $q_{sm}^{LU}(\rho_s^L, v_m^L, L^*, \tau^*)$ of a given observable trail yields $\kappa < -1.4$, then all underdense trails with $q > q_{sm}^{LU}(\rho_s^L, v_m^L, L^*, \tau^*)$ will also pass through resonance at some time $t > \tau^*$. Therefore, PC METEORLINK Version 1.0V employs Eq. 3.7 to approximate the amplification of the transversely polarized wave at the underdense trail.

The PC METEORLINK Version 1.0 program employs Eq. 3.7 for all underdense trails in both the MR and DC calculation. This approximation overemphasizes the role that resonance plays in these calculations, particularly in the magnitude of the underdense trail contribution to the DC value. To minimize the effect on the DC calculation, both Versions 1.0 and 1.0V of the METEORLINK program employ an increased value of diffusion rate ($D_U > D$) to simulate the rapid decline of the resonance condition.

Calculation of the MR contribution for each *potential* underdense usable trail begins with the calculation of $q_{sm}^{LU}(\rho_s^L, v_m^L, L^*, \tau^*)$ from Eq. 3.3 followed by the calculation of the corresponding minimum mass from Eq. 3.1a. The burst duration contribution to the DC value is determined for

19. V. A. Bronshten, *Physics of Meteoric Phenomena*, Table 23, D. Reidel, Boston, 1983, p. 217.

all line density values $q > q_{sm}^{LU}(\rho_s^L, \mathbf{v}_m^L, L^*, \tau^*)$. In other words, q is known and $\tau_{sm}^{LO}(\rho_s^L, \mathbf{v}_m^L, L^*, \tau^*)$ must be determined from

$$\tau_{sm}^{LO}(\rho_s^L, \mathbf{v}_m^L, L^*, \tau^*) = \frac{1}{a_2^{LU}} \left[\ln(l^* q^2 / a_1^{LU}) - a_3^{LU} \right] \quad (3.9)$$

which gives the received power duration above P_r^* for a meteor trail meeting the observability criteria $(\rho_s^L, \mathbf{v}_m^L)$.

Overdense Trail-Scatter Model

Once the minimum underdense line density $q_{sm}^{LU}(\rho_s^L, \mathbf{v}_m^L, L^*, \tau^*)$ is computed, both Versions 1.0 and 1.0V compute the transition line density to the overdense trail model. This transition has been shown [20] to achieve a maximum value of

$$q_{sm}^T = \frac{2\sqrt{\pi} \sin(\gamma_{sm}) r_0 \Phi_{sm}^T}{\lambda r_e} \quad (3.10)$$

where Φ_{sm}^T is the amount of phase error imparted to the propagating wave within the trail. The threshold value chosen for Φ_{sm}^T signifies the amount of phase error induced by multiple scattering permitted before the overdense model is determined to be applicable. Thus, both PC METEORLINK Versions 1.0 and 1.0V compute q_{sm}^T and $q_{sm}^{LU}(\rho_s^L, \mathbf{v}_m^L, L^*, \tau^*)$. If $q_{sm}^{LU}(\rho_s^L, \mathbf{v}_m^L, L^*, \tau^*) \leq q_{sm}^T$, then

$$q_{sm}^*(\rho_s^L, \mathbf{v}_m^L, L^*, \tau^*) = q_{sm}^{LU}(\rho_s^L, \mathbf{v}_m^L, L^*, \tau^*)$$

and both underdense and overdense trails are considered adequate to meet the usability criteria. Otherwise, an overdense trail model is determined to produce all usable trails meeting the observability criteria.

In PC METEORLINK Version 1.0, the overdense trail scatter coefficients are given by

$$a_1^{LO} = \frac{32\pi^2}{r_e^2 \lambda^2} r_1 r_2 (r_1 + r_2) \sin^2(\gamma_{sm}) \quad (3.11a)$$

$$a_2^{LO} = 4 \cos^2(\phi_s) D \quad (3.11b)$$

$$a_3^{LO} = r_0^2 \cos^2(\phi_s) \quad (3.11c)$$

$$a_4^{LO} = \frac{\pi^2}{\lambda^2} r_e^2 \quad (3.11d)$$

with the classical expression for path loss given by

20. H. Brysk, "Electromagnetic scattering from high-density meteor trails," *IRE Trans. Ant. Prop.*, AP-7, December 1959, pp. S330-S336.

$$L_{sm}^O(t) = \left[a_1^{LO} \sqrt{(a_2^{LO} t + a_3^{LO}) \ln \left(\frac{a_4^{LO} q}{a_2^{LO} t + a_3^{LO}} \right)} \right]^{-1} \quad (3.12)$$

Refraction in the underdense portion of the trail surrounding the overdense column reduces the scattered power [21]. This effect has been approximated in PC METEORLINK Version 1.0V by replacing $\sin^2(\gamma_{sm}) = 1 - \sin^2(\phi_s) \cos^2(\beta_{sm})$ with $1 - \sin^\xi(\phi_s) \cos^2(\beta_{sm})$ in Eq. 3.11a and $\cos^2(\phi_s)$ in Eqs. 3.11b and 3.11c with $\cos^\xi(\phi_s)$, where $\xi = 0.3$ for $\beta_{sm} = 0^\circ$ and $\xi = 1.7$ for $\beta_{sm} = 90^\circ$. The Version 1.0V program interpolates the remaining values of ξ in $[0^\circ, 90^\circ]$ from the expression $\xi = 2.0 - 1.7 \cos(\beta_{sm})$. In a recent development, empirical evidence suggests that ξ is better approximated by $\xi = 2.0 - 1.7 \cos^3(\beta_{sm})$ [22]. The coefficients for the overdense trail model used by Version 1.0V are given by

$$a_1^{LO} = \frac{32\pi^2}{r_e^2 \lambda^2} r_1 r_2 (r_1 + r_2) [1 - \sin^\xi(\phi_s) \cos^2(\beta_{sm})] \quad (3.13a)$$

$$a_2^{LO} = 4 \cos^\xi(\phi_s) D \quad (3.13b)$$

$$a_3^{LO} = r_0^2 \cos^\xi(\phi_s) \quad (3.13c)$$

$$a_4^{LO} = \frac{\pi^2}{\lambda^2} r_e \quad (3.13d)$$

These coefficients are used in Eq. 3.12 to compute the maximum allowable path loss to meet the usability requirements

The classic overdense trail model yields burst durations far in excess of measured values [23]. Both versions of the PC METEORLINK program account for the effects of neutral particle attachment to reduce these predicted values to observed quantities. In other words, the line density q decays exponentially with time according to

$$q = q_{sm}^{LO} \exp(-\beta_A n_A t) \quad (3.14)$$

where

β_A = attachment rate determined from atmospheric measurements at the trail scatter point

n_A = volume density of neutral particles involved in the attachment process at the scatter point

Typical values for the product $\beta_A n_A$ vary between 0.005 and 0.015.

21. L. A. Manning, "Oblique echoes from over-dense meteor trails," *J. Atmos. Terr. Phys.*, Vol. 14, April 1959, pp. 82-93.

22. D. Meisel, *personal communication*.

23. D. W. R. McKinley, *Ibid.*, p. 217.

The MAPL value for the modified overdense trail can then be computed from the propagation path *gain* function

$$g(t) = [I_{sm}^o(t)]^{-1} = a_1^{LO} \sqrt{(a_2^{LO} t + a_3^{LO}) \ln \left(\frac{a_4^{LO} q_{sm}^{LO} \exp(-\beta_A n_A t)}{a_2^{LO} t + a_3^{LO}} \right)} = a_1^{LO} f^{1/2} \quad (3.15)$$

where $f^{1/2} = \sqrt{(a_2^{LO} t + a_3^{LO}) \ln \left(\frac{a_4^{LO} q_{sm}^{LO} \exp(-\beta_A n_A t)}{a_2^{LO} t + a_3^{LO}} \right)}$. Eq. 3.15 is a transcendental function in the

time variable t , thus complicating the calculation of the line density q_{sm}^{LO} such that a maximum MAPL value of L^* dB is achieved for at least τ^* seconds. In both PC METEORLINK Versions 1.0 and 1.0V, therefore, Eq. 3.15 is approximated by a three-term Taylor's series expansion of Eq. 3.15 about the time t_{max}^{LO} at which $g(t)$ given by Eq. 3.15 is maximized, that is, the MAPL value is minimized and maximum trail-scattered power is received from an overdense trail. The time t_{max}^{LO} is found using Newton's method to find the single root of the expression

$$\left. \frac{dg}{dt} \right|_{t=t_{max}^{LO}} = \frac{1}{2} a_1^{LO} f^{-1/2} \left. \frac{df}{dt} \right|_{t=t_{max}^{LO}} = 0 \quad (3.16a)$$

or

$$\left. \frac{df}{dt} \right|_{t=t_{max}^{LO}} = a_2^{LO} \ln \left(\frac{a_4^{LO} q_{sm}^{LO} \exp(-\beta_A n_A t_{max}^{LO})}{a_2^{LO} t_{max}^{LO} + a_3^{LO}} \right) - a_2^{LO} t_{max}^{LO} - (a_2^{LO} + a_3^{LO}) = 0 \quad (3.16b)$$

The Taylor's series approximation $g(t)$ becomes

$$g(t) \cong g(t_{max}^{LO}) + \left. \frac{dg}{dt} \right|_{t=t_{max}^{LO}} (t - t_{max}^{LO}) + \frac{1}{2} \left. \frac{d^2 g}{dt^2} \right|_{t=t_{max}^{LO}} (t - t_{max}^{LO})^2 \quad (3.17a)$$

or since $\left. \frac{dg}{dt} \right|_{t=t_{max}^{LO}} = 0$ at $t = t_{max}^{LO}$, Eq. 3.17a reduces to the concave-down parabola defined by

$$g(t) \cong g(t_{max}^{LO}) + \frac{1}{2} \left. \frac{d^2 g}{dt^2} \right|_{t=t_{max}^{LO}} (t - t_{max}^{LO})^2 \quad (3.17b)$$

which is symmetric about $t = t_{max}^{LO}$. This second order expansion requires the second derivative of $g(t)$ given by

$$\frac{d^2 g}{dt^2} = \frac{1}{2} a_1^{LO} \left(f^{-1/2} \frac{d^2 f}{dt^2} - \frac{1}{2} f^{-3/2} \frac{df}{dt} \right) \quad (3.18a)$$

where

$$\frac{d^2 f}{dt^2} = -a_2^{LO} \left(\beta_A n_A + \frac{a_2^{LO}}{a_2^{LO} t + a_3^{LO}} + 1 \right) \quad (3.18b)$$

The parabolic approximation in Eq. 3.18b achieves the desired value $g^* = 1/l^*$ at the two times t_1 and t_2 such that

$$g(t_1) = g\left(t_{\max}^{LO} - \frac{\tau^*}{2}\right) = g^* \text{ and } g(t_2) = g\left(t_{\max}^{LO} + \frac{\tau^*}{2}\right) = g^*$$

Substituting either t_1 or t_2 into Eq. 3.17b yields

$$g^* = g(t_{\max}^{LO}) + \frac{1}{8} \frac{d^2 g}{dt^2} \bigg|_{t=t_{\max}^{LO}} (\tau^*)^2 \quad (3.19)$$

The duration of the received signal above P_r^* , that is, the duration of the minimum path gain value at or above g^* , is then given by

$$\tau_{sm}^{LO} = \sqrt{8 \left[g^* - g(t_{\max}^{LO}) \right] \bigg/ \frac{d^2 g}{dt^2} \bigg|_{t=t_{\max}^{LO}}} \quad (3.20)$$

Given the overdense line density q , Eq. 3.20 determines the corresponding burst duration above P_r^* .

4. MB LINK PERFORMANCE

4.1 Meteor Rate

In the Version 1.0 program, the arrival rate of meteors meeting the observability and usability criteria, $(\rho_s^s, \hat{\mathbf{v}}_m^L)$ and (L^*, τ^*) , respectively, is given by

$$\dot{N} = \int_{x_L^L}^{x_L^u} \int_{y_L^L}^{y_L^u} \int_{z_L^L}^{z_L^u} \int_{\alpha_M^L}^{\alpha_M^u} B_s(z_L) Q_{\alpha\beta}^* \left(\rho_s^s, \hat{\mathbf{v}}_m^L, L^*, \tau^* \right) |\hat{\mathbf{v}}_{m3}^L \sin(\alpha_M)| d\alpha_M dz_L dy_L dx_L \quad (4.1a)$$

where

$$Q_{\alpha\beta}^* = (s-1) X_{sp} \left(q_{0z}, \hat{\mathbf{v}}_m^O \right) \int_{v_L q_{sm}^*}^{v_u} \int_{\hat{\mathbf{v}}_m^L}^{\infty} \frac{p_{v_a, \hat{\mathbf{v}}_m^L}(v, \hat{\mathbf{v}}_m^L)}{p_{\hat{\mathbf{v}}_m^L}(\hat{\mathbf{v}}_m^L)} \left[\frac{q_{0z}}{\cos(\chi_{sm})} \right]^{s-1} q^{-s} dq dv \quad (4.1b)$$

with $q_{sm}^* = q_{sm}(\rho_s^s, \hat{\mathbf{v}}_m^O, L^*, \tau^*)$ and

x_L^u = maximum value of x_L for modeled scatter points above (x_L, y_L) in the L plane, serving as the upper limit for down-range integration of link-usable sporadic meteor flux values

y_L^l = minimum value of y_L for modeled scatter points above (x_L, y_L) , serving as the lower limit on cross-range integration of link-usable sporadic meteor flux values

y_L^u = maximum value of y_L , serving as the upper limit on cross-range integration of link-usable sporadic meteor flux values

α_m^l = minimum value of trail orientation angle α_m in the M plane determined by β_s ($\alpha_m^l = \pi$)

α_m^u = maximum value of α_m determined by β_s ($\alpha_m^u = 2\pi$)

q_{sm}^* = minimum required trail line density meeting the observability requirement $(\rho_s^L = \langle x_L, y_L, z_L \rangle, \hat{v}_m^O = \hat{f}(x_L, y_L, z_L, \alpha_m))$, where \hat{f} is a vector-valued function, as well as the usability requirements (L^*, τ^*)

q_{sm}^T = trail line density threshold corresponding to the observability requirement $(\rho_s^L = \langle x_L, y_L, z_L \rangle, \hat{v}_m^O = \hat{f}(x_L, y_L, z_L, \alpha_m))$ as well as the signal wavelength λ .

Values for z_L^l and z_L^u are determined from the corresponding trail-scatter point height limits $h_s^l = 80$ km and $h_s^u = 120$ km above (x_L, y_L) are given by

$$z_L^l = \left[(R_E + h_s^l)^2 - x_L^2 - y_L^2 \right]^{1/2} - \left[R_E^2 - \left(\frac{d_{12}^L}{2} \right)^2 \right]^{1/2} \quad (4.2a)$$

and

$$z_L^u = \left[(R_E + h_s^u)^2 - x_L^2 - y_L^2 \right]^{1/2} - \left[R_E^2 - \left(\frac{d_{12}^L}{2} \right)^2 \right]^{1/2} \quad (4.2b)$$

with

$$d_{12}^L = |x_2^L - x_1^L|$$

where $\rho_1^L = (x_1^L, 0, 0)$ and $\rho_2^L = (x_2^L, 0, 0) = (-x_1^L, 0, 0)$ are the x_L -axis points along the zenith to antenna sites $j = 1, 2$ and R_E is the earth's radius. The parameter $X_{sp}(q_{0z}, \hat{v}_m^O)$ is the total flux of meteors (number/km²/steradian/minute) producing a zenith line density $q_{0z} = 4.9 \times 10^{12}$ electrons

per meter with trail direction vector $\hat{\mathbf{v}}_m^0$. These tabular values were determined [24] from radar measurements [25] performed in the former Soviet Union at Kazan (earth coordinates) and at Mogadishu (earth coordinates) in Somalia [26]. The zenith line density is as the line density of a trail formed by the parent meteor traveling vertically downward.

The term $B_s(z_L)$ in Eq. 4.1a accounts for transformation of the integration over solid angle into an integration over height z_L and angle α_M . This transformation yields the expressions [27]

$$B_s(z_L) = \beta_1 - \beta_2 = \frac{\beta_1''}{b_r} - \frac{(\hat{r}_{L13} + \hat{r}_{L23})(b_3 - b_2 - b_1)}{b_r^3} \quad (4.3a)$$

$$\beta_1'' = \frac{1 - (\hat{r}_{L13})^2}{r_1} + \frac{1 - (\hat{r}_{L23})^2}{r_2} \quad (4.3b)$$

$$b_1 = (\hat{r}_{L11} + \hat{r}_{L21}) \left(\frac{\hat{r}_{L11} \hat{r}_{L13}}{r_1} + \frac{\hat{r}_{L21} \hat{r}_{L23}}{r_2} \right)$$

$$b_2 = (\hat{r}_{L12} + \hat{r}_{L22}) \left(\frac{\hat{r}_{L12} \hat{r}_{L13}}{r_1} + \frac{\hat{r}_{L22} \hat{r}_{L23}}{r_2} \right)$$

$$b_3 = (\hat{r}_{L13} + \hat{r}_{L23}) \beta_1''$$

$$b_r = |\hat{\mathbf{r}}_{L1} + \hat{\mathbf{r}}_{L2}|$$

$$\hat{r}_{L11} = \frac{x_L - x_1^L}{r_1} \quad \hat{r}_{L21} = \frac{x_L - x_2^L}{r_2}$$

$$\hat{r}_{L12} = \frac{x_L}{r_1} \quad \hat{r}_{L22} = \frac{y_L}{r_2}$$

$$\hat{r}_{L13} = \frac{z_L}{r_1} \quad \hat{r}_{L23} = \frac{z_L}{r_2}$$

and the R-vector magnitudes

$$r_j = \sqrt{(x_L - x_j^L)^2 + y_L^2 + z_L^2} \quad j = 1, 2$$

24. J. A. Pupyshv, Methods of statistical examination of varying sporadic meteor burst radiant density (SMRD) over the celestial sphere, *Radiowave Meteor Propagation*, Kazan State U. P., Vol. 15, Kazan, Russia, 1980, Technical Information Service, American Institute of Aeronautics and Astronautics, Document A82-16532 (in Russian).

25. O. I. Belkovic and J. A. Pupyshv, The variation of sporadic meteor radiant density and the mass law exponent over the Celestial Sphere, *Physics and Dynamics of Meteors*, R. Kresak and P. M. Millman, eds., pp. 373-381, D. Reidel, Dordrecht, Holland, 1968.

26. N. T. Svetashkova, Density variations of meteor flux along the earth's orbit, *Middle Atmospheric Program: Handbook for MAP*, Vol. 25, R. G. Roper (ed.), Government Printing Office, Washington, DC, August 1987, pp. 311-320.

27. R. I. Desourdis, *Ibid.*, pp. 144-146.

where the R-vectors are defined by

$$\mathbf{r}_j = \langle (x_L, y_L, z_L) - (x_j^L, y_j^L, z_j^L) \rangle, \text{ for } j = 1, 2$$

and the trail scatter point $\rho_s^L = (x_L, y_L, z_L)$ and the antenna coordinates (x_1^L, y_1^L, z_1^L) and $(x_{2j}^L, y_{2j}^L, z_{2j}^L)$. The meteor speed integration limits v_l and v_u are bounded by 11 km/s and 75 km/s, respectively.

The PC METEORLINK Version 1.0 program uses a meteor velocity distribution consisting of single values of average meteor speed for each value of radiant elongation angle ε . In symbols

$$p_{v_a, \hat{\mathbf{v}}_m^L}(v_a, \hat{\mathbf{v}}_m^L) = c_a n(\varepsilon) \delta_D[v - \bar{v}(\varepsilon)] \quad (4.4)$$

where $\bar{v}(\varepsilon)$ is the average geocentric meteor speed at elongation e and δ_D is the Dirac delta function. The use of this approximate velocity distribution in Eq. 4.1b permits simplification in the expression for $Q_{\alpha\beta}^*$ as follows

$$\begin{aligned} Q_{\alpha\beta}^* &= (s-1) X_{sp}(q_{0z}, \hat{\mathbf{v}}_m^O) \int_{v_l}^{v_u} \int_{q_{sm}^*}^{\infty} \frac{p_{v_a, \hat{\mathbf{v}}_m^L}(v, \hat{\mathbf{v}}_m^L)}{p_{\hat{\mathbf{v}}_m^L}(\hat{\mathbf{v}}_m^L)} \left[\frac{q_{0z}}{\cos(\chi_{sm})} \right]^{s-1} q^{-s} dq dv \\ &= X_{sp}(q_{0z}, \hat{\mathbf{v}}_m^O) \int_{v_l}^{v_u} \frac{p_{v_a, \hat{\mathbf{v}}_m^L}(v, \hat{\mathbf{v}}_m^L)}{p_{\hat{\mathbf{v}}_m^L}(\hat{\mathbf{v}}_m^L)} \left[\frac{q_{0z}}{q_{sm}^* \cos(\chi_{sm})} \right]^{s-1} dv \\ &= X_{sp}(q_{0z}, \hat{\mathbf{v}}_m^O) \int_{v_l}^{v_u} \frac{c_a n(\varepsilon) \delta_D[v - \bar{v}(\varepsilon)]}{c_a n(\varepsilon)} \left[\frac{q_{0z}}{q_{sm}^* \cos(\chi_{sm})} \right]^{s-1} dv \\ &= X_{sp}(q_{0z}, \hat{\mathbf{v}}_m^O) \int_{v_l}^{v_u} \delta_D[v - \bar{v}(\varepsilon)] \left[\frac{q_{0z}}{q_{sm}(\rho_s^S, v \hat{\mathbf{v}}_m^L, L^*, \tau^*) \cos(\chi_{sm})} \right]^{s-1} dv \\ &= X_{sp}(q_{0z}, \hat{\mathbf{v}}_m^O) \left[\frac{q_{0z}}{q_{sm}(\rho_s^S, \bar{v}(\varepsilon) \hat{\mathbf{v}}_m^L, L^*, \tau^*) \cos(\chi_{sm})} \right]^{s-1} \end{aligned} \quad (4.5)$$

where $q_{sm}^* = q_{sm}(\rho_s^S, \mathbf{v}_m^L, L^*, \tau^*) = q_{sm}(\rho_s^S, v \hat{\mathbf{v}}_m^L, L^*, \tau^*)$. Finally, the mass-rate exponent used in the Version 1.0 program was determined from

$$s = 1.9 + 0.12\varepsilon + 0.01\varepsilon^2$$

where ε is the elongation angle.

The term $X_{sp}(q_{0z}, \hat{\mathbf{v}}_m^0)$ can be converted to the sporadic meteor flux $\Theta_{sp}(m_{0z}, \hat{\mathbf{v}}_m^0)$ is the rate of sporadic meteors exceeding the minimum mass $m_0 = m_{0z} / \cos(\chi_{sm})$ with radiant $\hat{\mathbf{v}}_m^L$ (zenith angle χ_{sm}) arriving per square kilometer per steradian per minute. The complete distribution of sporadic radiants $\Theta_{sp}(m_{0z}, \hat{\mathbf{v}}_m^0)$ over the Celestial Sphere is shown in the appendix for each month. Given this distribution, it is then possible to express the MR value in PC METEORLINK Version 1.0V as

$$\dot{N} = \int_{x_L^l}^{x_L^u} \int_{y_L^l}^{y_L^u} \int_{z_L^l}^{z_L^u} \int_{\alpha_M^l}^{\alpha_M^u} B_s(z_L) Q_{\alpha\beta}^* \left(\rho_s^S, \hat{\mathbf{v}}_m^L, L^*, \tau^* \right) \left| \hat{\mathbf{v}}_m^L \sin(\alpha_M) \right| d\alpha_M dz_L dy_L dx_L \quad (4.6a)$$

where

$$\begin{aligned} Q_{\alpha\beta}^* &= (s-1) \Theta_{sp}(m_{0z}, \hat{\mathbf{v}}_m^0) \int_{v_l}^{v_u} \int_{m_{sm}^*}^{\infty} \frac{p_{v, \hat{\mathbf{v}}_m^L}(v, \hat{\mathbf{v}}_m^L)}{P_{\hat{\mathbf{v}}_m^L}(\hat{\mathbf{v}}_m^L)} m_0^{s-1} m^{-s} dm dv \\ &= \Theta_{sp}(m_{0z}, \hat{\mathbf{v}}_m^0) \int_{v_l}^{v_u} \frac{p_{v, \hat{\mathbf{v}}_m^L}(v, \hat{\mathbf{v}}_m^L)}{P_{\hat{\mathbf{v}}_m^L}(\hat{\mathbf{v}}_m^L)} \left(\frac{m_0}{m_{sm}^*} \right)^{s-1} dv \\ &= \Theta_{sp}(m_{0z}, \hat{\mathbf{v}}_m^0) \int_{v_l}^{v_u} \frac{p_{v, \hat{\mathbf{v}}_m^L}(v, \hat{\mathbf{v}}_m^L)}{P_{\hat{\mathbf{v}}_m^L}(\hat{\mathbf{v}}_m^L)} \left[\frac{m_0}{m_{sm}(\rho_s^S, v \hat{\mathbf{v}}_m^L, L^*, \tau^*)} \right]^{s-1} dv \end{aligned} \quad (4.6b)$$

with

$$m_{sm}^* = m_{sm}(\rho_s^S, v \hat{\mathbf{v}}_m^L, L^*, \tau^*) \quad (4.7)$$

and the velocity distribution is given by Eq. 2.1.

Both Versions 1.0 and 1.0V of PC METEORLINK used Gauss quadrature to integrate the expressions for arrival rate, \dot{N} , or MR value. In general, both programs compute the quadrature formula from

$$I\{f\} = \int_{u_1}^{u_2} f(u) du$$

can be approximated by quadrature formula of the form

$$I_N\{f\} = \sum_i^{N_u} w_i f(u_i)$$

where the N_u coefficients w_i and corresponding points u_i are chosen to minimize the quadrature error $|I\{f\} - I_N\{f\}|$. Applying this quadrature formula to approximate the MR-value integration in PC METEORLINK Version 1.0 yields

$$\dot{N} = \sum_i^{N_x} \sum_j^{N_y} \sum_k^{N_z} \sum_l^{N_\alpha} w_i w_j w_k w_l \delta^4 \dot{N}(x_i, y_j, z_k, \alpha_l) \quad (4.8a)$$

where

$$\delta^4 \dot{N}(x_i, y_j, z_k, \alpha_l) = B_s(z_k) Q_{\alpha\beta}^* |\hat{v}_{m3}^L \sin(\alpha_m)| \quad (4.8b)$$

The L-system notation for the values x_i, y_j , and z_k is assumed as well as M-system notation for α_l . The elements $Q_{\alpha\beta}^*$, $B_s(z_k)$, and \hat{v}_{m3}^L are functions of x_i, y_j, z_k , and α_l . The calculation values x_i, y_j, z_k , and α_l for quadrature are defined by

$$\begin{aligned} x_i: x_L^l \leq x_i \leq x_L^u \text{ for } i = 1, 2, \dots, N_x \\ y_j: y_L^l \leq y_j \leq y_L^u \text{ for } j = 1, 2, \dots, N_y \\ z_k: z_L^l \leq z_k \leq z_L^u \text{ for } k = 1, 2, \dots, N_z \\ \alpha_l: \alpha_m^l (= \pi) \leq \alpha_l \leq \alpha_m^u (= 2\pi) \text{ for } l = 1, 2, \dots, N_\alpha \end{aligned}$$

The values for x_i, y_j, z_k , and α_l , and the corresponding coefficient weights w_i, w_j, w_k , and w_l are specified according to the requirements imposed by the quadrature technique, or techniques, employed.

PC METEORLINK Version 1.0V employs similar quadrature formula as the Version 1.0 program with the addition of the meteor speed integration. The MR value computed by the Version 1.0V program is given by

$$\dot{N} = \sum_i^{N_x} \sum_j^{N_y} \sum_k^{N_z} \sum_l^{N_\alpha} \sum_p^{N_v} w_i w_j w_k w_l w_p \delta^5 \dot{N}(x_i, y_j, z_k, \alpha_l, v_p) \quad (4.9a)$$

where the integration limits, quadrature points, and numbers of points are identical in meaning to the Version 1.0 program and

$$v_p: v_a^l \leq v_p \leq v_a^u \text{ for } p = 1, 2, \dots, N_v$$

define the integration limits and point for meteor speed. The function $Q_{\alpha\beta}^*$ is given by Eq. 4.6b, however, rather than Eq. 4.5.

The "ratio of q values" approach founded on Eq. 4.5 was employed in PC METEORLINK Version 1.0 (translated VAX version). It is apparent from Figure 2.1, however, that the velocity density function is not well characterized at all elongation angles by a single-valued function. As a result, the ratio of m values $(m_0/m_{sm}^*)^{s-1}$ varies with velocity and is scaled by the probability ratio $p_{v_a, \hat{v}_m^L}(v_a, \hat{v}_m^L)/p_{\hat{v}_m^L}(\hat{v}_m^L)$ determined from the empirical velocity density function shown in Figure 2.1. For this reason, Version 1.0V of the PC METEORLINK program was developed to employ a more realistic model of the meteor velocity distribution in predicting MB link MR and DC values using Eq. 4.6b.

4.2 Duty Cycle

The percent of time for which the received trail-scattered signal exceeds P^* , defines the MB link DC value. Given the minimum electron line density q_{sm}^* , the PC METEORLINK Version 1.0 program computes this DC value as

$$\dot{T} = \int_{x_L^l}^{x_L^u} \int_{y_L^l}^{y_L^u} \int_{z_L^l}^{z_L^u} \int_{\alpha_M^l}^{\alpha_M^u} B_s(z_L) \left[\int_{q_{sm}^*}^{q_{sm}^T} m_q(q) \tau_q^U(q) dq + \int_{q_{sm}^T}^{\infty} m_q(q) \tau_q^O(q) dq \right] d\alpha_M dz_L dy_L dx_L \quad (4.10a)$$

where

$$m_q(q) = (1-s) X_m(\hat{v}_m^O) \left[q_{0z} \cos(\chi_{sm}) \right]^{s-1} |\hat{v}_{m3}^L \sin(\alpha_m)| q^{-s} \quad (4.10b)$$

for $q_{sm}^* \leq q_{sm}^T$, and

$$\dot{T} = \int_{x_L^l}^{x_L^u} \int_{y_L^l}^{y_L^u} \int_{z_L^l}^{z_L^u} \int_{\alpha_M^l}^{\alpha_M^u} B_s(z_L) \int_{q_{sm}^*}^{\infty} m_q(q) \tau_q^O(q) dq d\alpha_M dz_L dy_L dx_L \quad (4.11)$$

for $q_{sm}^* > q_{sm}^T$. The parameter $X_m(\hat{v}_m^O)$ is the flux of meteors with trail unit vector \hat{v}_m^O in the ORBITAL system producing trails with minimum zenith line density of $q_{0z} = 4.9 \times 10^{12}$ electrons per meter.

In Version 1.0V of the PC METEORLINK program, the q integrations are replaced by the double integral of meteor speed v and mass m . Since the meteor mass m_{sm} can be represented as the product $m_{sm} = C_{sm} q_{sm}$, then burst duration $\tau_q(q) = \tau_q[m / C(P_s^S, \mathbf{v}_m^L)] = \tau_m(m)$ and the Version 1.0V expression for the DC value becomes

$$\dot{T} = \int_{x_L^l}^{x_L^u} \int_{y_L^l}^{y_L^u} \int_{z_L^l}^{z_L^u} \int_{\alpha_M^l}^{\alpha_M^u} B_s(z_L) \int_{v_l}^{v_u} \frac{P_{v_a, \hat{v}_m^L}(v, \hat{v}_m^L)}{P_{\hat{v}_m^L}(\hat{v}_m^L)} \left[\int_{m_{sm}^*}^{m_{sm}^T} m_m(m) \tau_m^U(m) dm + \int_{m_{sm}^T}^{\infty} m_m(m) \tau_m^O(m) dm \right] dv d\alpha_M dz_L dy_L dx_L \quad (4.12a)$$

where

$$m_m(m) = (s-1) m_0^{s-1} \Theta_{sp}(m_{0z}, \hat{v}_m^L) |\hat{v}_{m3}^L \sin(\alpha_m)| m^{-s} \quad (4.12b)$$

and $m_{sm}^* = m_{sm}(\rho_s^S, v_{\hat{v}_m^L}, L^*, \tau^*) \leq m_{sm}^T$, the threshold value of mass such that $m_{sm}^T = C_{sm} q_{sm}^T$. If $m_{sm}^* > m_{sm}^T$, then

$$\dot{T} = \int_{x_L^l}^{x_L^u} \int_{y_L^l}^{y_L^u} \int_{z_L^l}^{z_L^u} \int_{\alpha_M^l}^{\alpha_M^u} B_s(z_L) \int_{v_l}^{v_u} \frac{P_{v_a, \hat{v}_m^L}(v, \hat{v}_m^L)}{P_{\hat{v}_m^L}(\hat{v}_m^L)} \int_{m_{sm}^T}^{\infty} m_m(m) \tau_m^O(m) dm dv d\alpha_M dz_L dy_L dx_L \quad (4.13)$$

This result indicates that the burst duration contribution from a single meteor trail is theoretically independent of the Version 1.0 and Version 1.0V model algorithms. The rate of occurrence of meteors producing this duration differs between the two programs, however, because Version 1.0V employs the meteor flux $\Theta_{sp}(m_{0z}, \hat{v}_m^L)$ of meteors exceeding a minimum mass while Version 1.0 uses the flux $X_{sp}(q_{0z}, \hat{v}_m^O)$ of meteors producing trails exceeding a minimum electron line density.

The numerical quadrature employed by PC METEORLINK Version 1.0 to compute the DC value is given by

$$\dot{T} = \sum_i^{N_x} \sum_j^{N_y} \sum_k^{N_z} \sum_l^{N_\alpha} w_i w_j w_k w_l B_s(z_k) \left[\sum_{n_U}^{N_U} w_{n_U} m_q(q_{n_U}) \tau_q^U(q_{n_U}) + \sum_{n_O}^{N_O} w_{n_O} m_q(q_{n_O}) \tau_q^O(q_{n_O}) \right] \quad (4.14a)$$

for $q_{sm}^* \leq q_{sm}^T$ and

$$\dot{T} = \sum_i^{N_x} \sum_j^{N_y} \sum_k^{N_z} \sum_l^{N_\alpha} w_i w_j w_k w_l B_s(z_k) \sum_{n_O}^{N_O} w_{n_O} m_q(q_{n_O}) \tau_q^O(q_{n_O}) \quad (4.14b)$$

for $q_{sm}^* > q_{sm}^T$. As in the MR quadrature, the L-system notation for the values x_i, y_j , and z_k is assumed as well as M-system notation for α_l . The elements $B_s(z_k)$, $m_q(q_{n_U} \text{ or } q_{n_O})$, $\tau_q^U(q_{n_U})$, $\tau_q^O(q_{n_O})$, and \hat{v}_m^L in Eqs. 4.14 are functions of x_i, y_j, z_k , and α_l . The calculation values x_i, y_j, z_k , and α_l for quadrature were defined for the MR calculation while q_{n_U} and q_{n_O} are defined by

$$q_{n_U}: q_{sm}^* \leq q_{n_U} \leq q_{sm}^T \text{ for } n_U = 1, 2, \dots, N_U$$

and

$$q_{n_O}: q_{sm}^T \leq q_{n_O} \leq q_{max}^O \text{ for } n_O = 1, 2, \dots, N_O$$

if $q_{sm}^* \leq q_{sm}^T$, and

$$q_{n_O}: q_{sm}^* \leq q_{n_O} \leq q_{max}^O \text{ for } n_O = 1, 2, \dots, N_O$$

if $q_{sm}^* > q_{sm}^T$, where q_{max}^O is a suitably large value of electron line density such that the corresponding MR contribution is negligible, for example, $q_{max}^O = 1 \times 10^{20}$ epm. The values for q_{n_U} and q_{n_O} and the corresponding coefficient weights w_{n_U} and w_{n_O} are specified according to the requirements imposed by the specific quadrature technique employed. PC METEORLINK uses Gauss quadrature for all numerical integrations.

The Version 1.0V of PC METEORLINK program adds a sixth quadrature to account for the integration over meteor speed v . Using the expression $m_{sm} = C_{sm} q_{sm}$ and the definitions of q integration points, define the meteor mass integration points

$$m_{n_U}: m_{sm}^* \leq m_{n_U} \leq m_{sm}^T \text{ for } n_U = 1, 2, \dots, N_U$$

and

$$m_{n_o}: m_{sm}^T \leq m_{n_o} \leq m_{\max}^O \text{ for } n_o = 1, 2, \dots, N_o$$

if $m_{sm}^* \leq m_{sm}^T$ and

$$m_{n_o}: m_{sm}^* \leq m_{n_o} \leq m_{\max}^O \text{ for } n_o = 1, 2, \dots, N_o$$

for $m_{sm}^* > m_{sm}^T$. The meteor speed integration points defined for the MR calculation are

$$v_p: v_a^l \leq v_p \leq v_a^u \text{ for } p = 1, 2, \dots, N_v$$

Combining the mass and speed quadrature in the DC calculation yields

$$\dot{T} = \sum_i^{N_x} \sum_j^{N_y} \sum_k^{N_z} \sum_l^{N_\alpha} w_i w_j w_k w_l B_s(z_k) \sum_p^{N_v} w_p \left[\sum_{n_U}^{N_U} w_{n_U} m_m(m_{n_U}) \tau_m^U(m_{n_U}) + \sum_{n_o}^{N_o} w_{n_o} m_m(m_{n_o}) \tau_m^O(m_{n_o}) \right] \quad (4.15)$$

for $m_{sm}^* \leq m_{sm}^T$ and

$$\dot{T} = \sum_i^{N_x} \sum_j^{N_y} \sum_k^{N_z} \sum_l^{N_\alpha} w_i w_j w_k w_l B_s(z_k) \sum_p^{N_v} w_p \sum_{n_o}^{N_o} w_{n_o} m_m(m_{n_o}) \tau_m^O(m_{n_o}) \quad (4.16)$$

for $m_{sm}^* > m_{sm}^T$.

SCIENTIFIC & TECHNICAL REPORT

(Theoretical Model)

September 5, 1995

Prepared by

**Communications Engineering Laboratory
Telecommunications and Information Systems Division
Science Applications International Corporation
261 Cedar Hill St., Bldg 'C'
Marlborough, Massachusetts 01752**

1. INTRODUCTION

1.1 Summary

This report presents work performed for the Phillips Laboratory by Science Applications International Corporation (SAIC) to convert its proprietary VAX-based METEORLINK meteor-burst computer model to software capable of operation on an IBM-compatible personal computer (PC). The VAX version of METEORLINK was written in FORTRAN 77 using several VAX VMS-unique features for I/O and pseudo-structured programming. The PC METEORLINK program was written in the Borland Turbo C++ language by directly translating the original FORTRAN source code. This translation was completed successfully and several test cases were performed using the VAX and PC versions driven by the same input parameters. These test cases demonstrated essentially identical results with the exception of insignificant numerical differences due to the different computing platforms. The initial PC translation of the VAX METEORLINK program was designated "Version 1.0" of the "PC METEORLINK" computer program.

SAIC sought to improve the MB modeling algorithms employed in the PC METEORLINK program, Version 1.0, by adding an empirical meteor velocity distribution, a meteor mass-based distribution of sporadic meteor flux, and several other improved algorithms. The addition of the meteor velocity distribution required the addition of additional integration loops for meteor speed for each modeled meteor radiant. This enhanced version of the PC METEORLINK program has been designated "Version 1.0V". A measurement-prediction comparison has been performed using Version 1.0V of the PC METEORLINK program with comparisons drawn to results obtained with the VAX METEORLINK program in several earlier publications [1, 2, 3]. The results of this comparison exhibit improvement of model behavior in several respects, but the amount of speed dependence produces distortion in the normal diurnal variation in excess of anticipated values. Although this distortion is apparent, and indicates that better empirical models should be considered, the overall model predictions represent an improvement over the Version 1.0 capability to accurately model the performance of an MB communications link.

METEORLINK Version 1.0V calibration and validation were performed with data taken from three MB-link measurement campaigns, including the Greenland Meteor Burst Test Bed [4], the Jodrell Bank Engineering Station [5] in the United Kingdom, and Kazan State University [6] in Russia. The results show that both Versions 1.0 and 1.0V of the PC METEORLINK program yield similar accuracy although the two models differ significantly in their calculation of the usable meteor rate (MR) and duty cycle (DC). The complete results of the Greenland Test Bed measurement-prediction comparison with

-
1. R. I. Desourdis, Jr., S. C. Merrill, J. H. Wojtaszek and K. Hernandez, Meteor burst link performance sensitivity to antenna pattern, power margin and range, *IEEE MILCOM'88 Conf. Proc.*, Vol. 1, October 1988, pp. 14.5.1-14.5.7.
 2. R. I. Desourdis, Jr., J. C. Ostergaard, and A. D. Bailey, "Meteor burst computer model validation using high-latitude measurements," *IEEE MILCOM'91 Conf. Proc.*, Vol. 2, McLean, Virginia, November 1991, pp. 22.1.1-22.1.5.
 3. R. I. Desourdis, et. al., "Advanced Meteor-Burst Radio for Multi-Media Communications," *IEEE MILCOM'94 Conf. Proc.*, Vol. 2, Ft. Monmouth, New Jersey, October 1994, pp. 685-689.
 4. R. I. Desourdis, Jr., V. V. Sidorov, A. V. Karpov, R. G. Huziashev, L. A. Epictetov, and D. W. Brown, "A Russian meteor burst communications experiment and measurement-prediction comparison," *IEEE MILCOM'92 Conf. Proc.*, Vol. 1, San Diego, October 1992, pp. 1.6.1-1.6.5.
 5. A. C. B. Lovell, *Meteor Astronomy*, University Press, Oxford, New York, 1954, pp. 112-115.
 6. R. I. Desourdis, Jr., V. V. Sidorov, A. V. Karpov, R. G. Huziashev, L. A. Epictetov, and D. W. Brown, *Ibid.*.

Version 1.0 and Version 1.0V predictions appear in Appendix A of a companion report [7]. A comparison of model prediction accuracy for the Greenland measurements alone is shown in Figure 1.1 and described in Section 4 of this report. Figures 1.2a and 1.2b are plots of the daily-average MR value measured at Jodrell Bank in 1950-51 with the corresponding Version 1.0 and 1.0V predictions. The complete set of month by month Jodrell Bank predictions are provided in of a companion report [7]. Although development of Version 1.0V was motivated in part due reduce the excessive METEORLINK prediction for the Autumn MR values, the effect was not altered by incorporating a more accurate meteor velocity distribution. Other physical parameters, such as the sporadic meteor flux density or meteor velocity distributions, may have produced or maintained this phenomena. Finally, MB measurements performed in Russia during April (radar) and May (forward scatter) were compared with Version 1.0V predictions as shown in the scatter plots of Figures 1.3a and 1.3b.

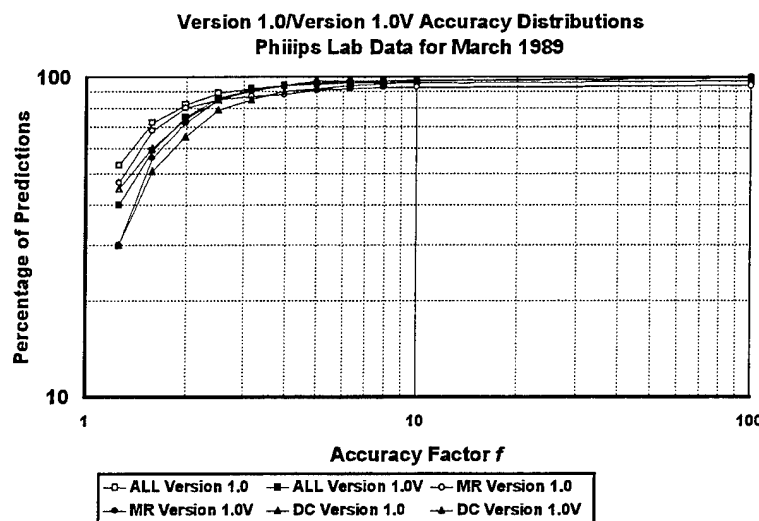


Figure 1.1 Greenland prediction accuracy comparison

There reports were written as part of this effort in addition to translation and modification of the original VAX FORTRAN version of METEORLINK. into a Turbo C++ program for the PC. The software is accompanied by a "User's Guide" addressing both Versions 1.0 and 1.0V of the PC METEORLINK program. It must be noted that the Version 1.0V files can be "read" by the Version 1.0 program, but use of Version 1.0 input files with Version 1.0V will lead to an I/O error. For example, the number of meteor speed integration points is a required input parameter, although the Version 1.0 program does not use this parameter. The second report describes many of the PC METEORLINK algorithms, particularly those which were altered in developing Version 1.0V from Version 1.0. Algorithms shared by both programs, particularly the development of the geometric model of meteor trail scatter,

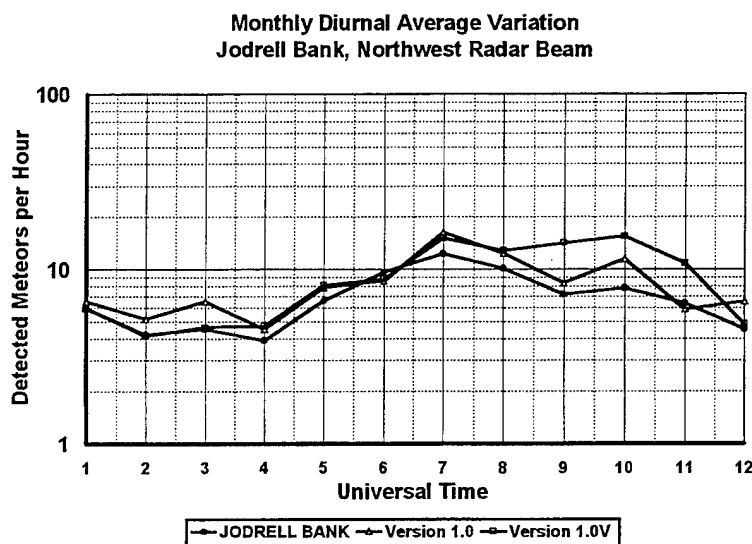


Figure 1.2a Monthly MR Comparison for the Northwest Beam

were referenced from a recent publication [8]. Finally, this report and the associated Appendices A and B of the companion report [7] present preliminary results from the measurement-prediction comparison performed using Phillips Lab data collected in Greenland and radar data collected in England at Jodrell Bank, respectively, as well as the Kazan measurements.

This report describes the algorithms employed in the PC METEORLINK Version 1.0 and 1.0V C++ computer programs used to produce the measurement-prediction comparison results described in this report and other publications [1, 2, 3]. The reader will note that many of the basic derivations assumed in this report were published elsewhere [7].

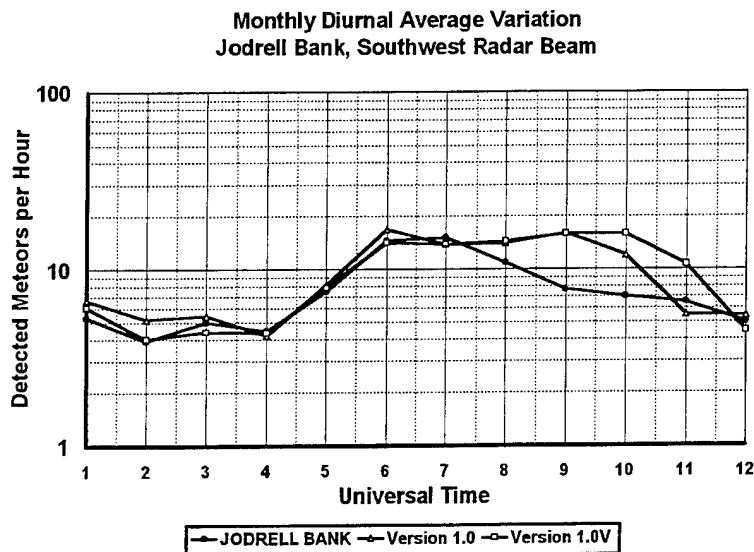


Figure 1.2b Monthly MR Comparison for the Southwest Beam

1.2 Background

This technical manual describes the algorithms employed in the PC METEORLINK computer program, Versions 1.0 and 1.0V. The "1.0V" Version employs "velocity-based" prediction algorithms intended to increase model fidelity and, ultimately, improve MB-link performance predictions. These algorithms include the integration of usable meteor rate with respect to meteor speed using an empirical distribution for meteor velocity. In addition, Version 1.0V replaces the Version 1.0 sporadic meteor distribution based on minimum electron line density with the corresponding distribution of sporadic meteors whose mass exceeds a minimum specified value. Finally, the height of maximum ionization is determined numerically as a function of meteor speed and maximum trail electron line density.

The PC METEORLINK program is authored in the C++ language and was originally translated directly from the FORTRAN 77 version developed for the VAX 3600. In other words, PC METEORLINK Version 1.0 is intended to reproduce the current VAX METEORLINK Version 1.40 results as closely as possible given the difference in platforms. An earlier version of the VAX METEORLINK program was provided to the Phillips Laboratory as part of a contract executed to calibrate and, subsequently, validate the VAX METEORLINK program. The measurements of meteor arrival rate (MR), duty cycle (DC), and other link-performance parameters used in this validation were extracted from the extensive meteor-burst data base collected in Greenland by the Phillips Laboratory [9]. In fact, a limited validation of the PC METEORLINK Version 1.0V program was performed using

8. R. I. Desourdis, "Modeling and Analysis of Meteor Burst Communications," Chapter 3, *Meteor Burst Communications: Theory and Practice*, John Wiley & Sons, New York, March, 1993, pp. 59-342.

9. *The RADC High Latitude Meteor Scatter Test Bed*, by J. C. Ostergaard, J. E. Rasmussen, M. J. Sowa, J. M. Quinn, and P. A. Kossey, RADC-TR-86-74 ADA180550, Hanscom Air Force Base, Massachusetts, July 1986, Unlimited Distribution.

a subset of the data employed in the original VAX METEORLINK validation. This Version 1.0V validation is described in a companion report [10].

1.3 Assumptions

This report uses symbols and definitions adopted by Chapter 3 of *Meteor Burst Communications: Theory and Practice* [11]. This book chapter provides a detailed derivation of the algorithms employed in the original VAX METEORLINK program as well as complete validation results not previously published. This report will not attempt to reproduce material presented in this book except to the extent that it is necessary to explain the differences between the PC METEORLINK Version 1.0V and Version 1.0. It will also be assumed that the reader is familiar with the terminology of meteor-burst communications, such as meteor rate, duty cycle, underdense meteor rate, etc. and the fundamentals of meteor astronomy and physics.

Appendix A in Chapter 3 of *Meteor Burst Communications: Theory and Practice* contains a complete development of useful coordinate systems for modeling MB links. In this report, only the LINK (L), METEOR (M), and ORBITAL coordinate systems defined in this reference will be employed. Many other coordinate systems are defined in this reference, but these three systems can be used to meet the objectives of this technical report. The L and M systems are used to determine the spatial orientations of meteor trails essential to effective radiowave scattering, i.e., *link-observable* meteor trails. The O system is used to represent these link-observable trails using the coordinate conventions used to define the incident flux of sporadic meteors and the meteor velocity distribution.

57.4-MHz Meteor Radar at Kazan in Russia
500 W, 5-El Yagi @ 327 deg, -114 dBm RSL

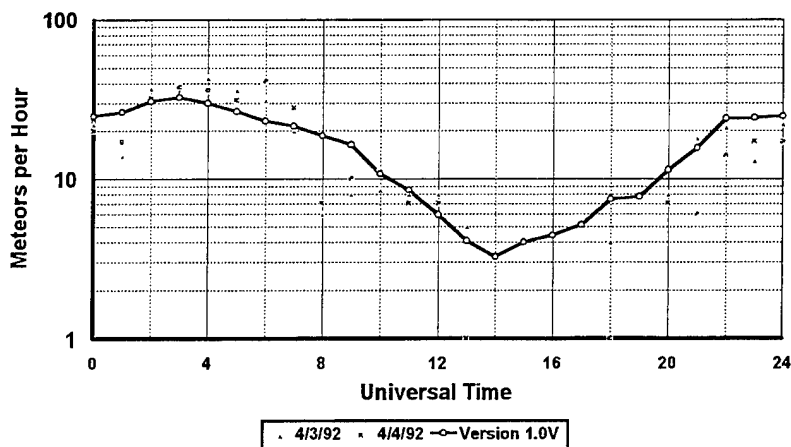


Figure 1.3a Kazan radar (backscatter) measurements

57.4-MHz Moscow-Kazan MB Link in Russia
700 W, 5-El Yagis, -114 dBm RSL

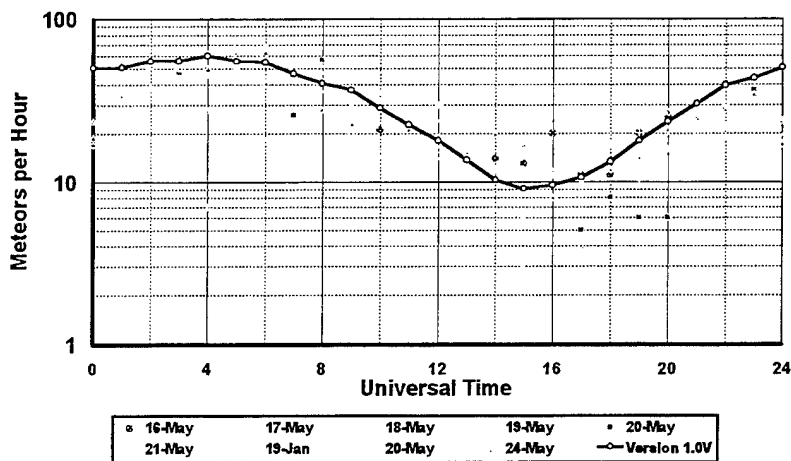


Figure 1.3b Moscow-Kazan forward-scatter MB link

10. Science Applications International Corporation, *Scientific and Technical Report*, Contract # F19628-93-C-0082, CDRL A003, Marlborough, Mass., September 1995.

11. R. I. Desourdis, "Modeling and Analysis of Meteor Burst Communications," Chapter 3, *Meteor Burst Communications: Theory and Practice*, John Wiley & Sons, New York, March, 1993, pp. 59-342.

2. ALGORITHM DEVELOPMENT

2.1 Technical Background

The development of the VAX METEORLINK computer program was described in a recent publication [12], with those model algorithms differing in Versions 1.0 and 1.0V of the PC METEORLINK described in a companion report [13]. This latter report presented the algorithms used in the PC METEORLINK program, but it did not explain how these algorithms were identified, evaluated, and ultimately selected for the model. This report describes this process, presents the results, and suggests further developments to improve model predictions. In addition, the first measurement-prediction comparison for validation of the PC METEORLINK Version 1.0V approach is also presented. Validation results for the VAX METEORLINK and PC METEORLINK Version 1.0 programs have been published in previous works [14].

2.2 Model Development

The development of any model purporting to mimic natural processes is often a combination of both theoretical and empirical algorithms. This combination is particularly necessary in the development of an MB channel model because most of the atmospheric and meteoric processes affecting MB communications are only knowable indirectly from measurement. In other words, theoretical models of radiowave scatter from meteor trails and associated atmospheric phenomena are suggested, developed, and validated from observed light and reflected radiowaves. As a result, there is significant uncertainty in both the validity of specific mathematical formulations derived from these measurements as well as the combination of formulations which produce the most accurate prediction of MB-link performance.

The principle meteoric parameters which govern the accuracy of METEORLINK Version 1.0V are the ionization coefficient, $\beta_I(v)$, the initial trail radius, $r_0(v, h_t)$, the diffusion rate, $D(h_t)$, the maximum ionization height, H_{\max} , the underdense/overdense electron line density threshold, q_{sm}^T , the mass-rate exponent, $s(\epsilon)$, and the minimum mass of the meteor flux density distribution, m_0 . Several expressions for the ionization coefficient have been developed, including

$$(1) \beta_I(v) = 2.6 \times 10^{-6} (v_{\text{kmps}} - 8.15)^3 \quad [15] \quad (2.1a)$$

$$(2) \beta_I(v) = 1.5 \times 10^{-21} v_{\text{cm/s}}^{3.12} \quad [16] \quad (2.1b)$$

$$(3) \beta_I(v) = 4.36 \times 10^{-24} v_{\text{cm/s}}^{3.42} \quad [5] \quad (2.1c)$$

$$(4) \beta_I(v) = 8.4 \times 10^{-7} (v_{\text{kmps}} - 8.8)^{3.5} \quad [5] \quad (2.1d)$$

12. R. I. Desourdis, "Modeling and Analysis of Meteor Burst Communications," Chapter 3, *Meteor Burst Communications: Theory and Practice*, John Wiley & Sons, New York, March, 1993, pp. 59-342.

13. Science Applications International Corporation, *R&D Equipment Information (User's Guide)*, Contract # F19628-93-C-0082, CDRL A005, Marlborough, Mass., September 1995..

14. R. I. Desourdis, Jr., J. C. Ostergaard, and A. D. Bailey, "Meteor burst computer model validation using high-latitude measurements," *IEEE MILCOM'91 Conf. Proc.*, Vol. 2, McLean, Virginia, November 1991, pp. 22.1.1-22.1.5.

15. R. I. Desourdis, Jr., V. V. Sidorov, A. V. Karpov, R. G. Huziashev, L. A. Epictetov, and D. W. Brown, "A Russian meteor burst communications experiment and measurement-prediction comparison," *IEEE MILCOM'92 Conf. Proc.*, Vol. 1, San Diego, October 1992, pp. 1.6.1-1.6.5.

16. V. A. Bronshten, *Physics of Meteoric Phenomena*, Table 23, D. Reidel, Boston, 1983, p. 213.

$$(5) \beta_I(v) = 4.0 \times 10^{-25} v_{cm/s}^{3.5} [5] \quad (2.1e)$$

$$(6) \beta_I(v) = 1.0 \times 10^{-28} v_{cm/s}^4 [5] \quad (2.1f)$$

$$(7) \beta_I(v) = 9.5 \times 10^{-29} v_{cm/s}^4 [5] \quad (2.1g)$$

$$(8) \beta_I(v) = 10^{-28} v_{cm/s}^4 [5] \quad (2.1h)$$

$$(9) \beta_I(v) = 5.5 \times 10^{-38} v_{cm/s}^{5.4} [5] \quad (2.1i)$$

where $v_{km/s}$ and $v_{cm/s}$ are meteor speed in meters per second and centimeters per second, respectively. These expressions are plotted versus meteor speed in Figure 1. As the figure shows, these expressions span two orders of magnitude and exhibit different rate-of-increase dependence of $\beta_I(v)$ with meteor speed v . Each of these expressions was used to determine which formula resulted in the "best" measurement-prediction comparison, both in terms of absolute value and trends.

The classical expressions for the initial trail radius $r_0(v, h_t)$ are independent of meteor speed and are given by:

$$(1) r_0(h_t) = 10^{0.075h_t - 7.9} [17] \quad (2.2a)$$

$$(2) r_0(h_t) = 10^{0.075h_t - 7.2} [6] \quad (2.2b)$$

Intuitively, the initial radius should be dependent on meteor speed as well as trail height h_t . In fact, two other expressions derived more recently than Eqs. 2.2, which include both the effects of meteor speed and atmospheric particle density (versus trail height), are given by:

$$(3) r_0(v, h_t) = 7.35 \times 10^6 v_{cm/s} / n_a(h_t) [18] \quad (2.2c)$$

$$(4) r_0(v, h_t) = 2.58 \times 10^8 v_{cm/s}^{0.8} / n_a(h_t) [7] \quad (2.2d)$$

These expressions are plotted in Figure 2 for heights of 90, 100, and 110 km above sea level for Eqs. 2.2c and 2.2d.

The ambipolar diffusion rate, $D(h_t)$, determines the duration of individual meteor bursts and has been empirically determined as a function of trail height. The classical expression for diffusion rate is given by:

$$(1) D(h_t) = 10^{0.067h_t - 5.6} [19] \quad (2.3a)$$

which was determined as a regression curve fit to height measurements with diffusion rate as the independent variable. In METEORLINK, however, the height is known and the diffusion rate is sought. For this reason, PC METEORLINK also includes the expression for $D(h_t)$ derived from the regression of D-values with h_t as the independent variable. This latter expression can be determined from the published linear regression results [20] to yield:

17. D. W. R. McKinley, *Meteor Science and Engineering*, McGraw-Hill, New York, 1961, p. 199.

18. V. A. Bronshten, *Ibid.*, p. 217.

19. D. W. R. McKinley, *Ibid.*, p. 202.

20. E. L. Murray, Ambipolar diffusion of a meteor trail and its relation with height, *Planet. Space Sci.*, Vol. 1, 1959, pp. 125-129.

$$(2) \quad D(h_t) = 10^{0.0225h_t - 1.58} \quad (2.3b)$$

which is plotted with Eq. 2.3a in Figure 3.

The height of maximum ionization, H_{\max} , is the height at which the meteoric ionization achieves its maximum value along its flight through the atmosphere. Three basic expressions were considered for H_{\max} , including:

$$(1) \quad H_{\max} = \text{constant (typically, 93-96 km)} \quad [21] \quad (2.4a)$$

$$(2) \quad H_{\max} = 0.39 v_{\text{km/s}} + 78.0 \quad [22] \quad (2.4b)$$

$$(3) \quad H_{\max} = 44.0 \log_{10}(v_{\text{km/s}}) - 4.4 \log_{10}(q_{\max}) + 82.0 \quad [23] \quad (2.4c)$$

where q_{\max} is the maximum ionization achieved at H_{\max} . In practice, q_{\max} is a function of H_{\max} so a root-finding algorithm must be employed to solve

$$H_{\max} - 44.0 \log_{10}(v_{\text{km/s}}) + 4.4 \log_{10}[q_{\max}(H_{\max})] - 82.0 = 0$$

for the proper value of H_{\max} .

The underdense/overdense threshold q_{sm}^T is the value of line density used by PC METEORLINK Version 1.0V to determine whether the underdense or overdense trail model is used to compute the minimum usable mass. Although q_{sm}^T has been traditionally approximated as a constant value, such as 0.75×10^{14} or 2.4×10^{14} electrons per meter, all METEORLINK versions use the expression

$$q_{sm}^T = 2\pi^{1/2} \sin(\gamma_{sm}) r_0(v, h_t) \Phi_{sm}^T / \lambda r_e \quad [24] \quad (2.5)$$

where γ_{sm} is the angle between the transmit R-vector and the meteor trail, r_e is the classical electron radius, and Φ_{sm}^T is the upper bound on scattered signal phase shift delineating the onset of overdense trail scatter. This expression accounts for the dependence of the threshold value on signal wavelength as well as trail geometry, meteor velocity, and height above sea level.

The mass-rate exponent, $s(\epsilon)$, determines the MR value associated for a meteor of mass m according to $c_\epsilon m^{-s(\epsilon)}$, where c_ϵ is a constant dependent on meteor velocity. In the VAX METEORLINK versions, the mass-rate exponent is given by

$$s(\epsilon) = 1.9 + 0.12\epsilon + 0.01\epsilon^2 \quad [25] \quad (2.6)$$

21. R. I. Desourdis, Jr., V. V. Sidorov, A. V. Karpov, R. G. Huziashev, L. A. Epictetov, and D. W. Brown," *Ibid.*.

22. D. W. R. McKinley, *Ibid*, p. 129.

23. *Ibid*, p. 181.

24. H. Brysk, "Electromagnetic scattering from high-density meteor trails," *IRE Trans. Ant. Prop.*, AP-7, December 1959, pp. S330-S336.

25. N. T. Svetashkova, Density variations of meteor flux along the earth's orbit, *Middle Atmospheric Program: Handbook for MAP*, Vol. 25, R. G. Roper (ed.), Government Printing Office, Washington, DC, August 1987, pp. 311-320.

This dependence of mass-rate exponent on elongation angle could be due to inaccurate modeling of the meteor velocity distribution in using radar measurements to determine $s(\epsilon)$. For this reason, the PC METEORLINK Version 1.0V assumes that $s(\epsilon) = \text{constant}$, set between 2.0 and 2.5.

Finally, the minimum meteor mass m_0 is the minimum mass of meteors included in the sporadic meteor flux density distribution. The sporadic flux references [26] reference the same Kazan and Mogadishu radar measurements while referencing m_0 values ranging from 3.0×10^{-5} grams to 5.5×10^{-5} grams. Minimum mass values were reported for the same data set at values as high as 1.0×10^{-3} grams, although this value was probably due to scaling of the data by the author to achieve particular results.

3. SOFTWARE DEVELOPMENT

Any computer model employing empirically and theoretically-derived expressions from a variety of researchers must be adjusted so that it yields accurate measurement-prediction comparisons for a known data set. This process, called "calibration," is intended to yield the most accurate prediction model for use in predicting performance to "unfamiliar" inputs, that is, model "validation". The need for calibration is particularly true when expressions used in the model are developed by researchers using a variety of theoretical assumptions and experimental techniques over many years. This situation is the case in MB communications and in the field of meteor physics and astronomy in general. In the case of PC METEORLINK Version 1.0V, these adjustments include the use of different combinations of Eqs. 2.1 through 2.6 as well as values of m_0 within the referenced range. In addition to selection of the most appropriate expression, the individual constants within each expression could be adjusted to achieve the best overall agreement between measurement and prediction. Ideally, minimum adjustment to the various coefficients would be necessary to achieve an acceptable measurement-prediction comparison. Hopefully, the calibrated model would produce accurate predictions over the full range of input parameters for the intended model applications.

4. RESULTS

4.1 Phillips Lab

The METEORLINK computer model was used to predict the MR and DC values recorded on an experimental MB link operated in Greenland by the Phillips Laboratory (PL) and established by the Rome Air Development Center (RADC) in 1984 [27]. The results of the absolute analysis and accompanying discussion presented in this section were derived from previous work [28]. These measurements were recorded on the Greenland Meteor Burst Test Bed for one-way MB links operating from Sondrestrom AFB to Thule AFB (1200 km). These links operated at 45, 65, 85, and 104 MHz using resonant five-element Yagi antennas on each frequency. METEORLINK predictions of MR, DC, underdense trail MR (UMR), underdense trail DC (UDC), the underdense percentage of the (%UMR), and the underdense percentage of the duty cycle (%UDC) were compared with the corresponding

26. J. A. Pupyshv, T. K. Filimonova, and T. V. Kazakova, Maps of the distribution over the entire celestial sphere of the sporadic meteor radiant density, *Radiowave Meteor Propagation*, No. 15, Kazan State U. P., Kazan, Russia, 1980, Document A82-16533, Technical Information Service, American Institute of Aeronautics and Astronautics, (in Russian).

27. *The RADC High Latitude Meteor Scatter Test Bed*, by J. C. Ostergaard, J. E. Rasmussen, M. J. Sowa, J. M. Quinn, and P. A. Kossey, RADC-TR-86-74 ADA180550, Hanscom Air Force Base, Massachusetts, July 1986, Unlimited Distribution.

28. R. I. Desourdis, Jr., J. C. Ostergaard, and A. D. Bailey, "Meteor burst computer model validation using high-latitude measurements," *IEEE MILCOM'91 Conf. Proc.*, Vol. 2, McLean, Virginia, November 1991, pp. 22.1.1-22.1.5.

measurements for 45, 65, 85 and 104 MHz; minimum RSL-values of -120, -110 and -100 dBm; and 12 times per day for a total of five months. The PL measurements performed for horizontally polarization were used in this calibration and validation effort.

Measured data consists of calibrated received signal level (RSL) samples recorded throughout any propagation event, typically trail-scatter or sporadic E, whenever the transmitted signal from Sondrestrom is identified. Trail-scattered signals are detected and recorded digitally for PL post-processing. Noise powers are periodically recorded and receiver measurements are monitored and periodically re-calibrated. Measurement post-processing classifies sampled events as trail-scatter or sporadic E, distinguishes between underdense and overdense trail RSL behavior [29], and yields the bi-hourly MR and DC for RSL values (P_r^*) exceeding specified thresholds. In addition, average noise measurements versus frequency and time are processed, typically showing the expected decrease in Galactic noise power with increasing frequency as well as its characteristic 2-3 dB diurnal variation. An important attribute of the PL measurement-derived MR and DC values is that noise uncertainty can be eliminated from the measurement-prediction comparisons.

Input parameters for METEORLINK predictions corresponding to the Greenland measurements were derived directly from the ST-link configuration. A subset of these comparison results spanning the full range of observed model accuracy were used in the calibration and validation efforts. NEC-computed antenna electric field patterns were generated by PL engineers and used for the 45, 65, 85, and 104 MHz antennas. The antenna foregrounds at the Thule receive site permitted pattern calculations assuming smooth-earth ground reflections. The Sondrestrom patterns were generated using NEC-computed free-space patterns modified to account for ground reflections produced by asymmetrical terrain blockage in the antenna foreground. Both transmit and receive antennas were pointed along the boresight to the opposite end of the link. A transmit power of 29.45 dBW was assumed at the input to each Sondrestrom transmit antenna. Plots of PC METEORLINK Version 1.0 and Version 1.0V prediction accuracy are presented in Appendix A.

4.2 Jodrell Bank

A meteor radar was constructed and operated at the Jodrell Bank Experimental Station of the University of Manchester, England beginning in 1949 [30]. The radar's mission was to measure the hourly rate of sporadic meteors as well as to determine the radiants of both major and minor meteor streams [31]. In the radar case, the scattering ellipsoid becomes a sphere and the potential common volume is maximized for omni-directional antenna patterns. The Jodrell Bank results, however, consist of MR-values measured with highly directional antenna beams. Thus MR predictions of the Jodrell Bank measurements must track the interaction between narrow-beamed antennas, spherically-dispersed hot spots and trail backscatter to reproduce the observed diurnal variation.

The Jodrell Bank ($2^\circ 18' \text{ W}$, $53^\circ 14' \text{ N}$) measurements were performed at a frequency of 72 MHz using two independent antenna arrays, each illuminating different portions of the sky. Each array

29. J. A. Weitzen, "A Data Base Approach to Analysis of Meteor Burst Data," *Radio Science*, Vol. 22, January, 1987, pp. 133-140.

30. A. C. B. Lovell, *Meteor Astronomy*, University Press, Oxford, New York, 1954, pp. 112-115.

31. A. Aspinall, J. A. Clegg and G. S. Hawkins, "A Radio Echo Apparatus for the Delineation of Meteor Radiants," *Philosophical Magazine*, Vol. 7, No. 42, pp. 504-514.

reportedly [32] consisted of six horizontally polarized six-element Yagi antennas with 6 dB beamwidths in the horizontal and vertical planes of 10° and a corresponding peak gain of approximately 24 dBi at an elevation angle of 8.5° . The two arrays were placed at equal distances from either side of the building containing the transmitter and receiver. The antenna beams were fixed to point along different bearings, 242° (southwest beam) and 292° (northwest beam) clockwise from true north, respectively. It has been separately stated that the antenna bearings were $\pm 25^\circ$ of true west [33] for the sporadic meteor survey, although the former values were used in this measurement-prediction comparison.

The radar's peak transmitter power was 5 kW (37 dBW) and its minimum detectable power P_r^* was 7×10^{-14} W (-102 dBm). A burst duration, i.e., radar pulse, of 8 μ s duration was employed with a repetition rate of 150 pulses per second. Dual pulses spaced 300 μ s apart were used to minimize noise spoofing of the scrolled photographic recording of received pulses. Transmissions were made on both antennas simultaneously but receptions were recorded through separate receive chains from each antenna. Thus the transmitted power into each antenna was about 2.5 kW. Plots of received pulses during the Geminid (December) meteor shower of 1949 clearly show the stream radiant passing through the southwest beam and then, about one hour later, passing through the northwest beam, as the earth rotates in the stream [34].

Average hourly MR-values were derived from continuous radar measurements that spanned contiguous months from October 1949 through September 1951 [35]. In other words, the averaged MR-values for each hour represent the average of all MR-values collected for that hour in each day of the specified month. MR-values attributed to known meteor showers were extracted. Since the two antenna beams pointed to different bearings, two independent sets of averaged MR-values were obtained simultaneously. No statistical fluctuation (error bars) were provided for these measurements. Otherwise, these results provide an excellent source of validation data for measurement-prediction comparisons of diurnal and seasonal variation.

METEORLINK predictions were performed using the documented radar parameters, although no NEC-generated pattern was available to model the Yagi arrays. Instead, an antenna pattern for two vertically stacked (half-wavelength separation) horizontally polarized 12-element Yagis at five wavelengths height was used to approximate the Jodrell Bank array. The 3 dB beamwidths were increased to about 35° in the horizontal plane and 40° in the vertical plane with a corresponding reduction in peak gain to about 18 dBi at an elevation angle of 8° . This pattern was oriented at both 292° and 242° clockwise from true north, thus approximating the southwest and northwest antenna beams, respectively, of the Jodrell Bank radar.

A 5 kW transmitter output power, P_t , was assumed into each antenna, unlike the 2.5 kW used by the Jodrell Bank radar. As in the measurements, a frequency (f_{MHz}) of 72 MHz was assumed with a required received power P_r^* of -102 dBm. A required burst duration of 10 ms was assumed to account for the radar repetition rate (150 per second) with "average" offset from the start of a burst until the arrival of a radar pulse. The additional 3 dB of transmit power into each antenna somewhat offset the difference in actual versus modeled peak antenna gains. Nevertheless, the assumed antenna patterns can

32. *Ibid.*, pg. 506.

33. A. C. B. Lovell, *Ibid.*, pg. 112.

34. A. Aspinall, J. A. Clegg and G. S. Hawkins, *Ibid.*, pg. 511.

35. A. C. B. Lovell, *Ibid.*, pg. 114.

only be considered an approximation to the actual patterns. Since the modeled antenna illuminates a greater sky volume than the Jodrell radar antenna (wider main beam, albeit with reduced power gain), the absolute MR-values would be expected to vary somewhat between measurement and prediction. The data used in this study was collected for the period from October 1950 through September 1951. The prediction-measurement comparison for the Jodrell Bank data is presented in Appendix B.

4.3 Calibration and Validation

The PC METEORLINK Version 1.0V program was used to predict the MR, DC, UMR, UDC, %UMR, and %UDC for the 45-MHz ST link at -120 dBm, the 85-MHz link at -120 and -100 dBm, and the 104-MHz link at -100 dBm. These links were modeled for four times of day, 0, 6, 12, and 18 hr. local time (LT). All PL results are presented as the ratio, or validation measure, given by

$$v_m = \log\left(\frac{\text{METEORLINK predicted value}}{\text{Greenland MB Test Bed measurement}}\right)$$

so the factor 2.0 corresponds to 0.3 and 0.5 corresponds to -0.3. The Jodrell Bank MR measurements for the northern radar beam in January were used to support additional calibration of the model. The actual MR values are plotted along with the corresponding predictions to illustrate the observed diurnal behavior as well as to compare measurement with predictions from both Versions 1.0 and 1.0V of PC METEORLINK. The PL and Jodrell Bank data used for calibration are presented in the indices shown at the beginning of Appendices A and B, respectively. These predictions were performed iteratively until the average values of MR, DC, UMR, UDC, %UMR, and %UDC were within factors of 0.5 and 2.0 of the corresponding measurements.

Several combinations of Eq. 2.1-2.6 were evaluated to produce the results shown in Appendices A and B. Eq. 2.1i, namely

$$(9) \beta_1(v) = 5.5 \times 10^{-38} v_{cmpr}^{5.4} [5] \quad (4.1)$$

was found necessary to produce the proper diurnal variation, particularly for the Jodrell Bank data set. The initial trail radius

$$(3) r_0(v, h_t) = 7.35 \times 10^6 v_{cmpr} / n_a(h_t) \quad (4.2)$$

was found necessary to create an acceptable relative magnitudes between the 45 and 85-MHz calibration results. The diffusion rate was modified from the original Eq. 2.3b

$$(2) D(h_t) = 10^{0.0225h_t - 1.58} \quad (4.3a)$$

to the smaller value

$$D(h_t) = 10^{0.0225h_t - 1.40} \quad (4.3b)$$

which differs by a factor of approximately 1.5 from the original expression. The height of maximum ionization was determined using the iterative approach based on the original expression

$$(3) H_{\max} = 44.0 \log_{10}(v_{kmpr}) - 4.4 \log_{10}(q_{\max}) + 82.0 \quad (4.4a)$$

modified to decrease the dependence on maximum line density according to

$$H_{\max} = 44.0 \log_{10}(\nu_{\text{kmps}}) - 3.3 \log_{10}(q_{\max}) + 82.0 \quad (4.4b)$$

The expression for threshold electron line density

$$q_{sm}^T = 2\pi^{1/2} \sin(\gamma_{sm}) r_0(\nu, h_t) \Phi_{sm}^T / \lambda r_e \quad (4.5)$$

and the mass exponent $s = 2.40$ in order to achieve an acceptable relationship between the 45 and 85-MHz PL results and the Jodrell Bank 72-MHz radar results. Finally, the minimum mass m_0 was set to a value of 6.5×10^{-4} gm to achieve an acceptable measurement-prediction comparison.

The validation predictions for the PL and Jodrell Bank measurements are presented in appendices A and B, respectively. Figure 3.1 shows a plot of the percentage of predictions within the factors f and $1/f$ plotted versus f along the abscissa. The PL MB-link predictions from both Versions 1.0 and 1.0 V show that more than half of the predictions at all four Greenland Test Bed frequencies lie within factors of 0.5 and 2.0 of the measured values for all MB-link performance measures. The figure shows that both PC METEORLINK versions exhibit similar accuracy, with Version 1.0 slightly more accurate for small errors ($f < 5$) and Version 1.0V is slightly more accurate for $f \geq 5$.

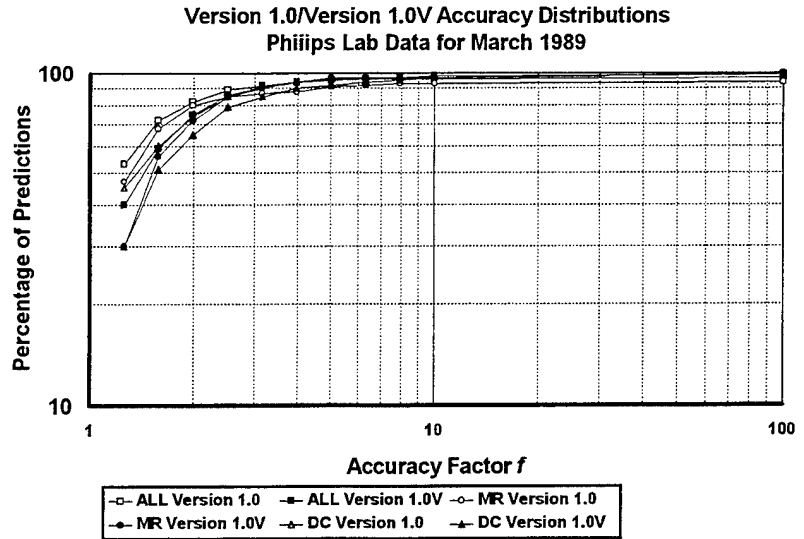


Figure 3.1 Comparison of model accuracy versus factor f

Similarly, the Jodrell Bank results show similar error factors for the early part of the year, that is, through August, with September and October results from Version 1.0V exhibiting optimistic (too high) MR values. Since the undulation in the validation measure varies with frequency, this effect (observed in the 45-MHz results) may not be associated with the ionization coefficient (fifth-power dependence) but with the antenna patterns. If lobes existed in locations other than those assumed in the modeling effort, than different calibration and validation results would have likely been the outcome.

4.4 Russian Measurements

Meteor radar measurements were performed in April, 1992 at Kazan (55° 0' N, 48° 48' E) using a five-element Yagi antenna at 9-m height over wet ground pointed at 327° east of north. Transmitter output power was 500 Watts and the minimum burst duration was 20 msec. Only two days of received signal level (RSL) samples were recorded because of equipment problems. The measured hourly MR-values above -114 dBm RSL are plotted in Figure 3.2. The classic diurnal variation is apparent as well as the significant day-to-day variation of the observed hourly MR-value from the same hour on subsequent days.

A forward scatter MB link was operated from Moscow (55° 30' N, 37° 36' E) to Kazan with hourly average MR-values available for May 16-24, 1992. Each link site employed a 5-element Yagi antenna at 9-m height over medium dry ground pointed along the link Great Circle path (GCP). The Moscow site

used 700-Watt transmitter output power and a 20-msec minimum burst duration above -114 dBm was required at the Kazan receive site. The measurement-prediction comparison results are shown in Figure 3.3. The nine days of link measurements exhibited the classic diurnal variation with higher rates than observed on the Kazan radar, probably due to the increased forward scattering angle and transmitter power of the Moscow-Kazan link. A significant day-to-day variation in measured hourly MR-values is apparent due to normal fluctuation in the incident meteor flux.

4.5 Summary of Results

The PL measurement-prediction comparison using the PC METEORLINK Version 1.0V program exhibited comparable accuracy to the Version 1.0 program. The Jodrell Bank Version 1.0V accuracy was also similar to the accuracy of the Version 1.0 results. Finally, the Kazan comparison showed that the Version 1.0V accuracy was somewhat better than the Version 1.0 results [36], albeit these results were not presented in this report. In all of these predictions, the discrepancies between prediction and measurement apparent in these results may be due to differences between the modeled and actual values of sporadic meteor radiant density, meteor velocity distributions, antenna patterns, atmospheric constants, trail physical parameters, and trail-scatter loss mechanisms. In particular, the apparent inaccuracy of Version 1.0V in September and October is apparently due to the appearance of significant flux approaching from greater elongation angles than during the other months (see the appendix in the companion technical report [37]). If these "lobes" in the flux were removed from the sporadic flux table, the Jodrell Bank measurement-prediction comparison results could be improved.

57.4-MHz Meteor Radar at Kazan in Russia
500 W, 5-El Yagi @ 327 deg, -114 dBm RSL

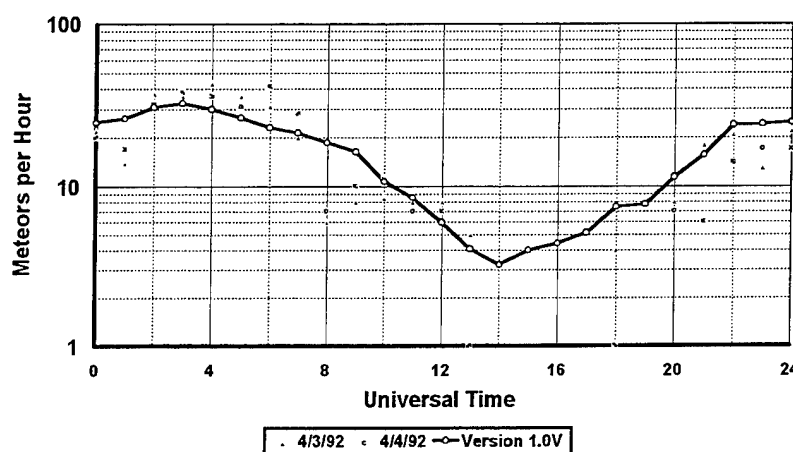


Figure 3.2 Kazan radar (backscatter) measurements

57.4-MHz Moscow-Kazan ME Link in Russia
700 W, 5-El Yagis, -114 dBm RSL

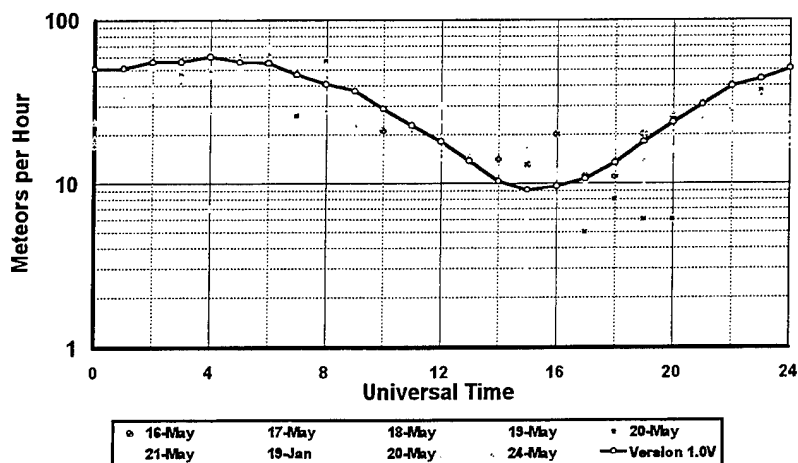


Figure 3.3 Moscow-Kazan forward-scatter MB link

36. R. I. Desourdis, Jr., V. V. Sidorov, A. V. Karpov, R. G. Huziashev, L. A. Epictetov, and D. W. Brown," *Ibid.*

37. Science Applications International Corporation, *Computer Software Product Item*, Contract # F19628-93-C-0082, CDRL A006, Marlborough, Mass., September 1995.

5. CONCLUSIONS AND RECOMMENDATIONS

Although PC METEORLINK Version 1.0V demonstrated slightly less accuracy in predicting the PL and Jodrell Bank results, SAIC believes that additional "fine tuning" of the Version 1.0V algorithms and physical constants will ultimately yield better accuracy than Version 1.0. This conclusion is based on the belief that the Version 1.0V model employs a more realistic velocity distribution, and other physical models, than Version 1.0. SAIC therefore recommends that the Version 1.0V programs be employed for future MB-link predictions as well as further model improvement efforts.

At this point, the Version 1.0V program should undergo another calibration effort to achieve better results than those published in this report, i.e., better than those provided by Version 1.0. SAIC believes that more than one set of physical models and their associated constant parameters will yield a "good" measurement-prediction comparison. In particular, the expression for ionization coefficient should further be considered for calibration efforts since the expression used in Version 1.0V yields excessive diurnal variation. Future efforts could investigate other expressions for the ionization coefficient not attempted during this limited effort.

6. APPENDIX A: GREENLAND TEST BED RESULTS

This appendix presents plots of the validation measure:

$$v_m = \log\left(\frac{\text{METEORLINK predicted value}}{\text{Greenland MB Test Bed measurement}}\right)$$

for the usable meteor rate (MR), link duty cycle (DC), underdense meteor rate (UMR), underdense duty cycle (UDC), underdense percentage of the MR value (%UMR), and the underdense percentage of the duty cycle (%UDC). The measurements used for this comparison were obtained by the Phillips Laboratory (then the Air Force Geophysics Laboratory) in Greenland in March of 1989. Each plot contains the results for both the original VAX METEORLINK (similar to PC METEORLINK Version 1.0) and PC METEORLINK Version 1.0V. The following table provides an index to help the reader locate specific results. The measurements used for the calibration data are shown in italic font in the table below.

Quantity	Rx Power (dBm)	Frequency [Figure # / Page #]			
		45 MHz	65 MHz	85 MHz	104 MHz
	-120 [A.1.1]	<i>A.1.1.1 / A-2</i>	A.1.1.2 / A-2	<i>A.1.1.3 / A-3</i>	A.1.1.4 / A-3
MR [A.1]	-110 [A.1.2]	A.1.2.1 / A-4	A.1.2.2 / A-4	A.1.2.3 / A-5	A.1.2.4 / A-5
	-100 [A.1.3]	A.1.3.1 / A-6	A.1.3.2 / A-6	<i>A.1.3.3 / A-7</i>	<i>A.1.3.4 / A-7</i>
	-120 [A.2.1]	<i>A.2.1.1 / A-8</i>	A.2.1.2 / A-8	<i>A.2.1.3 / A-9</i>	A.2.1.4 / A-9
DC [A.2]	-110 [A.2.2]	A.2.2.1 / A-10	A.2.2.2 / A-10	A.2.2.3 / A-11	A.2.2.4 / A-11
	-100 [A.2.3]	A.2.3.1 / A-12	A.2.3.2 / A-12	<i>A.2.3.3 / A-13</i>	<i>A.2.3.4 / A-13</i>
	-120 [A.3.1]	<i>A.3.1.1 / A-14</i>	A.3.1.2 / A-14	<i>A.3.1.3 / A-15</i>	A.3.1.4 / A-15
UMR [A.3]	-110 [A.3.2]	A.3.2.1 / A-16	A.3.2.2 / A-16	A.3.2.3 / A-17	A.3.2.4 / A-17
	-100 [A.3.3]	A.3.3.1 / A-18	A.3.3.2 / A-18	<i>A.3.3.3 / A-19</i>	<i>A.3.3.4 / A-19</i>
	-120 [A.4.1]	<i>A.4.1.1 / A-20</i>	A.4.1.2 / A-20	<i>A.4.1.3 / A-21</i>	A.4.1.4 / A-21
UDC [A.4]	-110 [A.4.2]	A.4.2.1 / A-22	A.4.2.2 / A-22	A.4.2.3 / A-23	A.4.2.4 / A-23
	-100 [A.4.3]	A.4.3.1 / A-24	A.4.3.2 / A-24	<i>A.4.3.3 / A-25</i>	<i>A.4.3.4 / A-25</i>
	-120 [A.5.1]	<i>A.5.1.1 / A-26</i>	A.5.1.2 / A-26	<i>A.5.1.3 / A-27</i>	A.5.1.4 / A-27
%UMR [A.5]	-110 [A.5.2]	A.5.2.1 / A-28	A.5.2.2 / A-28	A.5.2.3 / A-29	A.5.2.4 / A-29
	-100 [A.5.3]	A.5.3.1 / A-30	A.5.3.2 / A-30	<i>A.5.3.3 / A-31</i>	<i>A.5.3.4 / A-31</i>
	-120 [A.6.1]	<i>A.6.1.1 / A-32</i>	A.6.1.2 / A-32	<i>A.6.1.3 / A-33</i>	A.6.1.4 / A-33
%UDC [A.6]	-110 [A.6.2]	A.6.2.1 / A-34	A.6.2.2 / A-34	A.6.2.3 / A-35	A.6.2.4 / A-35
	-100 [A.6.3]	A.6.3.1 / A-36	A.6.3.2 / A-36	<i>A.6.3.3 / A-37</i>	<i>A.6.3.4 / A-37</i>

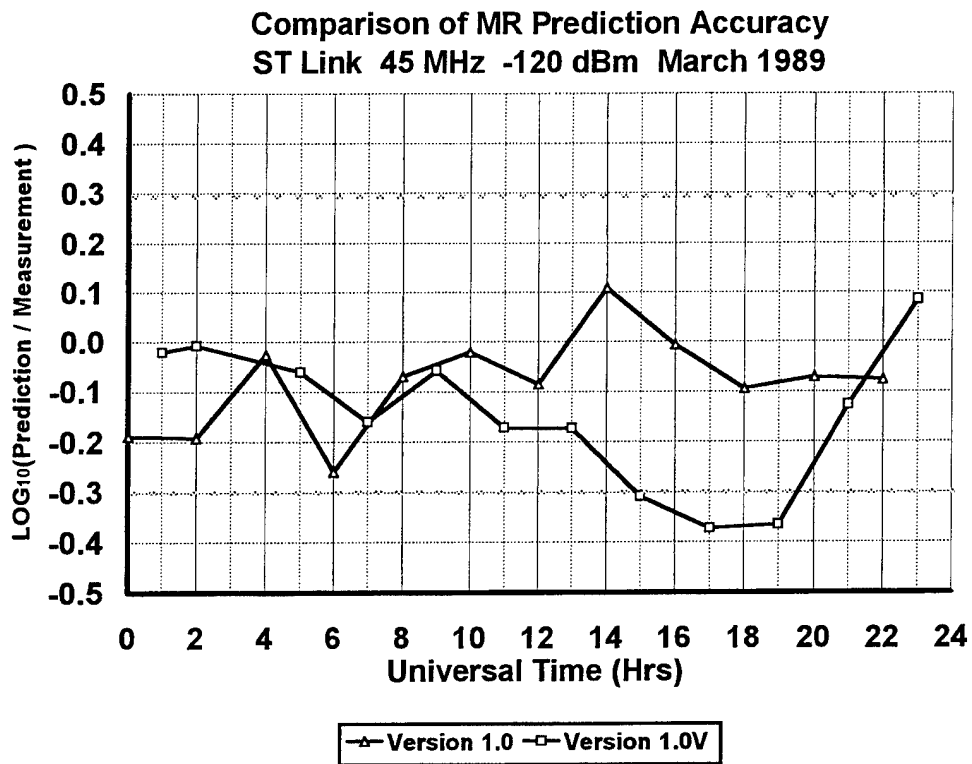


Figure A.1.1.1 MR Comparison at -120 dBm for 45 MHz

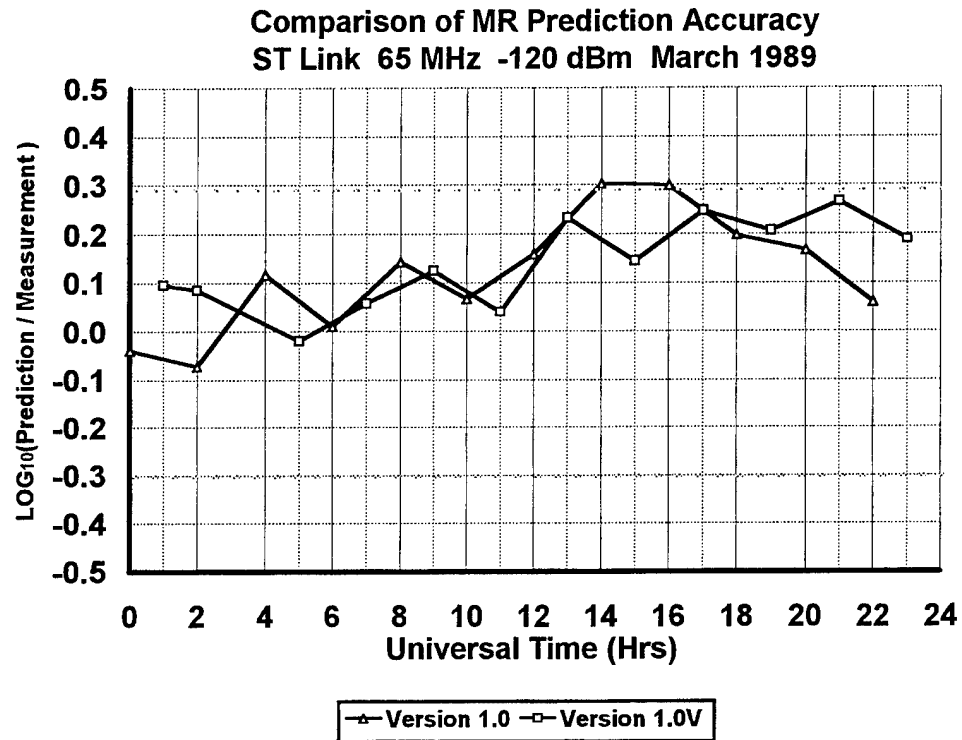


Figure A.1.1.2 MR Comparison at -120 dBm for 65 MHz

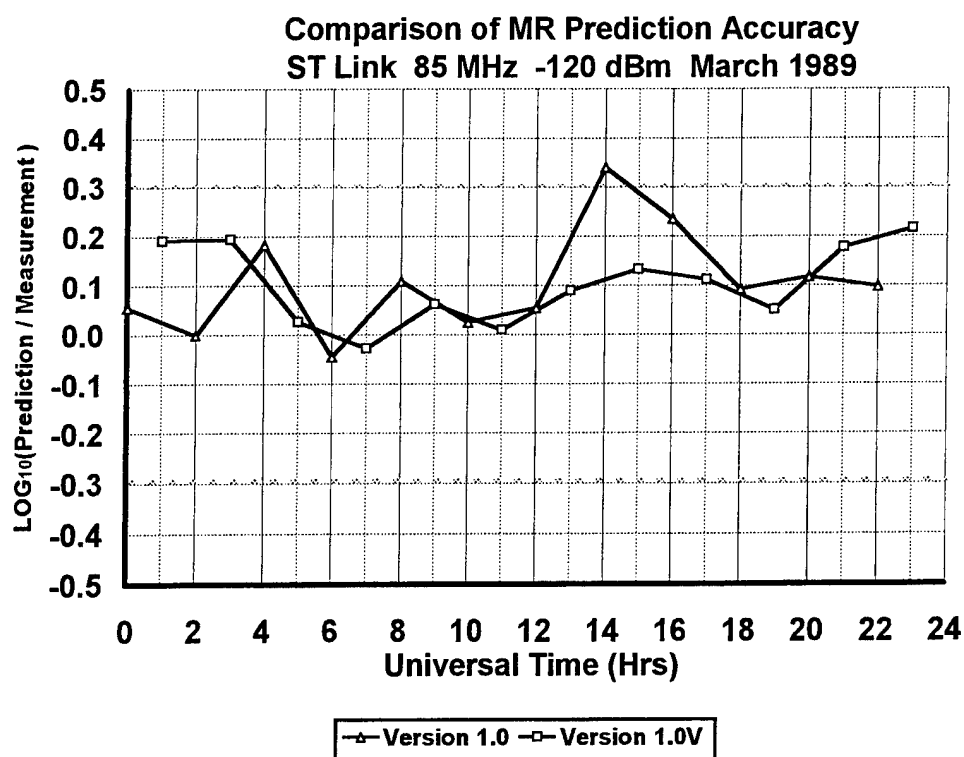


Figure A.1.1.3 MR Comparison at -120 dBm for 85 MHz

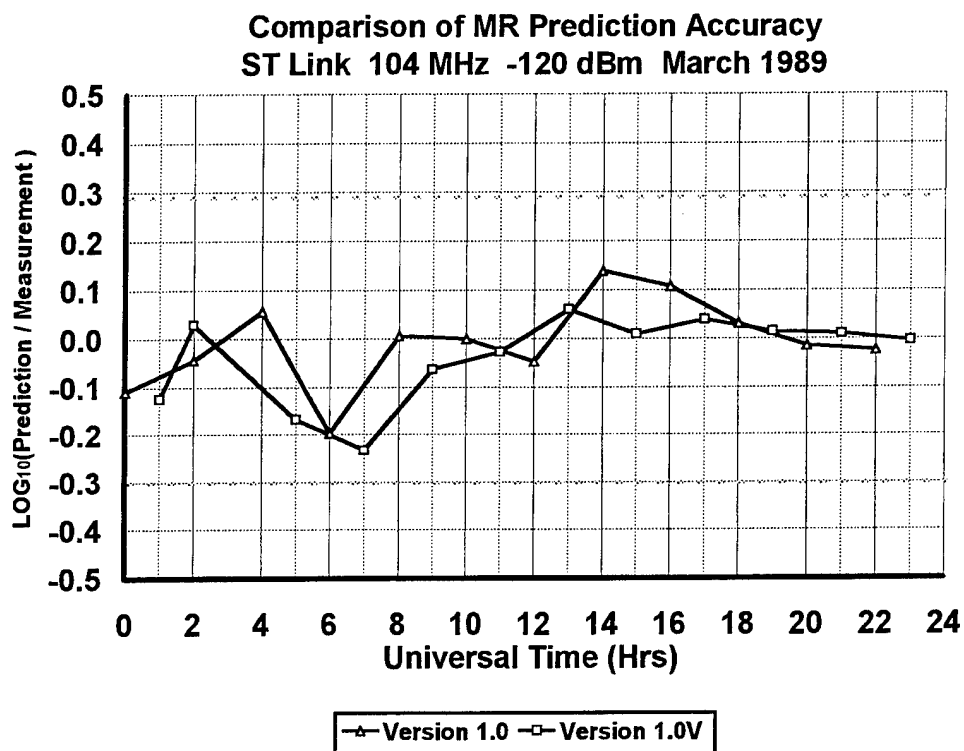


Figure A.1.1.4 MR Comparison at -120 dBm for 104 MHz

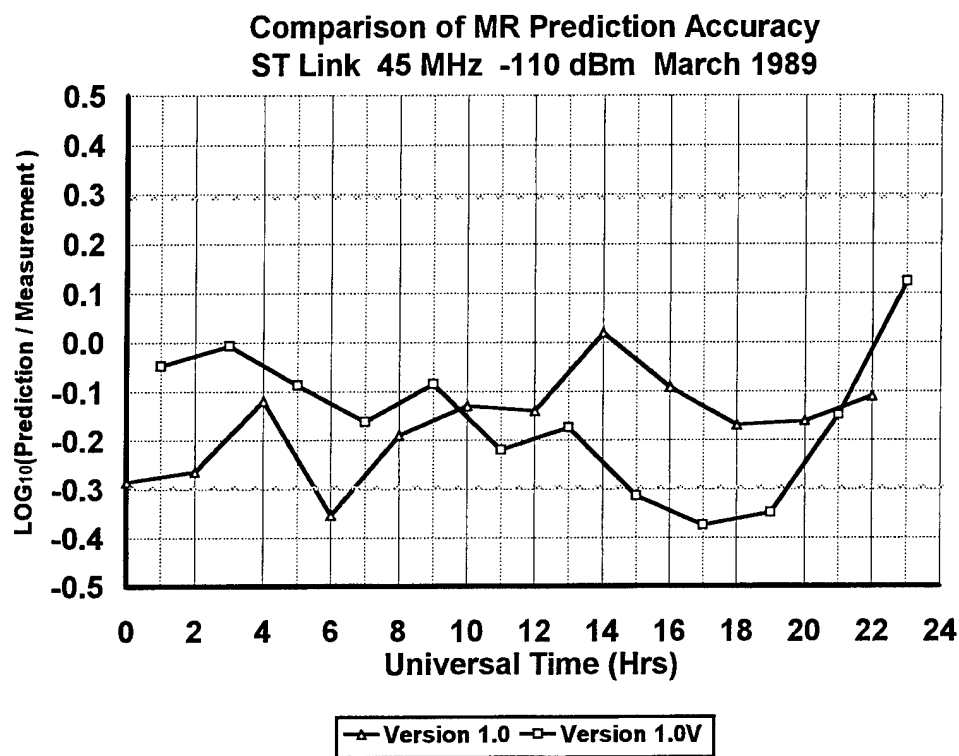


Figure A.1.2.1 MR Comparison at -110 dBm for 45 MHz

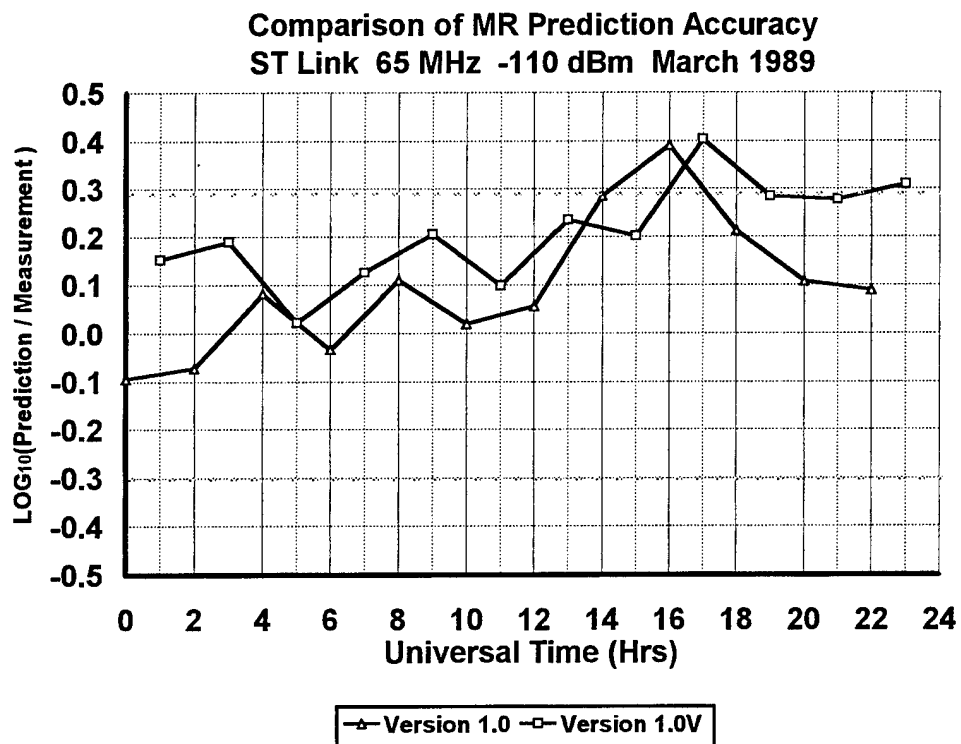


Figure A.1.2.2 MR Comparison at -110 dBm for 65 MHz

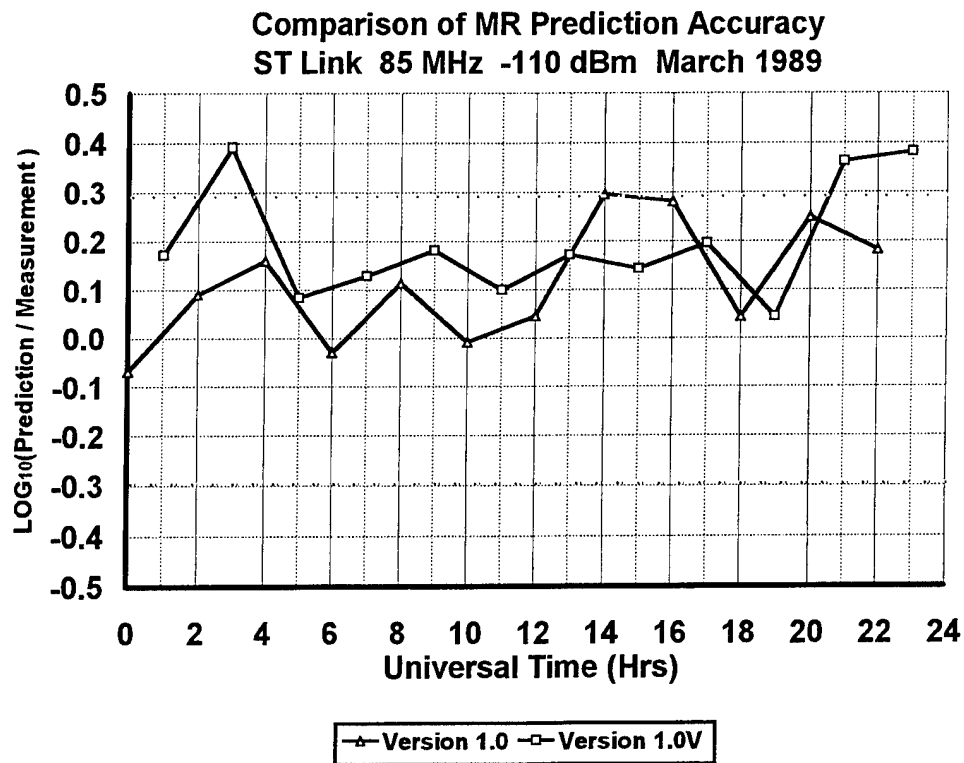


Figure A.1.2.3 MR Comparison at -110 dBm for 85 MHz

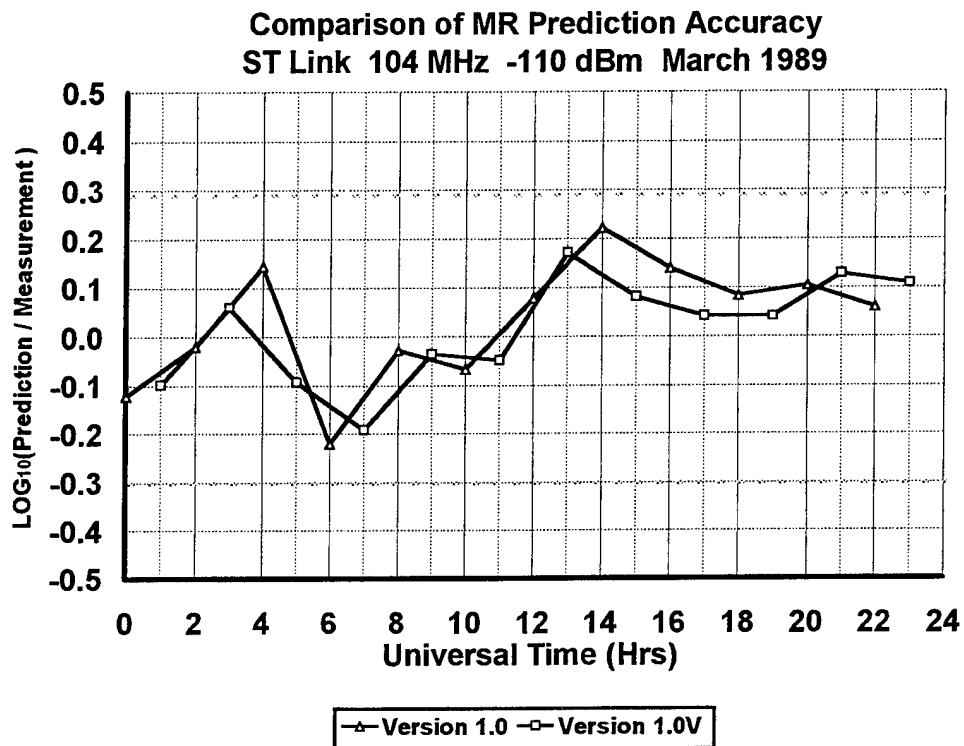


Figure A.1.2.4 MR Comparison at -110 dBm for 104 MHz

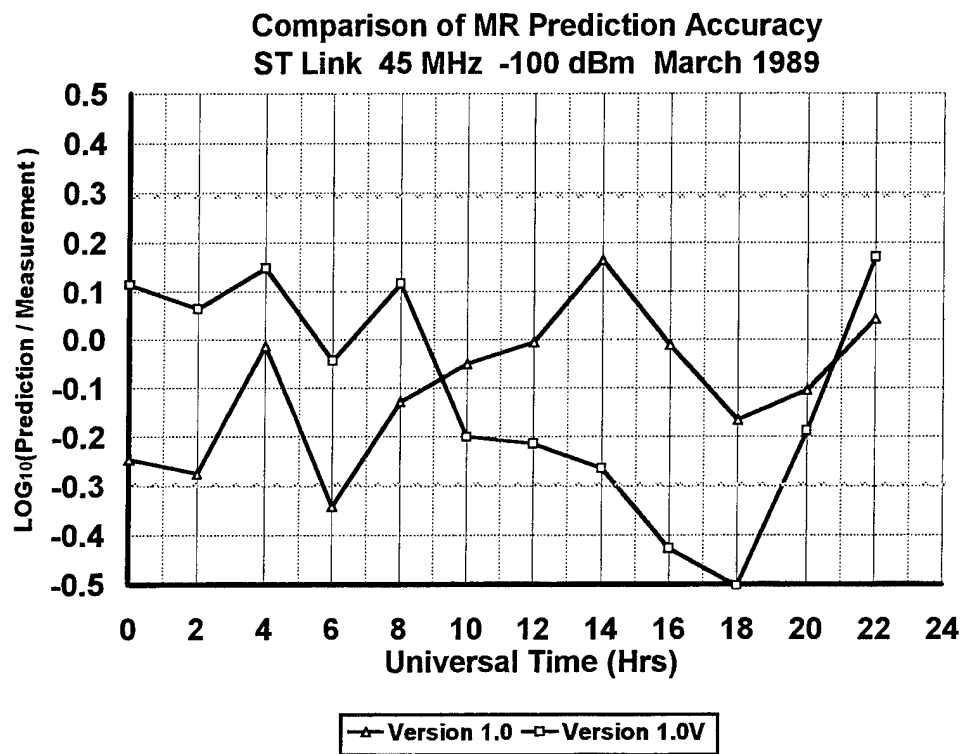


Figure A.1.3.1 MR Comparison at -100 dBm for 45 MHz

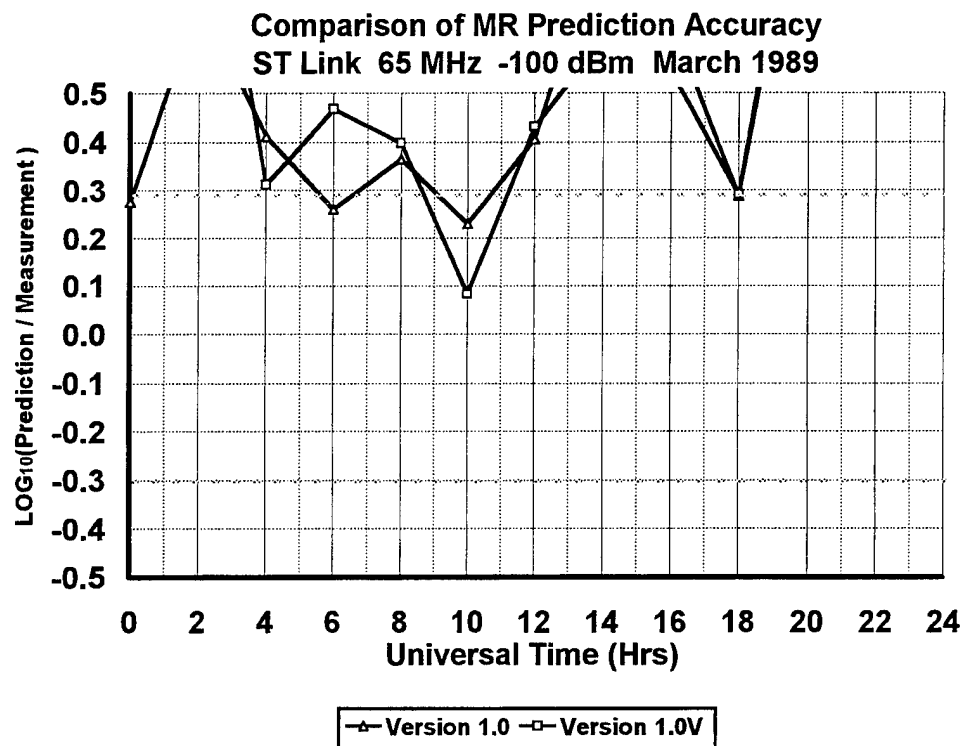


Figure A.1.3.2 MR Comparison at -100 dBm for 65 MHz

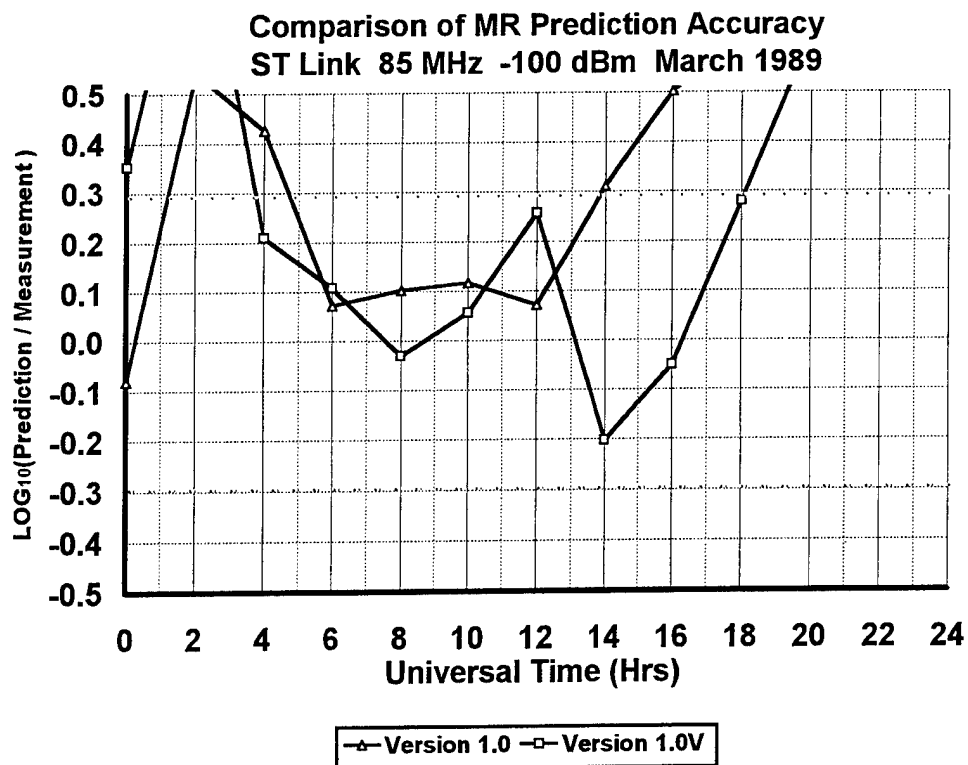


Figure A.1.3.3 MR Comparison at -100 dBm for 85 MHz

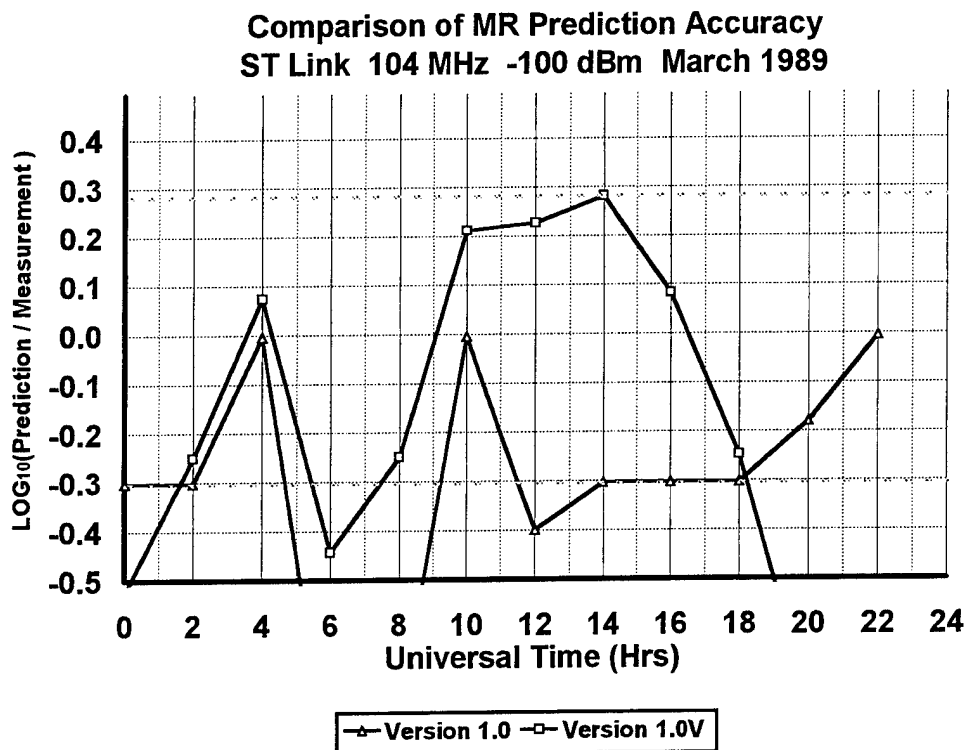


Figure A.1.3.4 MR Comparison at -100 dBm for 104 MHz

**Comparison of DC Prediction Accuracy
ST Link 45 MHz -120 dBm March 1989**

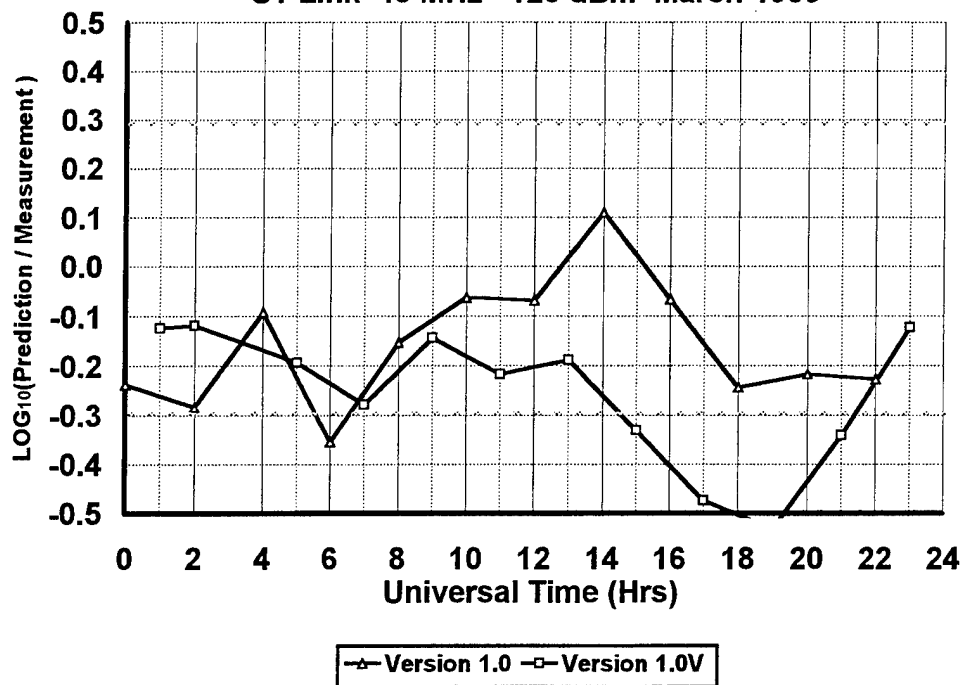


Figure A.2.1.1 DC Comparison at -120 dBm for 45 MHz

**Comparison of DC Prediction Accuracy
ST Link 65 MHz -120 dBm March 1989**

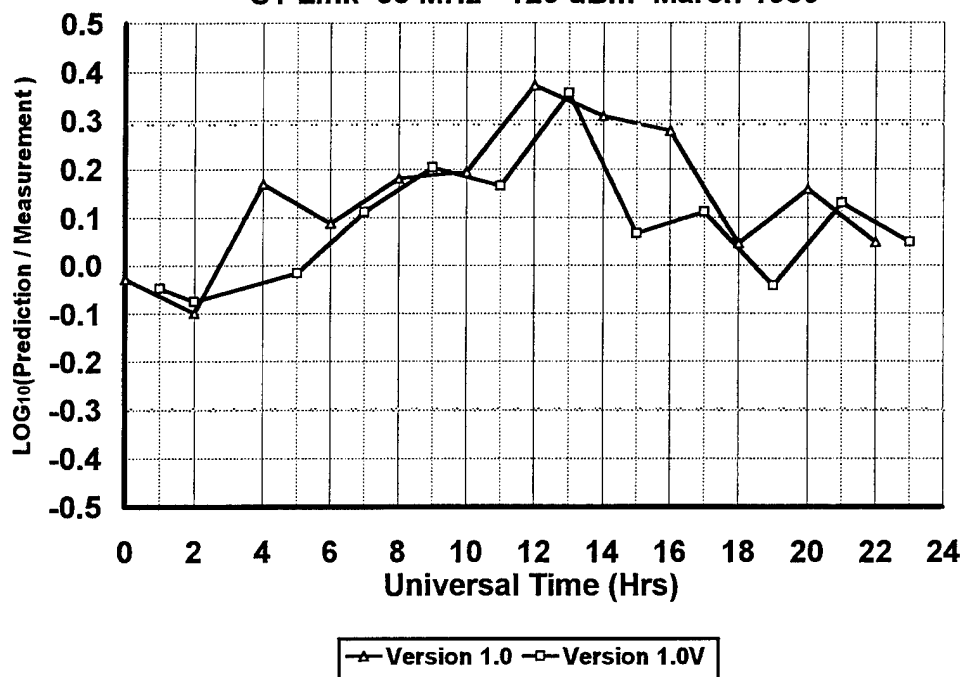


Figure A.2.1.2 DC Comparison at -120 dBm for 65 MHz

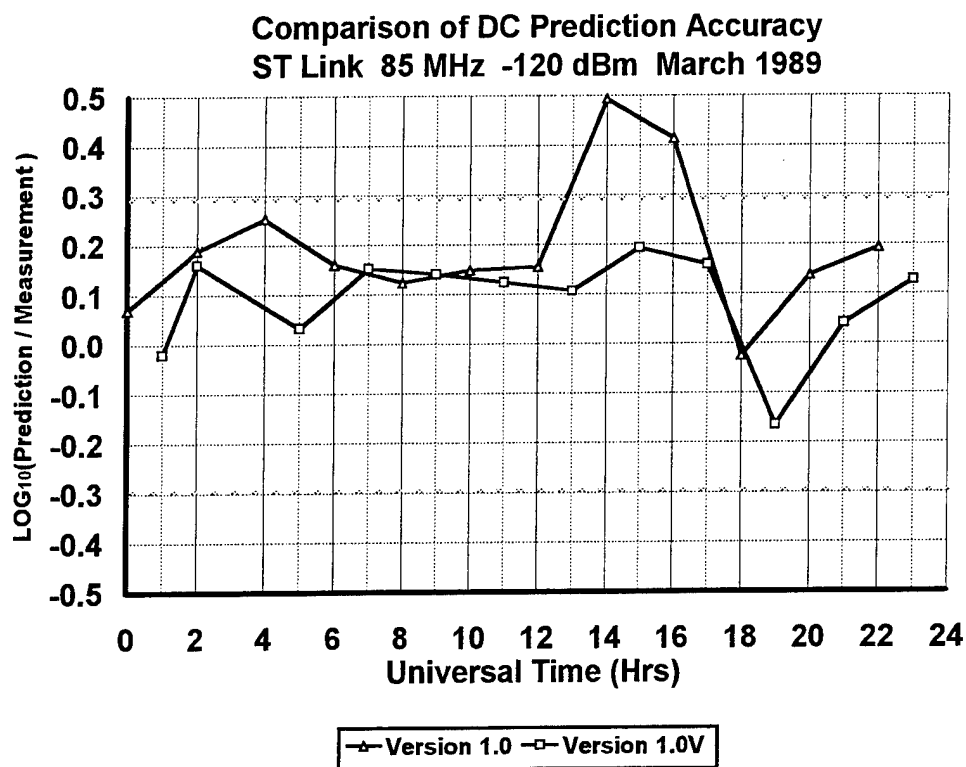


Figure A.2.1.3 DC Comparison at -120 dBm for 85 MHz

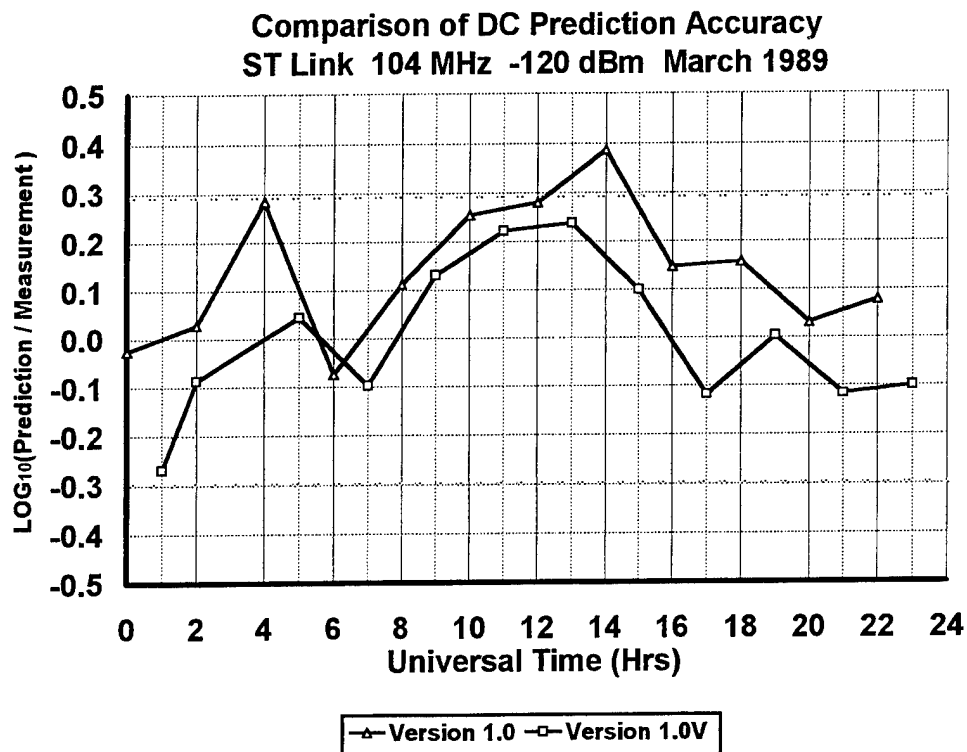


Figure A.2.1.4 DC Comparison at -120 dBm for 104 MHz

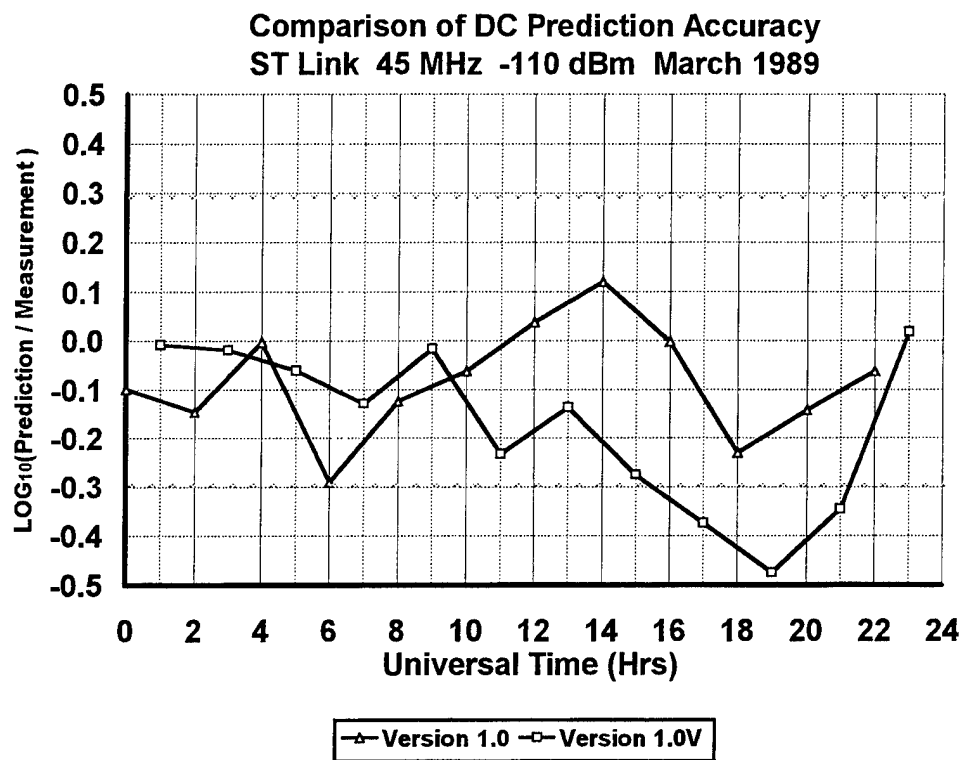


Figure A.2.2.1 DC Comparison at -110 dBm for 45 MHz

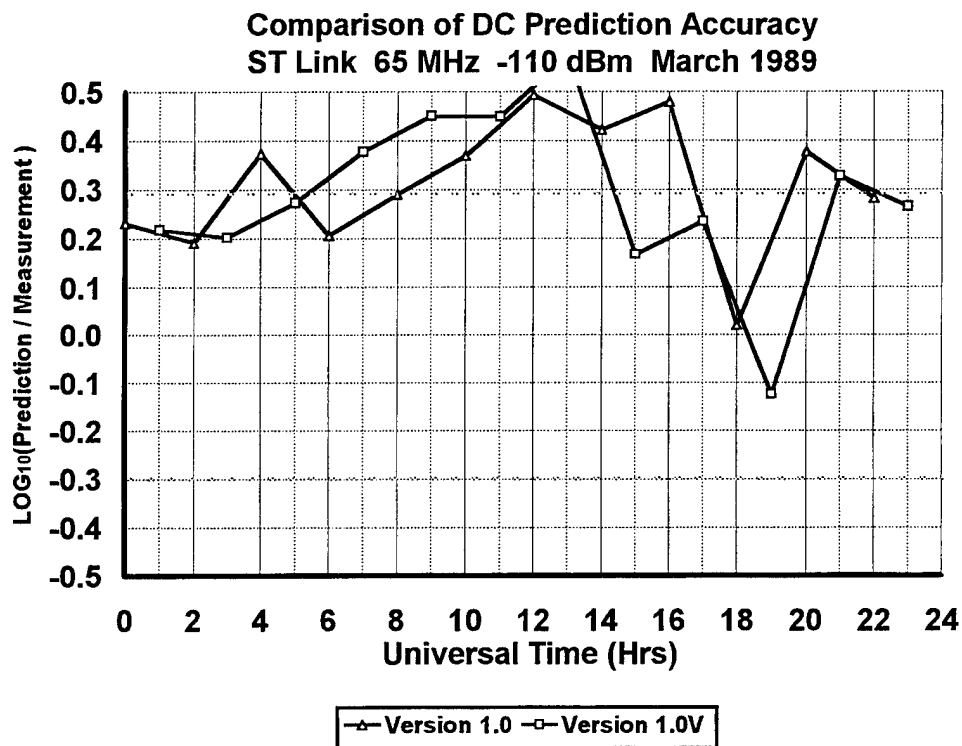


Figure A.2.2.2 DC Comparison at -110 dBm for 65 MHz

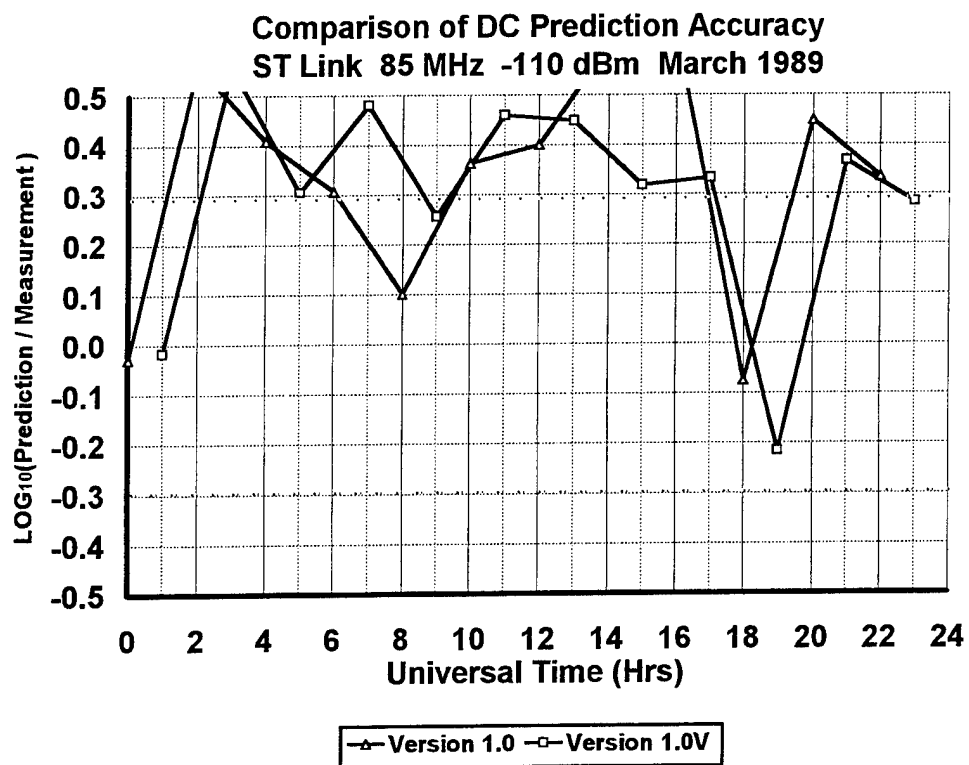


Figure A.2.2.3 DC Comparison at -110 dBm for 85 MHz

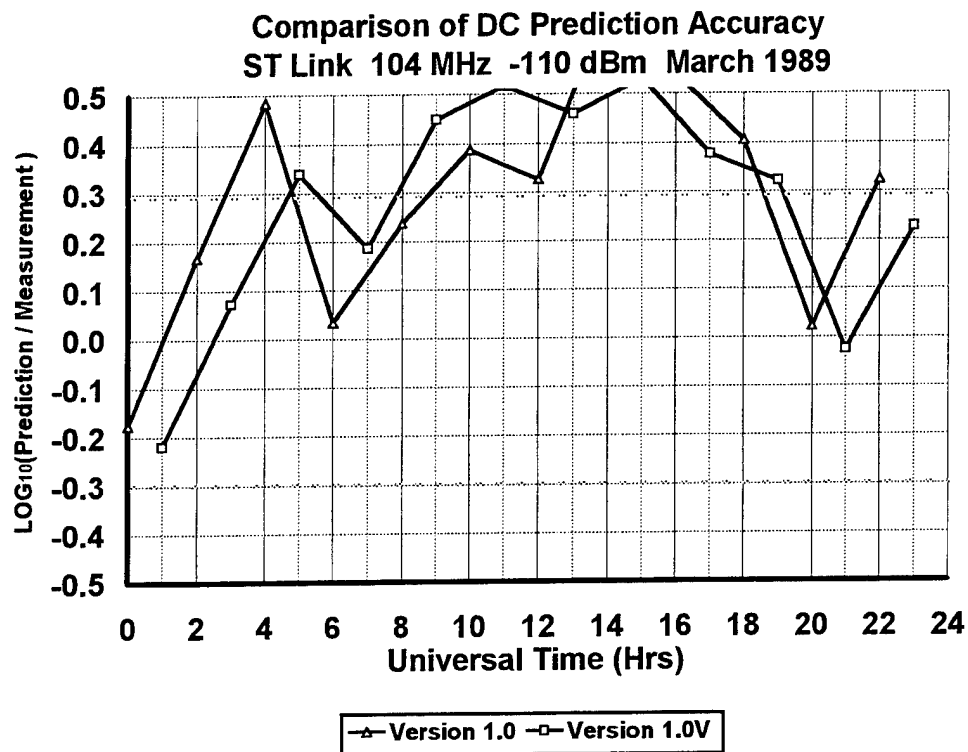


Figure A.2.2.4 DC Comparison at -110 dBm for 104 MHz

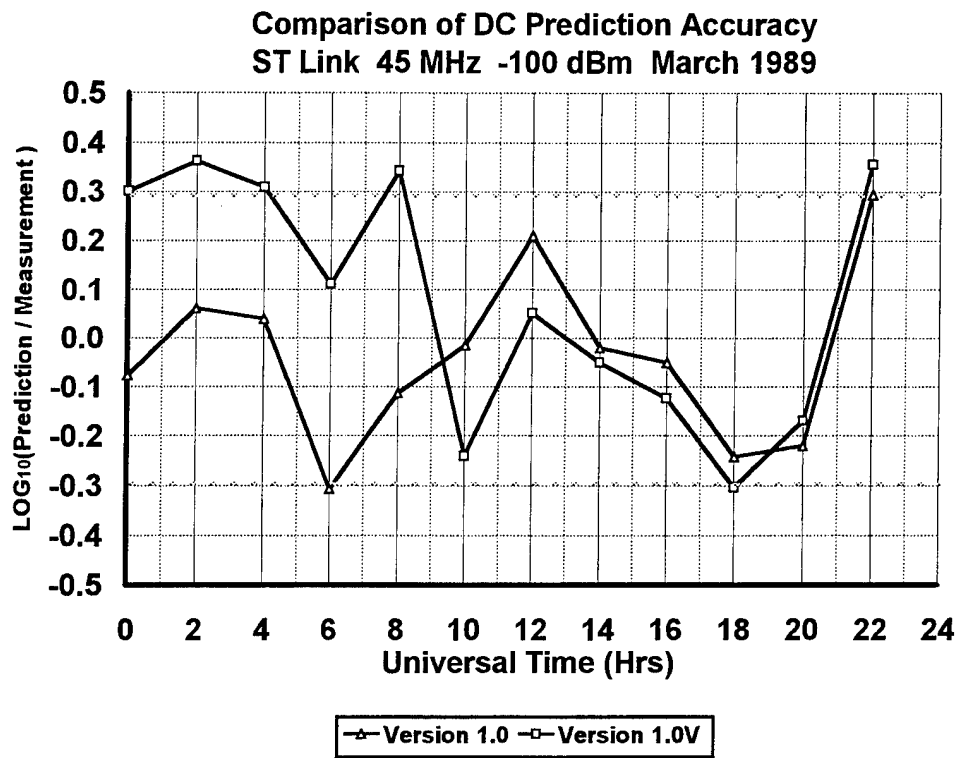


Figure A.2.3.1 DC Comparison at -100 dBm for 45 MHz

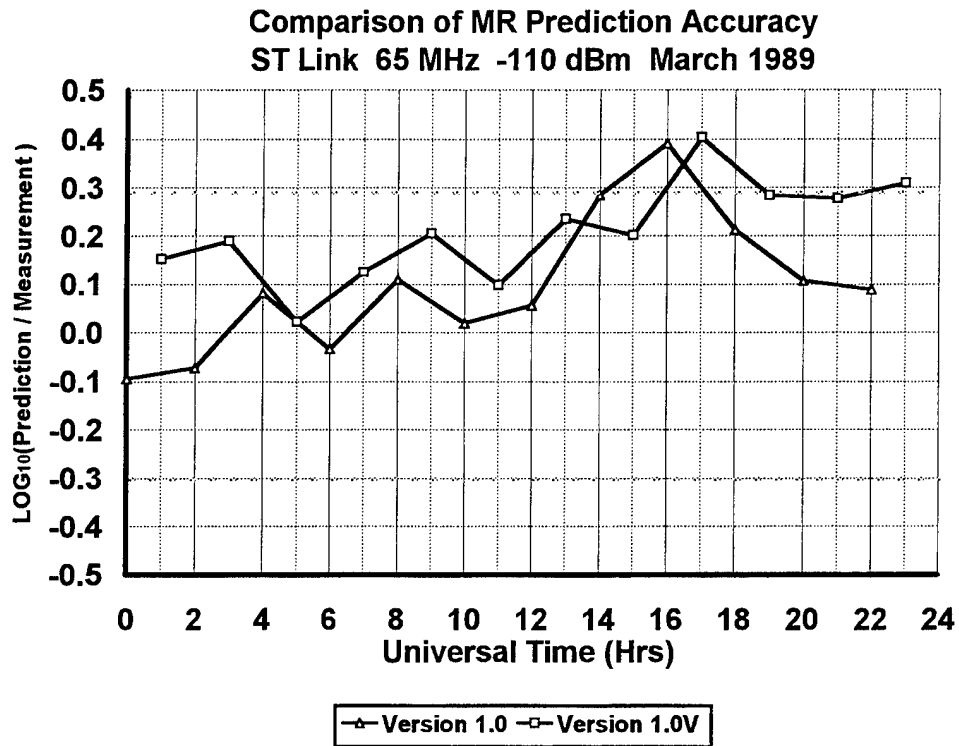


Figure A.2.3.2 DC Comparison at -100 dBm for 65 MHz

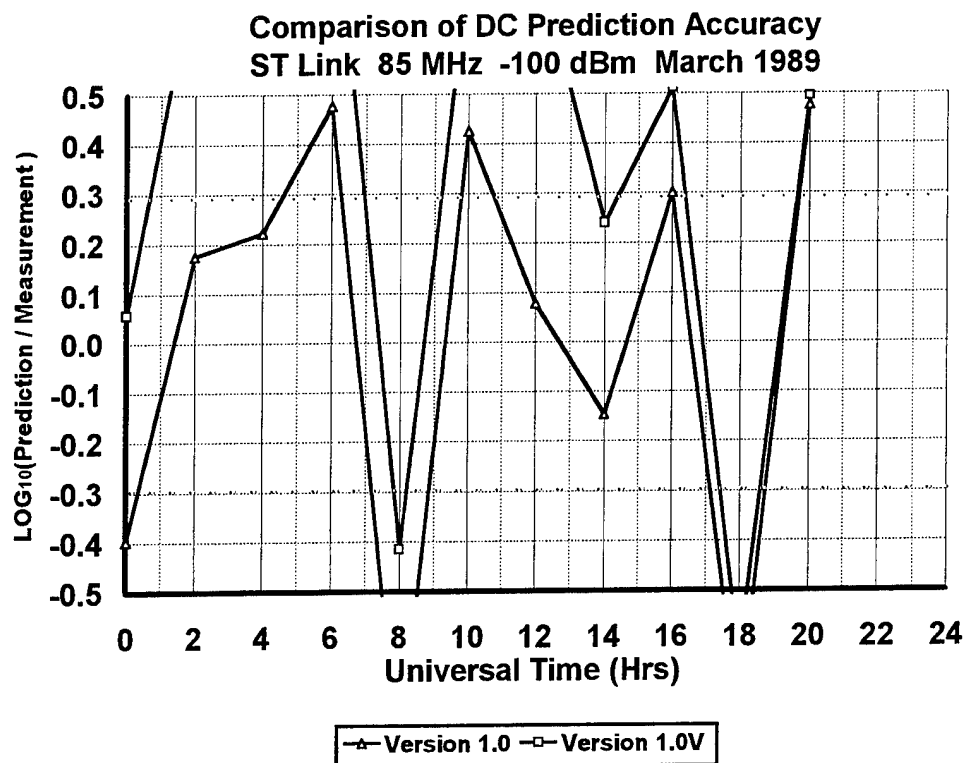


Figure A.2.3.3 DC Comparison at -100 dBm for 85 MHz

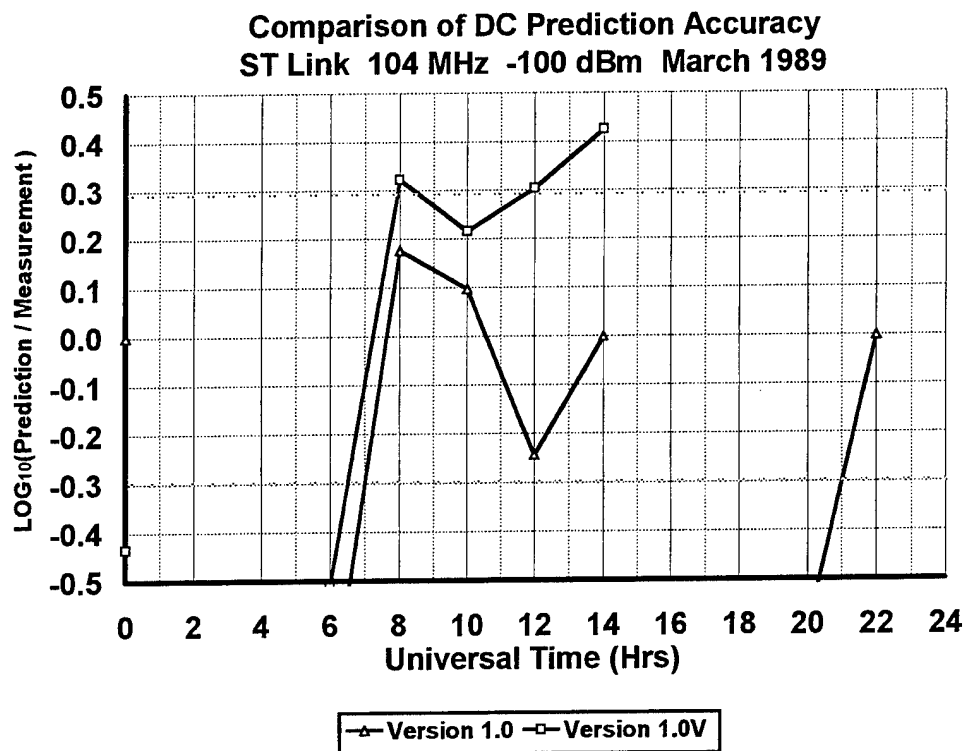


Figure A.2.3.4 DC Comparison at -100 dBm for 104 MHz

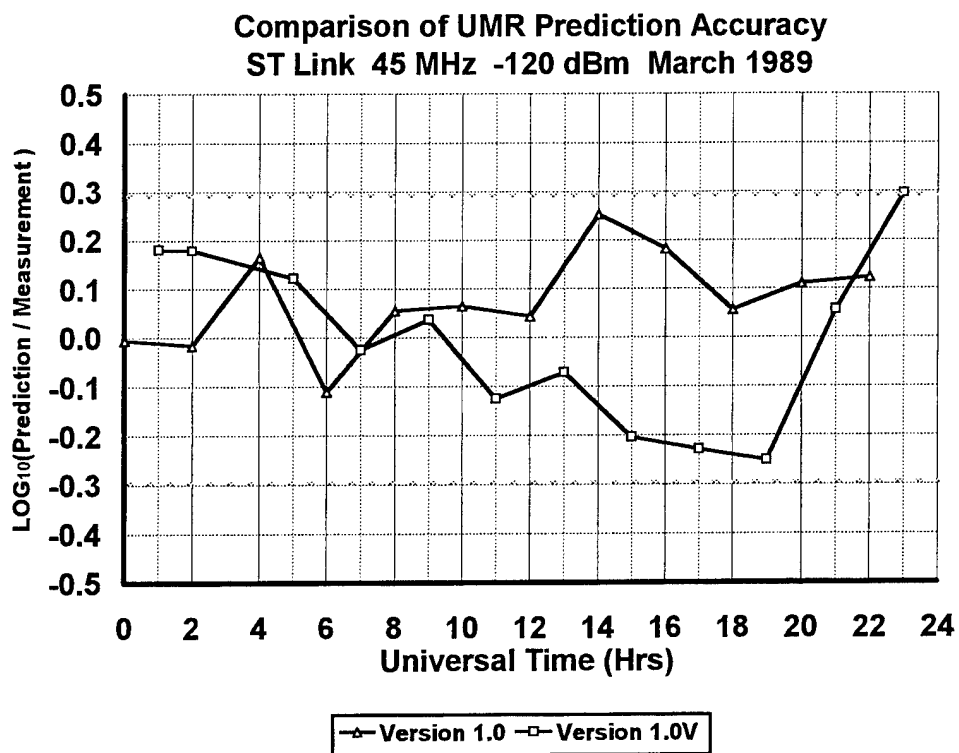


Figure A.3.2.1 UMR Comparison at -120 dBm for 45 MHz

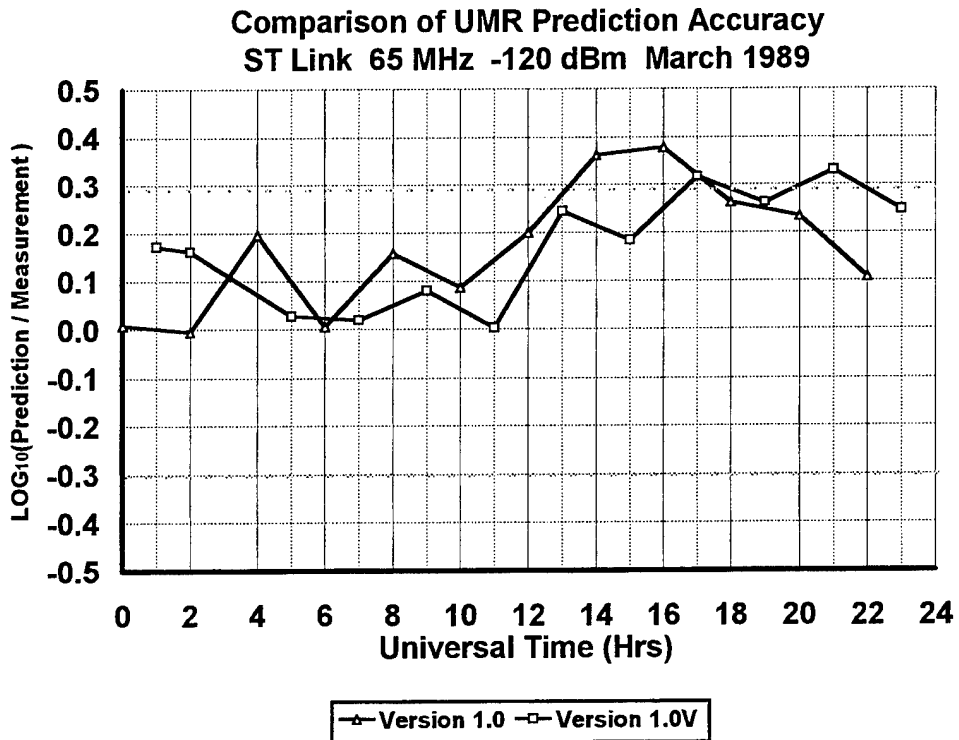


Figure A.3.2.2 UMR Comparison at -120 dBm for 65 MHz

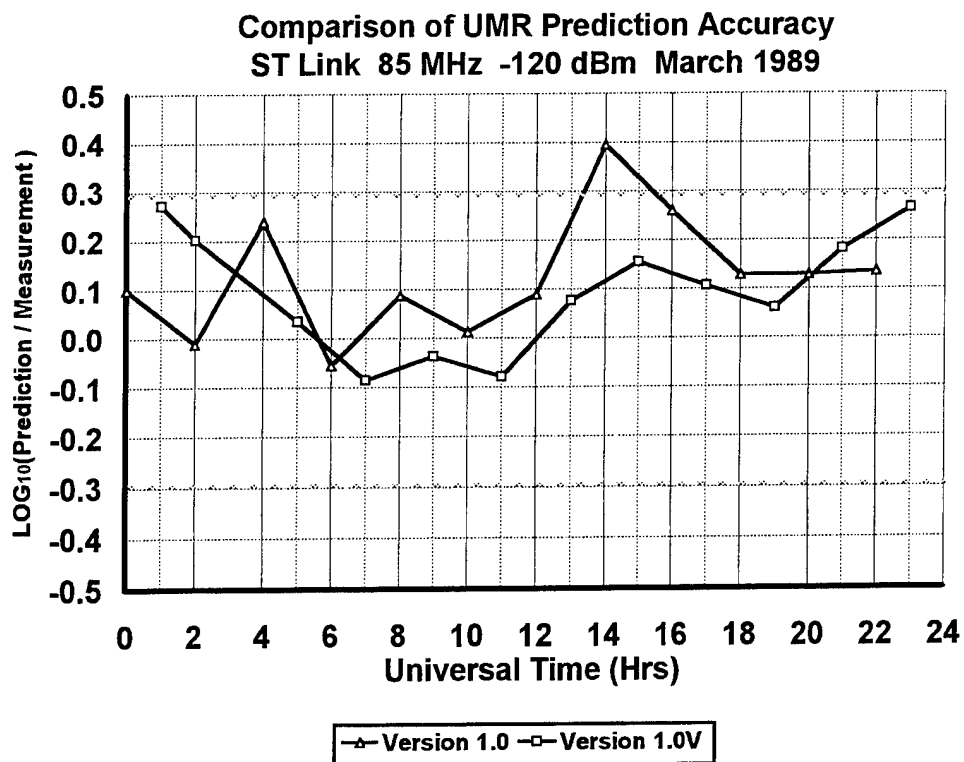


Figure A.3.2.3 UMR Comparison at -120 dBm for 85 MHz

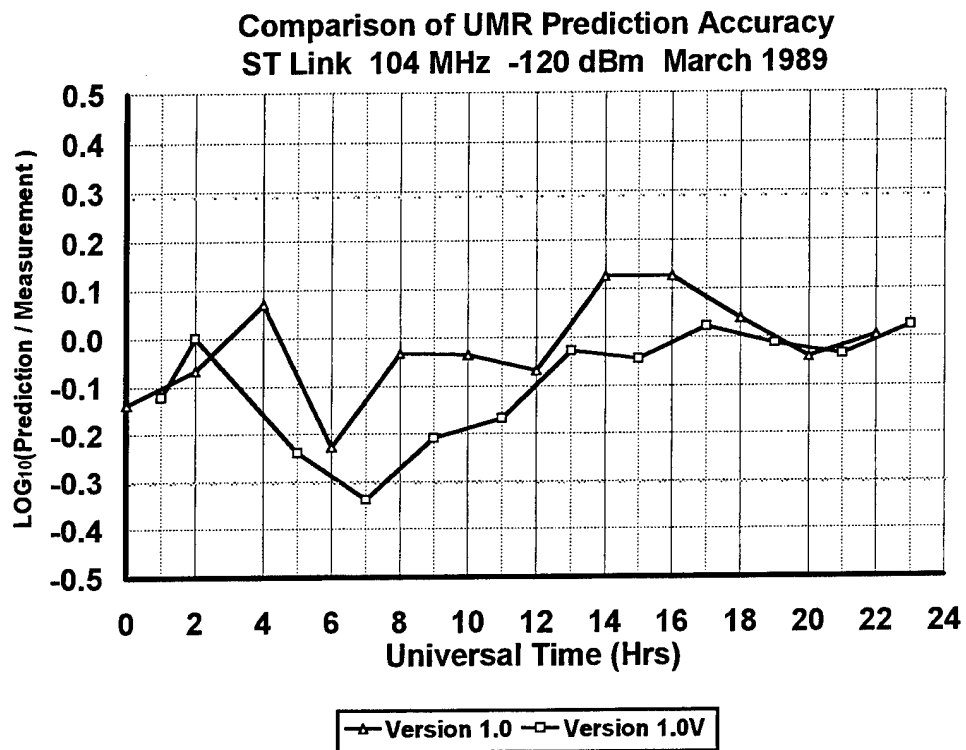


Figure A.3.2.4 UMR Comparison at -120 dBm for 104 MHz

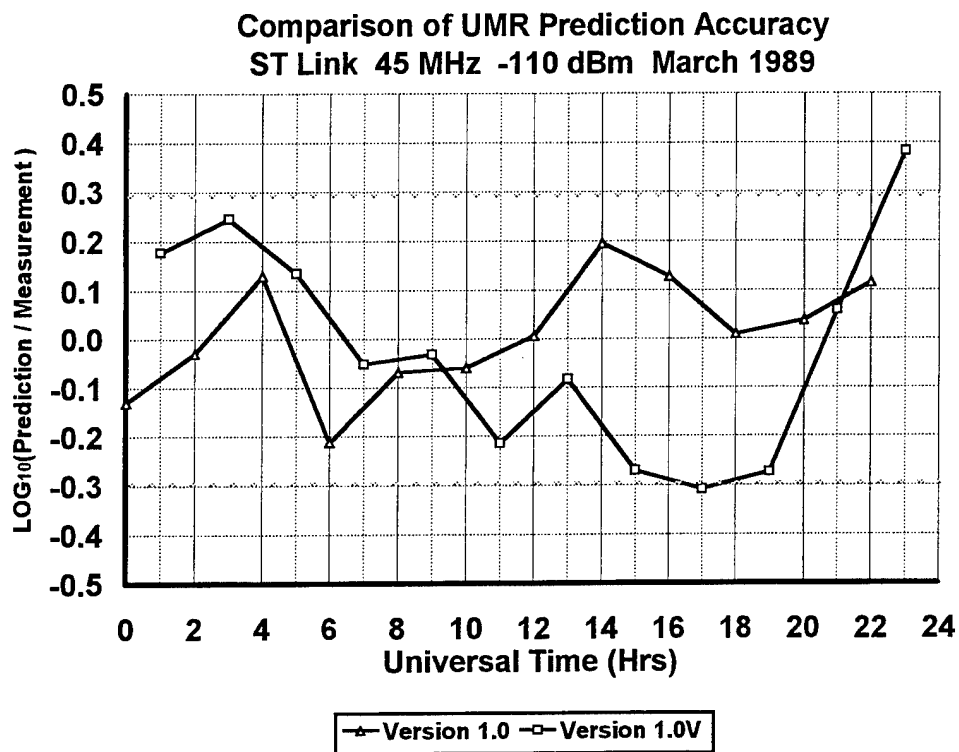


Figure A.3.2.1 UMR Comparison at -110 dBm for 45 MHz

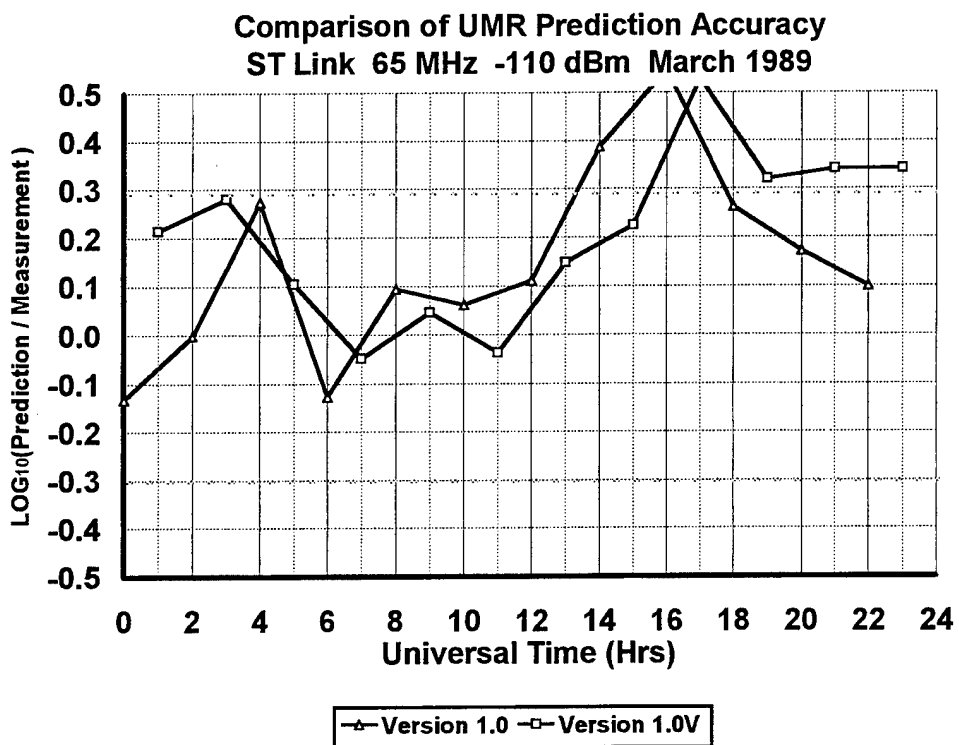


Figure A.3.2.2 UMR Comparison at -110 dBm for 65 MHz

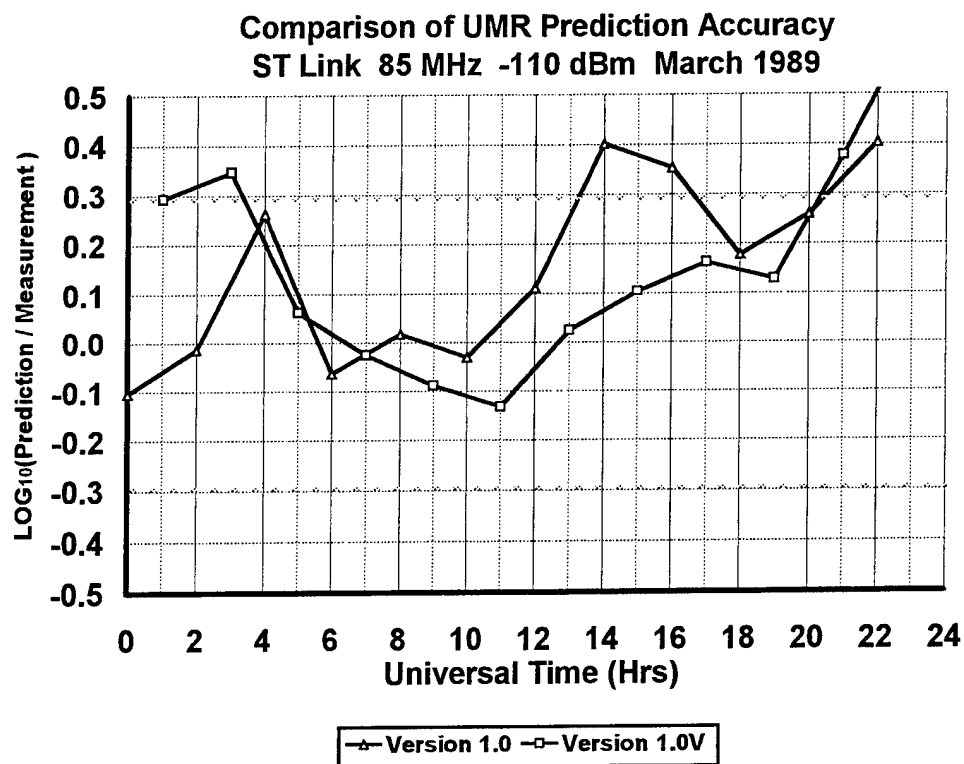


Figure A.3.2.3 UMR Comparison at -110 dBm for 85 MHz

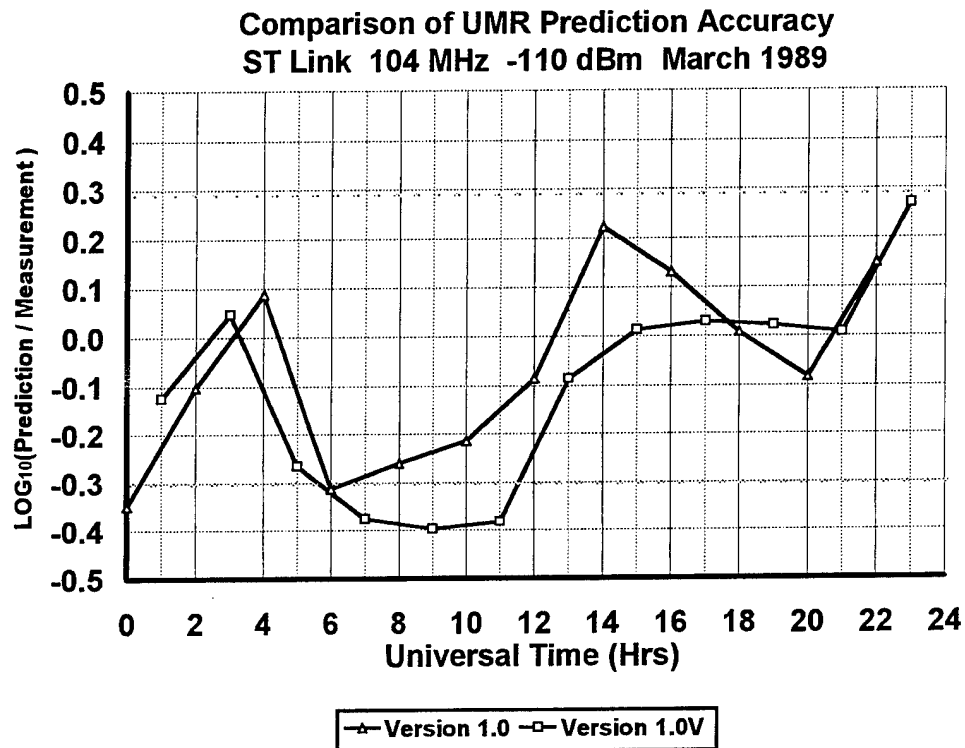


Figure A.3.2.4 UMR Comparison at -110 dBm for 104 MHz

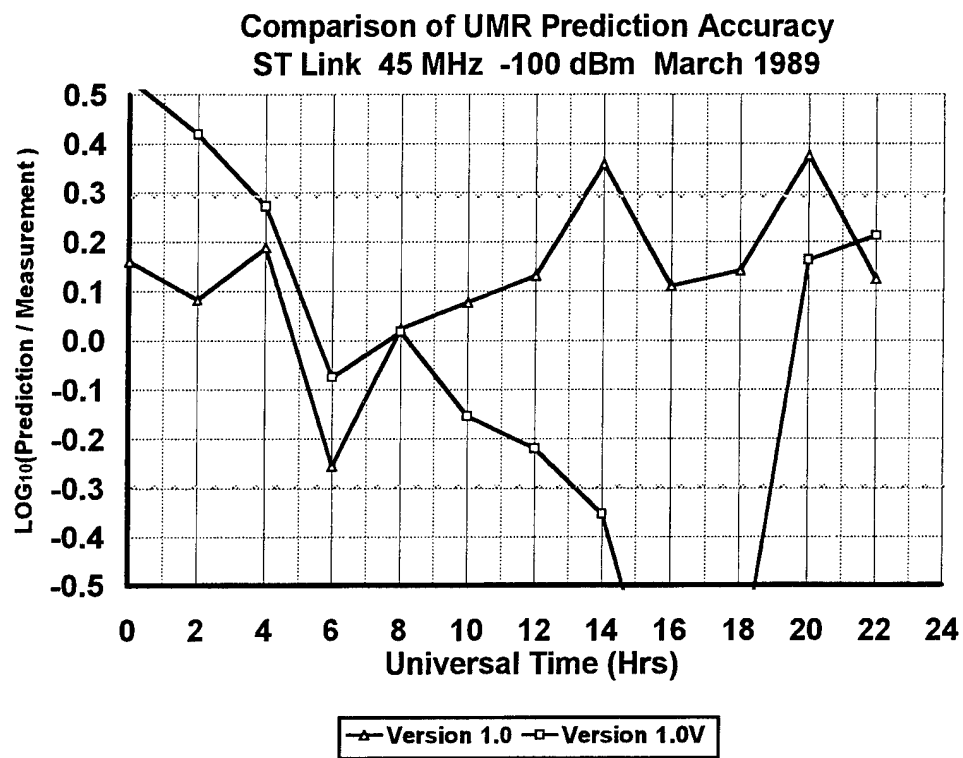


Figure A.3.3.1 UMR Comparison at -100 dBm for 45 MHz

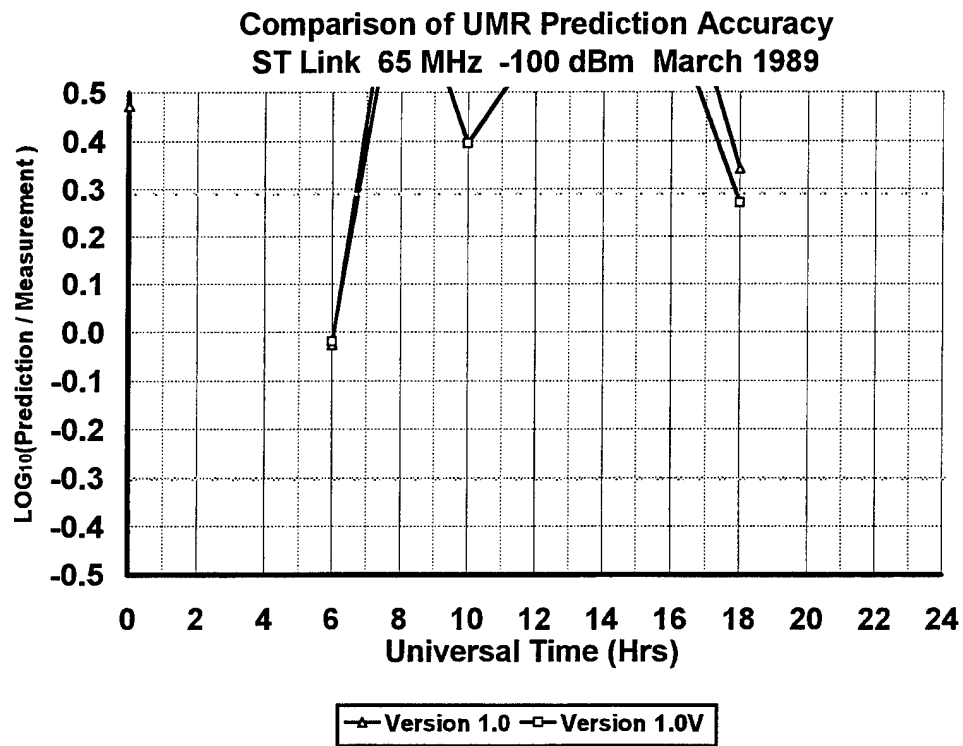


Figure A.3.3.2 UMR Comparison at -100 dBm for 65 MHz

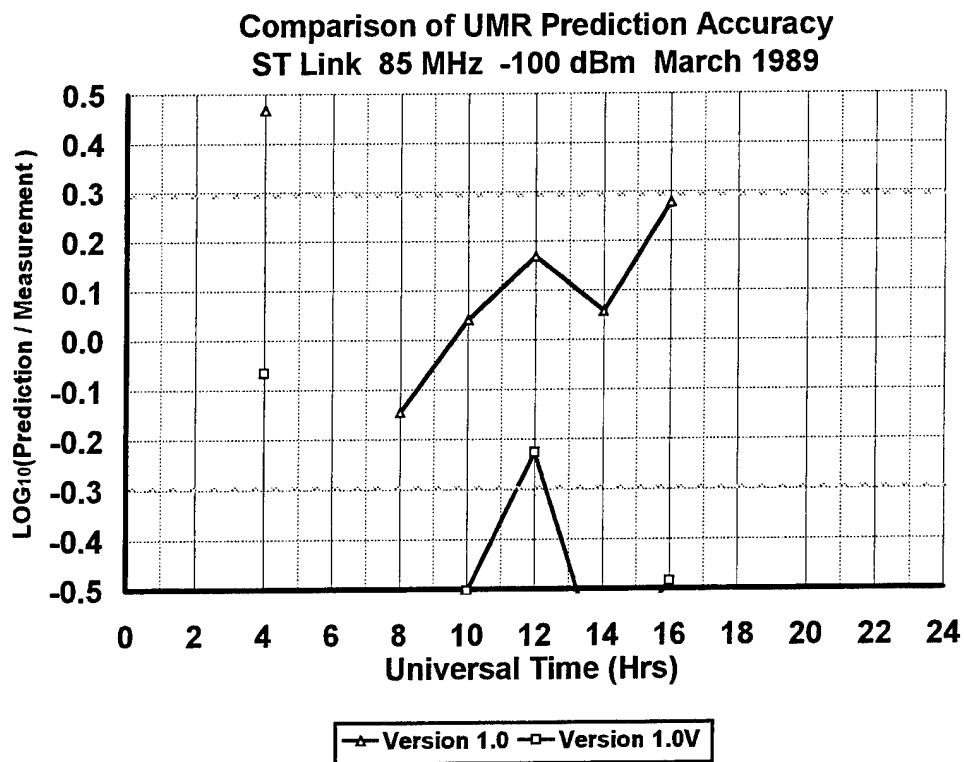


Figure A.3.3.3 UMR Comparison at -100 dBm for 85 MHz

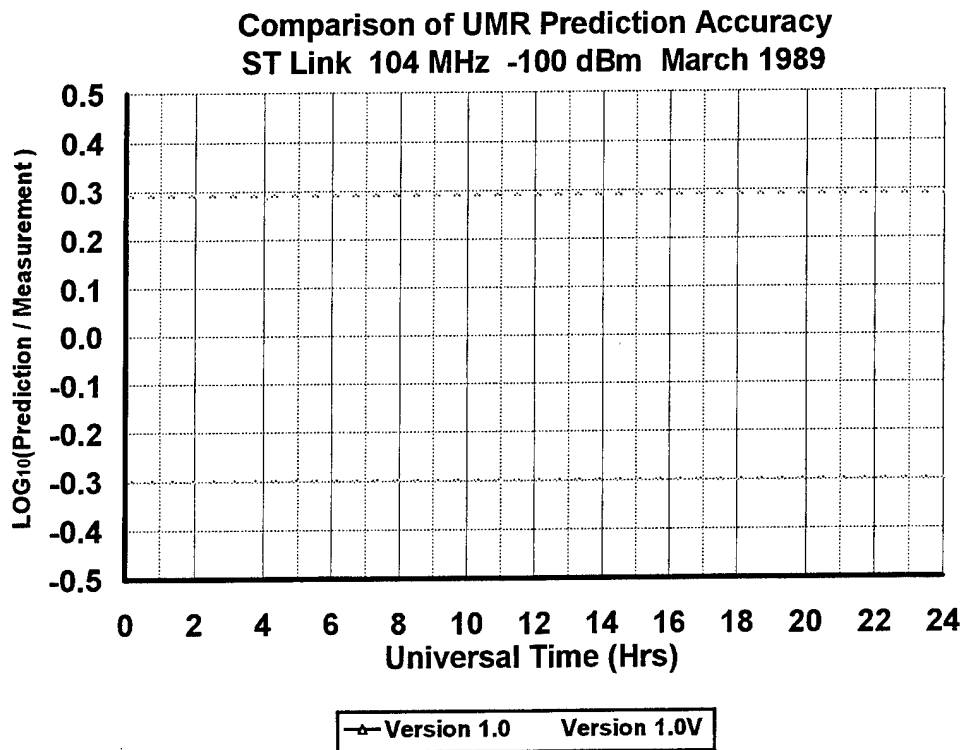


Figure A.3.3.4 UMR Comparison at -100 dBm for 104 MHz

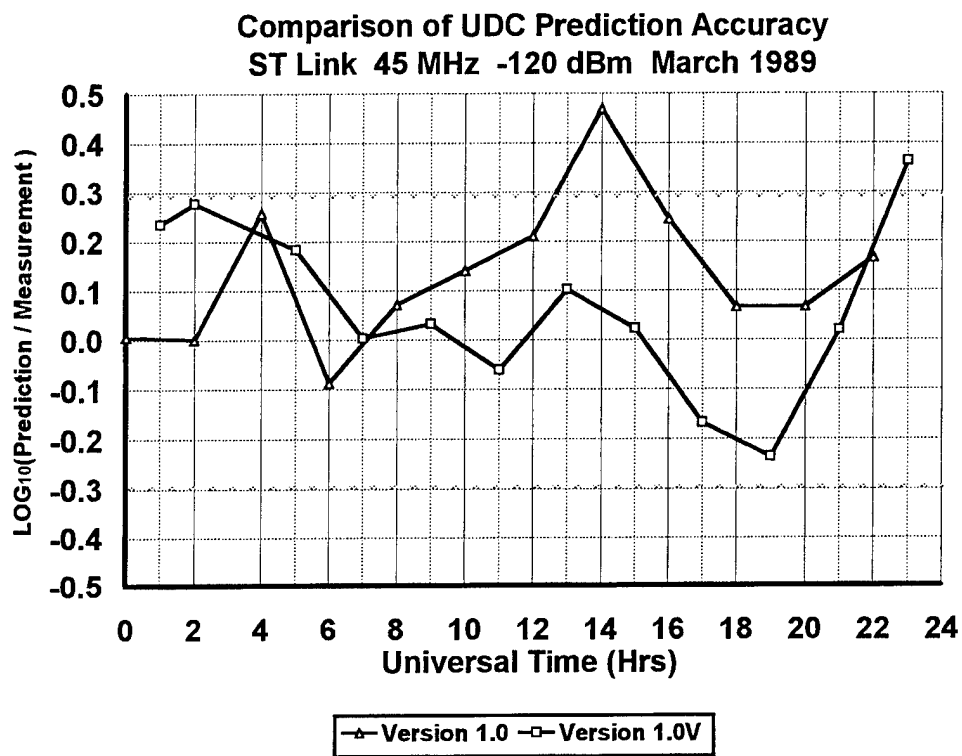


Figure A.4.1.1 UDC Comparison at -120 dBm for 45 MHz

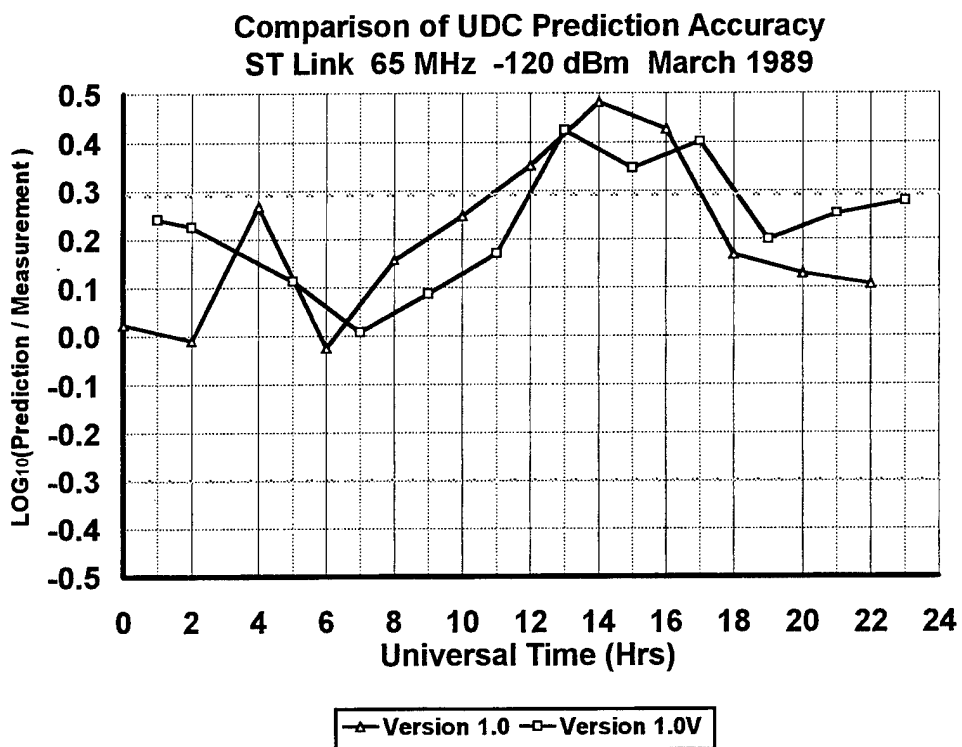


Figure A. 4.1.2 UDC Comparison at -120 dBm for 65 MHz

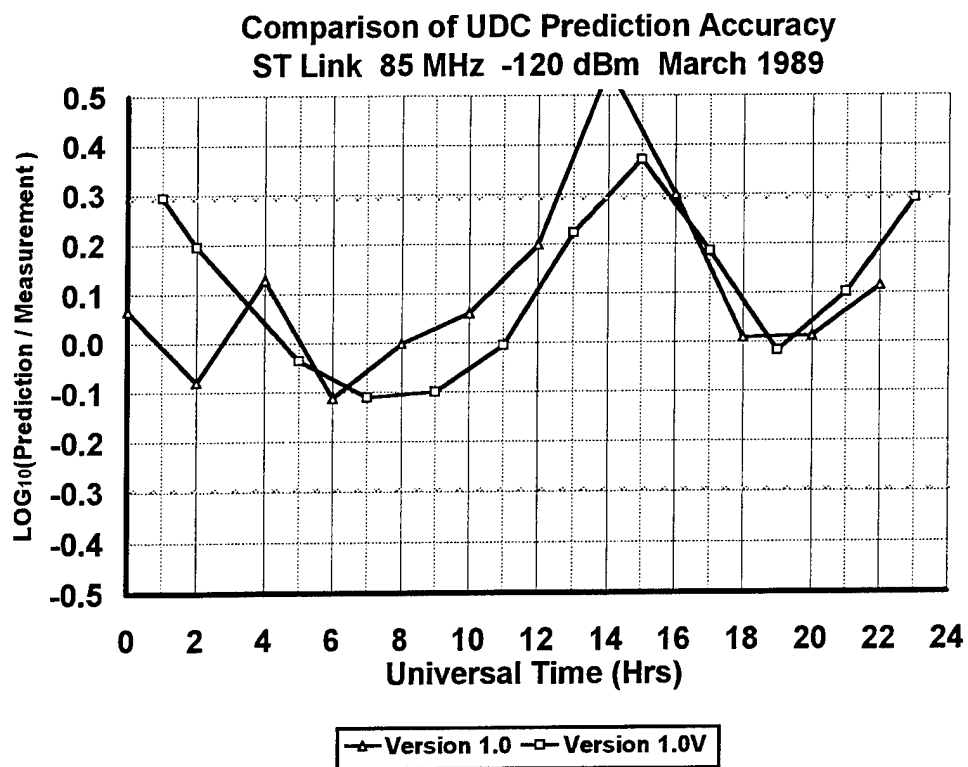


Figure A. 4.1.3 UDC Comparison at -120 dBm for 85 MHz

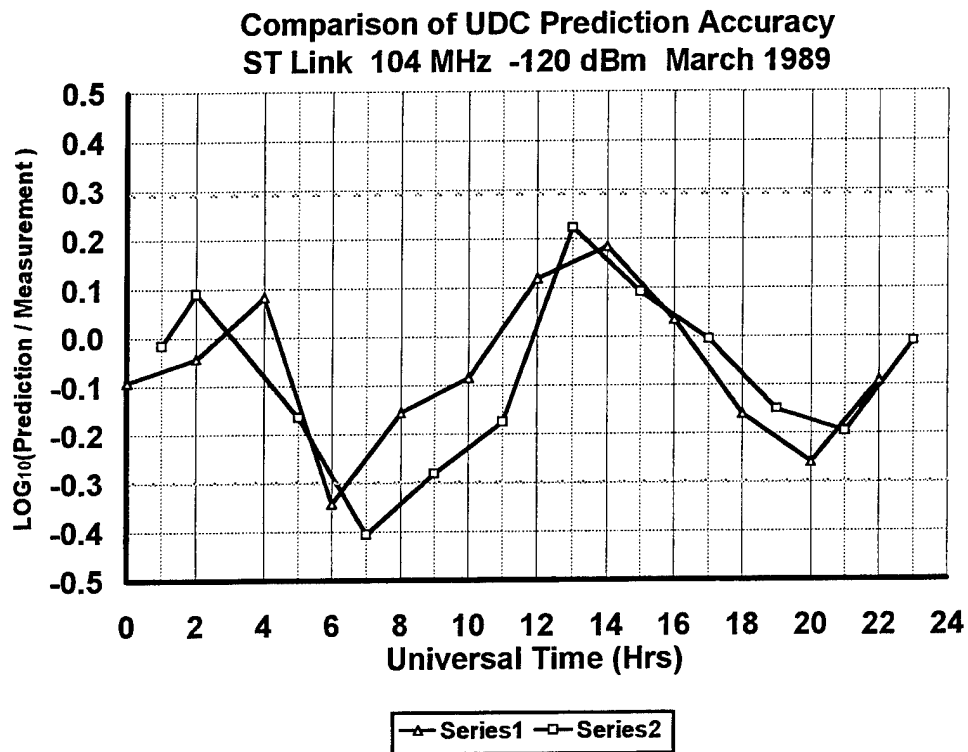


Figure A. 4.1.4 UDC Comparison at -120 dBm for 104 MHz

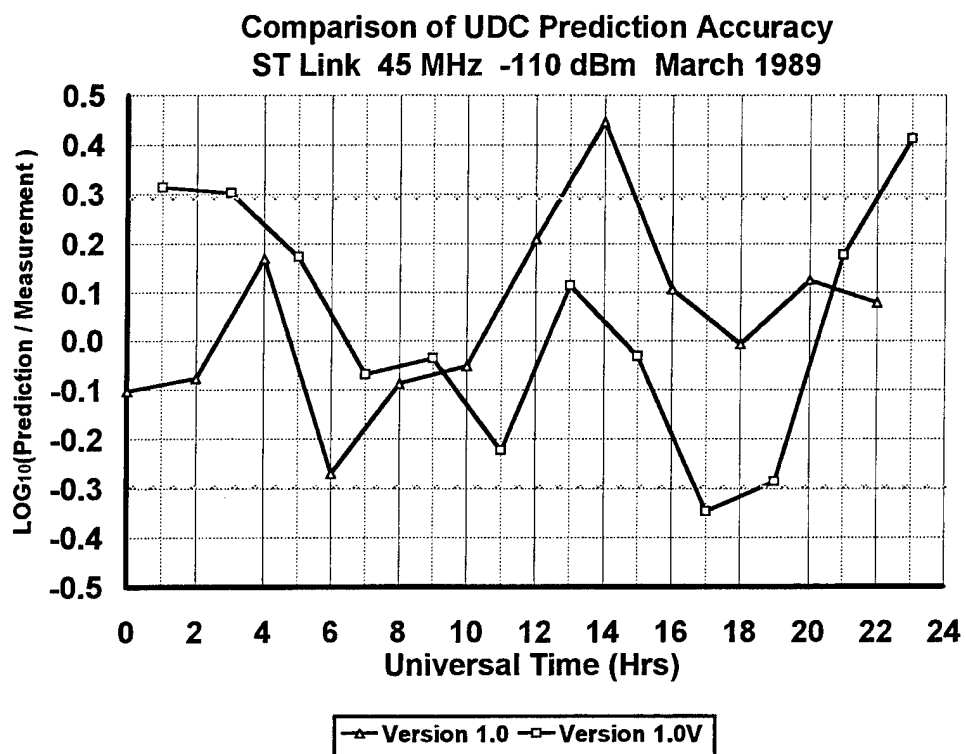


Figure A.4.2.1 UDC Comparison at -110 dBm for 45 MHz

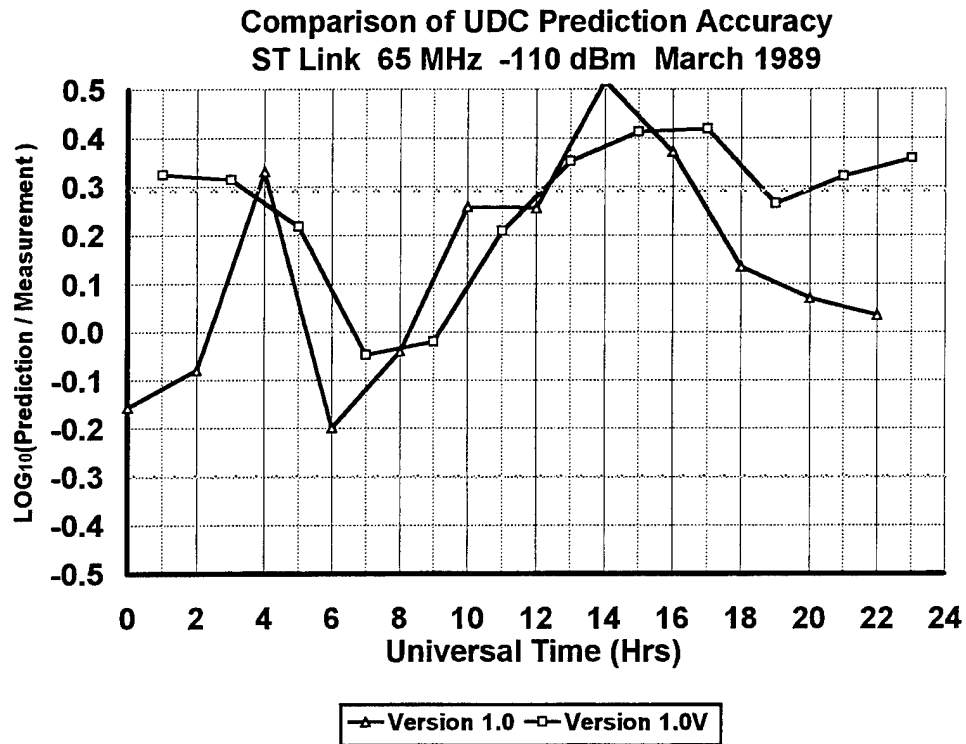


Figure A.4.2.2 UDC Comparison at -110 dBm for 65 MHz

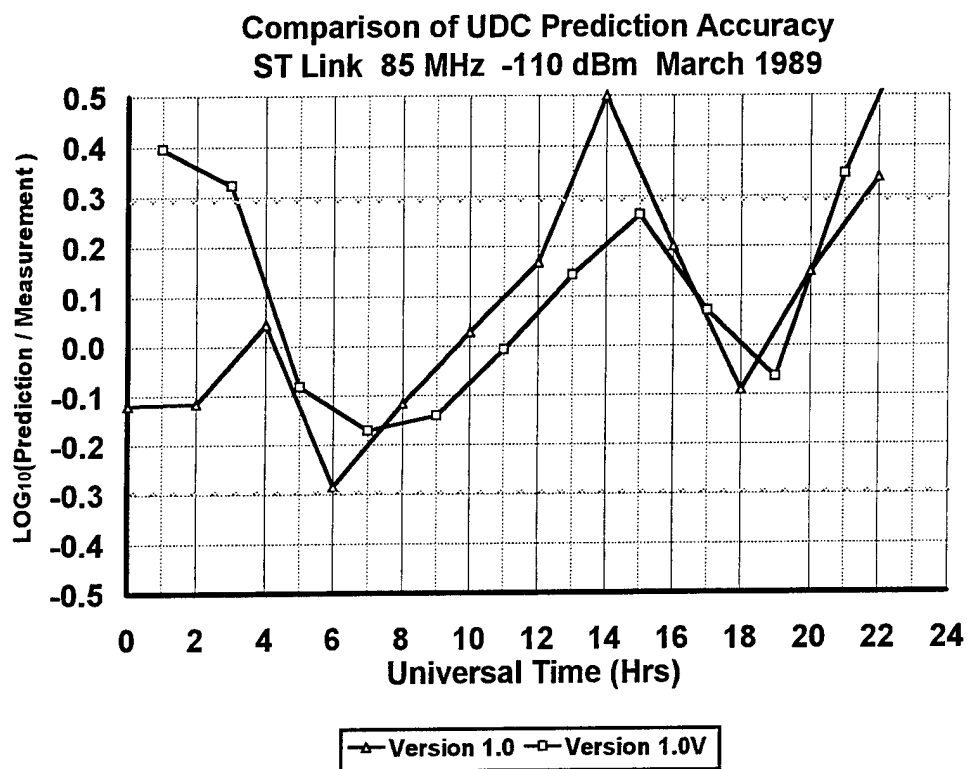


Figure A.4.2.3 UDC Comparison at -110 dBm for 85 MHz

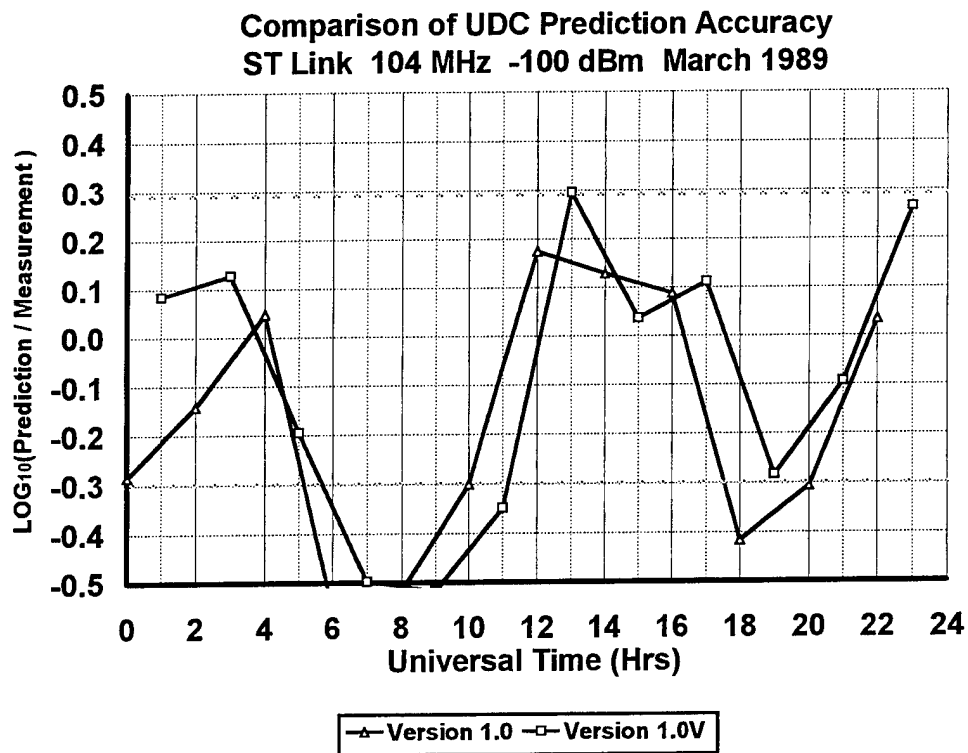


Figure A.4.2.4 UDC Comparison at -110 dBm for 104 MHz

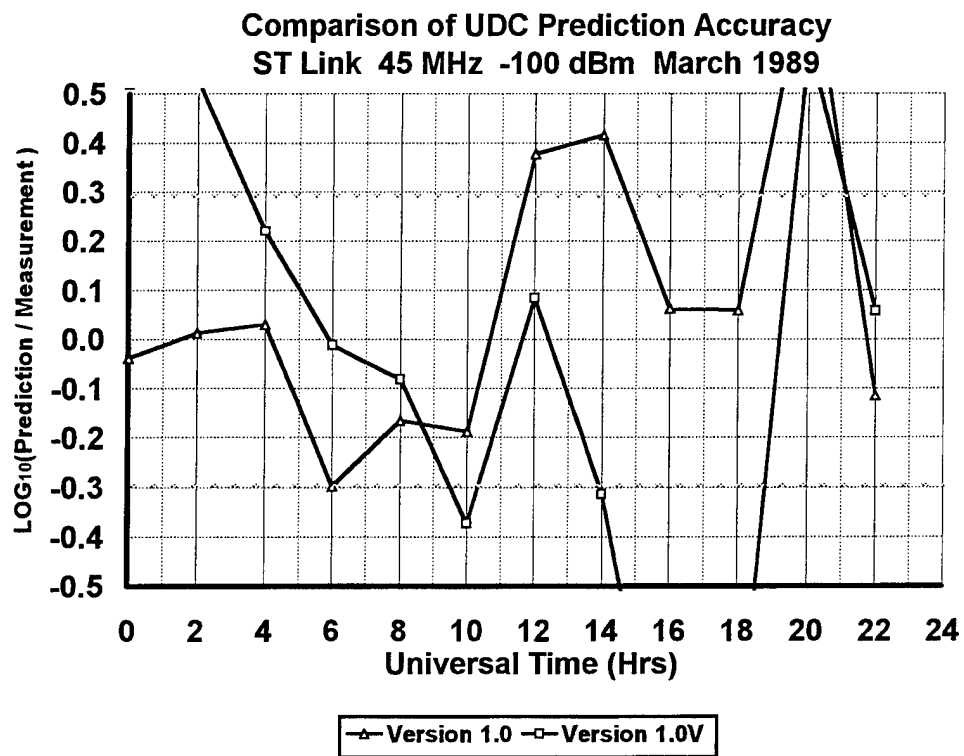


Figure A.4.3.1 UDC Comparison at -100 dBm for 45 MHz

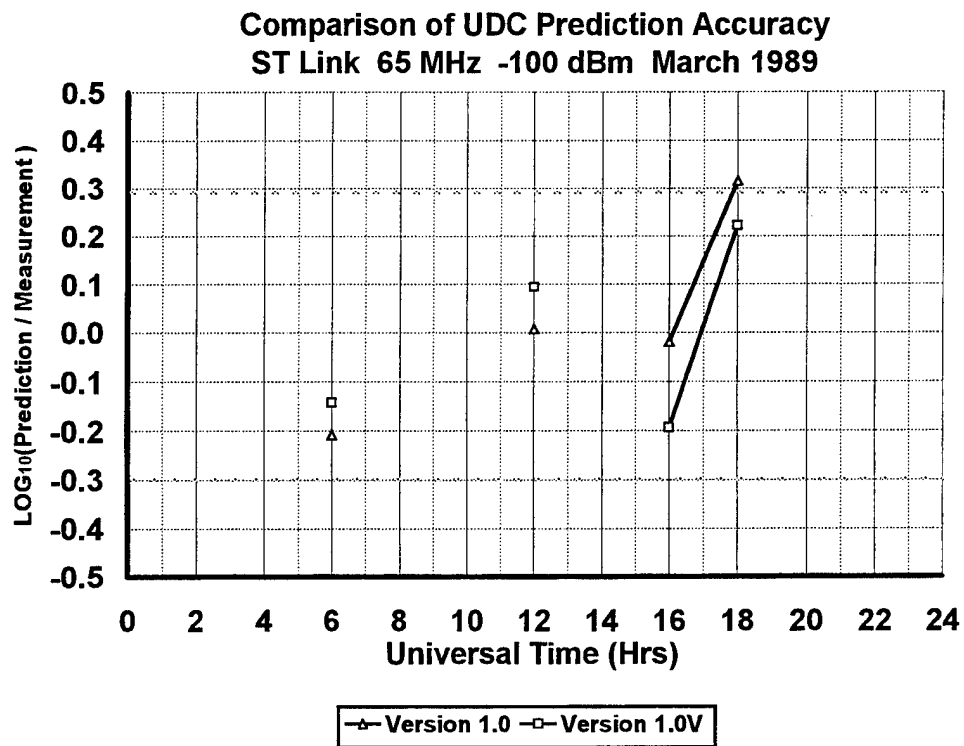


Figure A.4.3.2 UDC Comparison at -100 dBm for 65 MHz

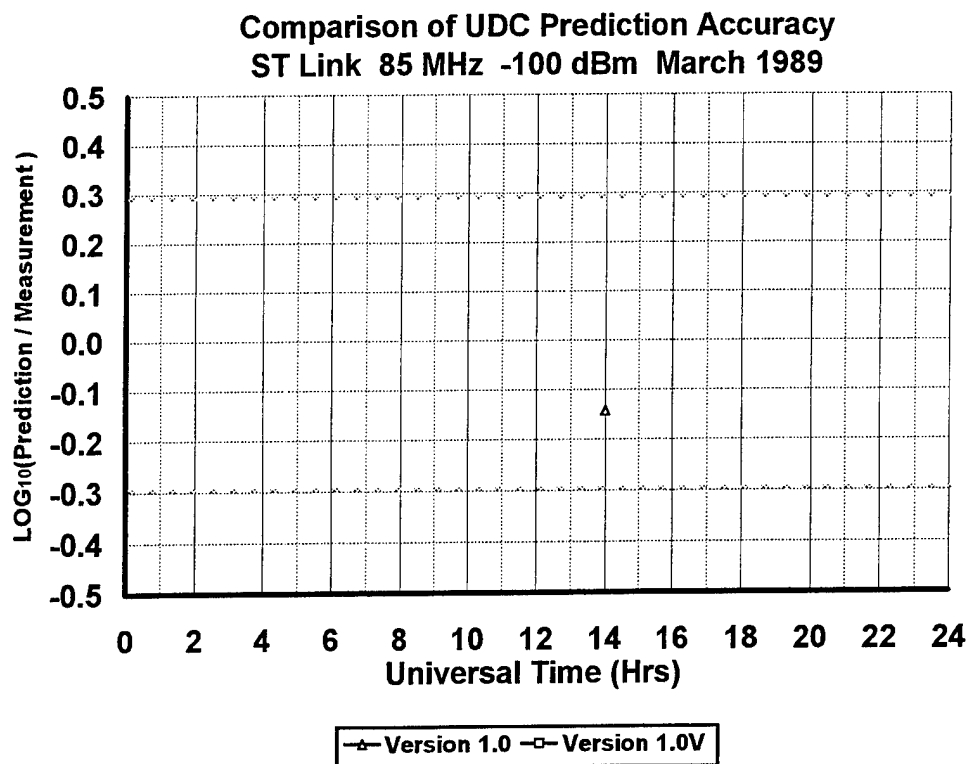


Figure A.4.3.3 UDC Comparison at -100 dBm for 85 MHz

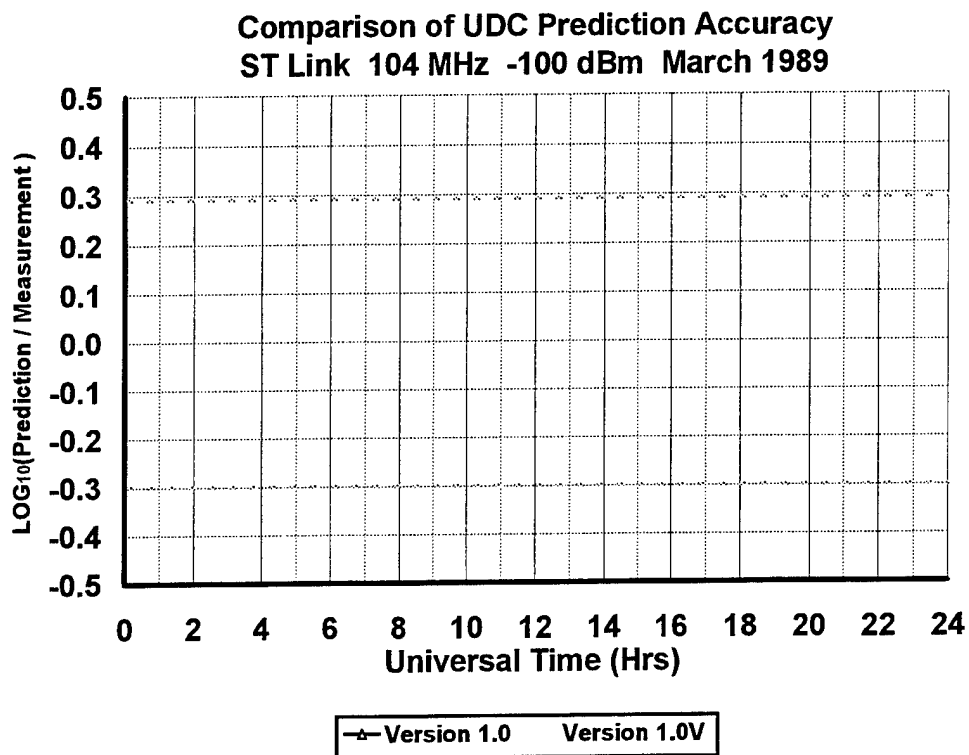


Figure A.4.3.4 UDC Comparison at -100 dBm for 104 MHz

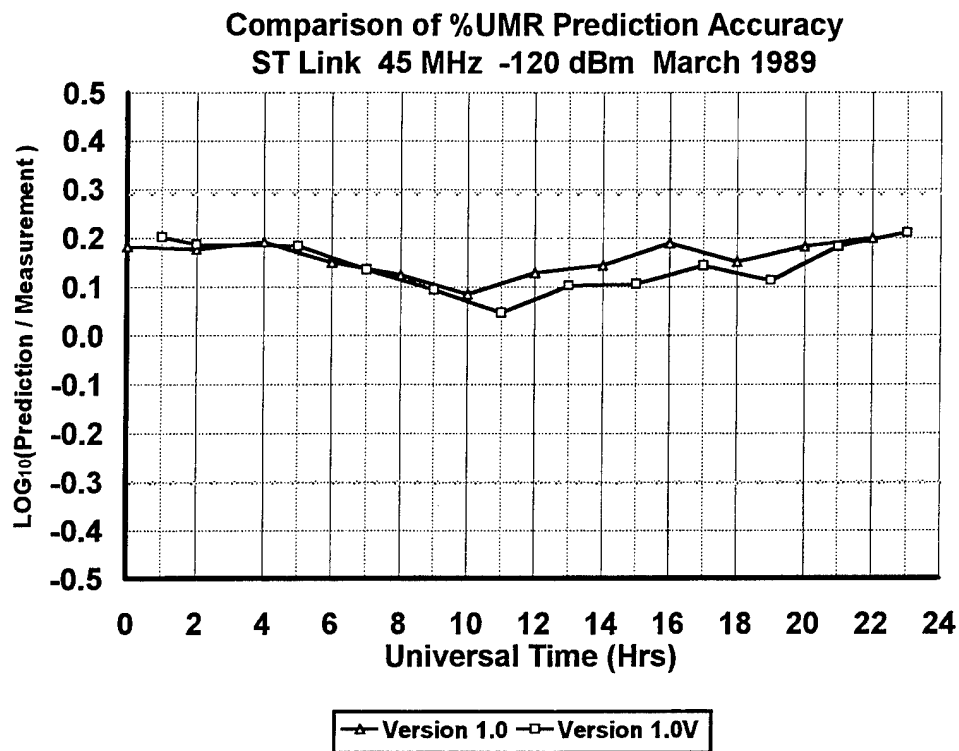


Figure A.5.1.1 %UMR Comparison at -120 dBm for 45 MHz

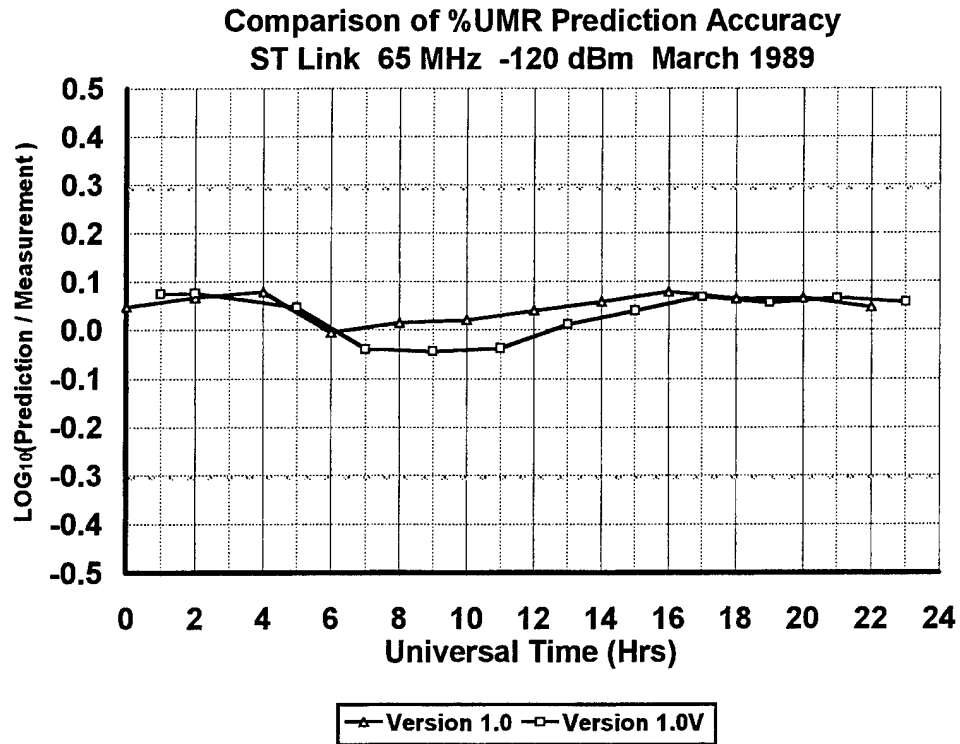


Figure A. 5.1.2 %UMR Comparison at -120 dBm for 65 MHz

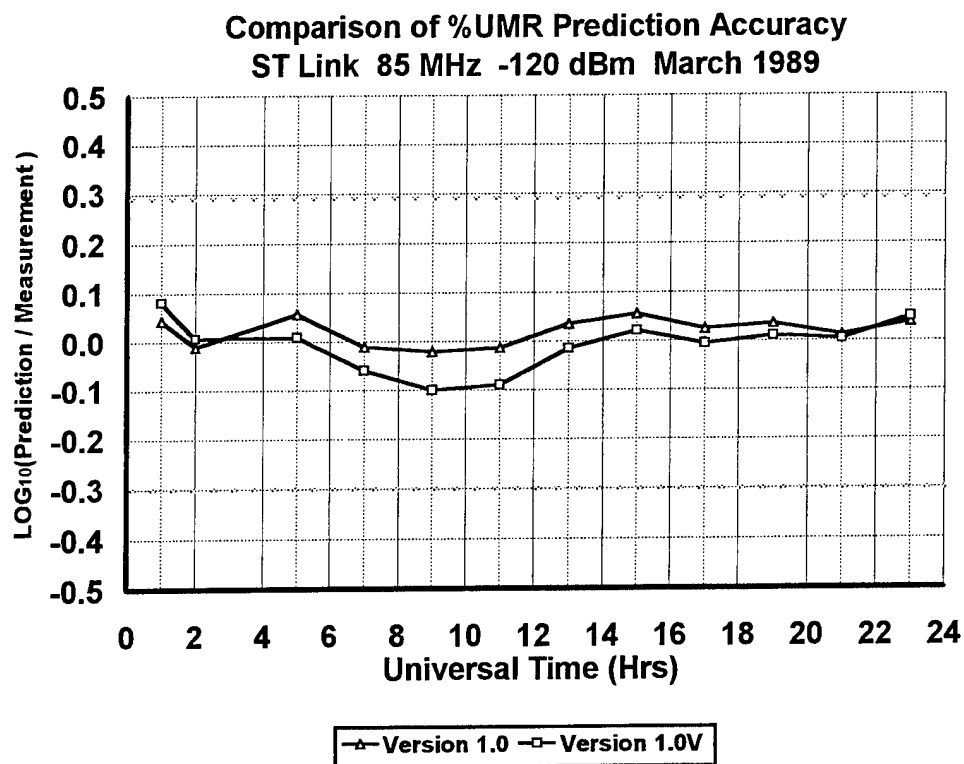


Figure A. 5.1.3 %UMR Comparison at -120 dBm for 85 MHz

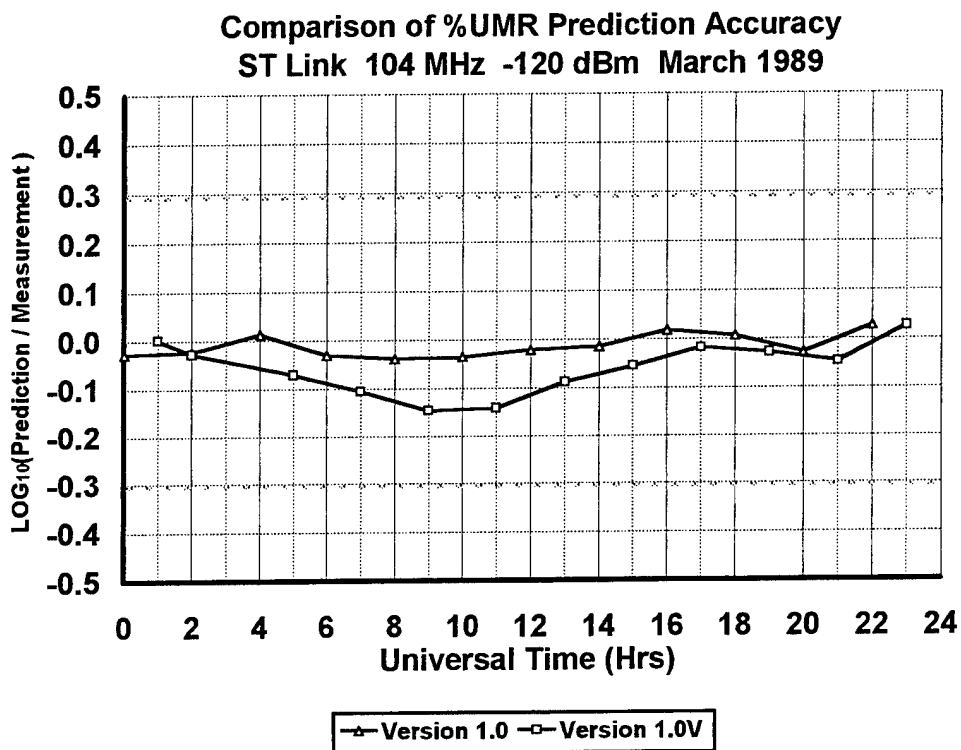


Figure A. 5.1.4 %UMR Comparison at -120 dBm for 104 MHz

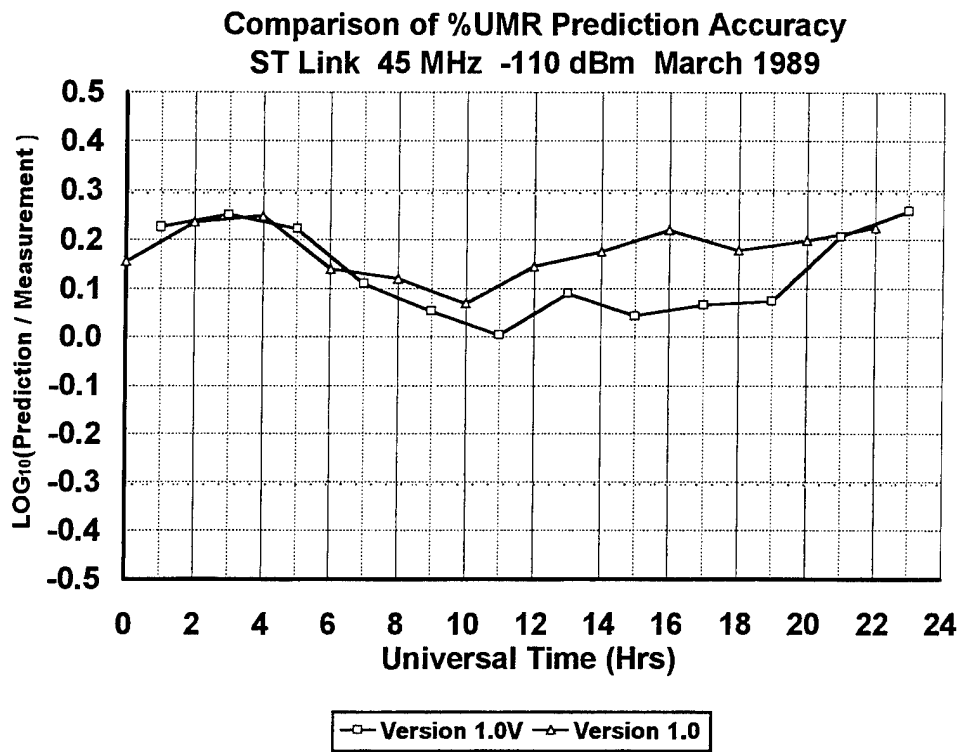


Figure A.5.2.1 %UMR Comparison at -110 dBm for 45 MHz

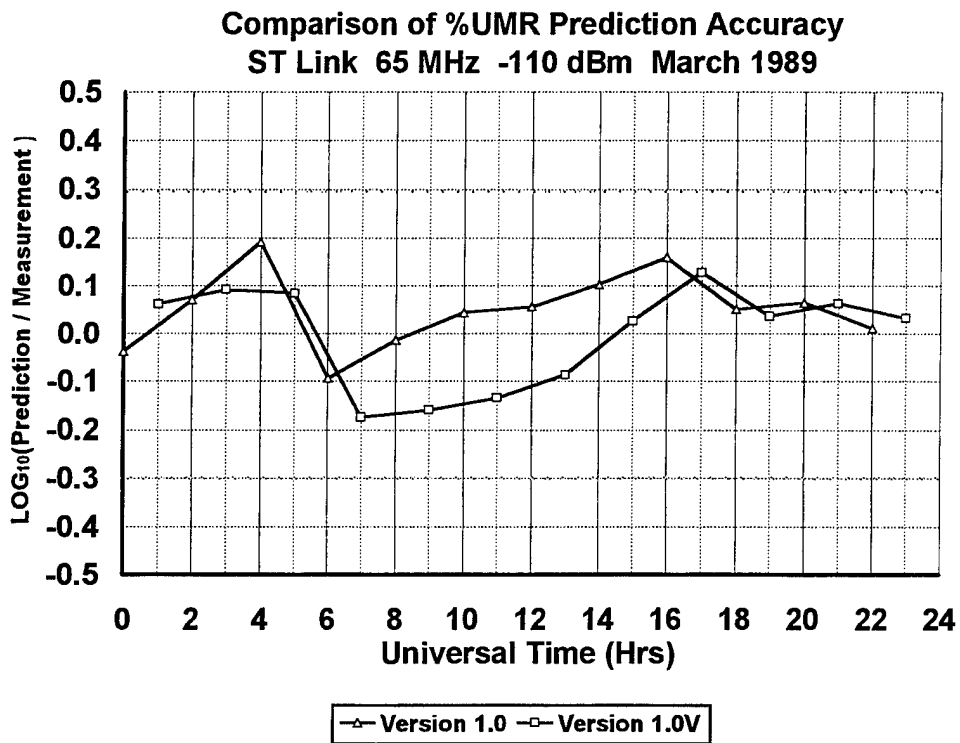


Figure A.5.2.2 %UMR Comparison at -110 dBm for 65 MHz

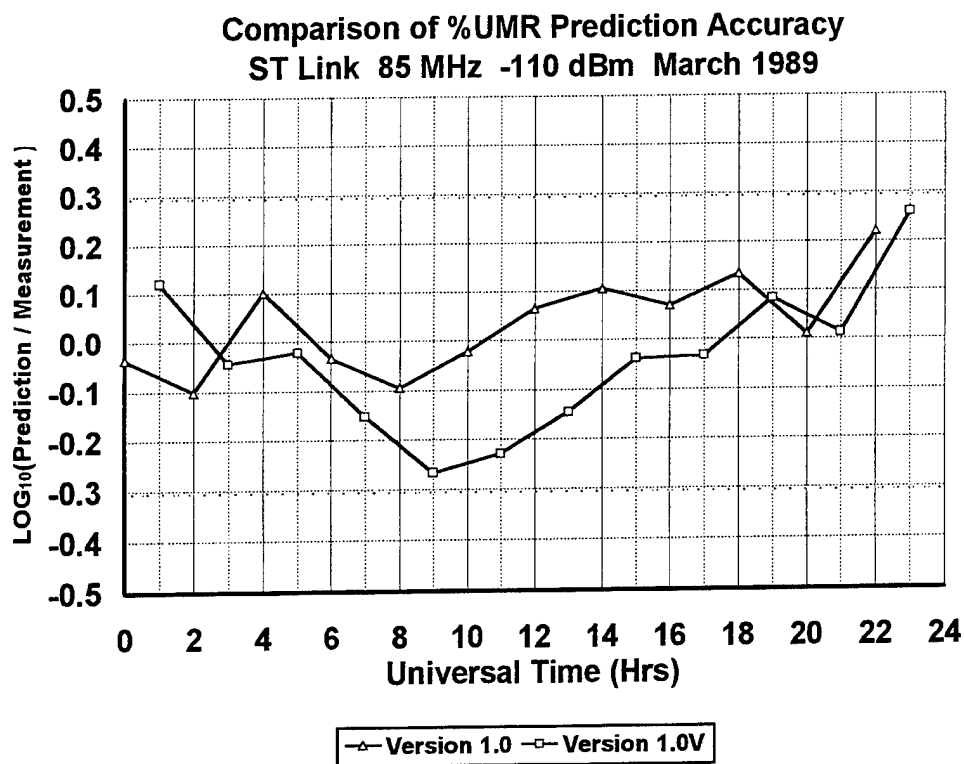


Figure A.5.2.3 %UMR Comparison at -110 dBm for 85 MHz

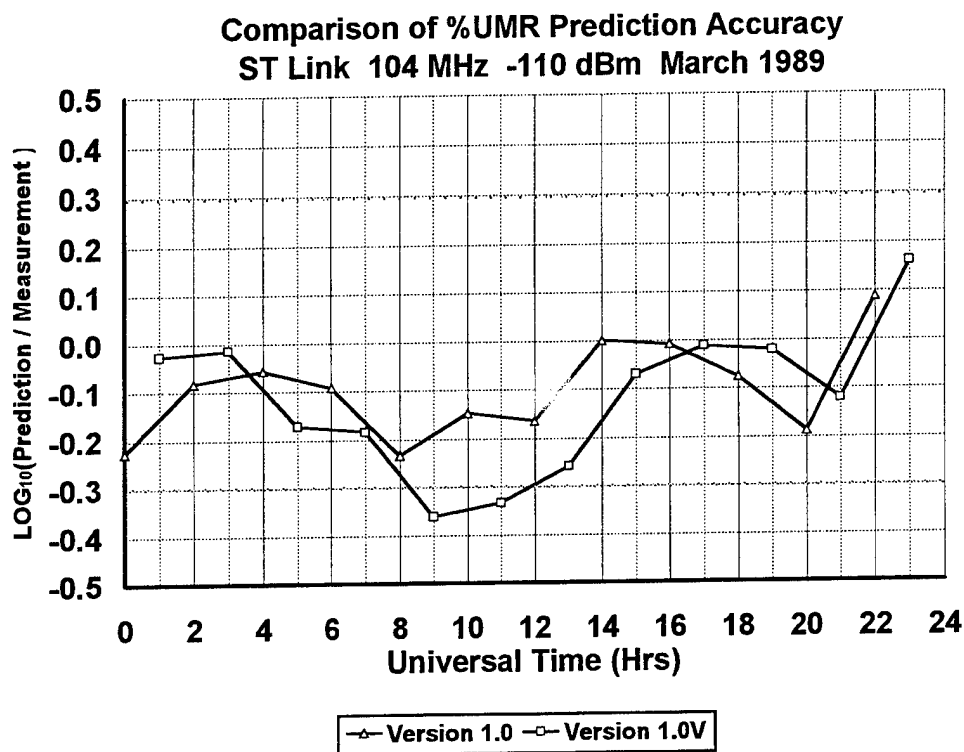


Figure A.5.2.4 %UMR Comparison at -110 dBm for 104 MHz

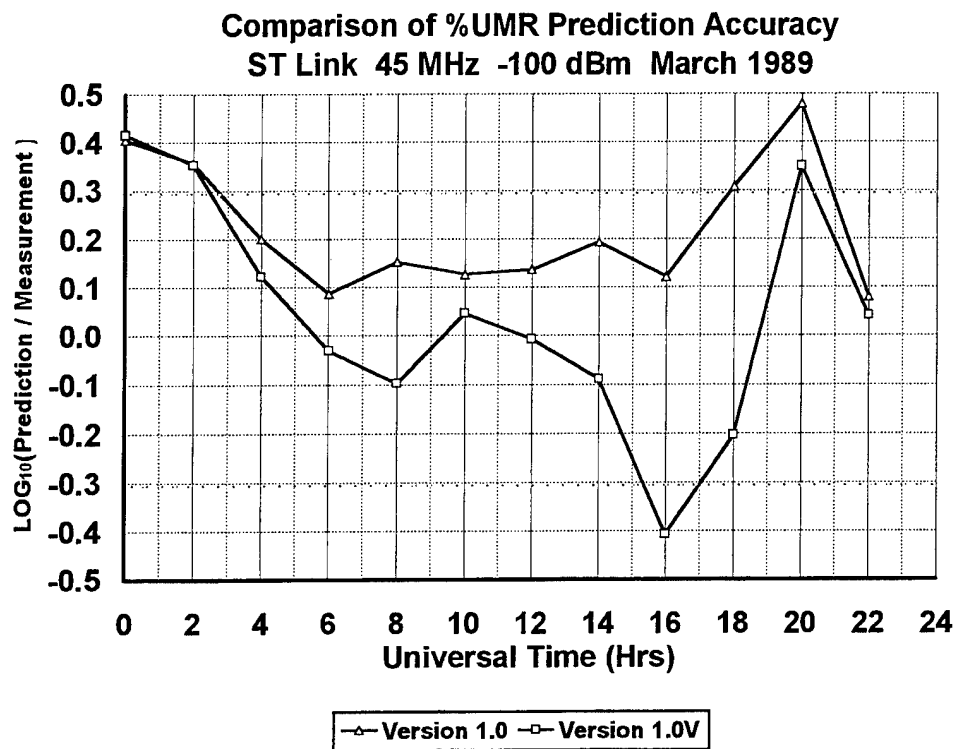


Figure A.5.3.1 %UMR Comparison at -100 dBm for 45 MHz

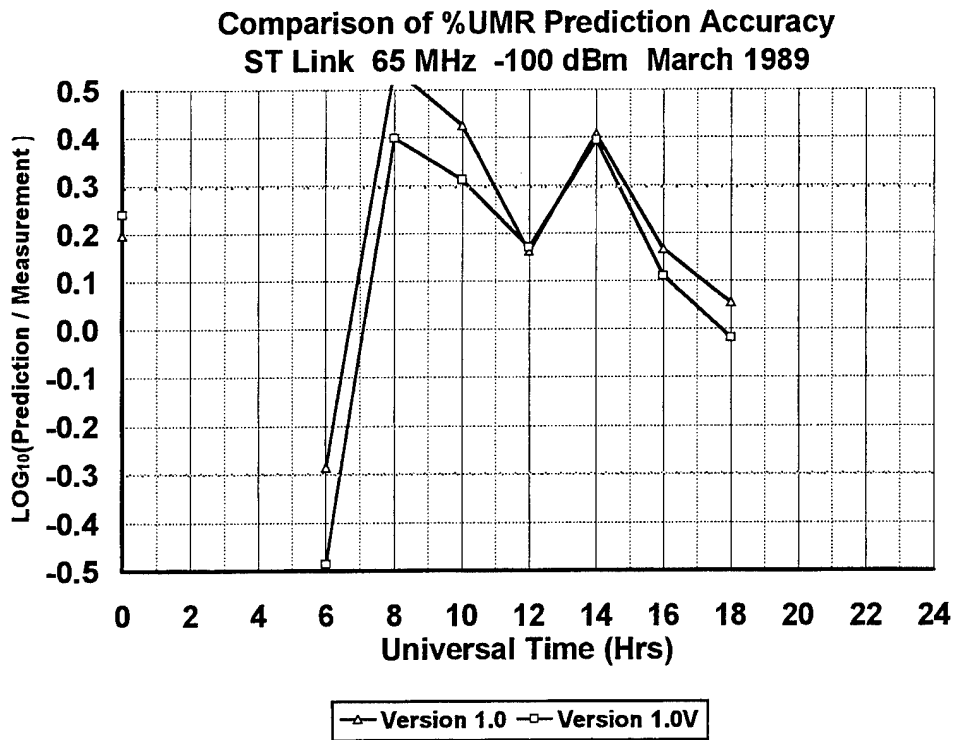


Figure A.5.3.2 %UMR Comparison at -100 dBm for 65 MHz

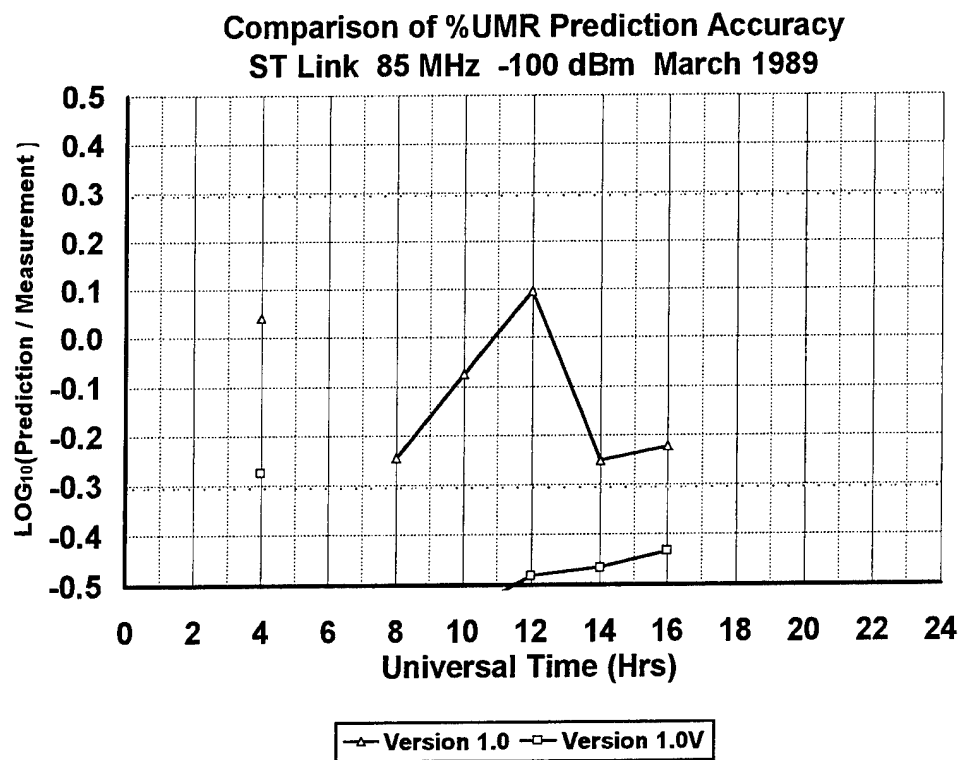


Figure A.5.3.3 %UMR Comparison at -100 dBm for 85 MHz

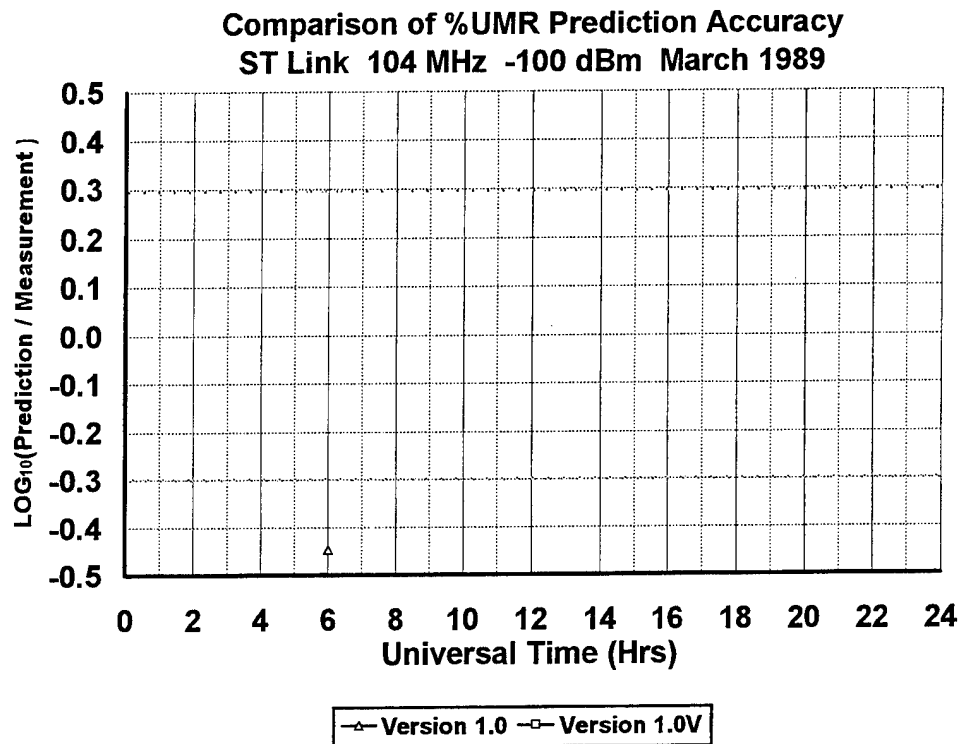


Figure A.5.3.4 %UMR Comparison at -100 dBm for 104 MHz

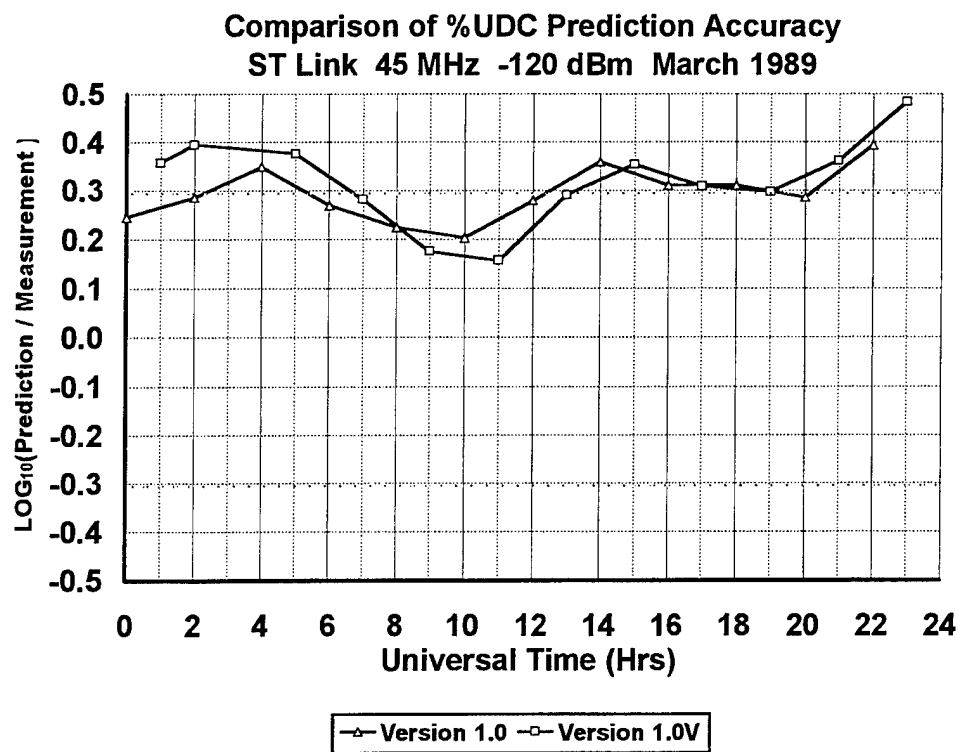


Figure A.6.1.1 %UDC Comparison at -120 dBm for 45 MHz

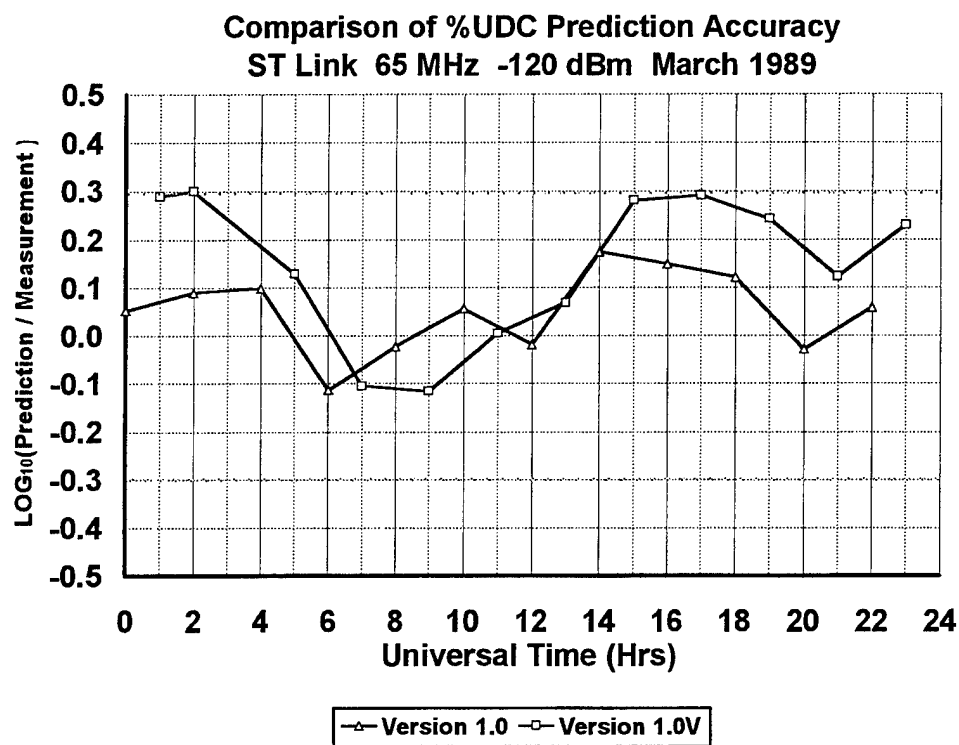


Figure A.6.1.2 %UDC Comparison at -120 dBm for 65 MHz

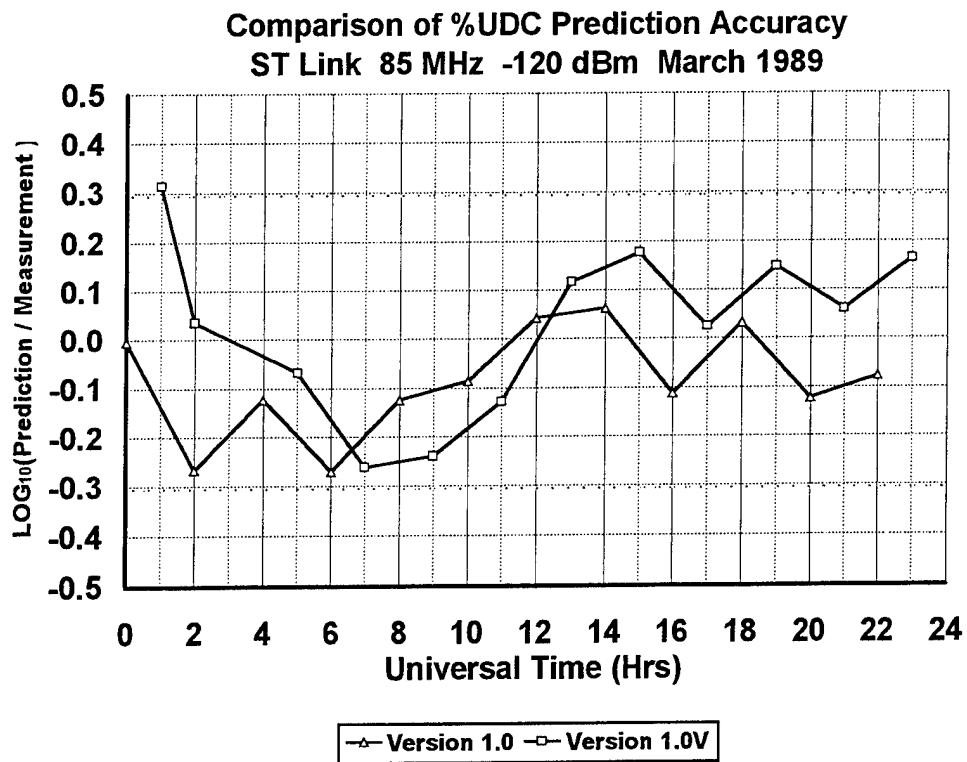


Figure A.6.1.3 %UDC Comparison at -120 dBm for 85 MHz

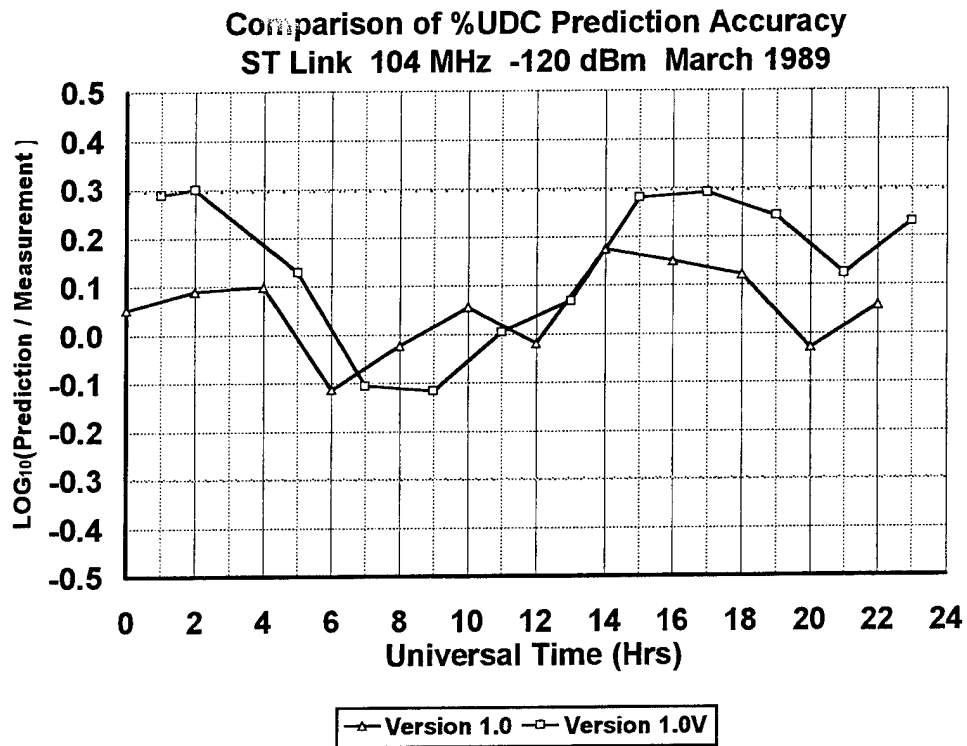


Figure A.6.1.4 %UDC Comparison at -120 dBm for 104 MHz

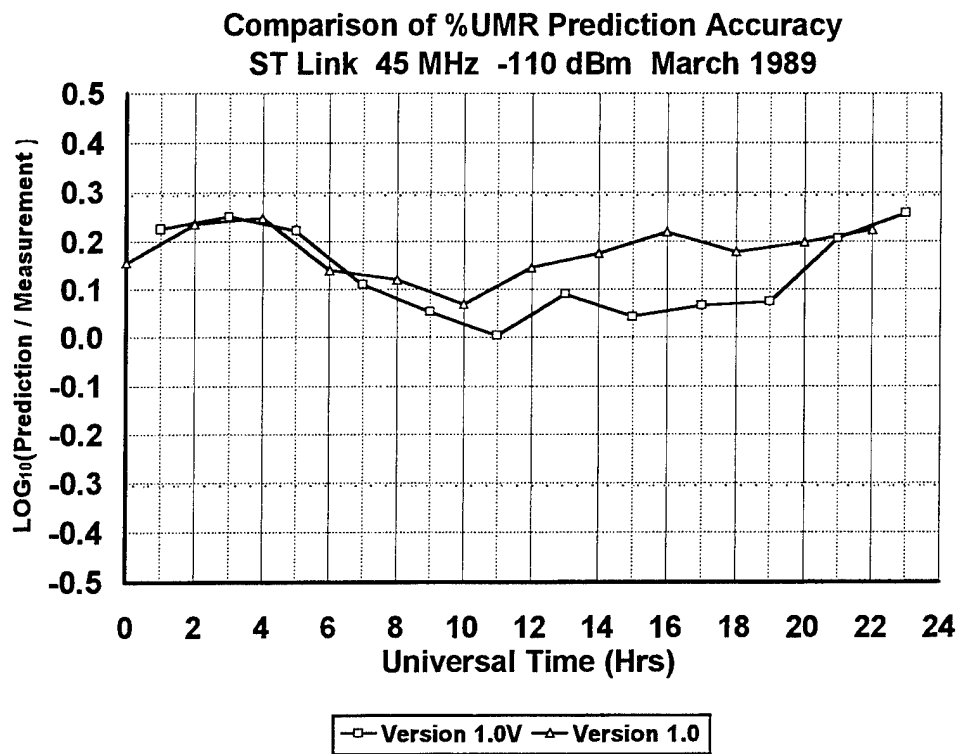


Figure A.6.2.1 %UDC Comparison at -110 dBm for 45 MHz

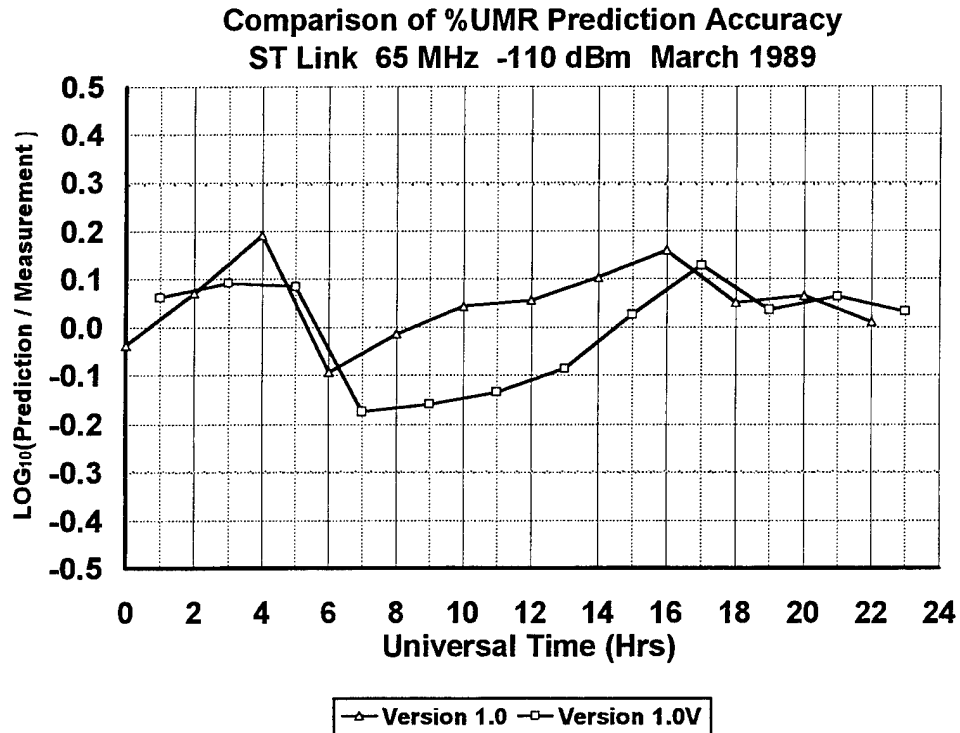


Figure A.6.2.2 %UDC Comparison at -110 dBm for 65 MHz

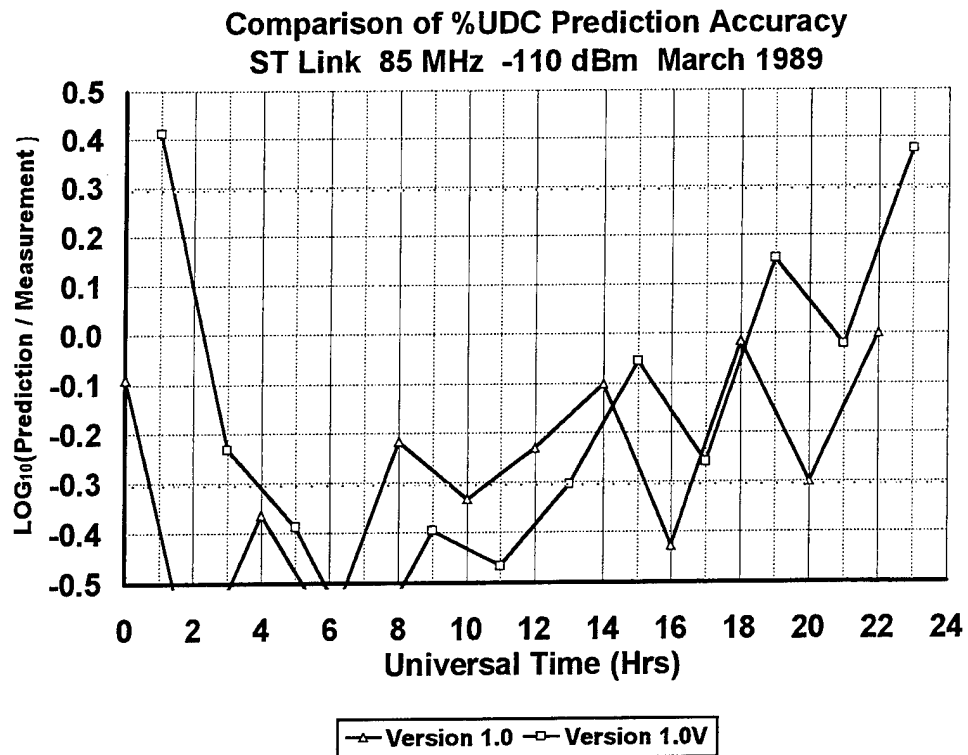


Figure A.6.2.3 %UDC Comparison at -110 dBm for 85 MHz

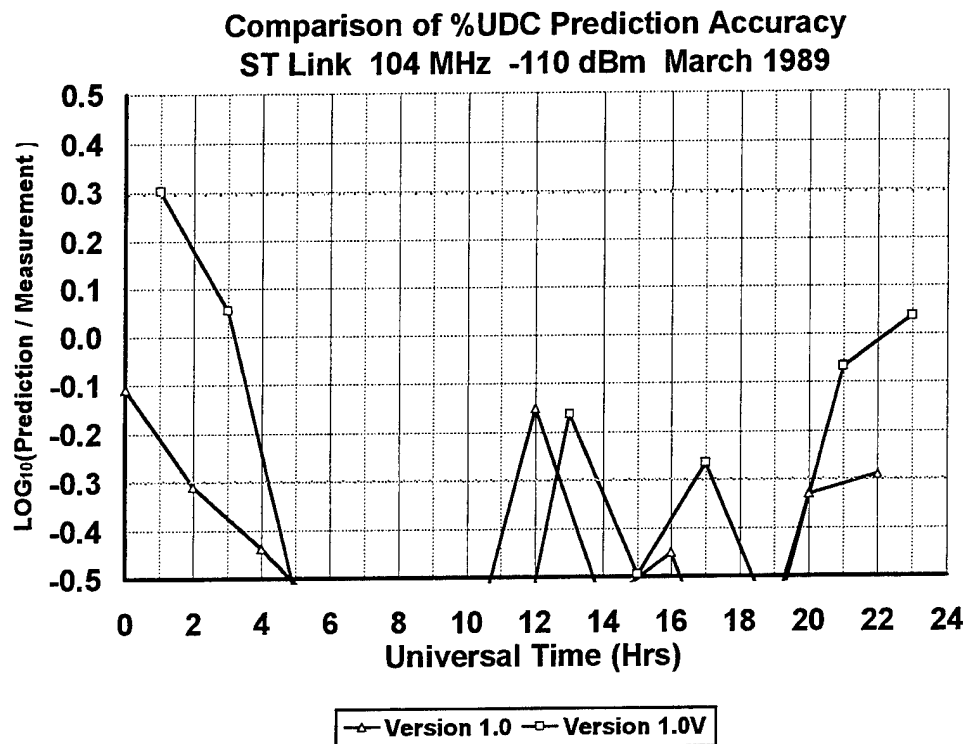


Figure A.6.2.4 %UDC Comparison at -110 dBm for 104 MHz

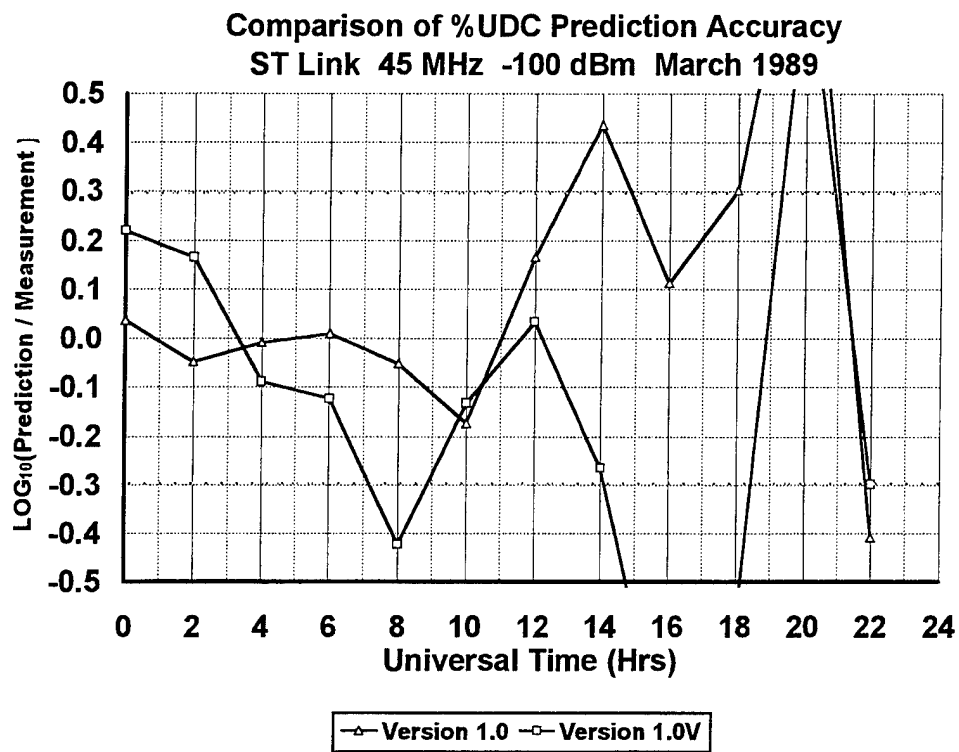


Figure A.6.3.1 %UDC Comparison at -100 dBm for 45 MHz

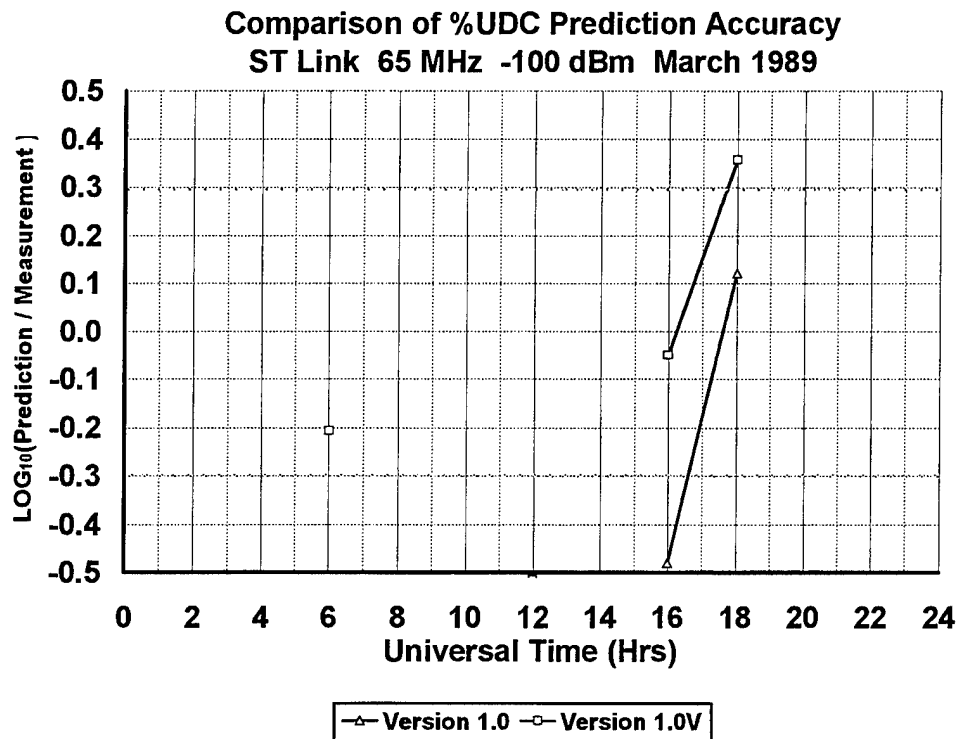


Figure A.6.3.2 %UDC Comparison at -100 dBm for 65 MHz

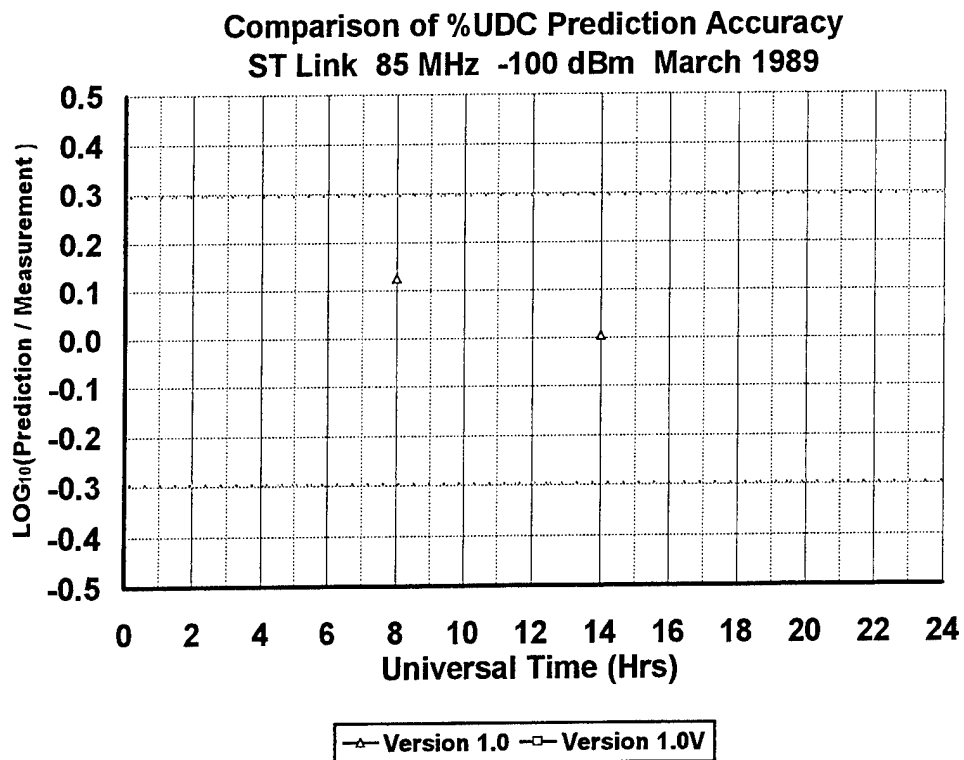


Figure A.6.3.3 %UDC Comparison at -100 dBm for 85 MHz

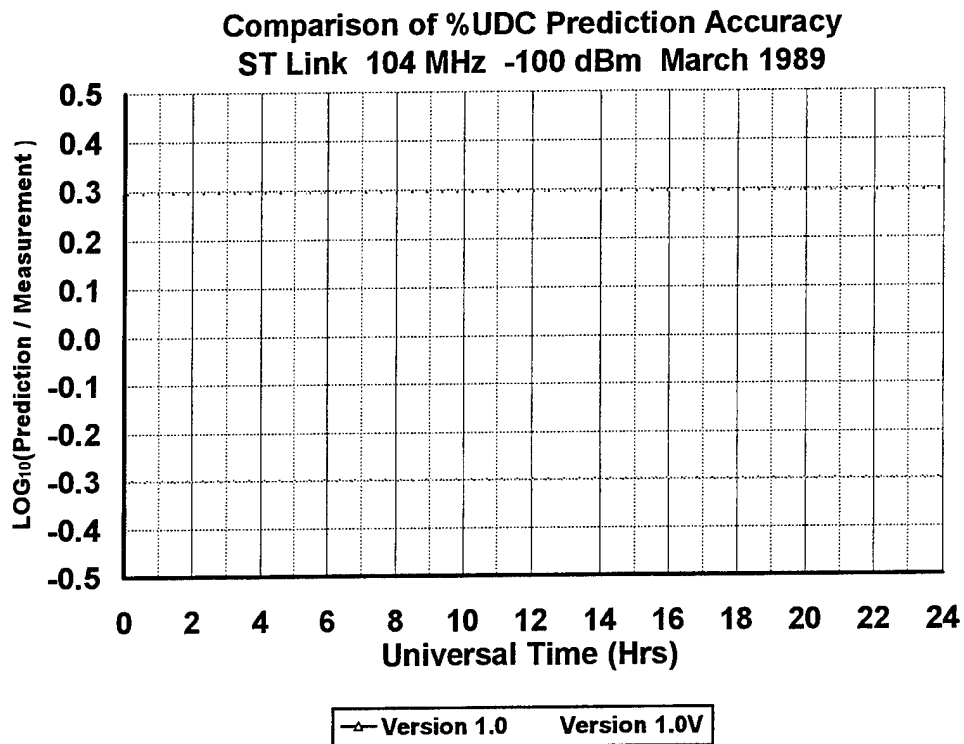


Figure A.6.3.4 %UDC Comparison at -100 dBm for 104 MHz

7. APPENDIX B: JODRELL BANK TEST BED RESULTS

This appendix presents plots of the usable meteor rate (MR) for the “northwest” and “southwest” antenna beams obtained at Jodrell Bank in Greenland in the years 1950 and 1951. Each plot contains the results for both the original VAX METEORLINK (similar to PC METEORLINK Version 1.0) and PC METEORLINK Version 1.0V. The following table provides an index into appendix B to help the reader locate specific results.

	Northwest Beam		Southwest Beam	
Month and Year	Figure #	Page #	Figure #	Page #
January 1951	B.1.1	B-2	B.1.2	B-2
February 1951	B.2.1	B-3	B.2.2	B-3
March 1951	B.3.1	B-4	B.3.2	B-4
April 1951	B.4.1	B-5	B.4.2	B-5
May 1951	B.5.1	B-6	B.5.2	B-6
June 1951	B.6.1	B-7	B.6.2	B-7
July 1951	B.7.1	B-8	B.7.2	B-8
August 1951	B.8.1	B-9	B.8.2	B-9
September 1951	B.9.1	B-10	B.9.2	B-10
October 1950	B.10.1	B-11	B.10.2	B-11
November 1950	B.11.1	B-12	B.11.2	B-12
December 1950	B.12.1	B-13	B.12.2	B-13
Monthly Average	B.13.1	B-14	B.13.2	B-14

**Diurnal variation in January, 1951
Jodrell Bank, Northwest Radar Beam**

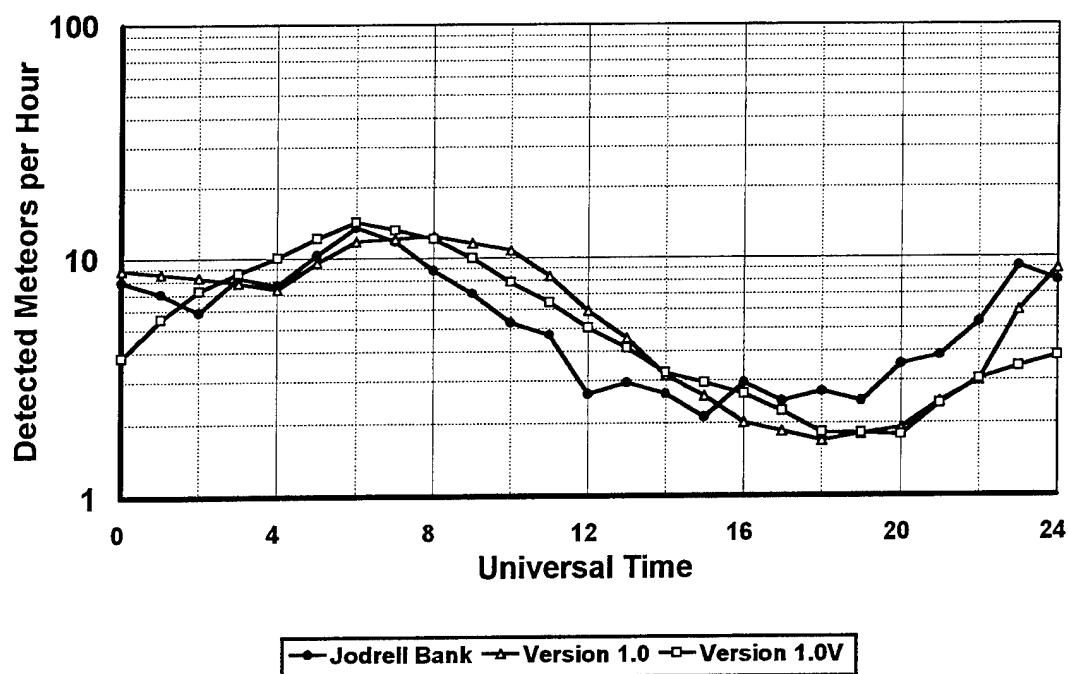


Figure B.1.1 MR Comparison for the Northwest Beam in January

**Diurnal variation in January, 1951
Jodrell Bank, Southwest Radar Beam**

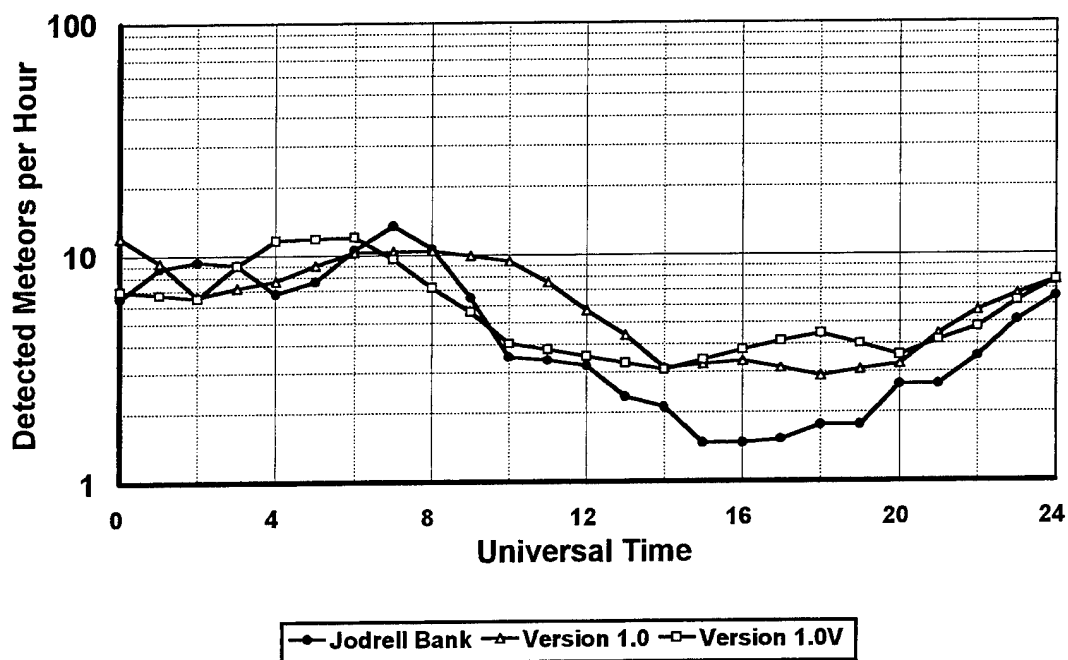


Figure B.1.2 MR Comparison for the Southwest Beam in January

**Diurnal variation in February, 1951
Jodrell Bank, Northwest Radar Beam**

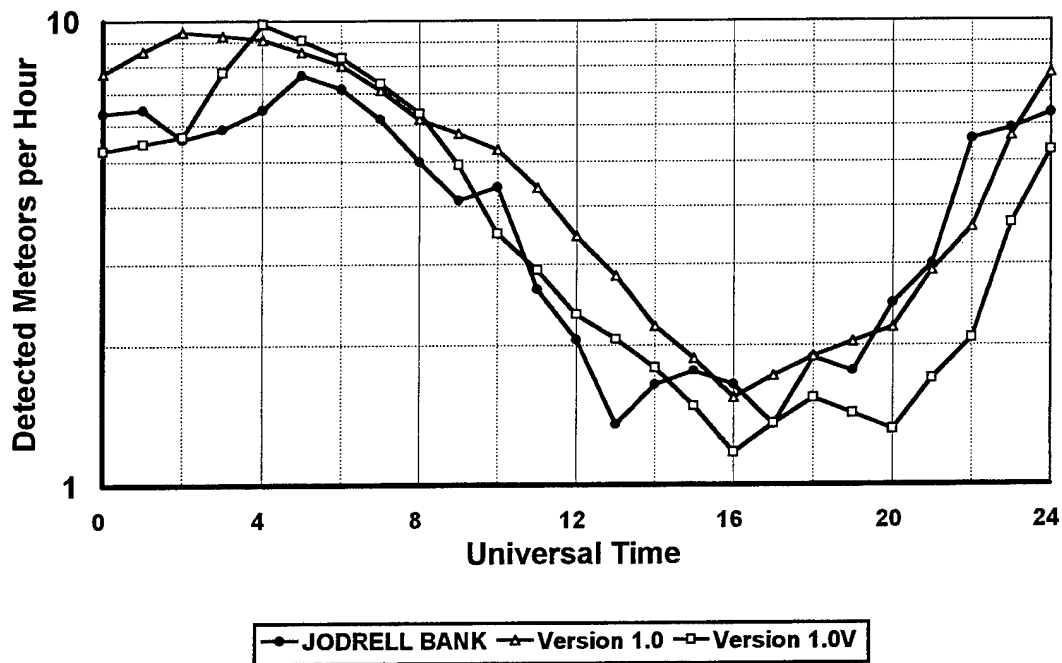


Figure B.2.1 MR Comparison for the Northwest Beam in February

**Diurnal variation in February, 1951
Jodrell Bank, Southwest Radar Beam**

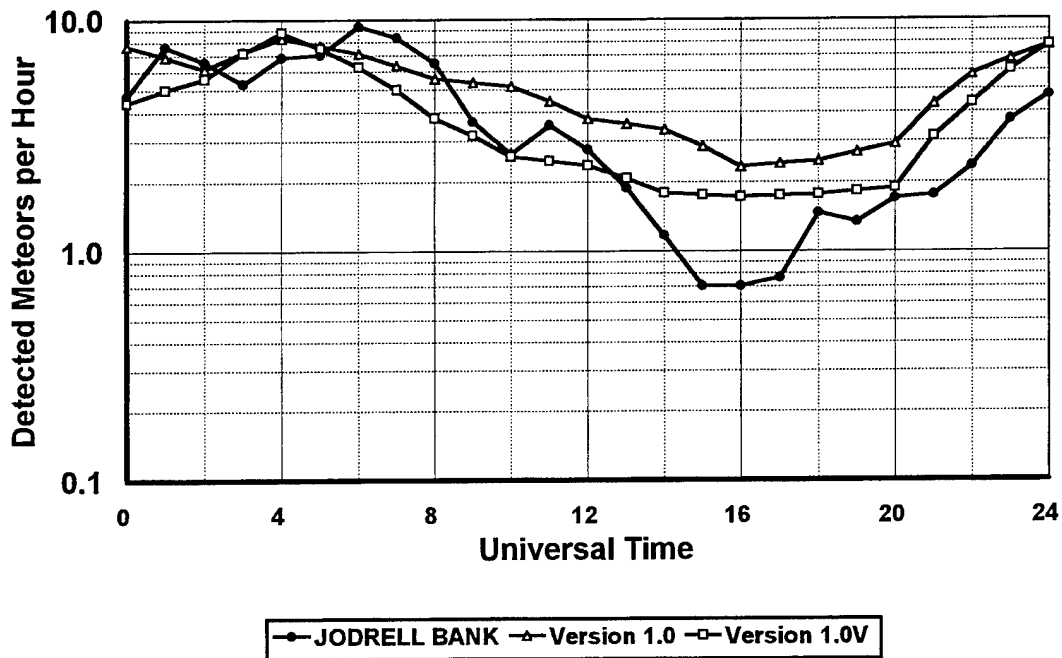


Figure B.2.2 MR Comparison for the Southwest Beam in February

**Diurnal variation in March, 1951
Jodrell Bank, Northwest Radar Beam**

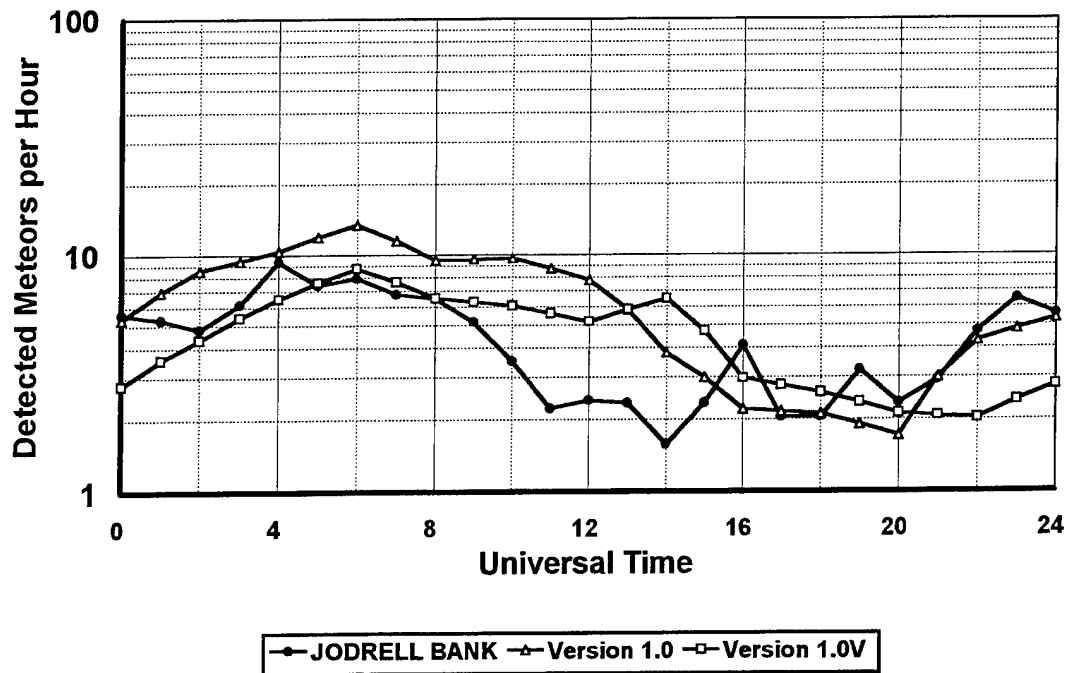


Figure B.3.1 MR Comparison for the Northwest Beam in March

**Diurnal variation in March, 1951
Jodrell Bank, Southwest Radar Beam**

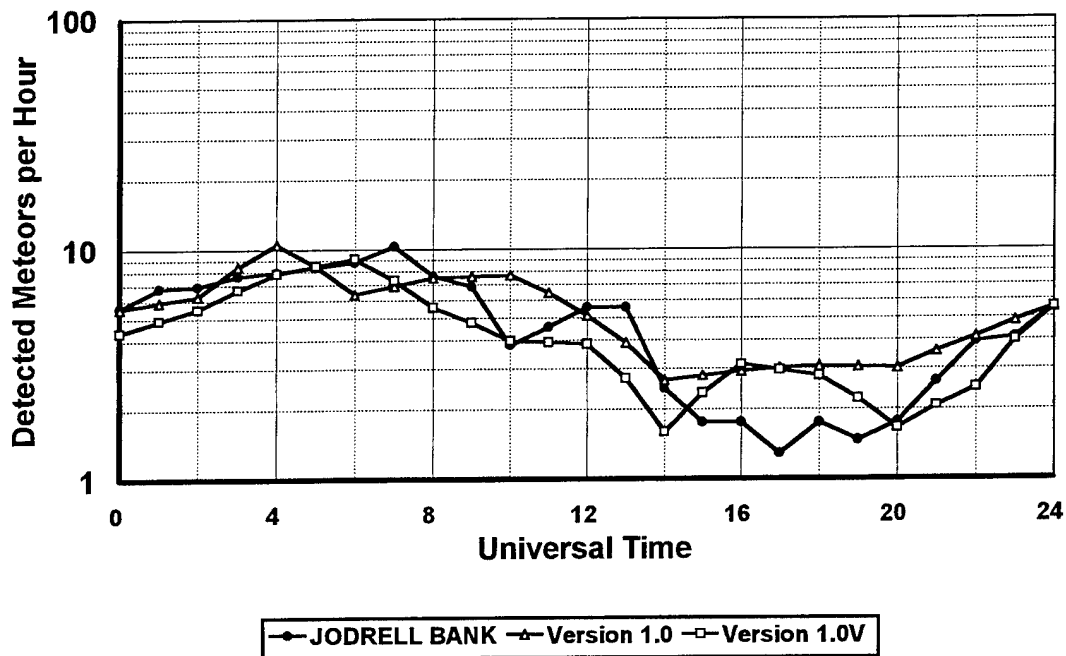


Figure B.3.2 MR Comparison for the Southwest Beam in March

**Diurnal variation in April, 1951
Jodrell Bank, Northwest Radar Beam**

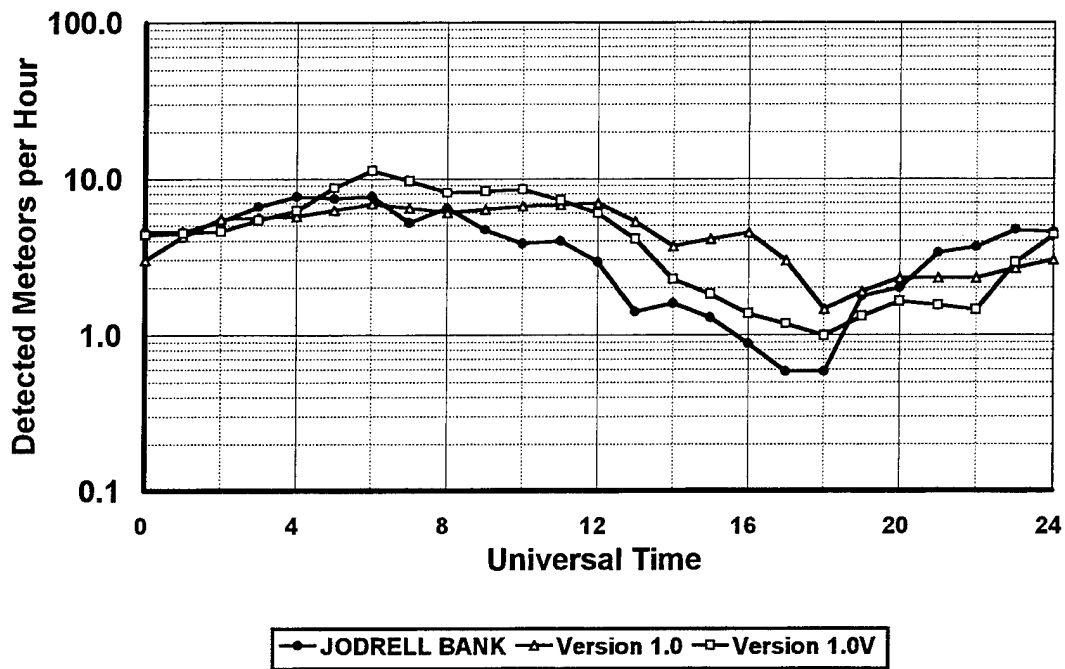


Figure B.4.1 MR Comparison for the Northwest Beam in April

**Diurnal variation in April, 1951
Jodrell Bank, Southwest Radar Beam**

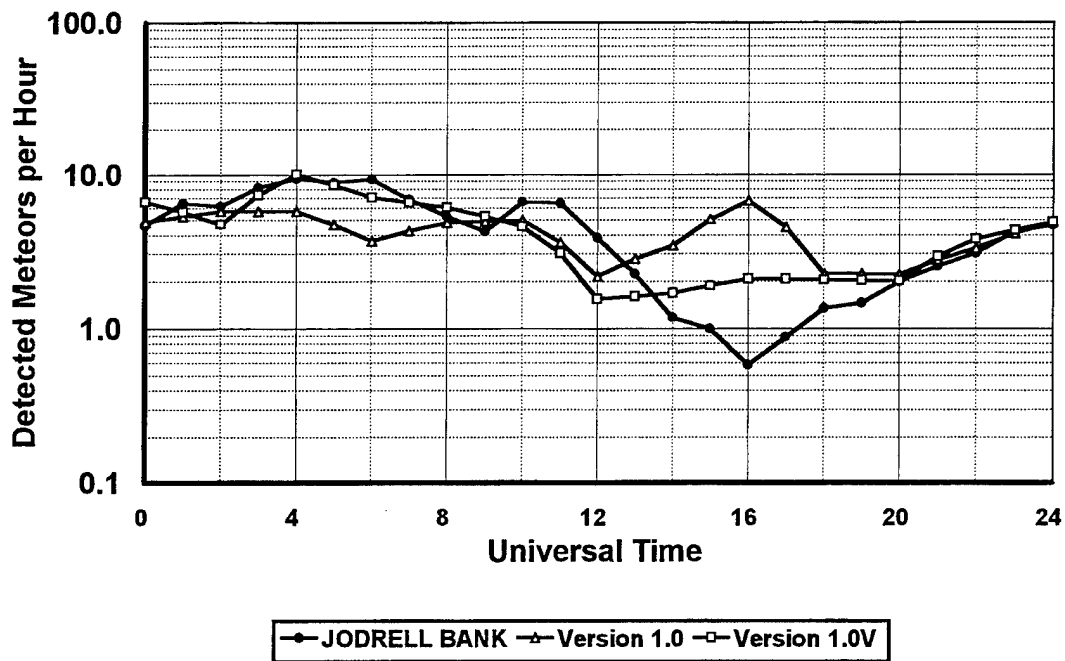


Figure B.4.2 MR Comparison for the Southwest Beam in April

Diurnal variation in May, 1951
Jodrell Bank, Northwest Radar Beam

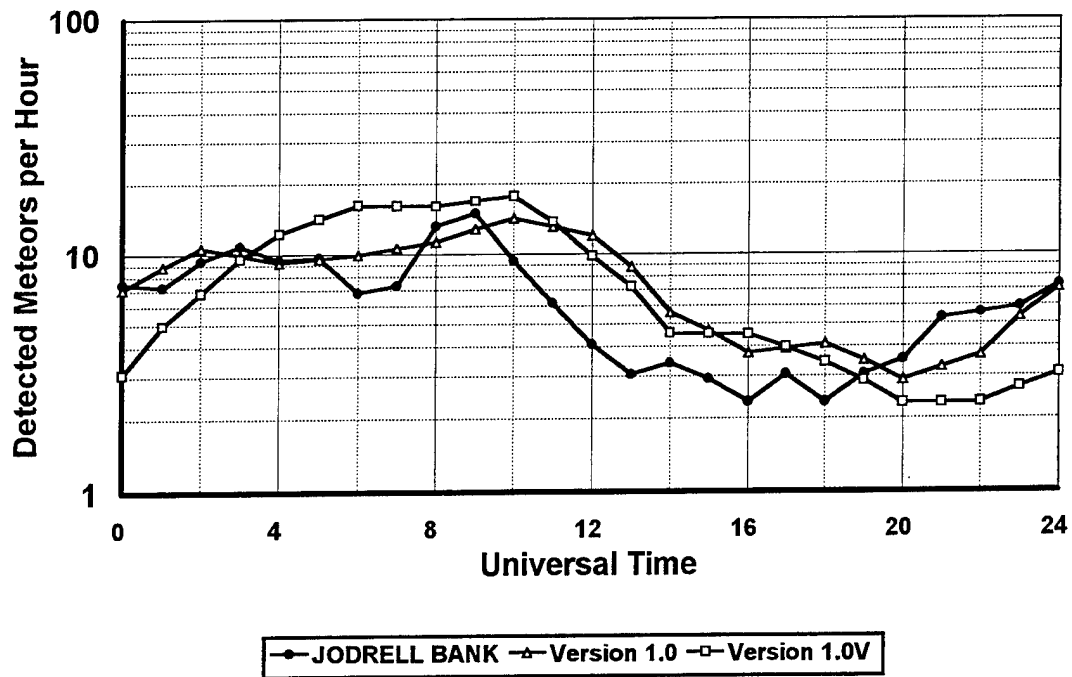


Figure B.5.1 MR Comparison for the Northwest Beam in May

Diurnal variation in May, 1951
Jodrell Bank, Southwest Radar Beam

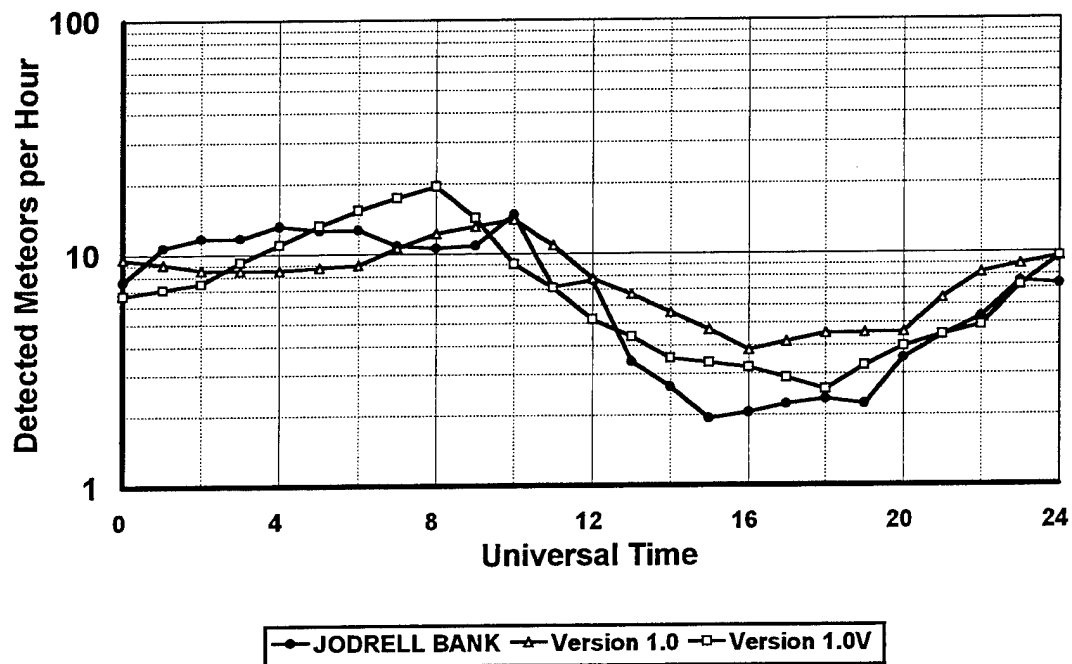


Figure B.5.2 MR Comparison for the Southwest Beam in May

**Diurnal variation in June, 1951
Jodrell Bank, Northwest Radar Beam**

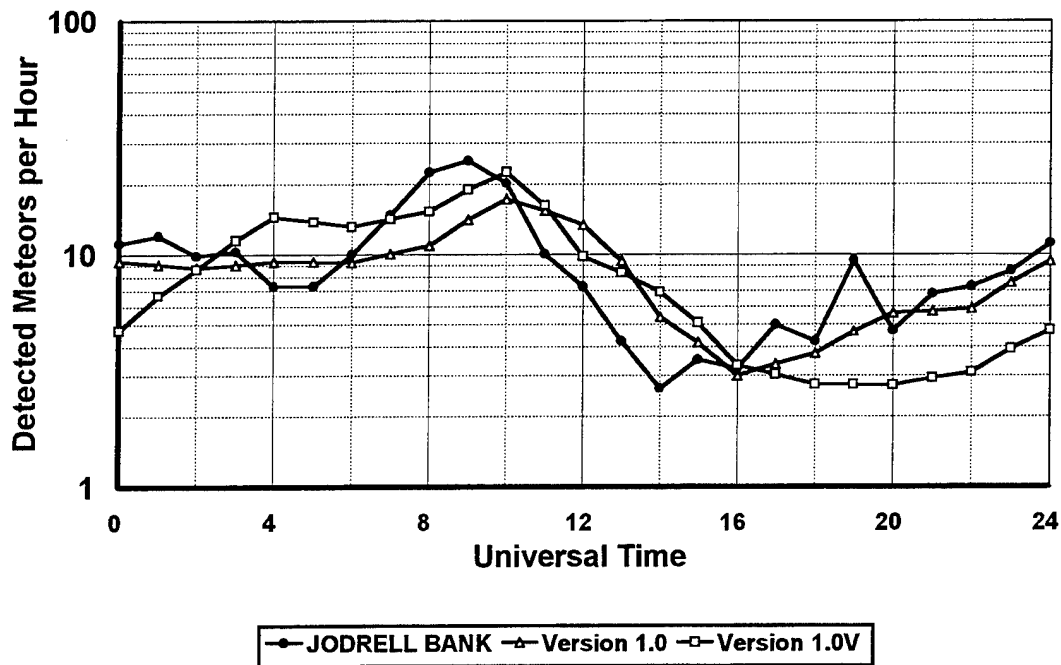


Figure B.6.1 MR Comparison for the Northwest Beam in June

**Diurnal variation in June, 1951
Jodrell Bank, Southwest Radar Beam**

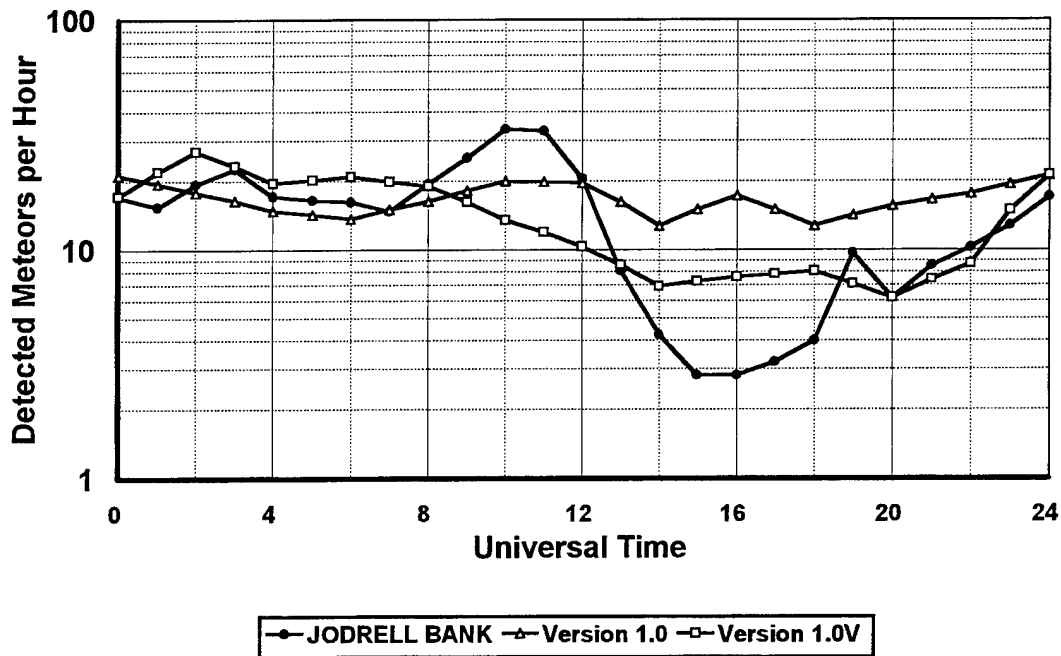


Figure B.6.2 MR Comparison for the Southwest Beam in June

**Diurnal variation in July, 1951
Jodrell Bank, Northwest Radar Beam**

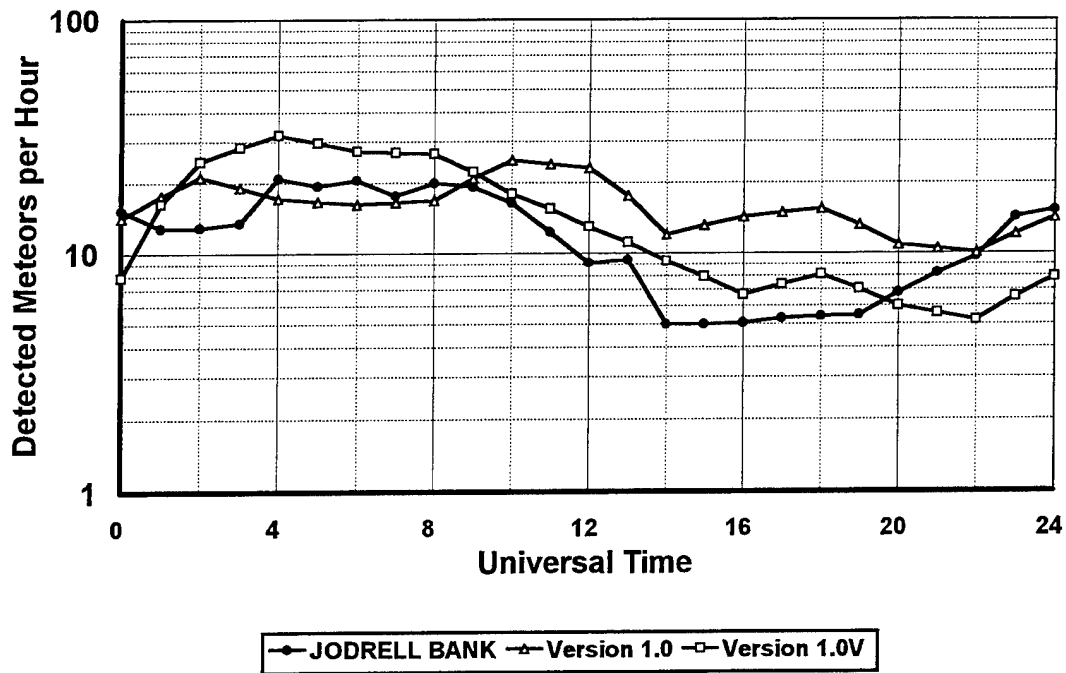


Figure B.7.1 MR Comparison for the Northwest Beam in July

**Diurnal variation in July, 1951
Jodrell Bank, Southwest Radar Beam**

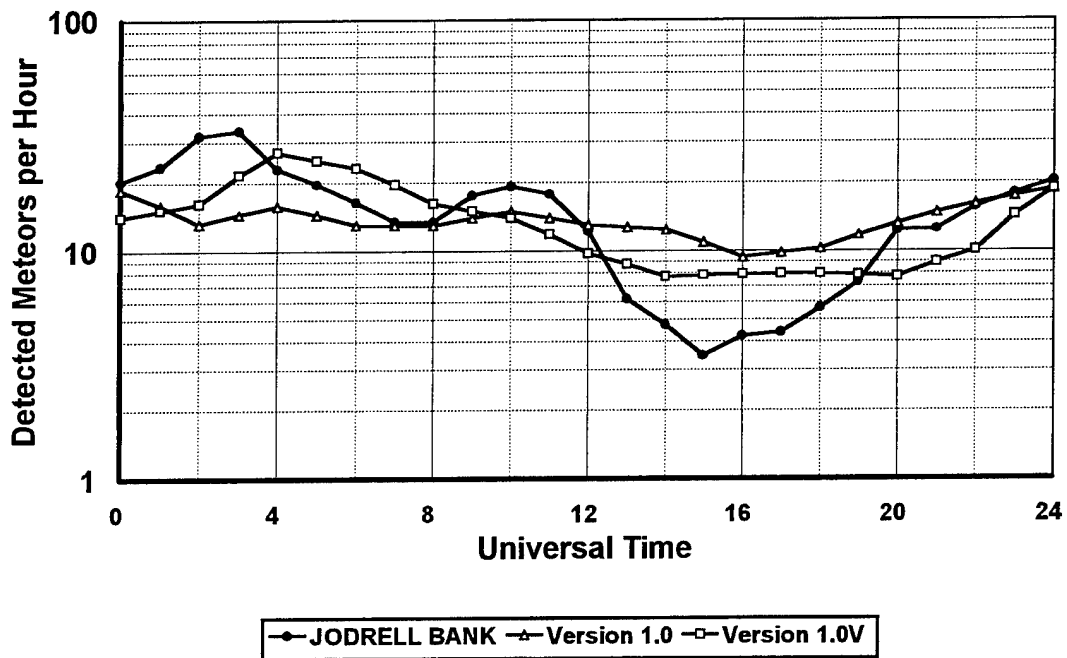


Figure B.7.2 MR Comparison for the Southwest Beam in July

Diurnal variation in August, 1951 Jodrell Bank, Northwest Radar Beam

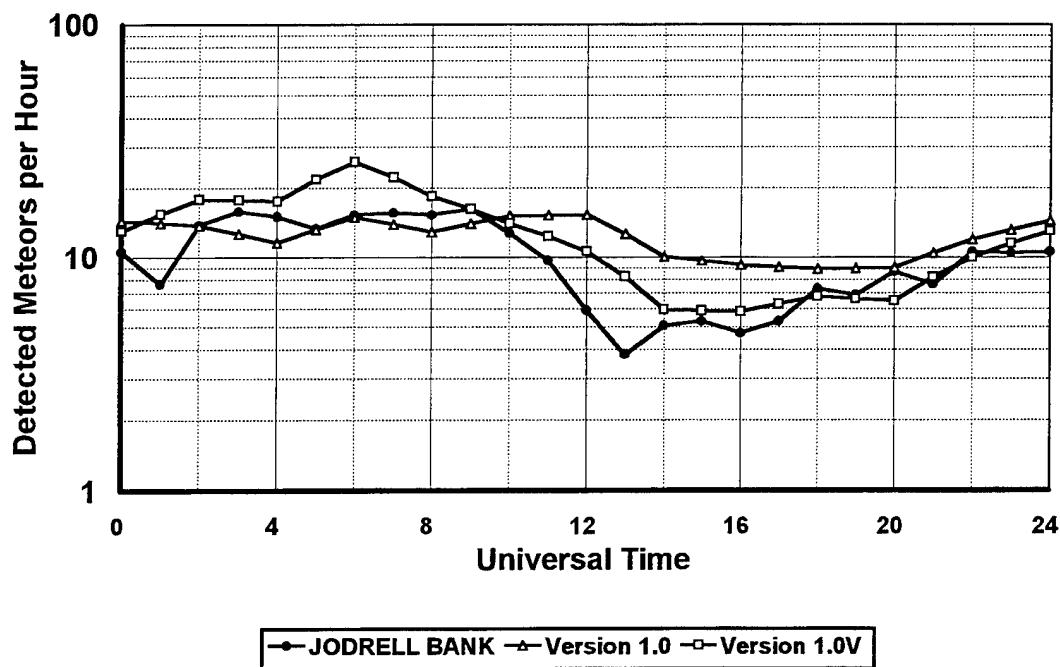


Figure B.8.1 MR Comparison for the Northwest Beam in August

Diurnal variation in August, 1951 Jodrell Bank, Southwest Radar Beam

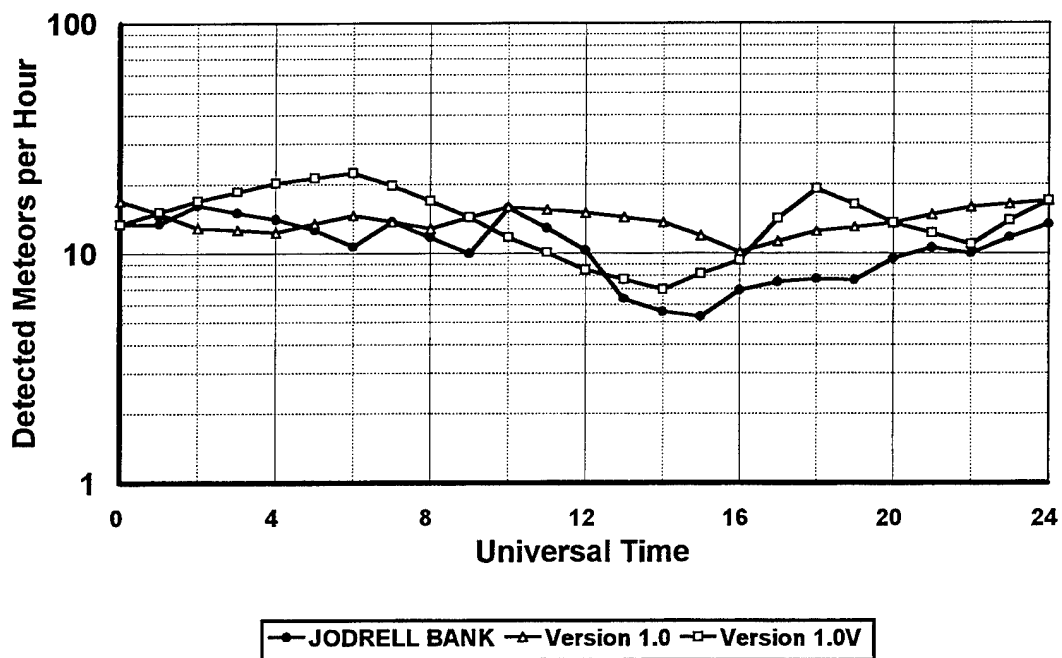


Figure B.8.2 MR Comparison for the Southwest Beam in August

**Diurnal variation in September, 1951
Jodrell Bank, Northwest Radar Beam**

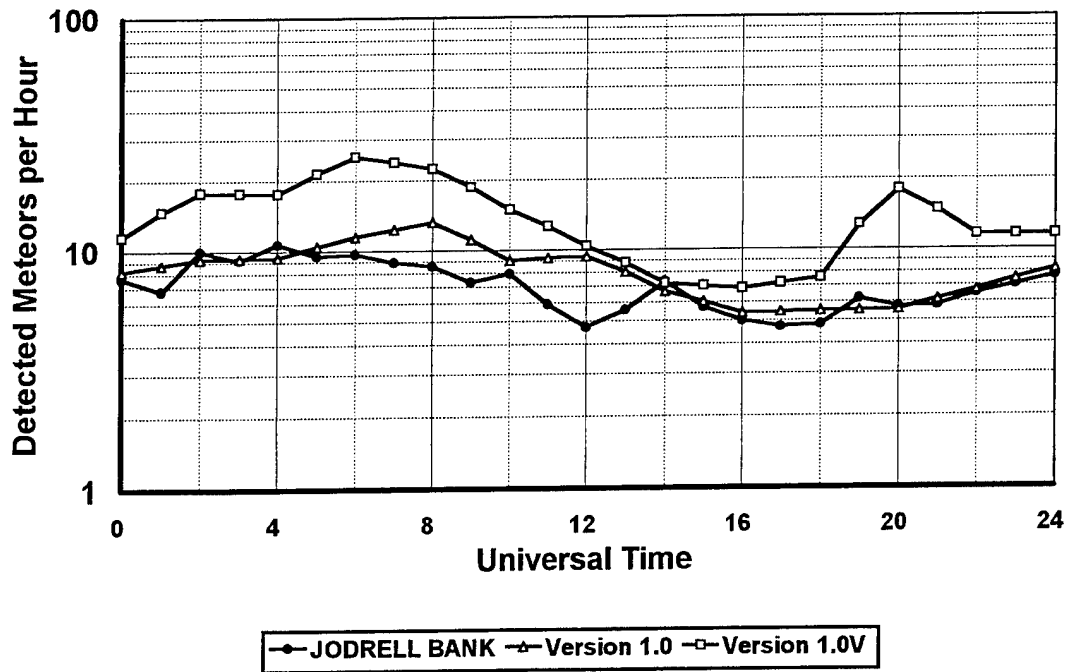


Figure B.9.1 MR Comparison for the Northwest Beam in September

**Diurnal variation in September, 1951
Jodrell Bank, Southwest Radar Beam**

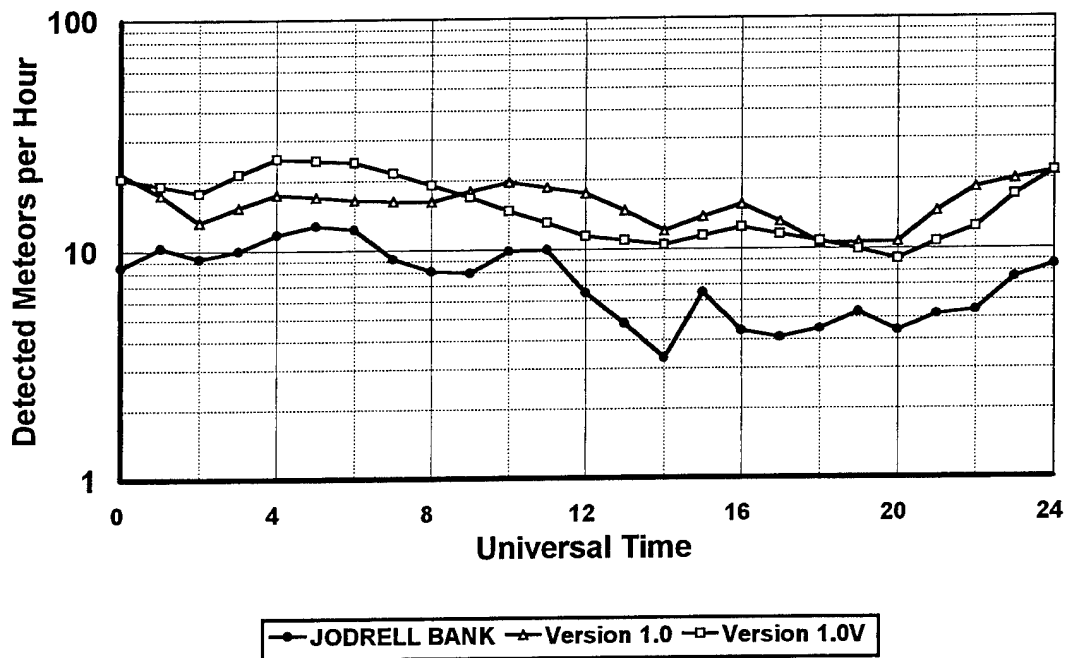


Figure B.9.2 MR Comparison for the Southwest Beam in September

Diurnal variation in October, 1950 Jodrell Bank, Northwest Radar Beam

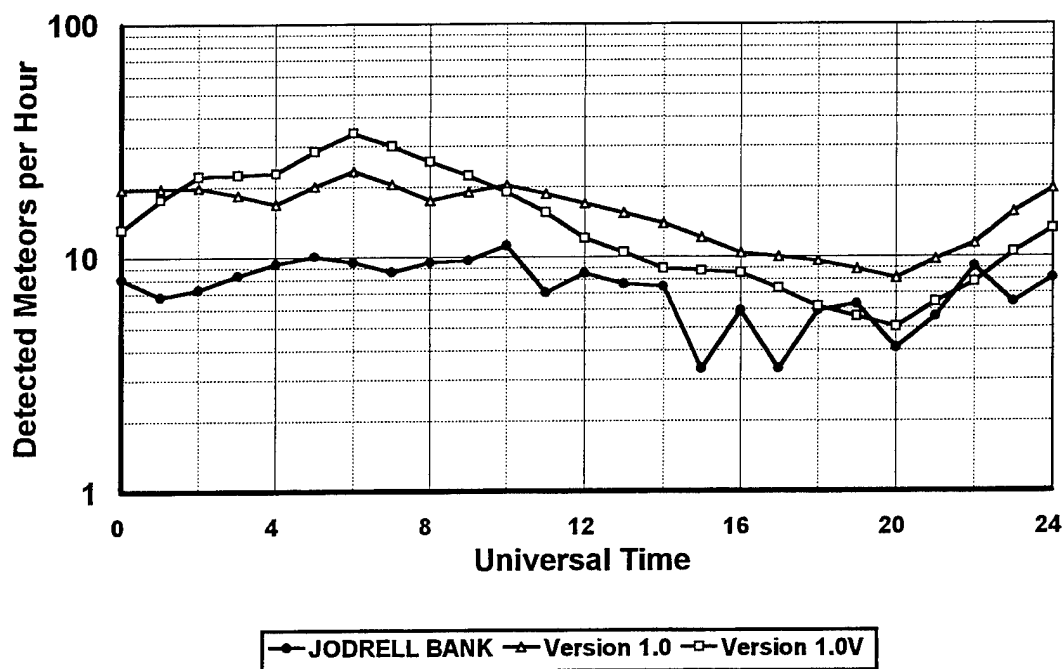


Figure B.10.1 MR Comparison for the Northwest Beam in October

Diurnal variation in October, 1950 Jodrell Bank, Southwest Radar Beam

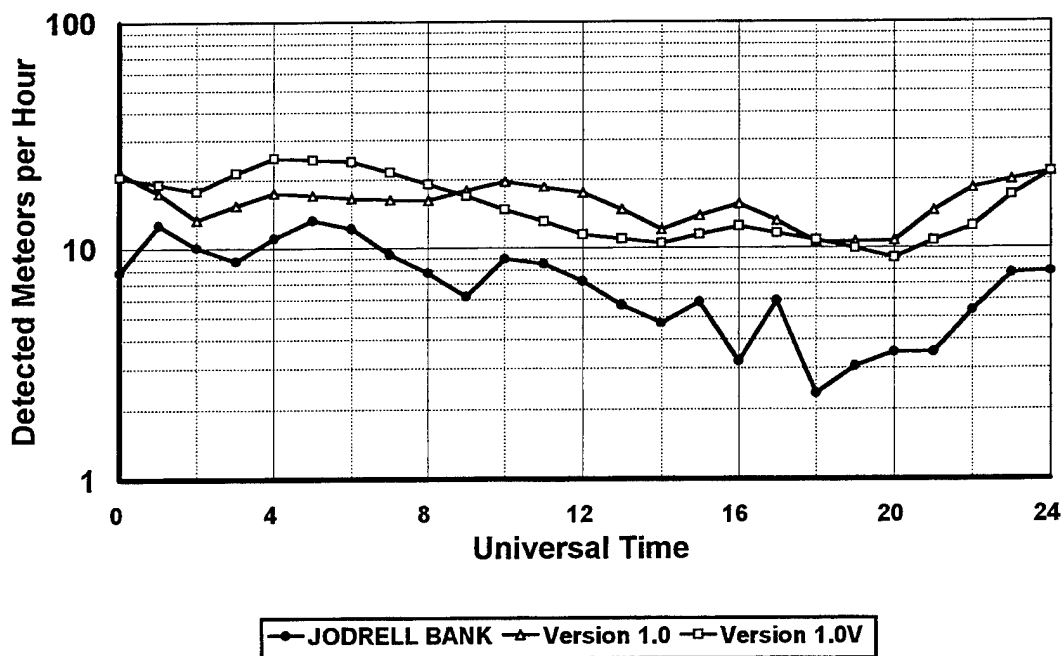


Figure B.10.2 MR Comparison for the Southwest Beam in October

**Diurnal variation in November, 1950
Jodrell Bank, Northwest Radar Beam**

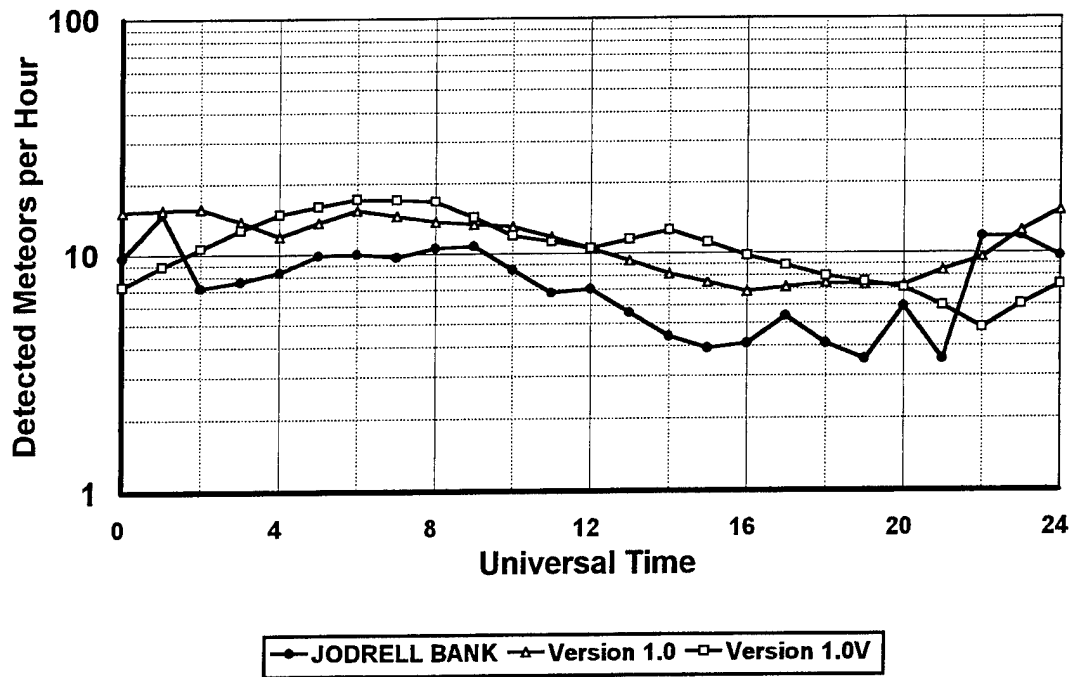


Figure B.11.1 MR Comparison for the Northwest Beam in November

**Diurnal variation in November, 1950
Jodrell Bank, Southwest Radar Beam**

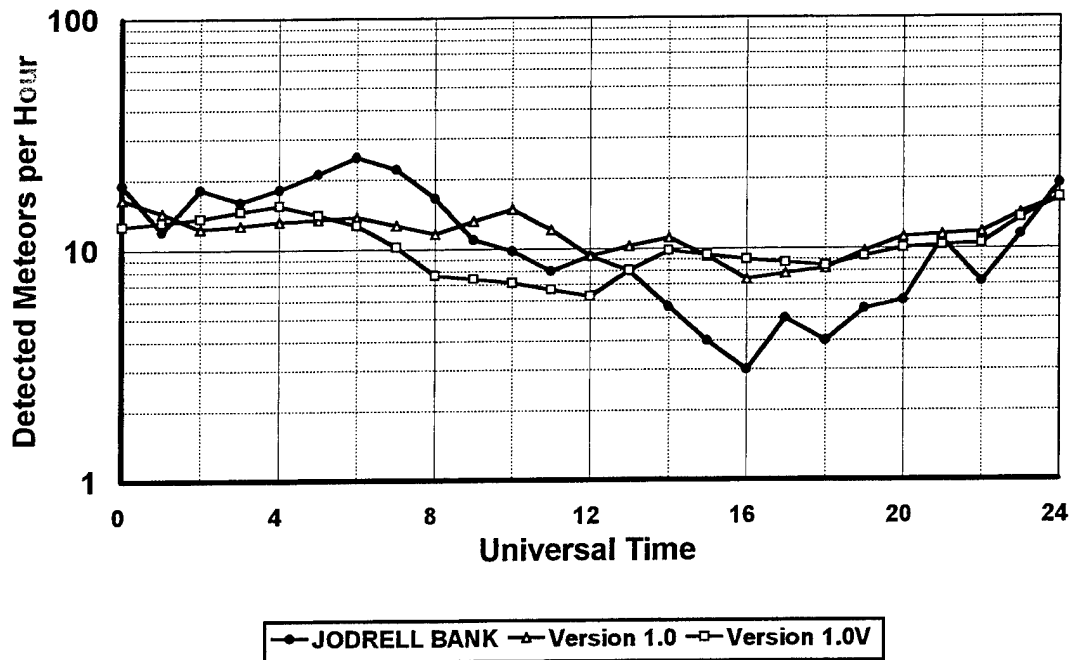


Figure B.11.2 MR Comparison for the Southwest Beam in November

**Diurnal variation in December, 1950
Jodrell Bank, Northwest Radar Beam**

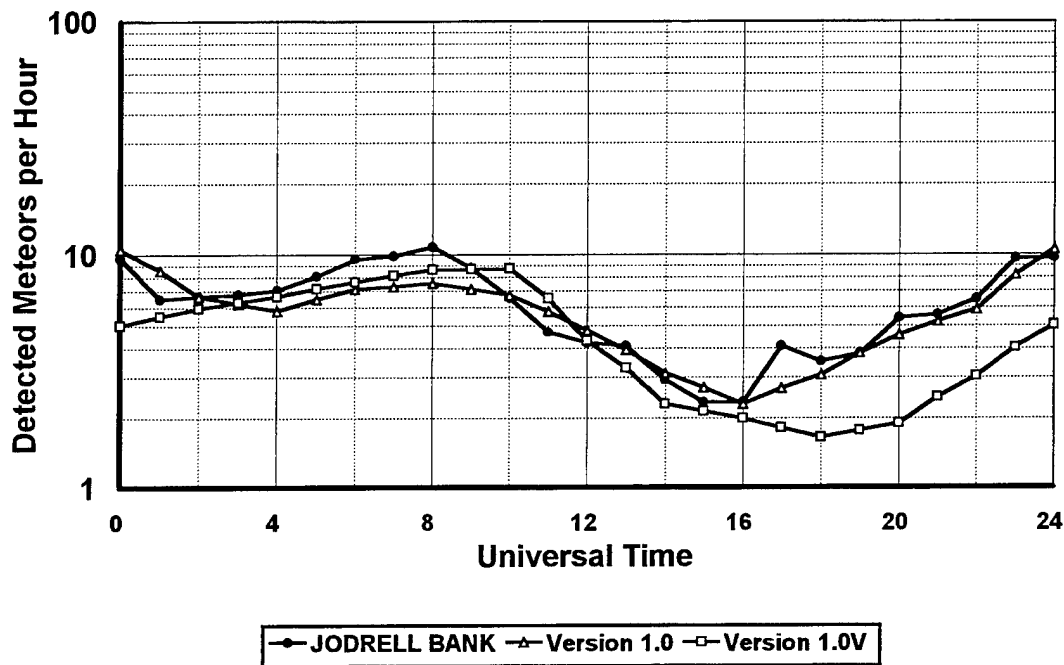


Figure B.12.1 MR Comparison for the Northwest Beam in December

**Diurnal variation in December, 1950
Jodrell Bank, Southwest Radar Beam**

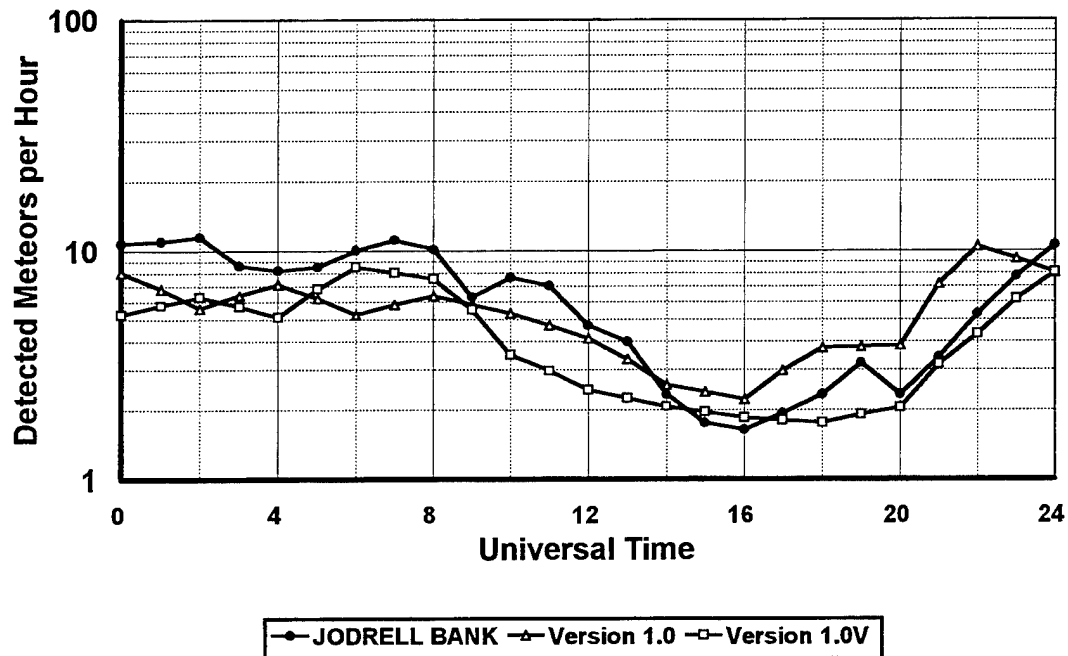


Figure B.12.2 MR Comparison for the Southwest Beam in December

Monthly Diurnal Average Variation Jodrell Bank, Northwest Radar Beam

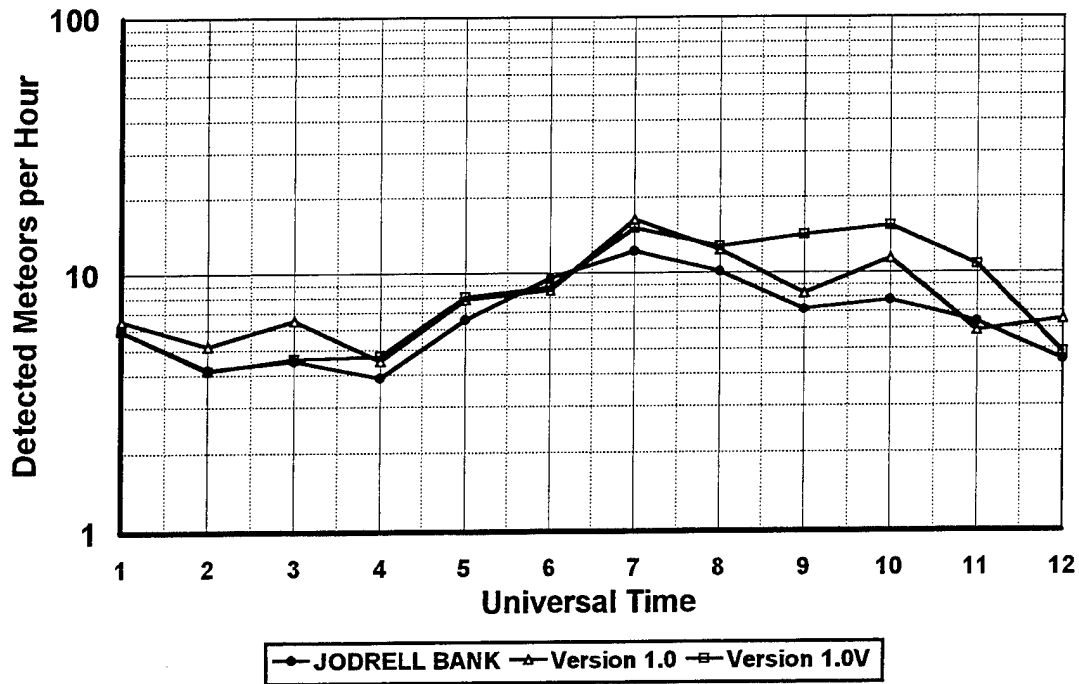


Figure B.13.1 Monthly MR Comparison for the Northwest Beam

Monthly Diurnal Average Variation Jodrell Bank, Southwest Radar Beam

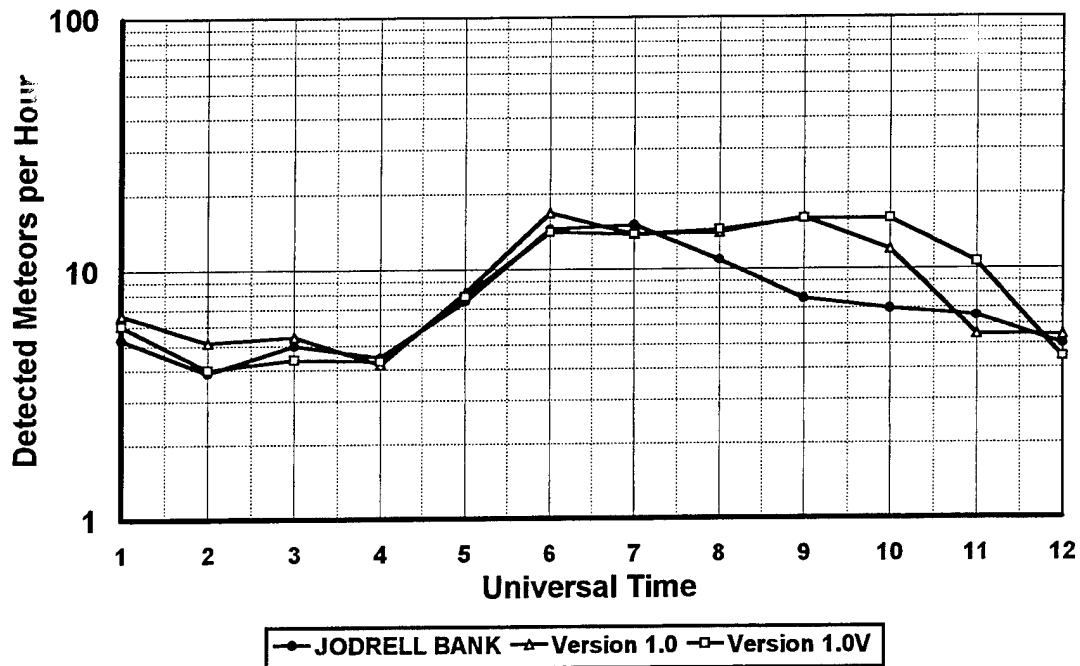


Figure B.13.2 Monthly MR Comparison for the Southwest Beam